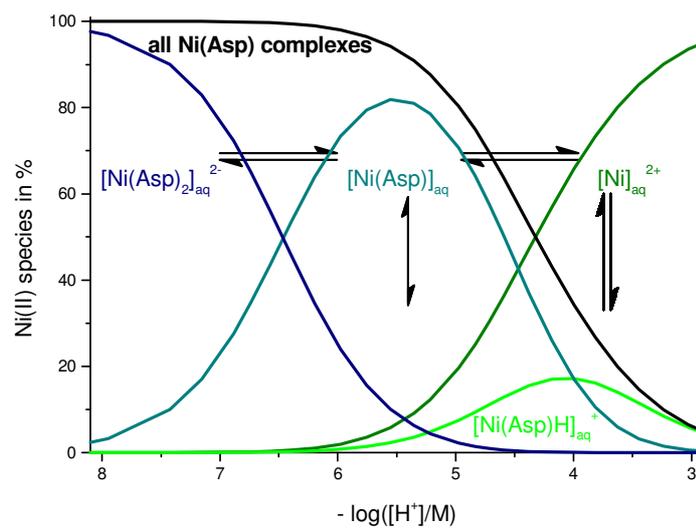


pH-Sensitive Binding of Nickel(II) Ions to Aspartic acid

Dissertation submitted in fulfilment of the requirements of the Doctor Degree of the Natural Sciences (Dr. rer. nat.) at the University of Bielefeld, Germany



The work was accomplished from January 2001 until March 2004 at the Faculty of Chemistry of the University of Bielefeld under the supervision of Prof. Dr. W. Knoche.

Date of Doctoral Final Examination (thesis defense): 25th May 2004

Examining Board:

Chairman: Prof. Dr. P. Jutzi

Examiners: 1. Prof. Dr. W. Knoche

2. Prof. Dr. E. Neumann

3. Dr. M. Letzel

Acknowledgements

Firstly, I would like to express my deep gratitude and thanks to my supervisor, Prof. Dr. W. Knoche for his ongoing help, guidance, dedication and for the opportunity to work in his research group in Germany. This was of great enrichment to me - personally, scientifically and culturally.

I am very grateful to my colleagues for their help throughout and pleasant working atmosphere, especially Dr. J. Kleimann and Dr. D. Leisner for the mathematical and computation assistance. Many thanks also go to Ms E. Ruano Herrero who worked for two months on this project during her stay in Bielefeld as Erasmus student, Mrs. B. Heidemann for her help in the stopped-flow experiments, Mrs. G. Heinze-Brückner from the Inorganic chemistry department for the IR and Raman experiments, Dr. M. Jost from the Organic chemistry department for his assistance and Dr. A. Mitschker from *BASF* who supplied us the polyaspartic acid sample.

I would also like to thank the Research Centre Jülich, the University of Bielefeld and the federal state North Rhine-Westphalia for the grants and financial assistance.

Special thanks are also due to my parents, Olga, Aldo and all my friends for their support of this endeavour.

Contents

CONTENTS	I
1. INTRODUCTION	1
Why complexation of nickel ions to aspartic acid ?	3
Why aspartic acid ?	3
Why nickel (II) ions?	4
Experiments in this Study	4
2. THERMODYNAMICS OF METAL COMPLEXATION	5
2.1 Factors affecting complex stability	5
2.1.1 Hardness and softness of the metal ion and of the coordinating ligands.....	5
2.1.2 The Chelate Effect	6
2.1.3 Sizes of chelate ring and metal ion.....	6
2.1.3.1 Chelate rings larger than six membered	8
2.2 UV/VIS Spectroscopy - electronic transitions in transition metal-amino acid complexes.....	9
2.2.1 Crystal Field Theory.....	9
3. KINETICS OF METAL COMPLEXATION.....	13
3.1 Factors affecting Metal Complexes Formation	13
3.1.1 Charge of the Metal ion	13
3.1.2 Charge of the Ligand.....	13
3.1.3 Charge of the Metal Complex.....	14
3.1.4 Charge Product of the Metal ion and Ligand	15
3.1.5 Ligand Structure	16
3.1.5.1 Kinetic chelate effect	16
3.1.5.2 Number and type of chelating groups	17
a) Amino-carboxylate ligands.....	17
b) Di-amine and di-carboxylate ligands.....	18
c) Oligo-amine ligands	18
d) Pyridinecarboxylates.	19
e) Other ligands.....	19
4. EXPERIMENTAL SECTION	21
4.1 Reagents.....	21
4.2 Instrumental and Experimental Methods	21
4.2.1 Potentiometric Titrations	21
4.2.2 Other Potentiometric measurements	23
4.2.3 UV-Vis-Spectrophotometry.....	23
4.2.3.1 pH-titrations	23
a. "Continuous flow" Experiments.....	23

b. “Automated titration” Experiments	23
4.2.3.2 Nickel(II) nitrate - titrations - Separate solution Experiments.....	24
4.2.3.3 Asp-titrations - Separate solution Experiments	24
4.2.4 IR and Raman Spectroscopy	25
4.2.5 Stopped-flow experiments	25
4.2.6 Processing of the data	26
5. RESULTS AND EVALUATION - THERMODYNAMICS	27
5.1 Protonation Equilibria of Aspartic acid	27
5.2 Complexation of Nickel (II) ions with Asp	29
5.2.1 Potentiometrical results	31
5.2.1.1 Potentiometrical analysis of the Complexation of Nickel (II) ions with Asp - Titration of nickel(II) ions and Asp with NaOH	31
5.2.2 Spectrophotometrical results	32
5.2.2.1 Analysing the spectral changes due to the formation of the various nickel(II)aspartate complexes	32
5.2.2.2 The binding mode of nickel(II) ions to poly-L-aspartic acid	41
5.3 Summary of Thermodynamics	42
6. RESULTS AND EVALUATION- KINETICS	43
6.1 Stopped-flow experiments	43
6.1.1 pH-Dependence of the Reaction Rate	43
6.1.1.1 Nickel(II) ions in excess	43
A) Fitting of the data assuming a water-release rate-determining step	47
B) Fitting of the data assuming a metal chelate ring-closure rate-determining step	52
6.1.1.2 Asp in excess	53
A) Fitting of the two-relaxation-time curves	55
i) Assuming a reaction scheme without the species NiLLH ⁺ and Ni(LH) ₂	60
Fitting of equations (6.54) and (6.55) for pCh > 6.....	61
Fitting of equations (6.54) and (6.55) for 3 < pCh < 8.	62
ii) Assuming a reaction scheme with the species NiLLH ⁺ and Ni(LH) ₂	63
6.1.2 Concentration-Dependence of the Reaction Rate	66
6.1.2.1 Dependence of the Reaction Rate on the Concentration of Nickel(II) ions; Nickel(II) ions in excess	67
6.1.2.2 Dependence of the Reaction Rate on the Aspartic Acid Concentration; Aspartic Acid in excess.....	68
6.1.2.3 Dependence of the Reaction Rate on the Buffer Concentration.....	71
6.1.3 Evaluation of Amplitudes	73
6.1.3.1 Single relaxation effect	73
6.1.3.2 Two relaxation effects	81
7. DISCUSSION	87
7.1 Thermodynamic Experiments.....	87

7.1.1 Potentiometrical Results	87
7.1.2 Spectrophotometrical results - analysing the spectral changes due to the formation of the various nickel(II)aspartate complexes.....	88
7.1.2.1 Asp-Ni Binding Mode	88
7.1.2.2 Ni(II) Binding Mode to protonated Asp and to PAsp	88
7.2 Kinetics	91
7.2.1 Stopped-flow experiments	91
7.2.1.1 pH-Dependence	92
7.2.1.1.1 Ni in excess	92
7.2.1.1.2 Asp in excess	94
7.2.1.2 Why is the formation of the 1:2 complex slower than the formation of the 1:1 complex?	101
7.3 Poly-L-Aspartic acid	105
8. SUMMARY.....	107
9. REFERENCES AND NOTES.....	111
10. APPENDIX	115
10.1 Experimental data.....	115
10.1.1 Potentiometrical data.....	115
10.1.2 Spectrophotometrical data	119
10.1.2.1 Uv-Vis Spectrophotometrical data	119
a) pH-titrations	119
b) Nickel(II) nitrate - titrations - Separate solution experiments.....	121
c) Asp-titrations - Separate solution experiments	121
10.1.2.2 IR and Raman data	122
a) IR Spectroscopy.....	122
b) Raman Spectroscopy.....	124
10.1.3 Kinetic data - Stopped-flow Experiments	126
10.2 The fitting programmes used	130
10.2.1 Fitting of Potentiometric and spectrophotometric data.....	130
10.2.2 Fitting of Kinetic data	134
10.3 Justification of the neglect of the quadratic terms in the derivation of the equation relating δA and $[H^+]$ (See section 6.1.3).....	134
10.4 Proof of the Integration for the evaluation of the amplitudes for two relaxation effects (See section 6.1.3.2).....	136

IV pH-Sensitive Binding of Nickel(II) Ions to Aspartic Acid

1. Introduction

Metal ion complexation is an interdisciplinary topic with applications in various fields. These include:

a) BIOTECHNOLOGY (with reference to heavy metal binding to anaerobic sludge)

For a better understanding of the interactions between heavy metals and sludge, A. Artola et. al., 1997, investigating heavy metal binding to anaerobic sludge, suggested that the main binding groups for metals in sludge are of amino acid type due to similarities observed between glycine-metal aqueous system and sludge-metal aqueous system.

b) ENVIRONMENTAL (with reference to water purification using biodegradable polyelectrolytes)

Water-soluble polymers, such as poly(vinyl alcohol), poly(ethylene glycol) and poly(acrylic acid) are widely used as cosmetics, paper additives, dispersants and detergent builders, but are hardly recovered or collected after use. Therefore, biodegradable substitutes for such non-biodegradable polymers having carboxylic acid groups are really desired in terms of the earth's environment. From an industrial point of view, biodegradable polymers must be produced at low cost and on industrial scale. Recently, the biotechnological production of L-aspartic acid with a low price and on an industrial scale has been realized. Moreover the thermal polycondensation of aspartic acid is known to easily produce poly(aspartic) acid, so that it has a great potential to resolve environmental problems, in particular, in the field of biodegradable water-soluble polymers.

c) GEOCHEMICAL (with reference to chemical reactions at soils and clays)

For a better understanding of the behaviour of environmental systems, in particular surface waters, sediments and soils. For this purpose, research on static (thermodynamic) and dynamic processes related to physical and colloid chemistry, biochemistry and biophysics are performed to determine amongst others the bioavailability of trace compounds to flora and fauna.

d) BIOMINERALISATION

The organic matrix in mollusc shells is involved in binding calcium and ultimately in producing the calcium carbonate crystals in the mineralization process of shell formation (see B. A. Halloran et.

al., 1995). S. Weiner et. al., 1975 reported that aspartic acid is involved in a significant portion of the protein sequence of the Ca^{2+} binding subunit.

e) AGRICULTURAL (with reference to controlled release of agricultural chemicals)

Research in functional biopolymers has focused on synthesis of polymers for controlled release of agricultural chemicals.

f) PLANT BIOCHEMISTRY (with reference to detoxification in plants)

The most important heavy metal binding and heavy metal detoxifying substances in plants are the peptides phytochelatins (see C. S. Cobbett, 2000).

g) MEDICAL;

Certain metal ions are essential to human life but are toxic at concentrations higher than a critical dose. Nickel is such an example, being an essential trace element (0.3 - 0.5 mg per day) but is toxic and carcinogenic at high concentrations (the lethal dose in rats being 50 mg), J. Emsley, 1994. The toxicity of metal ions is often associated with the degree of complexation to ligands, being toxic when present as free ions. Moreover, certain metal ion-enzyme interactions result in anti-inflammatory properties (Adamo F. et. al., 2001 and references therein); kidney stones formation, dental calculus, deposits formed in gout and atherosclerosis are also based on complexation reactions.

h) ANALYTICAL CHEMISTRY RESEARCH

Metal ion complexation is the basis of Ion-exchange Chromatography, Immobilized Metal Affinity Chromatography (IMAC) (see Gaberc-Porekar V. et. al., 2001), development of microsensors for the direct measurement of trace compounds *in situ*, with no or minimum sample handling e.g. sensors based on voltammetry, permeation liquid membrane (PLM); (sensors for environmental purposes, biomedical or industrial applications) and recently the use of amino acids and peptides as recognition elements in electrochemical sensors, J. J. Googing et al., 2001. The formation of chelates by polymers has widely been used for concentration, separation and extraction of metal ions.

i) SYNTHETIC CHEMISTRY RESEARCH

Metal ion complexation provides useful information about new potential masking agents. These are specific chelating agents which enhance the selectivity of extraction. For instance, in the

separation of metal ions, this is done by suppressing the extraction of interfering ions without suppressing the analytes. An example is the separation of nickel(II) from copper(II) with 8-hydroxyquinoline (see K. Watanabe et. al., 2001 and references therein).

Why complexation of nickel ions to aspartic acid ?

The environmental aspect is of considerable interest to us. Similar to other toxic heavy metal ions, the toxicity of Ni^{2+} is determined mainly by pH and its speciation. Furthermore, its uptake and transport can be promoted by complex formation with natural and anthropogenic ligands in soil solutions, water and biofluids. Therefore it is of great interest to understand the mechanisms and pathways of the formation of soluble Ni^{2+} -complexes with natural and anthropogenic ligands. After the thermodynamic and kinetic study of the complexation of nickel ions to

- a) side chain functionalities of synthetic polyelectrolyte and natural biopolymers (B. Goette, 2000, Kreczinski C., 2001, Engel, B., 2003)
- b) synthetic polyelectrolytes (S. Meyer, 1999) and
- c) natural biopolymers (Barwinski A., 2002, A. Schauer, 2001),

we embarked on a study of the thermodynamics and kinetics of the complexation reaction of nickel ions to aspartic acid.

Why aspartic acid ?

The following reasons motivated our choice of Asp as a ligand in our system:

- a) Asp is the building block of poly-aspartic acid, a biodegradable polyelectrolyte that is extensively used for water purification.
- b) Asp being a small molecule, makes it usable as a model for more complicated systems such as polyelectrolytes
- c) Furthermore, there is a great interest in the coordination ability of aspartic acid to metal ions from a biological point of view. Asp, being a small biologically important molecule, makes it usable as a model for more complex problems of biochemical interest, such as metal ion activation of enzymes, and the association of metals with proteins and polynucleotides.

Why nickel (II) ions?

- a) Commonly occurring heavy metal ion in industry
- b) reacts slow enough to be measured by P-Jump and Stopped Flow techniques.

Experiments in this Study

Since the binding and hence toxicity of Ni²⁺ is pH-dependent, the investigation was carried out at a large pH range. Additional to equilibrium studies, kinetic investigations were also performed on our system:

- a) to complement the thermodynamic results and
- b) since kinetic properties, especially at the molecular level, are potentially capable of yielding more specific information than equilibrium properties.
- c) whereas thermodynamic properties like association constants and formation enthalpies of such complexes are well known the kinetics and mechanisms have not been understood completely, although several studies have been performed on the kinetics of the reaction of Ni²⁺ with organic and inorganic acids.

In this study:

- a) the ionic strength I is defined as $I = \frac{1}{2} \sum_i z_i^2 c_i$ and is held constant at 0.1M, (z_i being the charge number of species i , whose concentration is c_i) such that
- b) the stability constants and protonation constants are defined as products of concentration instead of activities
- c) the activity coefficients are calculated according to the extended Debye-Hückel according to Davies (W. Davies, 1962): $\log f_i = -0.5z_i^2 \left(\frac{\sqrt{I \cdot M^{-1}}}{1 + \sqrt{I \cdot M^{-1}}} - 0.3I \cdot M^{-1} \right)$
- d) the activity of a species i is defined as: $a_i = c_i \cdot M^{-1} f_i$.

2. Thermodynamics of Metal Complexation

2.1 Factors affecting complex stability

The factors that influence the affinity of a ligand to different metals are numerous. These include

- the hardness/softness of the metal ion
- the hardness/softness of the coordinating side chains of the ligand
- the chelate effect
- the coordinating geometry of the complex
- ligand field stabilisation effects
- the ability of the metal to cause induced deprotonation of the coordinating functional groups ($-\text{COOH}$ and $-\text{NH}_3^+$ in the case of amino acids, and amide nitrogens in peptides); this depends on the compatibility of the hardness/softness of the metal ion with the corresponding ligand, for instance the order of peptide hydrogen displacement by metal ions is given by $\text{Pd}^{2+} > \text{Cu}^{2+} > \text{Ni}^{2+} > \text{Co}^{2+}$. The order relates to reasonably hard metal ions as they interact with hard amide ligands (J. J. Gooding et. al., 2001, pg 79)

2.1.1 Hardness and softness of the metal ion and of the coordinating ligands

The hardness of an element is directly correlated to its electronegativity, such that the most electronegative elements form the hardest donor atoms, as in F^{2-} or H_2O , and less electronegative elements such as C, P, or I are soft donors, as shown in figure 2.1.

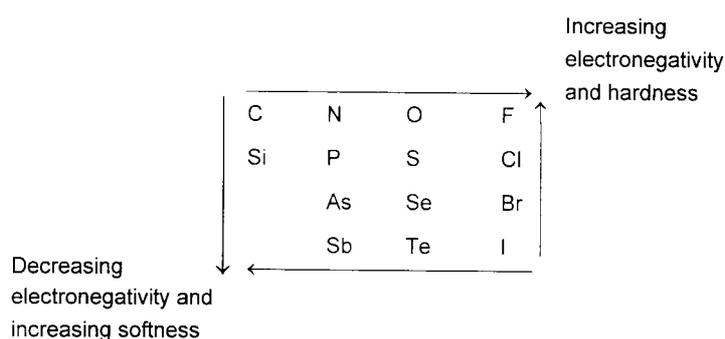


Figure 2.1 The distribution of hardness and softness in the Periodic Table as a function of the donor atom of the ligand, according to the **Hard and Soft Acids and Bases (HSAB)** classification of Pearson (see R. G. Pearson, 1967).

According to the HSAB classification, the periodic Table, can be divided into hard, soft, and borderline metal ions, as seen the figure below.

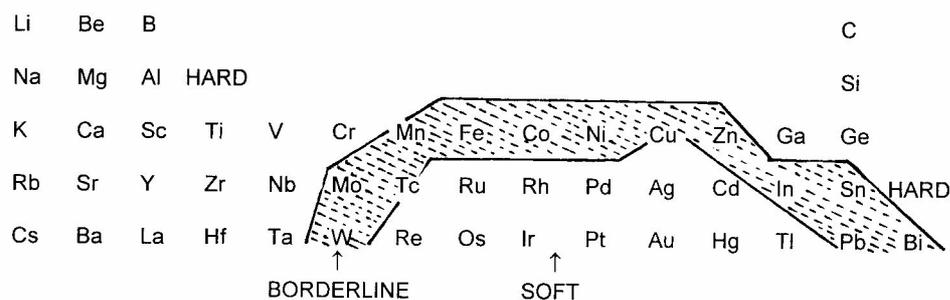


Figure 2.2 The distribution of hard, soft, and borderline metal ions in the periodic Table, according to the classification of Pearson.

Soft metal ions occur in a triangle in the center of the periodic Table, surrounded by metal ions of intermediate hardness, getting harder as one moves further from the soft metal ions.

The HSAB approach provides an indication of the type of ligand a metal ion is likely to prefer, but a more complete picture can be obtained by more detailed approaches, such as the **ligand field theory** (see section 2.2.1).

2.1.2 The Chelate Effect

The concept of a metal complex originated in the work of A. Werner, who in 1913 was awarded the first Nobel Prize in Inorganic chemistry (see G.B. Kauffman, 1981). The Chelate Effect, G. Schwarzenbach in 1952, refers to the increased stability for the complexes of chelating ligands as compared with those of open-chain monodentate analogues. This can be seen for instance when one compares the formation constants of Ni(II) with n-dentate oligoamines with the analogous complexes with ammonia (A. E. Martell and R. M. Smith, 1974-1989).

The increased stability is explained by the more negative entropy (more order) involved in the complexation reaction of n monodentate ligands in comparison to one n-dentate ligand to a central metal ion. The former case, involves the approach (and eventual collision) of n monodentate ligands from the bulk solution to the metal ion. In the oligodentate ligand, once the first donor atom is attached to the metal ion, it is much easier for the second and subsequent donor atoms to coordinate the metal ion than it is for the separate unidentate ligands since the subsequent donor atoms could move in only a restricted volume about the metal ion.

2.1.3 Sizes of chelate ring and metal ion

The chelate effect is also dependent on the size of the coordinating metal ion. The rule of ligand design states that: *"Increase of chelate ring size from five membered to six membered leads to an increase of selectivity of a ligand for smaller compared to larger metal ions"*.

This increase in complex stability for small metal ions relative to large metal ions on going from change of five membered to six membered chelate ring can be readily understood by reference to the low-strain form of cyclohexane. Cyclohexane, seen in figure 2.3, has in its chair conformer the minimum strain energy possible for a cycloalkane. All torsional angles are 60° , and the C-C-C bond angles are all the ideal value of 109.5° . The six membered chelate ring of 1,3-diaminopropane (TN) involving two nitrogens and a metal ion in place of three of the carbon atoms of cyclohexane will also be of very low strain energy (figure 2.3) as long as the metal ion is of about the same size and geometry as an sp^3 hybridized carbon atom. The ideal metal ion for coordination to TN thus has an N-M-N bond angle of 109.5° , and a short M-N bond length of about 1.6 \AA (figure 2.3 B), confirmed by calculations of the minimum strain energy of the TN ring as a function of both N-M-N angle and M-N bond length.

Analogously, the best size metal ion for the five membered chelate ring would be that having M-N bond lengths of 2.5 \AA , and N-M-N angles of about 70° (figure 2.3 C).

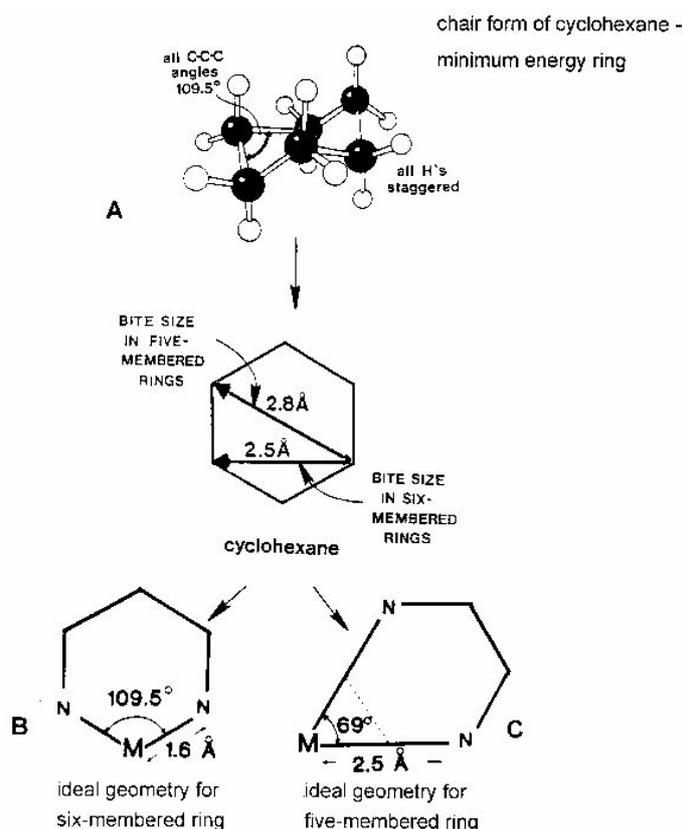


Figure 2.3

The relationship between the chair form of cyclohexane and the geometric requirements for a metal ion to form a minimum strain chelate ring involving the five membered chelate ring of EN (ethylenediamine) or the six membered ring of TN (1,3-diaminopropane). For an alkane to have the minimum strain energy, all torsion angles must be 60° , and the C-C-C angles should be 109.5° , as shown for the chair form of cyclohexane at (A). To maintain minimum strain energy, these torsion and bond angles should also be maintained in chelate rings, which can be derived from cyclohexane as shown. The resulting minimum strain requirements for the six membered chelate ring of TN are shown at (B), and those for the five membered chelate ring of EN are shown at (C). (Redrawn after Hancock R. D., 1990).

2.1.3.1 Chelate rings larger than six membered

The effect on $\log K_1^1$ for EDTA type ligands as the bridge connecting the two nitrogen donors together becomes longer is seen for a selection of metal ions in figure 2.4. Figure 2.4 shows that change in complex stability relative to the EDTA complex, $\Delta \log K$, for a variety of metal ions, as a function of n , the number of methylene groups in the bridge of the chelate ring involving the two nitrogen donors, as n increases from two to six. Figure 2.4 shows an initial change in complex stability as n increases from two to three which is related to metal ion size, as expected for increase in chelate ring size from five to six membered. Thereafter, there is a steady decrease in complex stability as n increases up to five, which is not strongly metal ion dependent. This suggests that increase in chelate ring size beyond five membered is not particularly useful as a ligand design tool for producing discrimination between different metal ions.

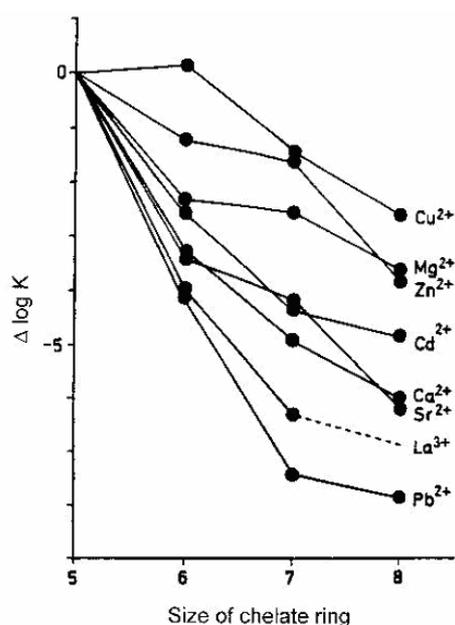


Figure 2.4 Variation of $\log K_1$ with chelate ring size in EDTA type analogues of the formula $(\sim\text{OOCCH}_2)_2\text{N}(\text{CH}_2)_n\text{N}(\text{CH}_2\text{COO}\sim)_2$. Chelate ring size varies from 5 ($n = 2$) to 8 ($n = 5$). The Variation is plotted as the change in stability, $\Delta \log K$, relative to the EDTA complex ($n = 2$) for each metal ion. Formation constants at 25°C and ionic strength 0.1. (Redrawn after R. D. Hancock, 1990)

¹ K_1 is the stability constant for one coordinated ligand to the central atom

2.2 UV/VIS Spectroscopy - electronic transitions in transition metal-amino acid complexes

Three general types of electronic transitions might be observed in transition metal – amino acid complexes: *intraligand*, *charge transfer*, and *ligand field*. The typical spectral region and molar absorptivity observed for these transitions are listed in the following table.

Table 2.1 Electronic Transitions

Band Type	Abbrev.	Selection Rule	Transition	Region	Typical Molar Absorption Coefficient
Intraligand	IL	symmetry allowed	$\pi \rightarrow \pi^*$, $n \rightarrow \pi^*$	usually UV	1000 ~ 50000
Metal to Ligand Charge Transfer	MLCT	symmetry allowed	$d \rightarrow \pi^*$	VIS or UV	1000 ~ 50000
Ligand to Metal Charge Transfer	LMCT	symmetry allowed	$\pi \rightarrow d$ or $\pi \rightarrow s$	VIS or UV	1000 ~ 50000
Ligand Field	dd	spin forbidden	$d \rightarrow d$	VIS or NIR	<1
Ligand Field	dd	Laporte forbidden	$d \rightarrow d$	VIS or NIR	<20 ~ 100
Ligand Field	dd	Laporte allowed	$d \rightarrow d$	VIS or NIR	ca. 250

Nickel(II) complexes contain the d^8 nickel cation, which prefers an octahedral or square planar coordination geometry. In these complexes, the ligand field transitions are usually well separated from the IL or CT transitions, thus simplifying the analysis of their spectra.

2.2.1 Crystal Field Theory

Crystal Field Theory was developed by Bethe and Van Vleck in 1930's and considers ligands to be simple, negative point charges, such that the bonding is assumed to be purely electrostatic². The interaction of these negative point charges with the d orbitals of the metal cation, splits the five d orbitals in a pattern determined by the geometry of the coordination. For instance for a 6-coordinate complex with octahedral geometry (as the hexa(aquo)nickel(II) ion), the five nickel(II) d orbitals are split into two sets: a triply degenerate set labelled t_{2g} (d_{xy} , d_{xz} , and d_{yz}), and a doubly degenerate set labelled e_g (d_z^2 and the $d_{x^2-y^2}$). The difference in energy between the t_{2g} and the e_g orbitals is known as the **crystal field splitting energy, (CFSE)**. The magnitude of CFSE depends upon both the metal ion (and its oxidation state) and the coordinating ligand and its value can be determined from the electronic spectra of coordination complexes. The variation in

² In **Ligand field theory** the metal electrons are allowed to be shared with electron pairs in the ligand molecular orbitals.

CFSE with the identity of the ligand has given rise to the spectrochemical series, in which the ligands are ranked from small CFSE to large CFSE. An abbreviated list is: $I^- < Br^- < Cl^- < OH^- < H_2O < NH_3 < en < CN^- < CO$.

A ligand such as I^- , which has a small CFSE is called a **weak field ligand**, whereas a ligand such as CN^- , has a large CFSE and is called a **strong field ligand**. The following table reveals the dependence of the CFSE upon both the metal cation and the ligand. The nickel(II) cation has relatively small CFSE values in comparison to other transition metal cations as Cr^{3+} and Fe^{3+} .

Table 2.1 Ligand Field Splitting Parameter, CFSE (cm^{-1}), of octahedral complexes

Metal Ion	Configuration	Cl^-	H_2O	NH_3	<i>en</i>
Cr^{3+}	d^3	13,700	17,400	21,500	21,900
Fe^{3+}	d^5	11,000	14,300	--	--
Ni^{2+}	d^8	7,500	8,500	10,800	11,500

A pictorial representation of the predicted energy levels and the respective electronic transitions as given by crystal field theory for the d^8 ion in an octahedral field is shown in figure 2.5. Such diagrams are known as *Orgel diagrams*, and allow for assignment of the various transitions observed for d^8 complexes.

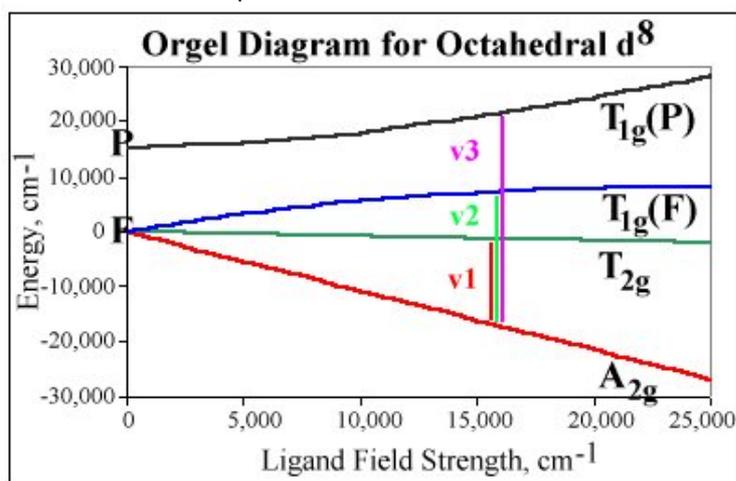


Figure 2.5

As shown in figure 2.5, the energy levels split into four distinct levels when the metal cation is placed in an octahedral field. Three of these levels arise from the F state of the uncomplexed cation, $^3A_{2g}$, $^3T_{2g}$, and $^3T_{1g}(F)$. The fourth level comes from the P state of the uncomplexed cation, $^3T_{1g}(P)$. The specific energy of each of these states, and thus the energies of the transitions between these states, is dependent upon the CFSE or *ligand field strength*. Three spin-allowed transitions from the ground state configuration, $^3A_{2g}$, are possible: v_1 , ($^3T_{2g} \leftarrow ^3A_{2g}$);

ν_2 , (${}^3T_{1g}(F) \leftarrow {}^3A_{2g}$); and ν_3 , (${}^3T_{1g}(P) \leftarrow {}^3A_{2g}$). The lowest ν_1 transition is typically in the near infrared region of electromagnetic radiation. This region is beyond the range of conventional UV/VIS spectrophotometers (~200 to 900 nm; 50000 to 11000 cm^{-1}) and below the range of conventional IR spectrophotometers (~4000 to 400 cm^{-1} ; 2500 to 25000 nm). On the other hand ν_3 is occasionally in the ultraviolet region. For the hexa(aquo)-nickel(II) complex these values are 8500 cm^{-1} (1176 nm), 13800 cm^{-1} (725 nm) and 25300 cm^{-1} (395 nm) respectively.

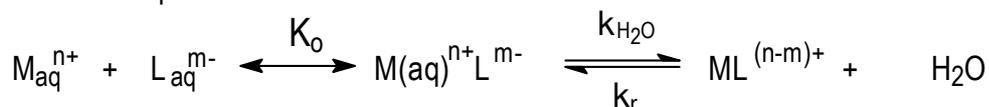
As the figure 2.5 indicates, as the ligand field strength of the ligand increases, all three transitions shift to higher energy (**blue shift**). Hence, the three d-d spin-allowed transitions, ${}^3T_{2g} \leftarrow {}^3A_{2g}$, ${}^3T_{1g}(F) \leftarrow {}^3A_{2g}$ and ${}^3T_{1g}(P) \leftarrow {}^3A_{2g}$ of the hexa(aquo)-nickel(II) complex are expected to shift to higher energy as the ligand field strength of the ligand increases, for instance due to complexation with amino group of Asp.

3. Kinetics of Metal Complexation

3.1 Factors affecting Metal Complexes Formation

3.1.1 Charge of the Metal ion

The formation of many inner-sphere metal complexes, ML from metal M and ligand L can be described in terms of a rapid pre-equilibrium, involving the formation of an outer sphere complex $M(H_2O)L$, followed by the rate-determining exchange of the ligand L for a molecule of water of the inner coordination sphere of the metal.



Scheme 3.1

The generally accepted mechanism (Eigen–Wilkins Mechanism, 1962) for the formation of a generalised metal-ligand complex ML, where $K_o = \frac{[M(aq)^{n+}L^{m-}]}{[M^{n+}][L^{m-}]}$, is the (apparent) association equilibrium constant of the first step, k_{H_2O} and k_r are the rate coefficients for the forward and backward reaction of the second equilibrium respectively.

The process is dominated by the rate coefficient k_{H_2O} , which depends on the strength of the metal-ion-water bond. The results of a large number of studies of the kinetics of formation of metal complexes, particularly those of nickel (II), with a wide variety of ligands led strong support to this mechanism (M. Eigen and R. G. Wilkins, 1966).

Later, finer details of the complex formation were investigated. This includes a study of the effects of charge and structure of the ligand, already coordinated as well as entering, on the rate and mechanism of the formation reaction. The difference in five and six-membered chelate formation and the nature of the donor atoms are among the structural factors which have been investigated.

3.1.2 Charge of the Ligand

In some cases the coordinated water of the metal ion is weakened by having several charged donor atoms in the ligand (e.g. CN^- , $EDTA^{4-}$ or OH^-), D. W. Margerum, 1976. Detailed study showed that a more decisive factor is the local charge density at the ligands present at the coordination sphere of the metal ion (binding strength relative to H_2O) and not the overall charge. The former determines the nucleophilicity of the ligand relative to the leaving water molecule.

G. G. Hammes and J. I. Steinfeld, 1962 reported that in contrast to the experiments with imidazole, the rate constants increase with additional substitution of glycine to the hexa(aquo)nickel(II) ion.

Predictions, however are sometimes difficult to establish. The COO^- group for instance has been reported to tend to loosen the hydration shell and increase $k_{\text{H}_2\text{O}}$, (G. G. Hammes and J. I. Steinfeld, 1962, K. Kustin et al, 1966 and A. Kowalak et al, 1967) and by others that this is not a general phenomenon, (D. W. Margerum and H. M. Rosen, 1967).

3.1.3 Charge of the Metal Complex

When one glycine is coordinated to the nickel ion, the rate of water substitution increases by a factor of 4 (G. G. Hammes and J. I. Steinfeld, 1962), table 3.1 (a).

Table 3.1 (n represents the number of ligands coordinated by the metal ion)

(a)

Glycine	$k_{\text{H}_2\text{O}}$ ($\text{M}^{-1}\text{s}^{-1}$)
n = 1	1.5×10^4
n = 2	6.0×10^4
n = 3	4.2×10^4

(b)

Imidazole	$k_{\text{H}_2\text{O}}$ ($\text{M}^{-1}\text{s}^{-1}$)
n = 1	5.0×10^3
n = 2	4.3×10^3
n = 3	2.4×10^3

Similar studies by the same authors with imidazole, resulted in no significant change in $k_{\text{H}_2\text{O}}$, table 3.1 (b). This is attributed to withdrawal of charge into the metal-ligand bond, which in turn loosens the binding between the metal ions and the remaining coordinated water molecules. Hence the water substitution becomes easier as the charge of the metal complex is reduced. This was later contradicted by studies carried where zinc in alkaline solutions reacted rapidly with porphyrins, when coordinated by 3 OH^- but slower with 4. Furthermore, later studies by M. Eigen concerning the substitution of NH_3 for H_2O with various nickel(II) complexes showed that the nitrogen coordination rather than the carboxylate coordination accelerates the water substitution of the metal complex. These and many other exceptions found later, suggest that it is not an easy task to predict trends in the rate of complexation reactions; each system may have its own particular mechanism.

This is seen for instance in the complexation reaction between Ni(II) and Co(II) with α - and β -aminobutyric acid. Whereas the rate constants for α -aminobutyric acid are consistent with the mechanism in which the release of water molecule from the metal ion's inner coordination sphere is rate determining, the slower reactions with β -aminobutyric acid are explained by the mechanism in which the chelate ring closure is the rate limiting step. The two mechanisms occur simultaneously, such that the reason why one becomes relatively slower and hence rate-determining depends on both the metal ion and ligand. This is clearly seen in the investigation by K. Kustin et al., 1966 concerning the complexation of Ni(II) and Co(II) to α - and β -alanine.

Analogous results to the α - and β -aminobutyric acid case, were reported for α - and β -alanine. However, for the complexation of β -alanine with Ni(II), the closure of the metal chelate ring was comparable to the water release step, while for Co(II) the metal chelate ring was slower than the water release step. With α -alanine, however Co(II) reacted significantly (20-25 times) faster than Ni(II), (G. G. Hammes and J. I. Steinfeld, 1962).

3.1.4 Charge Product of the Metal ion and Ligand

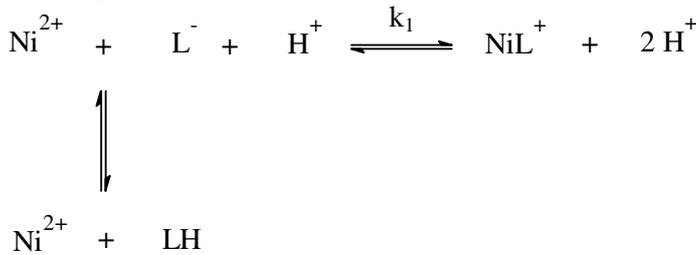
On the basis of mechanism shown in scheme 3.1,

$$\frac{1}{\tau} = k_{H_2O} \frac{K_o ([M^{n+}] + [L^{m-}])}{1 + K_o ([M^{n+}] + [L^{m-}])} + k_r$$

such that when $K_o ([M^{n+}] + [L^{m-}]) \ll 1$

$$\frac{1}{\tau} = k_{H_2O} K_o ([M^{n+}] + [L^{m-}]) + k_r.$$

Applying this to a simple ligand like glycine (represented as L^- in scheme 3.2), then $k_1 = K_o k_{H_2O}$.



Scheme 3.2

The term K_o is related to the charge number of the reactants, Z_M and Z_L , by equation (3.1)

$$K_o = \frac{4}{3} \pi N_A a^3 \exp\left(-\frac{Z_M Z_L e^2}{a \epsilon k T}\right) \quad (3.1)$$

where

K_o is the association constant of the two reactants in solution (in this case Ni^{2+} and L^-),

e is the elementary charge,

a is the distance of closest approach of the ions,

ϵ is the absolute solvent permittivity, and

k is Boltzmann's constant

T is the temperature

N_A is the Avogadro's constant.

Thus, the rate constant depends on the charge product of the metal ion and ligand $Z_M Z_L$ as follows:

$$\log(k_1 \cdot Ms) = \log\left(\frac{4}{3} \pi N_A a^3 k_{H_2O} \cdot Ms\right) - \frac{Z_M Z_L e^2}{2.3 a \epsilon k T} \quad (3.2)$$

Additionally, from a plot of $\log k_n$ against $-Z_M Z_L$ a linear plot is obtained (using “simpler” ligands with the charge present being reasonably localized), and from the slope, a value for a can be calculated. J. C. Cassatt and R. G. Wilkins, 1968 obtained 8.5\AA for the constant a for small peptides like tetraglycine.

This plot can also be used to supply information regarding the orientation of the NH_3^+ group relative to the COO^- in amino acids. By comparing the reactivity of a known neutral species (a model for an amino carboxylate ligand whose NH_3^+ and COO^- groups are very close to each other) with amino acids like glycine whose NH_3^+ and COO^- groups cannot be intramolecularly bonded.

3.1.5 Ligand Structure

3.1.5.1 Kinetic chelate effect

This effect describes the decrease in the rate of a complexation reaction by comparing the difficulty in forming a 6-membered ring as opposed to a 5-membered ring with an aminocarboxylic acid ligand. It explains for instance the decrease in the reaction rate observed for β -alanine as opposed to α -alanine. K. Kustin et al, 1966 attribute this to the fact that the structures of α -alanine and β -alanine are such that once attachment at the first site occurs, more energy is required to produce attachment at the second site for a 6-membered ring as opposed to a 5-membered ring. This results in a larger contribution to the energy of activation than the entropic “chelate effect” would indicate, as seen below.

The reasons for the higher energy barrier for a 6-membered ring closure are believed to be a) ring strain and b) additional entropy loss.

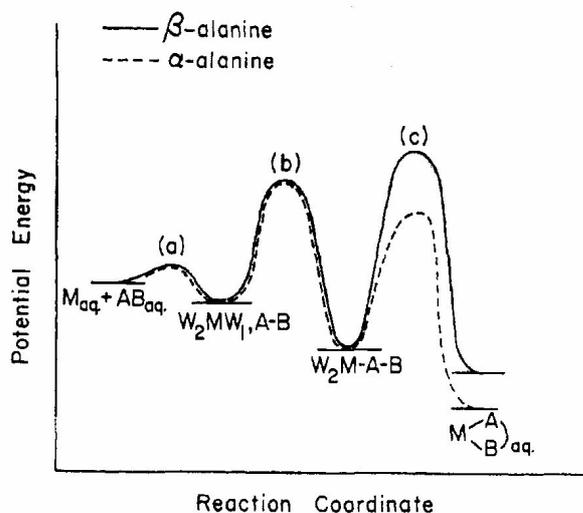


Figure 3.1 Superimposed potential energy diagrams for the metal-complex formation with α -alanine and β -alanine.

3.1.5.2 Number and type of chelating groups

Multidentate ligands have different binding modes and rates depending on the charge (and hence degree of protonation), number of and type of the individual ligand functional group. Of particular interest to us are ligands containing the amino and the carboxylate groups. However, complexity in behaviour is found, depending on the combination of these functional groups.

a) Amino-carboxylate ligands

A drastic reduction of the complexation rate was observed with monoprotection of the amino-carboxylate ligands. Mono-protonation of amino-carboxylate groups, for instance in iminodiacetic acid, IDA^{2-} ($\text{NH}(\text{CH}_2\text{COO}^-)_2$) and nitrilotriacetic acid, NTA^{3-} have shown an almost 10^5 decrease in reactivity, Table 3.1 .

Table 3.2

Amino-carboxylate ligand	k in $\text{M}^{-1} \text{s}^{-1}$	References
IDA^{2-}	4.5×10^4	T. J. Byadelek and A. H. Constant, 1965
IDAH^-	7.7×10^{-2}	
NTA^{3-}	4.8×10^5	T. J. Byadelek and M. L. Blomster, 1964
NTAH^{2-}	7.5	

(The above ligands were reacted with nickel(II) at 25°C , $I = 1.25$)

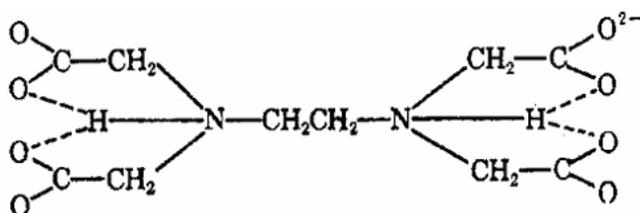
Furthermore, the presence of NH_3^+ group in for instance $^-\text{OOCCH}(\text{NH}_3^+)\text{COO}^-$ reduced the reactivity drastically, even with the favourable disposition of the carboxylate groups since the NH_3^+ group prevents chelation with Ni^{2+} ions. Since coordination cannot occur through primary attachment to the RNH_3^+ group, the first step of coordination must occur through the $-\text{COO}^-$ grouping of the amino acid. This is a labile arrangement with the breaking rate constant likely to be very much greater than the combined process of H^+ ionization from the $-\text{NH}_3^+$ residue and ring closure. The over-all rate constant would then be very much less than that for coordination of $\text{NH}_2\text{CH}_2\text{COO}^-$ where these unfavourable situations do not arise.

Another contributory factor to the unreactivity of the zwitterion may be the necessity to break down the strong intramolecular interactions (which may be electrostatic or hydrogen bonding in nature) which are believed to occur in the zwitterion form of the α -amino acids and α -aminooligocarboxylic acids. Infrared evidence has been used to indicate that, even with the oligocarboxylates such as NTAH^{2-} , all the available carboxylate groups interact in an equivalent manner with the single protonation site, (D. Chapman et al., 1963). Thus with these ligands also, intramolecular ring formation of the protonated form must be broken before coordination can

occur. The small but definite rate constants for reaction of NTAH^{2-} and IDAH^- may in fact result from the presence of the small amount of the neutral form ($\sim 10^{-3}$ %) in which the proton is associated with the carboxylate group and which therefore may be considered to be reactive.

Irrespective of the modus operandi of the effect, the fact that $\text{H}_2\text{EDTA}^{2-}$

(and $\text{C}_6\text{H}_{10}\text{N}_2(\text{CH}_2\text{COO}^-)_4(\text{H}^+)$), reacts with nickel(II) with a relatively high rate constant is interesting, since this di-protonated form approximates two joined halves of the unreactive IDAH^- and has the below suggested structure with protonation at the N atoms.



This result could be explained by the inclusion in equilibrium with the above structure of a small amount, of a form in which one or, less likely, two carboxylate groups have the proton associated with them, and which thus contains a free nitrogen able to coordinate in the first step.

b) Di-amine and di-carboxylate ligands

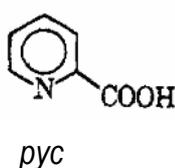
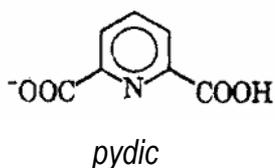
Non- and mono-protonated forms of diamines and dicarboxylates results differ by about 100-fold in reactivity towards nickel(II). This, is evidenced for instance by enH^+ whose rate constant for reaction with Ni^{2+} is about 10^2 less than that calculated for en ($4 \times 10^4 \text{ M}^{-1} \text{ s}^{-1}$), C. Cassatt and R. G. Wilkins, 1968. Similarly, HOCCOO^- and $\text{HOCCCH}_2\text{COO}^-$ have an even closer reactivity, compared with the corresponding dianionic forms, towards nickel(II), G. H. Nancollas and N. Sutin, 1966. Hence, monoprotonated dicarboxylates react easily, inspite of intramolecular hydrogen bonded structures due to the capability of that COOH grouping to coordinate even as a first step, unlike NH_3^+ .

c) Oligo-amine ligands

When complexing by the oligoamines is considered, however, the $\text{Ni}-\text{NH}_2$ bond formed is relatively stable to bond dissociation, and the completion of the ring with proton elimination occurs readily. Reinforcing evidence for this idea is the fact that $^+\text{N}(\text{CH}_3)_3\text{CH}_2\text{CH}_2\text{NH}_2$ reacts with nickel with a rate constant (4×10^2) similar to that of enH^+ ($6 \times 10^2 \text{ M}^{-1} \text{ sec}^{-1}$ at 25°C).

d) Pyridinecarboxylates.

The unreactivity of the zwitterion form is also seen in the saturated pyridine system, piperidine-2,6-dicarboxylate (pidic) (J. C. Cassatt and R. G. Wilkins, 1968). However, with the heterocyclic derivative, pyridine-2,6-dicarboxylate (pydic), an appreciable value for the reaction rate constant for the protonated form, is obtained ($5 \times 10^3 \text{ M}^{-1}\text{s}^{-1}$), while with the monocarboxylate pyridine-2-carboxylate (pyc) examination of the data at low pH indicates a small but definite residual rate constant ($30 \text{ M}^{-1} \text{ s}^{-1}$).

**e) Other ligands**

Similar differences to those observed for diamines and dicarboxylates were reported for the reaction of amp (2-aminomethylpyridine) and ampH⁺ (8.6×10^3 and $35 \text{ M}^{-1} \text{ sec}^{-1}$ respectively, J. C. Cassatt and R. G. Wilkins, 1968) and bipy and bipyH with nickel.

4. Experimental Section

4.1 Reagents

The following reagents were used:

- aspartic acid (Acros Organics, 98+%) in its acidic neutral form,
- poly-L-aspartic acid (sodium salt; molecular weight range 15000 – 50000 g/mol; degree of polymerisation: 244 (viscosity), 299 (light scattering), Sigma),
- nickel(II) nitrate hexahydrate (J. T. Baker Chemicals, 'Baker grade'),
- sodium chloride (Riedel de Haën, analytical reagent) - used for the adjustment of the ion strength
- standard HCl and NaOH solutions (Merck)
- pH indicators: methyl orange (Merck), bromophenol blue (Riedel de Haën), bromocresol green (Merck), chlorophenol red (Riedel de Haën) and bromothymol blue (Merck)
- Buffers: sodium formate (Merck, per analysi), anhydrous sodium acetate (Fluka, >99%), 2,6-lutidine (Fluka, purum)

All other reagents were with supplied by the company Merck and had a degree of purity *per analysi*.

Aspartic acid and buffer solutions were freshly prepared daily using triply distilled, carbon dioxide-free water, while the indicator solutions were prepared once weekly. This was done by stirring under vacuum until no more gas bubbles were observed. For large volumes, solutions were stirred under vacuum for about two hours while for smaller volumes a vacuum was created using a hand pump. All chemicals were used as supplied without further purification.

4.2 Instrumental and Experimental Methods

4.2.1 Potentiometric Titrations

Proton activity was measured using a glass electrode *Toledo InLab 412* (Mettler-Toledo GmbH, Giessen) which was calibrated, using a two-point calibration system as described by R. G. Bates (1962) illustrated below:

Calibration point I: 0.1M NaCl, 0.01M HCl; $p\text{cH} = 2.00$

Calibration point II: 0.1M NaCl, 0.001M HCl; 0.002M tris(hydroxymethyl)aminomethane;
 $p\text{cH} = 8.11$

Conditional constants and *pCH* are defined in section 5.1.

In order to estimate the error in the ligand titrations, a reference system was used consisting of a mixed-buffer solution (Perrin and Dempsey, 1974) whose conditional constants are well known, (see A. E. Martell and R. M. Smith, 1974 – 1989). This buffer mixture consisted of 0.002M of each of the following simple buffer substances: sodium formate, sodium acetate, maleic acid, imidazole, tris and lysine dissolved in triply distilled water and degassed by upward suction. The NaCl concentration was 0,096M so that the total $[Na^+]$ was exactly 0.1M for $I=0.1M$. 1ml of 1M HCl was added to 50ml of the buffer mixture prior to titration. The titrating NaOH solution was prepared using 0.1M Titrisol[®] (Merck GmbH) and degassed triply distilled water under argon atmosphere.

Furthermore, the mixed-buffer solution and aspartic acid solutions were degassed manually prior to each titration. All titrations were automated at $25.0 \pm 0.1^\circ C$ using a Titration Unit Titroline *alpha* (Schott Geräte GmbH, Hofheim) equipped with magnetic stirrer type TM 125 and keyboard mini PC type TZ 2825.

Aspartic acid was titrated separately with 0.1M NaOH and with 0.1M HCl due to its low first protonation constant K_{a1} . Four titrations were carried out:

- i) with ligand alone in order to determine its protonation constants, K_{a1} , K_{a2} and K_{a3}
- ii) with ligand and nickel ion, in the proportions ligand to metal, 1:1, 2:1 and 5:1, in order to determine the complexation constants of Asp to nickel(II) ions.

For each measurement, the pcH value was calculated using the known conditional constants of the buffer mixture components. This was then compared to the experimentally obtained calibration curve in order to calculate the error Δ_i involved.

$$\Delta_i = \text{pcH}(\text{Buffer}_{\text{exp},i}) - \text{pcH}(\text{Buffer}_{\text{theor},i}).$$

The errors Δ_i were interpolated and the interpolated error is termed " Λ_i ". Finally the pcH values of the aspartic acid titrations were corrected according to the equation:
$$\text{pcH}_{\text{corr},i} = \text{pcH}_{\text{exp},i} - \Lambda_i$$

An error estimate due to the electrode instability was also performed by comparing the two titration curves for the same buffer mixture, before the aspartic acid titration and after. The total error in the proton concentration, considering electrode instability and the accuracy of the buffers' conditional constants was estimated to be lower than 5%.

4.2.2 Other Potentiometric measurements

For the pH measurements of all the other solutions used, mostly involving single pH measurement, another two-point calibration system using standard buffers, R.G. Bates, 1962:

Calibration point I: 0.05M potassium hydrogen phthalate; pH=4.008

Calibration point II: 0.025M KH_2PO_4 , 0.025M $\text{Na}_2\text{HPO}_4 \cdot 2\text{H}_2\text{O}$; pH=6.865

The pH values were measured using combined glass electrodes connected to a Metrohm 605 pH-Meter at 25°C unless otherwise stated. The error was here estimated to be in the order of ± 0.02 pH units. The respective pCh values were calculated using the equation

$$\text{pCh} = \text{pH} + \log (f_1)$$

where f_1 is the activity coefficient for monocharged species ($f_1 = 0.785$ at $T = 25^\circ\text{C}$, $I = 0.1\text{M}$, Davies, 1962);

4.2.3 UV-Vis-Spectrophotometry

UV-Vis spectra were recorded using a double beam *Shimadzu* Spectrophotometer UV-2401PC.

For all experiments, the reference cuvette was filled with triply distilled water.

4.2.3.1 pH-titrations

a. “Continuous flow” Experiments

Solutions containing $5 \cdot 10^{-3}\text{M}$ Asp_0 , $2 \cdot 10^{-3}\text{M}$ Ni_0 and 0.1M NaCl were manually titrated with $5 \cdot 10^{-3}\text{M}$ Asp_0 , $2 \cdot 10^{-3}\text{M}$ Ni_0 , 0.1M NaCl and $5 \cdot 10^{-3}\text{M}$ NaOH at 25°C in a 250 mL conical flask connected to the 50 mm Suprasil continuous-flow cuvettes (Hellma). Simultaneously, the pH of the mixed solution in the conical flask was recorded potentiometrically.

b. “Automated titration” Experiments

i) Solutions containing $5 \cdot 10^{-3}\text{M}$ Asp_0 , 0.02M HCl, 0.1M NaCl and varying concentrations of nickel (II) nitrate ($1 \cdot 10^{-3}\text{M}$ or $2 \cdot 10^{-3}\text{M}$ Ni_0) were titrated with 0.1M NaOH at 25°C. The optical absorbance of the mixed solution in the conical flask was recorded simultaneously. 15 ml samples were taken at an interval of ca. 0.1pCh units and their spectrum recorded in the range 300 nm – 850 nm using a plastic pipette. Errors due to the manual transfer of the solutions from the titrating chamber to the 50 mm cuvettes were estimated to be less than 5% by comparing the experiment with a previous autotitration without any interruption.

ii) A solution containing 0.0435 g sodium L-polyaspartate³ (equivalent to 0.32 mM COO⁻ groups) in 15.6 ml of 0.25 M NaCl was set at pH 12 by adding 0.5 ml of 0.25 M NaOH in a 30 ml vial and titrated with 0.25 M HCl.

0.9 ml of 0.083 M Ni(NO₃)₂ were then added (equivalent to 0.15 mM COO⁻ groups), and the resulting solution titrated with 0.25 M NaOH (at a rate of 0.06 ml/minute) under argon atmosphere. The solutions were degassed manually prior to each titration. The 30 ml vial was connected to the 50 mm Suprasil continuous-flow cuvettes (Hellma) by means of a PVC tubing such that simultaneous spectra were recorded at intervals of ca. 0.1 pcH units in the range 300 nm – 850 nm.

4.2.3.2 Nickel(II) nitrate - titrations - Separate solution Experiments

Two types of Nickel(II) nitrate – titrations were carried out:

(a) at excess nickel(II) nitrate – to get information about the 1:1 complexes

Solutions containing 0.2·10⁻³ M Asp_o, varying Ni_o (0 M, 1·10⁻³ M to 1·10⁻² M in steps of 1·10⁻³ M), 5·10⁻³ M buffer and 0.1M NaCl were prepared in 25ml volumetric flasks. The pcH of the solution was then adjusted to 5.22 (using sodium acetate buffer) and 6.80 (using 2,6-lutidine buffer) by the addition of 1M NaOH/1M HCl. The solutions were then filtered using filters of pore size 0.45 μm supplied by the company *Sartorius* (in order to reduce noise in the spectra due to small dust particles) and investigated spectroscopically in 50 mm Suprasil cuvettes (Hellma).

(b) at excess aspartic acid – to get information about the 1:2 complexes

Solutions containing 1·10⁻² M Asp_o, varying Ni_o (0 M, 0.02·10⁻³ M to 0.2·10⁻³ M in steps of 0.02·10⁻³ M), 5·10⁻³ M buffer and 0.1M NaCl were prepared in 25mL volumetric flasks. The pcH of the solution was then adjusted to 5.22 (using sodium acetate buffer) and 6.80 (using 2,6-lutidine buffer) by the addition of 1M NaOH/1M HCl. The solutions were then filtered investigated spectroscopically as described in 4.2.3.2(a).

4.2.3.3 Asp-titrations - Separate solution Experiments

As in 4.2.3.2, two types of Asp – titrations were carried out:

(a) at excess nickel(II) nitrate – to get information about the 1:1 complexes

Solutions containing 2·10⁻³ M Ni_o, varying Asp_o (0 M, 0.04·10⁻³ M, 0.044·10⁻³ M, 0.05·10⁻³ M, 0.057·10⁻³ M, 0.067·10⁻³ M, 0.08·10⁻³ M, 0.1·10⁻³ M, 0.133·10⁻³ M, 0.2·10⁻³ M and 0.4·10⁻³ M),

³ the protonated form is summarised as PAsp

$5 \cdot 10^{-3}$ M buffer and 0.1M NaCl were prepared in 25ml volumetric flasks. The pH of the solution was then adjusted to 3.45, 4.00, 5.22 (using sodium acetate buffer) and 6.80 (using 2,6-lutidine buffer) by the addition of 1M NaOH/1M HCl. The solutions were then filtered and investigated spectroscopically as described in 4.2.3.2(a).

(b) at excess aspartic acid – to get information about the 1:2 complexes

Solutions containing $2 \cdot 10^{-3}$ M Ni₀, varying Asp₀ (0 M, $0.33 \cdot 10^{-3}$ M, $0.66 \cdot 10^{-3}$ M, $1 \cdot 10^{-3}$ M, $1.33 \cdot 10^{-3}$ M, $2 \cdot 10^{-3}$ M, $2.4 \cdot 10^{-3}$ M, $2.8 \cdot 10^{-3}$ M, $3.2 \cdot 10^{-3}$ M, $3.6 \cdot 10^{-3}$ M, $4 \cdot 10^{-3}$ M, $5 \cdot 10^{-3}$ M, $6 \cdot 10^{-3}$ M, $7 \cdot 10^{-3}$ M, $8 \cdot 10^{-3}$ M, $9 \cdot 10^{-3}$ M, $10 \cdot 10^{-3}$ M, $11 \cdot 10^{-3}$ M, $12 \cdot 10^{-3}$ M, $14 \cdot 10^{-3}$ M and $16 \cdot 10^{-3}$ M), $5 \cdot 10^{-3}$ M buffer and 0.1M NaCl were prepared in 25ml volumetric flasks. The pH of the solution was then adjusted to 3.45, 4.00, 5.22 (using sodium acetate buffer) and 6.80 (using 2,6-lutidine buffer) by the addition of 1M NaOH/1M HCl. The solutions were then filtered and investigated spectroscopically as described in 4.2.3.2(a).

4.2.4 IR and Raman Spectroscopy

Solutions containing 0.125 M Asp and 0.05 M Ni(NO₃)₂ were set to pH 3.50 (sample P), pH 6.00 (sample Q) and pH 10.50 (sample R). 20 ml of each sample was freeze-dried using liquid nitrogen and left overnight under vacuum. The resulting powders were then used for IR and Raman spectroscopy. Nickel(II) nitrate (sample Ni) and aspartic acid (sample Asp) samples were also performed for comparative purposes.

IR spectra were recorded on a Shimadzu spectrometer type FTIR-8300 in the range 4000 - 400 cm⁻¹ using KBr pellet technique under inert gas atmosphere. The Raman spectra were recorded on a Bruker spectrometer type IFS/66 FRA 106 (Nd-YAG-Laser $\lambda_0=1064$ nm) in the range 4000 - 400 cm⁻¹ using KBr pellet technique.

4.2.5 Stopped-flow experiments

The Stopped-flow experiments were performed on a combined diode-array Hewlett-Packard spectrophotometer model HP 8453 and stopped flow. For the experiments in the time range shorter than 5 seconds, another stopped-flow apparatus was used, set-up at our University Workshop. In both apparatus, the progress of reaction was monitored by the change in absorbance of a proton indicator coupled to our system and digitally stored in a personal computer. At least five experiments were carried out, and the data were accumulated in order to enhance the signal to noise ratio. The average curve was then calculated. A typical curve is shown in figure 4.1. The average curve was then fitted to a single or double exponential function to the relative change in absorbance by means of Marquardt's algorithm.

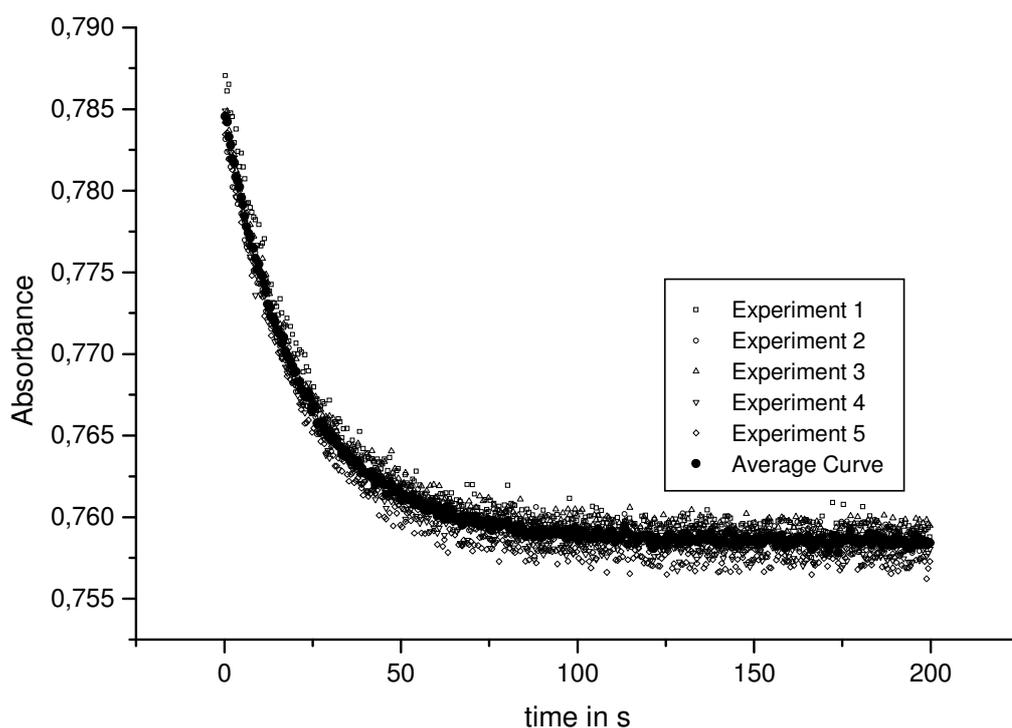


Figure 4.1

Absorption vs time curves for 5 repeated experiments and the calculated average curve for the reaction of Ni(II) ions with Asp for the case where Asp was present in excess;

$Ni_o = 2.5 \times 10^{-4}$ M, $Asp_o = 10^{-2}$ M, $I = 0.1$ M (NaCl), $buffer_o = 5 \cdot 10^{-3}$ M, $indicator_o = 2 \cdot 10^{-5}$ M, $pH = 5.60$.

4.2.6 Processing of the data

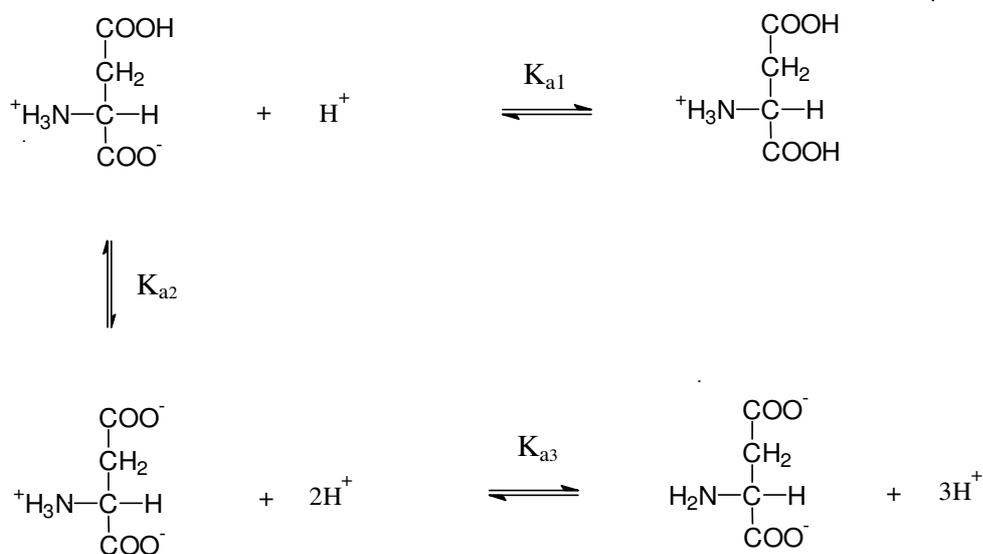
The diagrams and data analysis was performed with commercial standard programs of the company Microcal™ (Origin 5.0, Microcal software Inc., 1997, ChemWindow3, Softshell International, CS Chem 3D Ultra, Cambridge Soft.com, 2000), Microsoft® and Borland®. Experimental titrations and absorption data, as well as the kinetic data were recorded and analyzed by programs developed in the working group (see section 10.2).

The computation of the theoretical titration curve of the reference system (buffer mixture for the calibration of the pH values for the automated titrations) was performed with a program Titra (Altheide, 1999), which generates the titration process after input of all pK values, concentrations and volumes.

5. RESULTS AND EVALUATION - Thermodynamics

5.1 Protonation Equilibria of Aspartic acid

As is typical of amino acids, aspartic acid forms a zwitterion at neutral pH. In its fully protonated state, it is positively charged. It is therefore conveniently abbreviated as LH_3^+ , i.e. **L²⁺ is the abbreviation for $H_2N-CH(COO^-)-CH_2-COO^-$** . Two other partially protonated species exist, such that aspartic acid can exist in 4 different forms, as seen in scheme 5.1.



Scheme 5.1: Protonation Equilibrium of aspartic acid

In this study, the ionic strength is held constant at 0.1M (using NaCl) and it is assumed that the activity coefficients are constant. Thus, the equilibrium constants K_{a1} , K_{a2} and K_{a3} may be defined as products of concentration instead of activities, equations (5.1) to (5.3).

$$K_{a1} = \frac{[LH_2][H^+]}{[LH_3^+]} \quad (5.1)$$

$$K_{a2} = \frac{[LH^-][H^+]}{[LH_2]} \quad (5.2)$$

$$K_{a3} = \frac{[L^{2-}][H^+]}{[LH^-]} \quad (5.3)$$

This means that they are not the thermodynamic constants but the so-called *conditional constants* which depend on the ionic strength of the solution. Analogously the p_cH value is defined as $-\log([H^+]\cdot M^{-1})$.

The protonation constants were determined potentiometrically. Aspartic acid was titrated with 0.1M HCl and with 0.1M NaOH. The combined results are shown below, figure 5.1. pCH was measured as discussed in chapter 4.2.1.

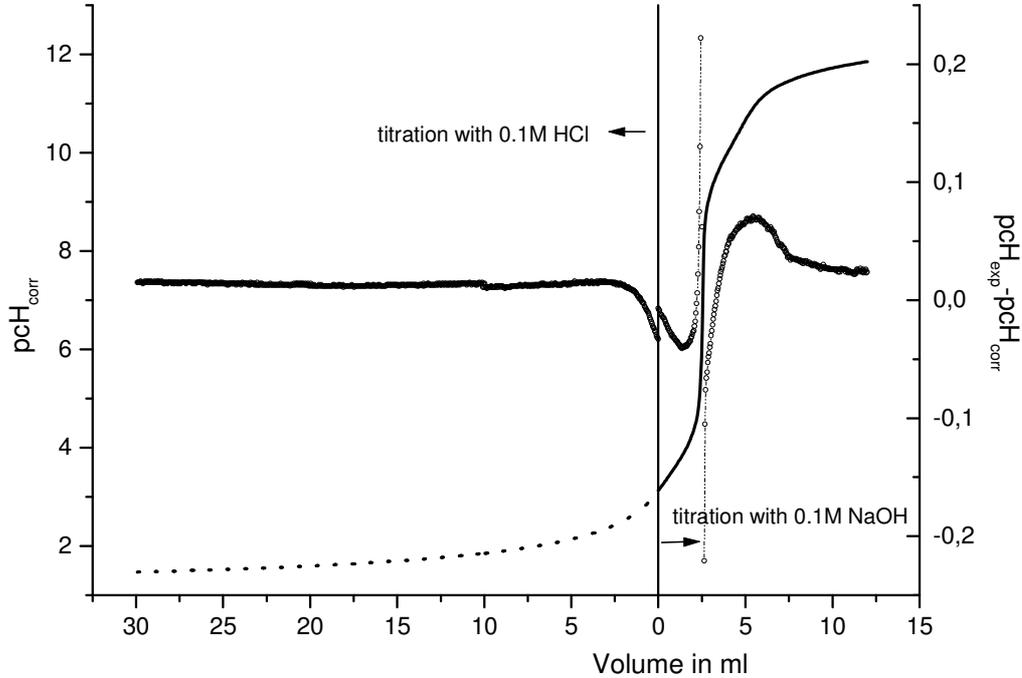


Figure 5.1

Titration of 50 ml of $5 \cdot 10^{-3}$ M Asp with 0.1M HCl (dotted line) and 0.1M NaOH (solid line); $I = 0.1$ M (NaCl); $T = 25^\circ\text{C}$. The circles (right-handed scale) show the deviation of the experimental data from the titration curve calculated.

From the titration curve the dissociation constants of Asp are obtained as the best fit of equation 5.4 to the experimental data. Equation 5.4 is obtained by combining equations (5.1) to (5.3) and (5.5) to (5.9).

$$\frac{[\text{H}^+] + B_o - \frac{K_w}{[\text{H}^+]} - A_o}{L_o} = \frac{\frac{[\text{H}^+]}{K_{a1}} - \frac{[\text{H}^+]^3}{K_{a1}K_{a2}K_{a3}} + 2}{1 + \frac{[\text{H}^+]}{K_{a1}} + \frac{[\text{H}^+]^2}{K_{a1}K_{a2}} + \frac{[\text{H}^+]^3}{K_{a1}K_{a2}K_{a3}}} \quad (5.4)$$

$$L_o = [\text{LH}_3^+] + [\text{LH}_2] + [\text{LH}^-] + [\text{L}^{2-}] \quad (5.5)$$

$$[\text{H}^+] + [\text{Na}^+] + [\text{LH}_3^+] = [\text{LH}^-] + 2[\text{L}^{2-}] + [\text{Cl}^-] + [\text{OH}^-] \quad (5.6)$$

$$[\text{Na}^+] = B_o + Y_o \quad (5.7)$$

$$[\text{Cl}^-] = A_o + Y_o \quad (5.8)$$

$$[\text{OH}^-] = K_w/[\text{H}^+] \quad (5.9)$$

$$A_o = [\text{HCl}]_o \quad (5.10)$$

$$B_o = [\text{NaOH}]_o \quad (5.11)$$

$$Y_o = [\text{NaCl}]_o \quad (5.12)$$

The ionic product of water is $K_w = 10^{-13.78} \text{ M}^2$ at $I = 0.1\text{M}$ and $T = 25^\circ\text{C}$.

Fitting function 5.4 yields the following values for the protonation constants $\text{p}K_{a1}$, $\text{p}K_{a2}$ and $\text{p}K_{a3}$ shown in table 5.1. Literature values of the constants are shown for comparison. The error ranges are the statistical errors added to 0.02 as electrode error.

Table 5.1

Fitted values for the protonation constants of Asp

	Results	Literature
$K_{a1} = \frac{[\text{LH}_2][\text{H}^+]}{[\text{LH}_3^+]}$	$-\log(K_{a1} \cdot \text{M}^{-1}) = 1.90 \pm 0.05$	1.93 + 0.01* 1.99 \diamond 1.87**
$K_{a2} = \frac{[\text{LH}^-][\text{H}^+]}{[\text{LH}_2]}$	$-\log(K_{a2} \cdot \text{M}^{-1}) = 3.74 \pm 0.03$	3.70 + 0.01* 3.69 \diamond 4.00** 3.60 \blacktriangle
$K_{a3} = \frac{[\text{L}^{2-}][\text{H}^+]}{[\text{LH}^-]}$	$-\log(K_{a3} \cdot \text{M}^{-1}) = 9.89 \pm 0.03$	9.63 + 0.01* 9.47 \diamond 9.75** 9.60 \blacktriangle

* A. E. Martell and R. M. Smith, Critical Stability Constants, Plenum Press, New York, (1974 -1989)

** R. N. Patel et. al., Indian J. Chem. Section A, 38 (8), 850-853, (1999)

\blacktriangle M. R. Patel et al., J. Indian Chem. Soc., 70 (6), 569 – 572, (1993)

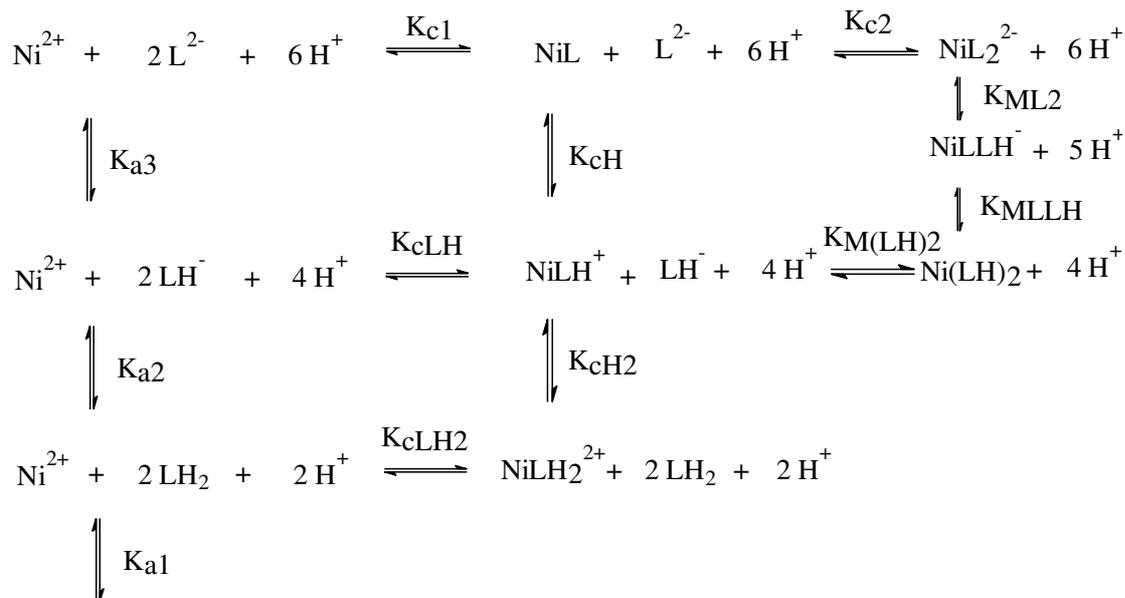
\diamond A. Pohlmeier and W. Knoche, International Journal of Chemical Kinetics, Vol. 28. , 125-136 (1996).

5.2 Complexation of Nickel (II) ions with Asp

In aqueous solution, nickel ions exist as hexa(aquo)-complexes. With Asp a 1:1 complex and a 1:2 complex are formed by substituting 1, 2 or 3 and 4, 5 or 6 respectively of these 6 coordinated water molecules. For simplification, the coordinated water molecules are omitted. The complexation is studied

- potentiometrically, by pH-titration of solutions of Asp and nickel nitrate with HCl and NaOH (see section 5.2.1);
- spectrophotometrically, by measuring the UV-Vis spectra of absorbance of solutions of Asp and nickel nitrate at different pH-values (see section 5.2.2).

Initially, all experimental results were fitted assuming reaction scheme 5.2. The structures of a bidentate, a tridentate and a hexadentate nickel(II) aspartate complexes are shown in figure 5.2.



Scheme 5.2 Complexation of nickel (II) ions with Asp

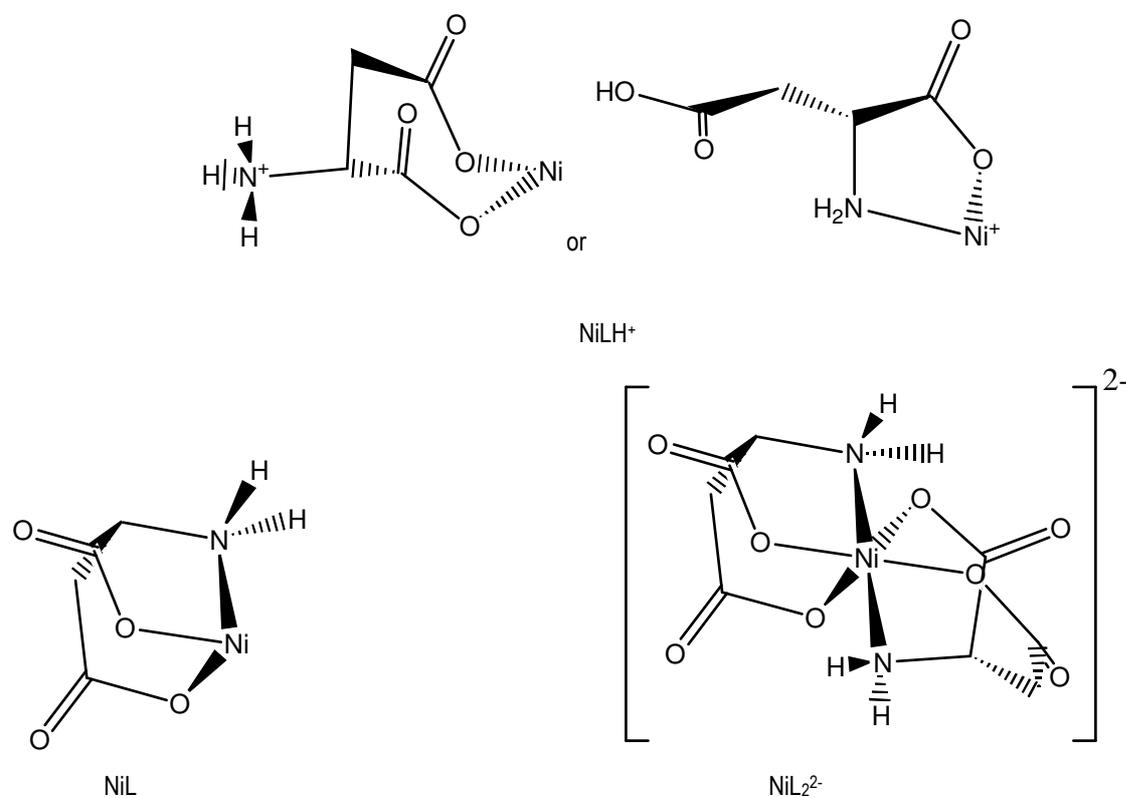


Figure 5.2
Structure of some of the nickel(II)aspartate complexes

5.2.1 Potentiometrical results

5.2.1.1 Potentiometrical analysis of the Complexation of Nickel (II) ions with Asp - Titration of nickel(II) ions and Asp with NaOH

Titration solutions containing $5 \cdot 10^{-3}$ M Asp, 0.02 M HCl and 0.1 M NaCl in the presence of varying concentrations of nickel nitrate ($1 \cdot 10^{-3}$ M or $2 \cdot 10^{-3}$ M) with 0.1 M NaOH at 25°C gives the results shown in figure 5.3. For $\text{pCh} < 3.0$ and $\text{pCh} > 11.0$ the curves are identical and hence not included in the figure.

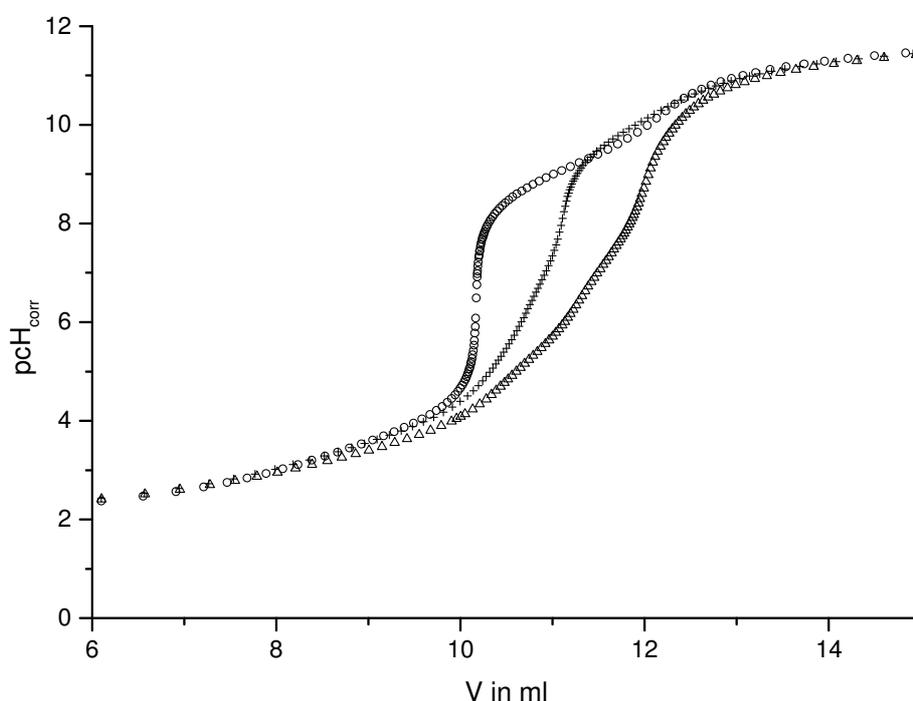


Figure 5.3

pH-titration curves of 40 ml of $5 \cdot 10^{-3}$ M Asp, 0.02 M HCl, 0.1 M NaCl and varying $\text{Ni}(\text{NO}_3)_2$ concentration with 0.1M NaOH at 25°C. The concentration of $\text{Ni}(\text{NO}_3)_2$ is 0, $1 \cdot 10^{-3}$ M and $2 \cdot 10^{-3}$ M (in the order of decreasing pCh at constant volume).

The experimental results are fitted according to scheme 5.2, using the quantity balances for nickel, aspartic acid and the electroneutrality balance, (equations 5.13 – 5.15) the protonation constants for Asp, (equations 5.1 – 5.3), the complexation constants of nickel(II) ions with Asp (equations 5.16 – 5.21) and two hydroxide complexes of nickel, (equations 5.22 – 5.23). The values for the complexation constants K_{c1} , K_{c2} , K_{cH} , K_{cLH2} , K_{MLLH} , K_{ML2} from the best fit are shown in Table 5.4.

$$L_o = [LH_3^+] + [LH_2] + [LH] + [L^{2-}] + [NiLH_2^{2+}] + [NiLH^+] + [NiL] + 2 \cdot [Ni(LH)_2] + 2 \cdot [NiLLH] + 2 \cdot [NiL_2^{2-}] \quad (5.13)$$

$$Ni_o = [Ni^{2+}] + [NiLH_2^{2+}] + [NiLH^+] + [NiL] + [Ni(LH)_2] + [NiLLH] + [NiL_2^{2-}] + [NiOH^+] + [Ni(OH)_2] \quad (5.14)$$

$$[H^+] + [Na^+] + [LH_3^+] + 2 \cdot [NiLH_2^{2+}] + [NiLH^+] + [NiOH^+] = [LH^-] + 2 \cdot [L^{2-}] + [Cl^-] \dots \\ \dots + [OH^-] + 2 \cdot [NiL_2^{2-}] \quad (5.15)$$

$$K_{c1} = \frac{[NiL]}{[Ni^{2+}][L^{2-}]} \quad (5.16)$$

$$K_{cH} = \frac{[NiLH^+]}{[NiL][H^+]} \quad (5.17)$$

$$K_{cLH_2} = \frac{[NiLH_2^{2+}]}{[NiLH^+][H^+]} \quad (5.18)$$

$$K_{c2} = \frac{[NiL_2^{2-}]}{[NiL][L^{2-}]} \quad (5.19)$$

$$K_{ML2} = \frac{[NiLLH^-]}{[NiL_2^{2-}][H^+]} \quad (5.20)$$

$$K_{MLLH} = \frac{[Ni(LH)_2]}{[NiLLH^-][H^+]} \quad (5.21)$$

$$K_M = \frac{[Ni^{2+}]}{[NiOH^+][H^+]} = 10^{9.996} M^{-1} * \quad (5.22)$$

$$K_{MOH} = \frac{[NiOH^+]}{[Ni(OH)_2][H^+]} = 10^{9.22} M^{-1} * \quad (5.23)$$

* C. F. Baes and R. E. Mesmer, The Hydrolysis of Cations, Wiley Interscience, (1976).

(For a more detailed description of the fitting procedure used, see section 10.2.1)

5.2.2 Spectrophotometrical results

5.2.2.1 Analysing the spectral changes due to the formation of the various nickel(II)aspartate complexes

The three d-d spin-allowed transitions, ${}^3T_{2g} \leftarrow {}^3A_{2g}$, ${}^3T_{1g}(F) \leftarrow {}^3A_{2g}$ and ${}^3T_{1g}(P) \leftarrow {}^3A_{2g}$ of the hexa(aquo)-nickel(II) complex exhibit a blue shift and a simultaneous increase in the absorption intensity upon complexation. The blue shift is attributed to the shift to higher energy as the ligand field strength of the ligand increases, due to complexation with amino group of Asp, (see Section 2.3.1.) while the observed increase in the absorption intensity is due to the fact that complexes

formed have no longer a centre of symmetry, making the d-d transitions 'less forbidden', F. A. Cotton and G. Wilkinson, 1995.

Hence, due to significantly different spectra produced, figure 5.4, the study of the formation of the different Asp complexes with nickel (II) ions can be followed spectroscopically in the range 350 nm to 850 nm.

Due to the low extinction coefficients typical of d-d transitions, the experiments were carried out in 5 cm cuvettes. Figure 5.4 shows the spectra of solutions of $\text{Ni}(\text{NO}_3)_2$ and Asp at different pH values.

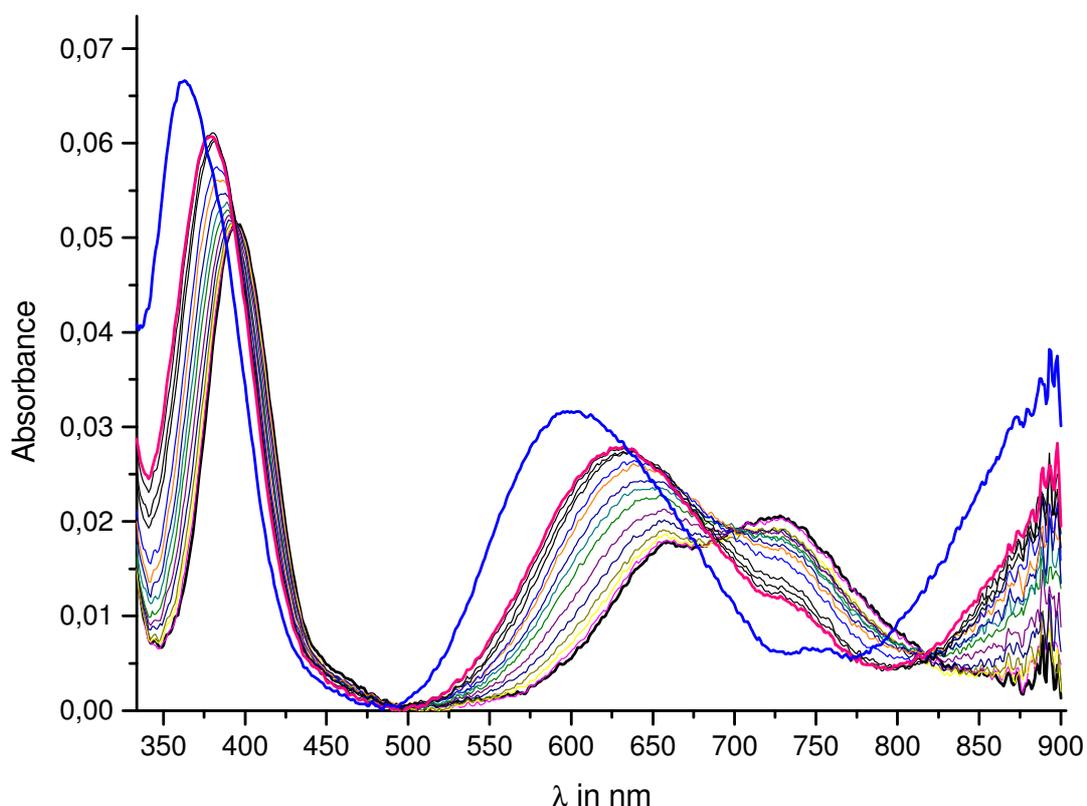


Figure 5.4

pH-dependence of the equilibrium absorption of $2 \cdot 10^{-3}$ M nickel(II) nitrate in the presence of $5 \cdot 10^{-3}$ M Asp and 0.1M NaCl at 25°C at pH 2.90, 3.92, 4.10, 4.29, 4.48, 4.70, 4.94, 5.08, 5.32, 5.46, 5.66, 6.09, 6.30, 6.50, 6.68 and 9.24 (in the order of increasing absorption at 600nm);

Since free Asp does not absorb in the studied region, Beer-Lambert's law includes the species shown in equation 5.24.

$$\frac{A}{d} = \epsilon_{\text{Ni}^{2+}} \cdot [\text{Ni}^{2+}] + \epsilon_{\text{NiLH}_2^{2+}} \cdot [\text{NiLH}_2^{2+}] + \epsilon_{\text{NiLH}^+} \cdot [\text{NiLH}^+] + \epsilon_{\text{NiL}} \cdot [\text{NiL}] + \epsilon_{\text{Ni}(\text{LH})_2} \cdot [\text{Ni}(\text{LH})_2] + \dots$$

$$\dots \epsilon_{\text{NiLLH}^-} \cdot [\text{NiLLH}^-] + \epsilon_{\text{NiL}_2^{2-}} \cdot [\text{NiL}_2^{2-}] + \epsilon_{\text{NiOH}^+} \cdot [\text{NiOH}^+] + \epsilon_{\text{Ni}(\text{OH})_2} \cdot [\text{Ni}(\text{OH})_2] \quad (5.24)$$

For the evaluation, equations (5.13) to (5.23) were combined with equation (5.24). In order to simplify the calculations, it was initially assumed that only the free nickel ions, the complexes NiL and NiL₂²⁻ are the absorbing species, such that equation (5.24) reduces to

$$\frac{A}{d} = \varepsilon_{Ni^{2+}} \cdot [Ni^{2+}] + \varepsilon_{NiL} \cdot [NiL] + \varepsilon_{NiL_2^{2-}} \cdot [NiL_2^{2-}] \quad (5.25)$$

The complexation constants and the respective extinction coefficients were obtained by fitting the experimental absorbance at different wavelengths with simulated absorbances, figure 5.5. Wavelengths were chosen for which significant variation of absorbance with pCh is shown. Figure 5.6 shows the deviation of the calculated from the experimentally obtained absorbance values. The fitted conditional constants pK_{c1} and pK_{c2} and extinction coefficients are shown in table 5.2 and table 5.3 respectively.

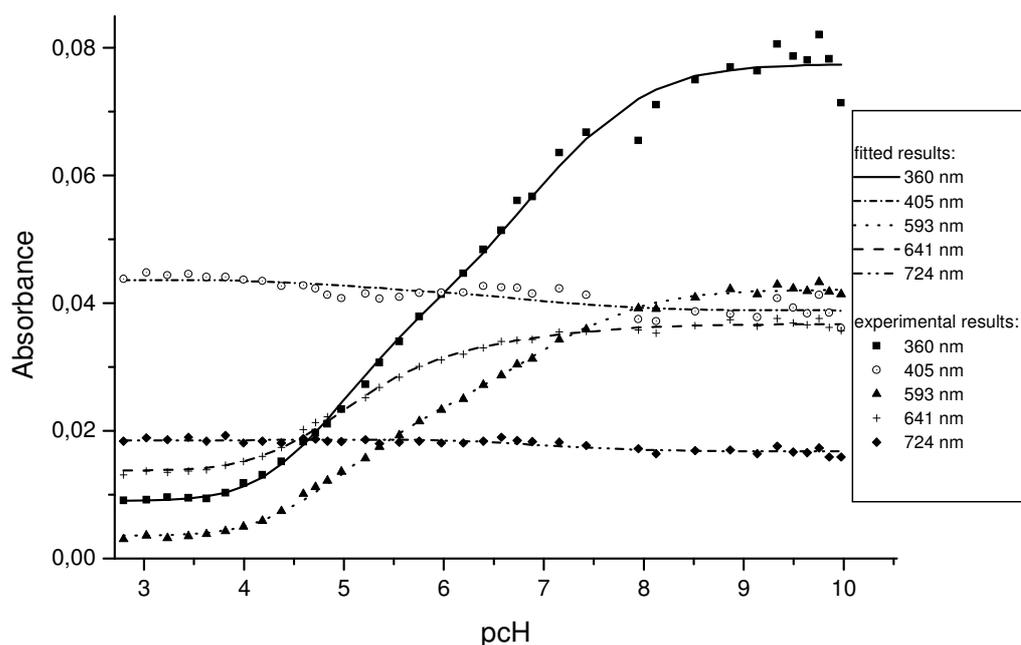


Figure 5.5

Fit of the pCh-dependencies of solutions of 2·10⁻³ M nickel(II) nitrate, 5·10⁻³ M Asp and 0.1M NaCl at 25°C at selected wavelengths using equation 5.25;

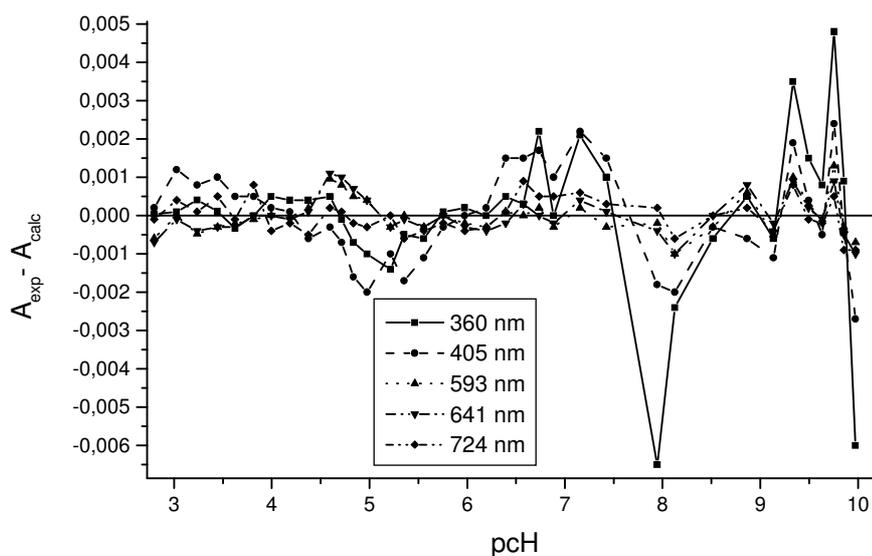


Figure 5.6

Deviation of the calculated from the experimentally obtained absorbances at selected wavelengths shown in figure 5.5; $A_{sp_0} = 5 \cdot 10^{-3} M$, $Ni_0 = 2 \cdot 10^{-3} M$, $I = 0.1 M$ (NaCl), $T = 25^\circ C$, $d = 5 cm$; autotitration with $0.1 M$ NaOH

Table 5.2

Fitted complexation constants

pK_{c1}	pK_{c2}	χ^2
7.22	5.53	2.21×10^{-4}

Table 5.3

Fitted extinction coefficients at selected wavelengths

Wavelength	724 nm	641 nm	593 nm	405 nm	360 nm
species	ϵ in $M^{-1}cm^{-1}$				
Ni^{2+}	1.85	1.38	0.36	4.36	0.90
NiL	1.87	3.33	2.37	4.18	4.08
NiL_2^{2-}	1.67	3.67	4.22	3.88	7.76

The large error at 360 nm is caused by the fact that for each pCH value the data points are recorded along a sharp variation of optical absorption with time at this wavelength (see figure 5.4).

The residuals in the basic pH range are substantially greater than the experimental errors, and therefore the assumption that only Ni^{2+} , NiL and NiL_2^{2-} are the absorbing species (equation 5.25) seem to be incorrect. Therefore all the possible nickel complexes shown in equation (5.24) were taken into account as possibly absorbing species. Additionally the potentiometric results shown in figure 5.3 were fitted together with the spectrophotometric results shown in figure 5.4. The fitted

extinction coefficients and the globally fitted conditional constants are shown in figure 5.7 and table 5.4 respectively.

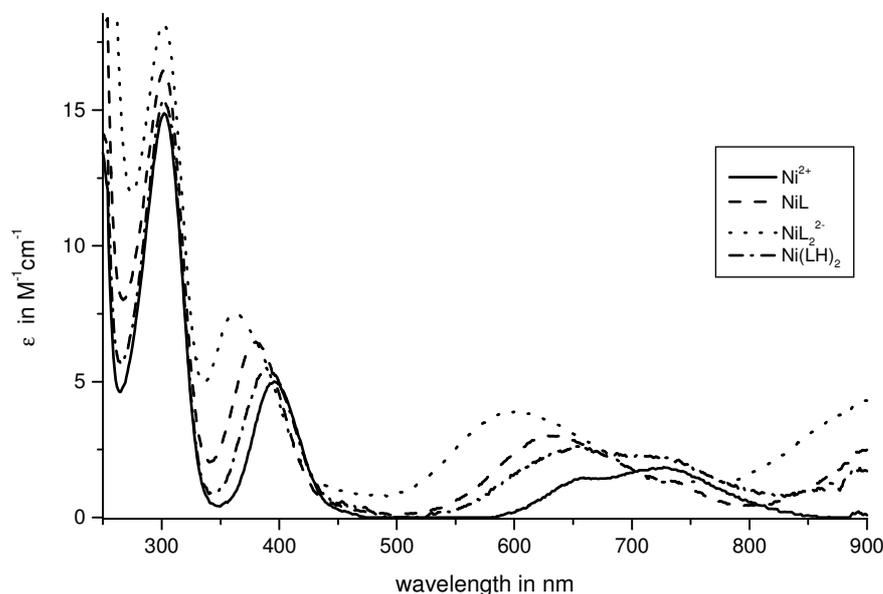


Figure 5.7

Calculated extinction coefficients as a function of wavelength; $Asp_0 = 5 \cdot 10^{-3} M$, $Ni_0 = 2 \cdot 10^{-3} M$, $I=0.1M$ (NaCl), $T=25^\circ C$, $d=5cm$; (For a more detailed description of the fitting procedure used, see Section 10.2.1)

Table 5.4

Fitted values for the complexation constants of Asp and Ni(II) ions in solution

	Results	Literature
$K_{c1} = \frac{[NiL]}{[Ni^{2+}][L^{2-}]}$	$\log(K_{c1} \cdot M) = 7.47 \pm 0.03$	$7.15 \pm 0.02^*$ 7.25^{**} 7.17^\blacktriangle
$K_{cH} = \frac{[NiLH^+]}{[NiL][H^+]}$	$\log(K_{cH} \cdot M) < 3.30$	4.05^*
$K_{cLH_2} = \frac{[NiLH_2^{2+}]}{[NiLH^+][H^+]}$	$\log(K_{cLH_2} \cdot M) < 1$	Not reported
$K_{c2} = \frac{[NiL_2^{2+}]}{[NiL][L^{2-}]}$	$\log(K_{c2} \cdot M) = 5.38 \pm 0.02$	$5.25 \pm 0.10^*$ 5.32^\blacktriangle
$K_{ML_2} = \frac{[NiLLH^+]}{[NiL_2^{2-}][H^+]}$	$\log(K_{ML_2} \cdot M) < 2$	Not reported
$K_{MLLH} = \frac{[Ni(LH)_2]}{[NiLLH^+][H^+]}$	$\log(K_{MLLH} \cdot M) < 9$	Not reported

* A. E. Martell and R. M. Smith, Critical Stability Constants, Plenum Press, New York, (1974 -1989)

** R. N. Patel et. al., Indian J. Chem. Section A, 38 (8), 850-853, (1999)

▲ M. R. Patel et al., J. Indian Chem. Soc., 70 (6), 569 – 572, (1993)

Figure 5.8 shows fitted extinction coefficients at five selected wavelengths and figure 5.9 shows the deviations of the calculated from the experimentally obtained absorbance values.

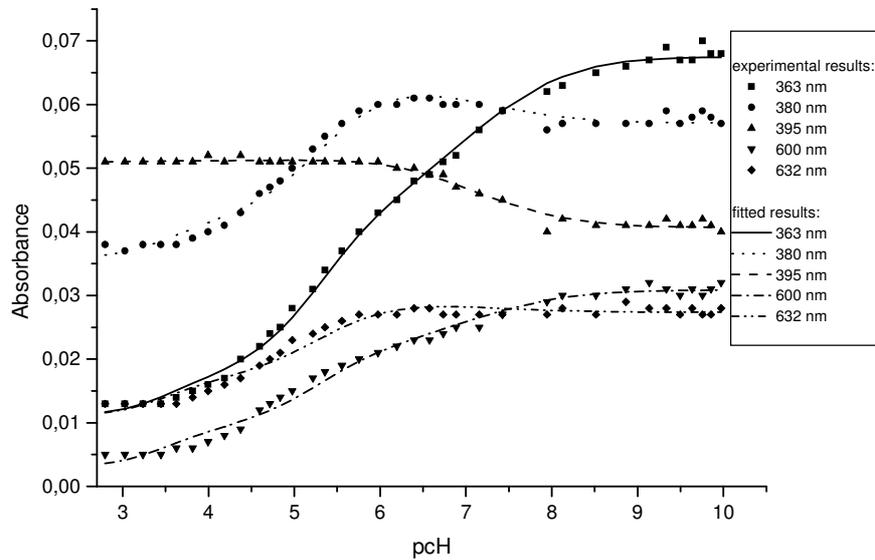


Figure 5.8

Fit of the pcH-dependencies of solutions of $2 \cdot 10^{-3}$ M nickel(II) nitrate, $5 \cdot 10^{-3}$ M Asp and 0.1M NaCl at 25°C at selected wavelengths using equation 5.24.

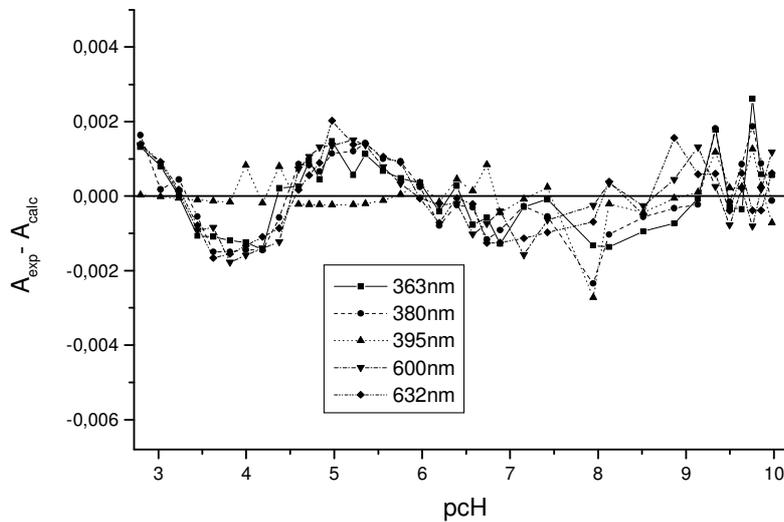


Figure 5.9

Deviations of the calculated from the experimentally obtained absorbances at selected wavelengths shown in figure 5.8; $Asp_0 = 5 \cdot 10^{-3}$ M, $Ni_0 = 2 \cdot 10^{-3}$ M, $I=0.1$ M (NaCl), $T=25^\circ\text{C}$, $d=5$ cm; autotitration with 0.1M NaOH.

Since as can be seen in table 5.4 it was not possible to determine the values of the constants K_{cLH_2} , K_{MLLH} , K_{ML_2} (due to very low concentrations of the species $Ni(LH)_2$, $NiLLH^-$ and $NiLH_2^{2+}$), the complexation constants were fitted again using a scheme involving only the species $NiLH^+$, NiL

and NiL_2^{2-} . Global fitting of the potentiometric results shown in figure 5.3 and the spectrophotometric results shown in figure 5.4 yielded the values for the complexation constants and the fitted extinction coefficients as shown in table 5.5 and figure 5.10 respectively.

Table 5.5

Fitted values for the complexation constants of Asp and Ni(II) ions in solution using a scheme involving only the species NiLH^+ , NiL and NiL_2^{2-} .

	Results	Literature
$K_{c1} = \frac{[\text{NiL}]}{[\text{Ni}^{2+}][\text{L}^{2-}]}$	$\log(K_{c1} \cdot M) = 7.20 \pm 0.04$	$7.15 \pm 0.02^*$ 7.25^{**} 7.17^\blacktriangle
$K_{cH} = \frac{[\text{NiLH}^+]}{[\text{NiL}][\text{H}^+]}$	$\log(K_{cH} \cdot M) = 4.29 \pm 0.22$	4.05^*
$K_{c2} = \frac{[\text{NiL}_2^{2-}]}{[\text{NiL}][\text{L}^{2-}]}$	$\log(K_{c2} \cdot M) = 5.27 \pm 0.03$	$5.25 \pm 0.10^*$ 5.32^\blacktriangle

* A. E. Martell and R. M. Smith, Critical Stability Constants, Plenum Press, New York, (1974 -1989)

** R. N. Patel et. al., Indian J. Chem. Section A, 38 (8), 850-853, (1999)

\blacktriangle M. R. Patel et al., J. Indian Chem. Soc., 70 (6), 569 – 572, (1993)

\diamond A. Pohlmeier and W. Knoche, International Journal of Chemical Kinetics, Vol. 28. ,125-136 (1996)

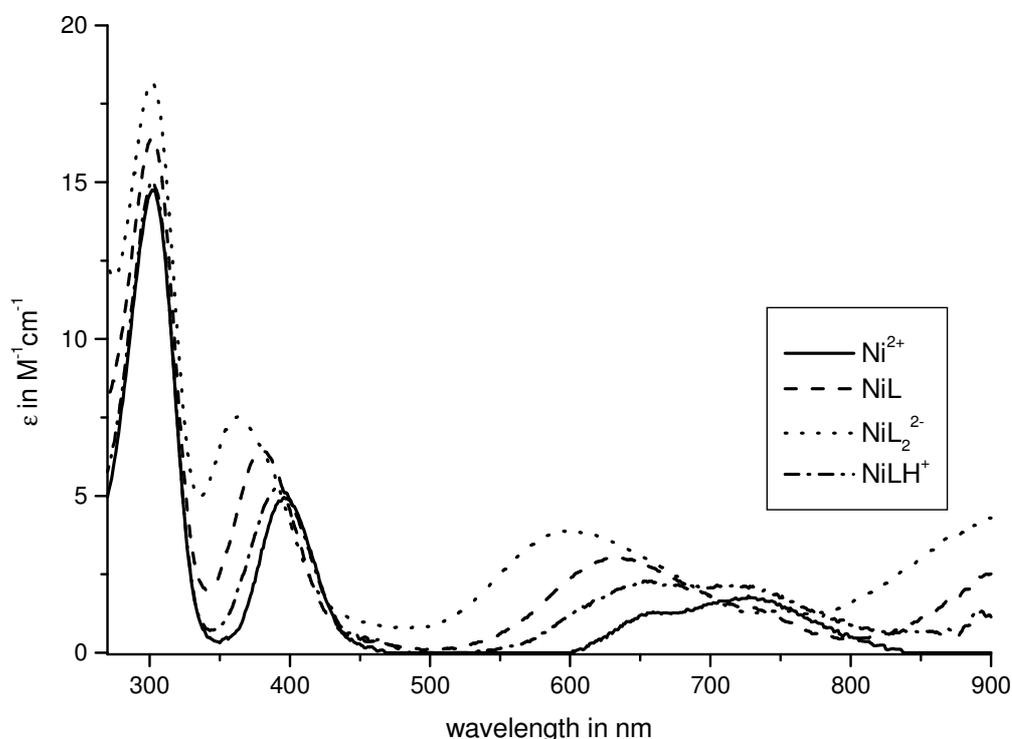


Figure 5.10

Calculated extinction coefficients as a function of wavelength using a scheme involving only the species NiLH^+ , NiL and NiL_2^{2-} ; $\text{Asp}_0 = 5.10^{-3} \text{ M}$, $\text{Ni}_0 = 2.10^{-3} \text{ M}$, $I=0.1 \text{ M}$ (NaCl), $T=25^\circ\text{C}$, $d=5 \text{ cm}$;

Figure 5.11 shows fitted extinction coefficients at five selected wavelengths for the scheme involving only the species NiLH^+ , NiL and NiL_2^{2-} . Figure 5.12 shows the corresponding deviations of the calculated from the experimentally obtained absorbance values.

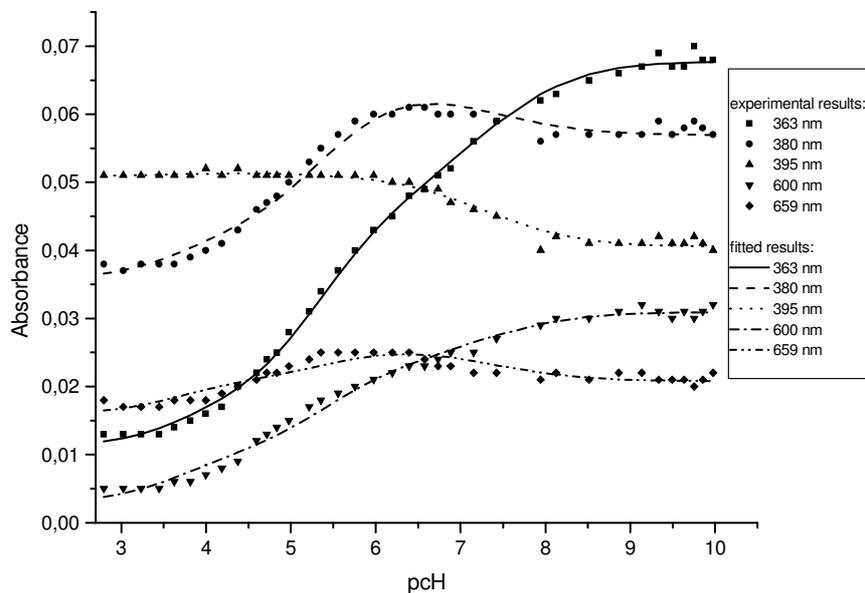


Figure 5.11

Fit of the pCH-dependencies of solutions of $2 \cdot 10^{-3} \text{ M}$ nickel(II) nitrate, $5 \cdot 10^{-3} \text{ M}$ Asp and 0.1 M NaCl at 25°C at selected wavelengths using a scheme involving only the species NiLH^+ , NiL and NiL_2^{2-} .

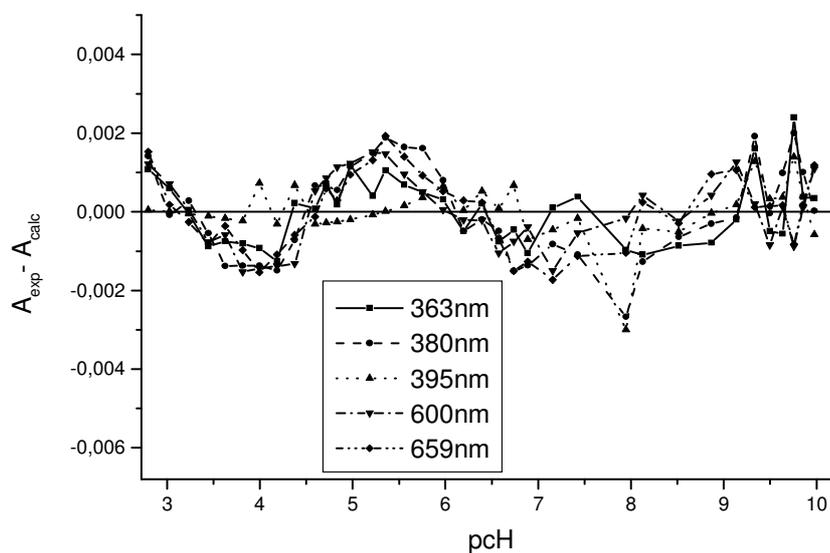


Figure 5.12

Deviations of the calculated from the experimentally obtained absorbances at selected wavelengths shown in figure 5.11; $\text{Asp}_0 = 5 \cdot 10^{-3} \text{ M}$, $\text{Ni}_0 = 2 \cdot 10^{-3} \text{ M}$, $I = 0.1 \text{ M}$ (NaCl), $T = 25^\circ \text{C}$, $d = 5 \text{ cm}$; autotitration with 0.1 M NaOH

Table 5.6 shows fitted extinction coefficients at five selected wavelengths.

Table 5.6

Fitted extinction coefficients at selected wavelengths

wavelength	659nm	600nm	395nm	380nm	363nm
species	ϵ in $M^{-1}cm^{-1}$				
Ni^{2+}	1.51 ± 0.06	0.15 ± 0.04	5.09 ± 0.09	3.46 ± 0.11	0.98 ± 0.06
NiL	2.63 ± 0.03	2.26 ± 0.03	5.15 ± 0.04	6.37 ± 0.06	4.51 ± 0.05
$NiLH^+$	2.16 ± 0.07	1.18 ± 0.05	5.13 ± 0.10	4.34 ± 0.13	1.91 ± 0.07
NiL_2	2.08 ± 0.03	3.08 ± 0.03	4.07 ± 0.03	5.71 ± 0.04	6.76 ± 0.04

The species distribution diagram for all the reactants and products is calculated from the protonation constants shown in table 5.1 and the complexation constants shown in table 5.5 and is shown in figure 5.13. The concentrations of $NiOH^+$ and $Ni(OH)_2$ are negligibly small.

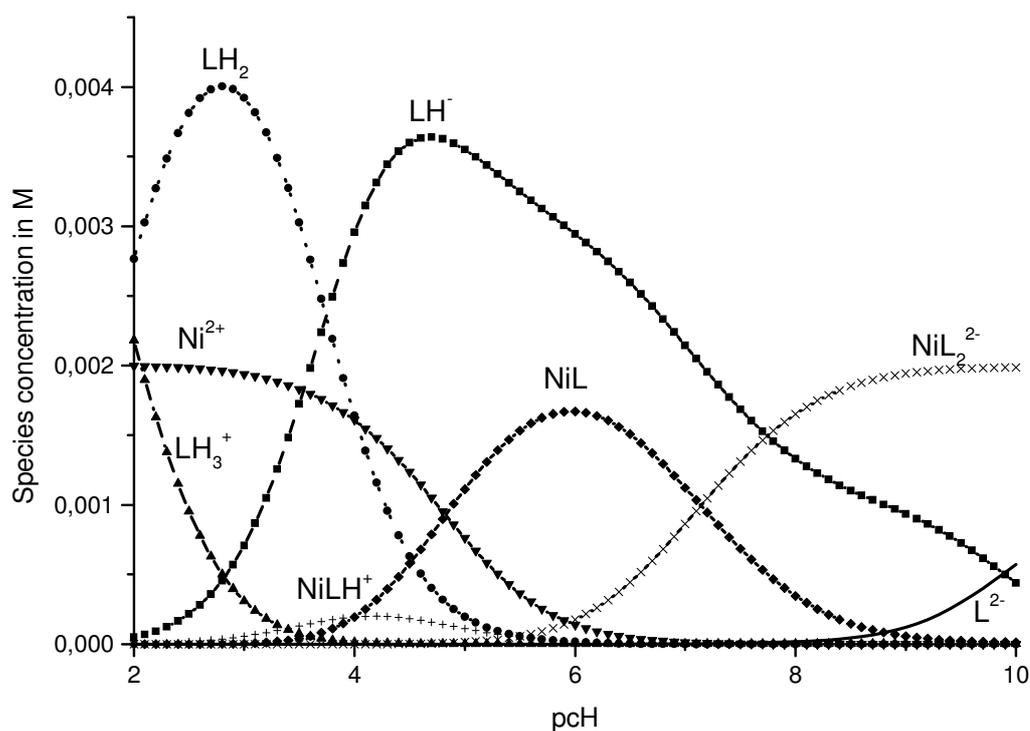


Figure 5.13

Species distribution diagram for the complexation of $Ni(II)$ ions with Asp from potentiometrical and spectrophotometrical titrations of 40 ml of $5 \cdot 10^{-3}$ M Asp, 0.02 M HCl, 0.1 M NaCl and $2 \cdot 10^{-3}$ M $Ni(NO_3)_2$ with 0.1 M NaOH at 25°C.

5.2.2.2 The binding mode of nickel(II) ions to poly-L-aspartic acid

Similarly to section 5.2.2.1, solutions of nickel(II) ions and poly-L-aspartic acid (sodium salt) were titrated with NaOH and monitored spectrophotometrically, figure 5.14. The measurements were done at $I = 0.25$ M in order to reduce the polyelectrolyte influence. The blue shifts in the spectra observed in solutions of nickel nitrate and Asp, figure 5.4 are not observed in figure 5.14. This indicates the absence of binding of the amino group to the nickel(II) ions.

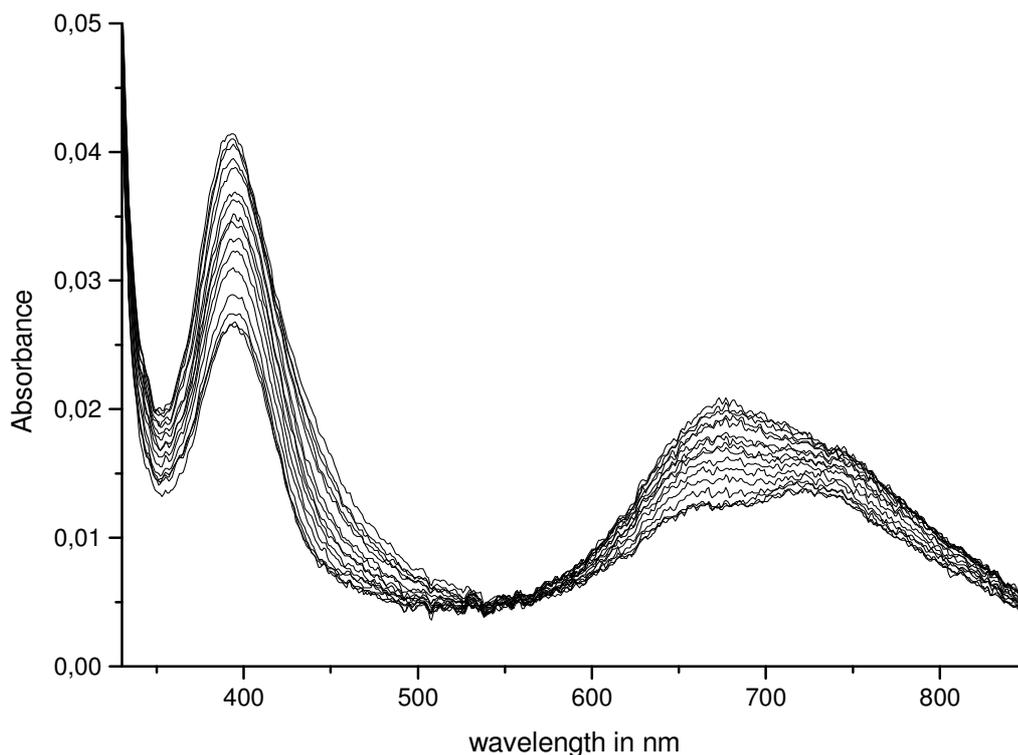


Figure 5.14

pH-dependence of the equilibrium absorption of nickel(II) ions in the presence of poly-L-aspartic acid, (PAsp); $PAsp_0 = 0.32 \times 10^{-3}$ val, $Ni_0 = 0.15 \times 10^{-3}$ val, (3.8×10^{-3} M) $d = 5$ cm, $I = 0.25$ M (NaCl); $T = 25^\circ\text{C}$ at pH 2 -12 (in the order of increasing absorption at 400 nm).

Only selected spectra are shown at pH 1.84, 4.83, 5.93, 7.57, 8.36, 8.53, 8.72, 8.8, 9.04, 9.14, 9.35, 9.39, 9.49, 9.54 and 9.85. No spectral change was observed from pH 9.85 to pH 12 in this wavelength range.

5.3 Summary of Thermodynamics

At equilibrium, all four differently protonated forms of aspartic acid need to be taken into account. At a neutral pH range, Asp occurs in its zwitterionic form (LH^- , see scheme 5.1). The protonation constants were determined potentiometrically. K_{a1} was determined with a lower accuracy in comparison to K_{a2} and K_{a3} since at such a low pCh value the functioning of the pH electrode becomes limiting. The protonation conditional constants obtained are shown in table 5.7.

Table 5.7: Fitted values for the protonation constants of Asp

	Results	Literature
$K_{a1} = \frac{[LH_2][H^+]}{[LH_3^+]}$	$-\log(K_{a1} \cdot M^{-1}) = 1.90 \pm 0.05$	$1.93 \pm 0.01^*$ 1.99^\diamond 1.87^{**}
$K_{a2} = \frac{[LH^-][H^+]}{[LH_2]}$	$-\log(K_{a2} \cdot M^{-1}) = 3.74 \pm 0.03$	$3.70 \pm 0.01^*$ 3.69^\diamond 4.00^{**} 3.60^\blacktriangle
$K_{a3} = \frac{[L^{2-}][H^+]}{[LH^-]}$	$-\log(K_{a3} \cdot M^{-1}) = 9.89 \pm 0.03$	$9.63 \pm 0.01^*$ 9.47^\diamond 9.75^{**} 9.60^\blacktriangle

* A. E. Martell and R. M. Smith, Critical Stability Constants, Plenum Press, New York, (1974 -1989)

** R. N. Patel et. al., Indian J. Chem. Section A, 38 (8), 850-853, (1999)

▲ M. R. Patel et al., J. Indian Chem. Soc., 70 (6), 569 – 572, (1993)

◇ A. Pohlmeier and W. Knoche, International Journal of Chemical Kinetics, Vol. 28., 125-136 (1996)

In aqueous solution, nickel(II) ions occur as an octahedral hexaquo complex. In the presence of Asp, mono- and di-aspartate complexes form of varying degree of protonation, depending on the solution pCh, however only the complexes NiL , $NiLH^+$ and NiL_2^{2-} could be accurately fitted. The complexation constants describing the stability of these species were determined potentiometrically and spectrophotometrically at constant temperature and ionic strength. The following values for the complexation constants were obtained:

Table 5.8: Fitted values for the complexation constants of Asp and Ni(II) ions in solution

	Results	Literature
$K_{c1} = \frac{[NiL]}{[Ni^{2+}][L^{2-}]}$	$\log(K_{c1} \cdot M) = 7.20 \pm 0.04$	$7.15 \pm 0.02^*$ 7.25^{**} 7.17^\blacktriangle
$K_{cH} = \frac{[NiLH^+]}{[NiL][H^+]}$	$\log(K_{cH} \cdot M) = 4.29 \pm 0.22$	4.05^*
$K_{c2} = \frac{[NiL_2^{2-}]}{[NiL][L^{2-}]}$	$\log(K_{c2} \cdot M) = 5.27 \pm 0.03$	$5.25 \pm 0.10^*$ 5.32^\blacktriangle

* A. E. Martell and R. M. Smith, Critical Stability Constants, Plenum Press, New York, (1974 -1989)

** R. N. Patel et. al., Indian J. Chem. Section A, 38 (8), 850-853, (1999)

▲ M. R. Patel et al., J. Indian Chem. Soc., 70 (6), 569 – 572, (1993)

6. RESULTS AND EVALUATION- Kinetics

6.1 Stopped-flow experiments

The kinetics of the complexation reaction between nickel(II) ions and Asp in solution were investigated using the Stopped-Flow technique. The progress of the reaction was monitored by the change in optical absorbance of a coupled proton indicator. The following indicators and respective buffers were used:

Table 6.1

Buffers and Indicators used for the different pH ranges

pH-Range	Buffer	Indicator
3.00 - 3.50	*Formate	Methyl Orange
3.00 - 3.50	*Formate	Bromomphenol Blue
3.50 - 5.00	*Acetate	Bromocresol Green
5.00 - 6.00	Acetate	Chlorophenol Red
6.00 - 8.00	2,6-Lutidin	Bromothymol Blue

* No Buffer was used in this pH-range when Asp was present in excess, since Asp functioned as an internal buffer due to its middle pK, pK_{a2}.

The use of buffers simplified the calculations due to the fact that the relative change in the proton concentrations was very small in comparison to the relative change in concentration of other reactants and products. Furthermore, the ratio of nickel(II) nitrate concentration to the Asp concentration or vice-versa was always greater than twenty such that pseudo-first order kinetics could be assumed. Each solution contained equal amounts of buffer, inert salt, and proton indicator.

6.1.1 pH-Dependence of the Reaction Rate

6.1.1.1 Nickel(II) ions in excess

Stopped-flow experiments were performed by mixing solutions of $2 \cdot 10^{-2}$ M Ni(NO₃)₂ with $5 \cdot 10^{-4}$ M Asp at different pCh values. The measurements can be fitted by single relaxation effects within experimental error. The results are shown in figure 6.1.

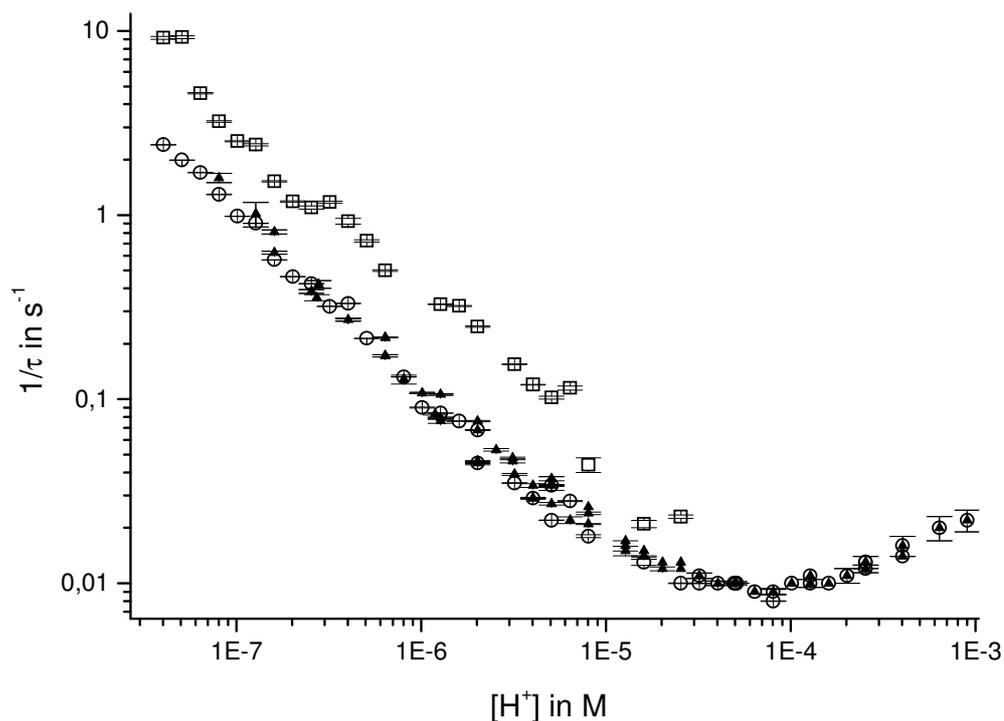


Figure 6.1

Reciprocal of the relaxation times of the reaction of Ni(II) ions with Asp;

$Ni_0 = 10^{-2}$ M, $Asp_0 = 2.5 \times 10^{-4}$ M, $I = 0.1$ M (NaCl), $buffer_0 = 5 \cdot 10^{-3}$ M, $indicator_0 = 2 \cdot 10^{-5}$ M; $T = 25^\circ\text{C}$

▲ : Data fitted to a single relaxation effect; □ and ○ : Data fitted to two relaxation effects

This fitting of absorption vs time results by a single relaxation effect leads to a small but systematic deviation of the fit from the measurements (see section 9.4.1.1) which therefore have also been evaluated assuming two relaxation effects, i.e.

$$A - A_{eq} = A_I e^{-\frac{t}{\tau_I}} + A_{II} e^{-\frac{t}{\tau_{II}}}$$

The relaxation times obtained by this fit are also shown in figure 6.1; the ratios of the relaxation amplitudes (A_{II} / A_I) and of the relaxation times τ_{II} / τ_I are shown in figure 6.2.

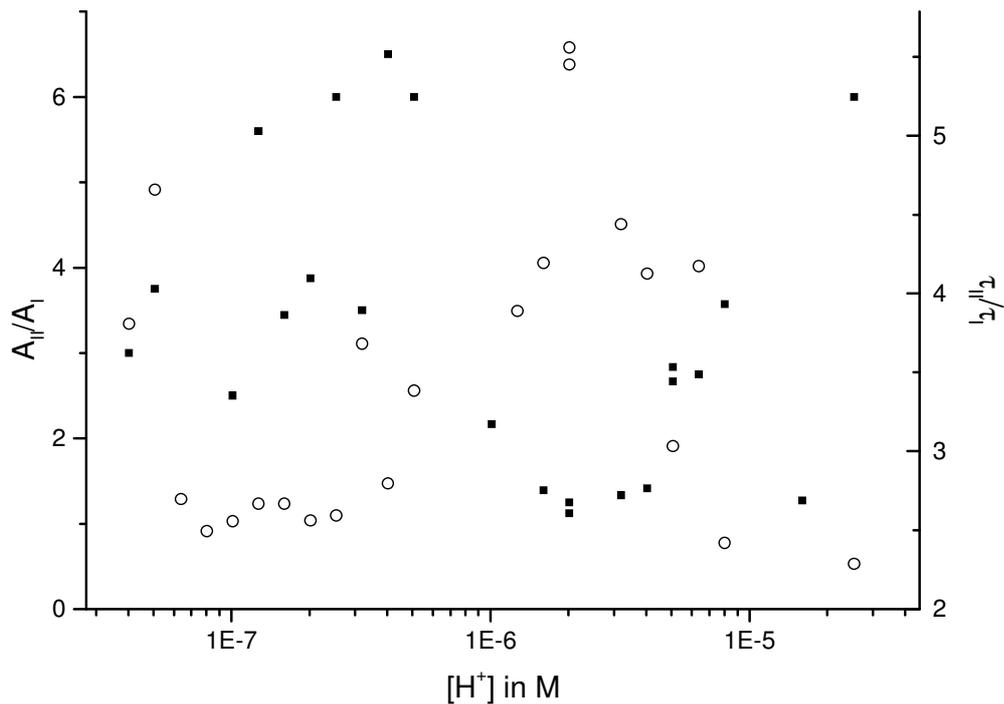


Figure 6.2

The ratio of the relaxation amplitudes (A_{II} / A_I ; ■) and of the relaxation times (τ_{II} / τ_I ; ○) for the case where the nickel(II) ions were in excess; I refers to the faster relaxation effect and II refers to the slower relaxation effect; $Ni_o = 10^{-2}$ M, $Asp_o = 2.5 \times 10^{-4}$ M, $I = 0.1$ M (NaCl), $buffer_o = 5.10^{-3}$ M, $indicator_o = 2.10^{-5}$ M; $T = 25^\circ\text{C}$

The figures show that:

- i) the longer relaxation time τ_{II} agrees well with the value for τ obtained from the fitting by a single relaxation effect
- ii) in most cases the ratio of the relaxation amplitudes (A_{II} / A_I) is large compared to unity
- iii) the ratio of the relaxation times $\tau_{II} / \tau_I \approx 4 \pm 1.5$
- iv) both ratios show a random dependence to the proton concentration.

Furthermore,

- a) the relationship relating the relaxation time to the proton concentration derived assuming two relaxation effects, gave the same equation as is obtained assuming a single relaxation effect
- b) the least square sum between experimental data and fitted curves does not improve significantly when fitting to two instead of one relaxation effect.

Therefore it is concluded that the shorter relaxation effect is most probably an artefact.

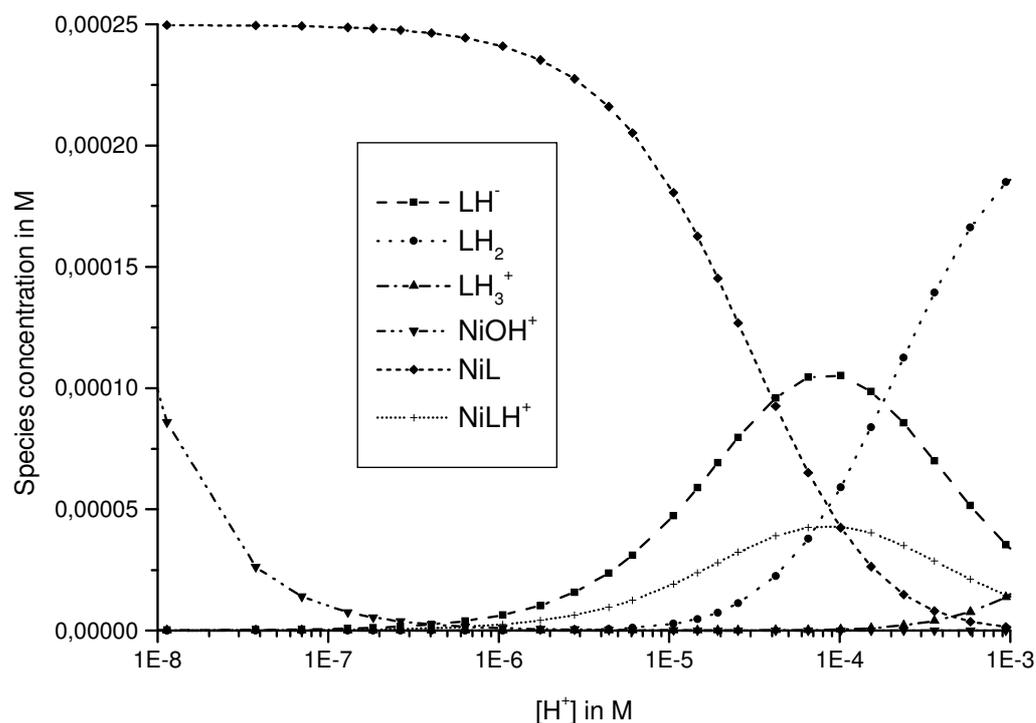
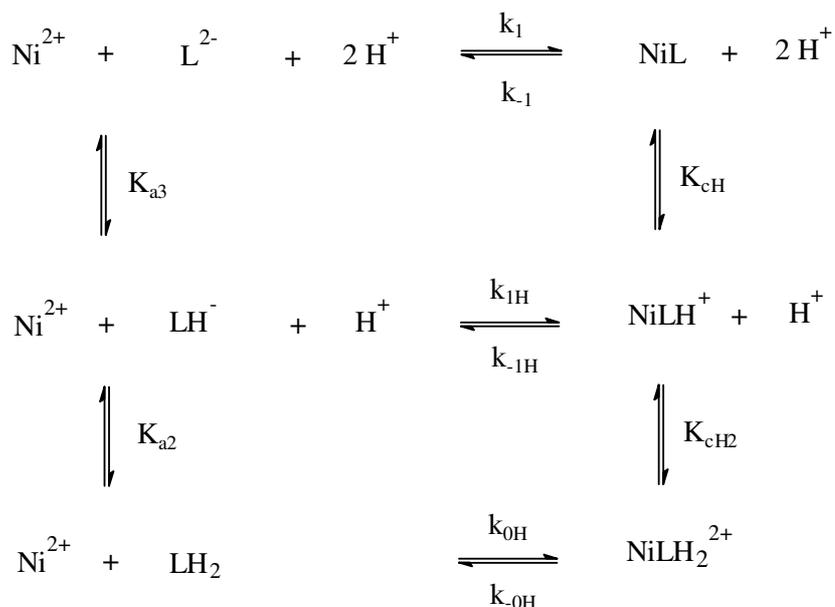


Figure 6.3

Species distribution diagram for the case where the nickel(II) ions were in excess; $Ni_0 = 10^{-2}$ M, $Asp_0 = 2.5 \times 10^{-4}$ M, $I = 0.1$ M (NaCl), $buffer_0 = 5 \cdot 10^{-3}$ M, $indicator_0 = 2 \cdot 10^{-5}$ M; $T = 25^\circ\text{C}$;

Figure 6.3 shows the species distribution diagram for the mixtures at equilibrium using the equilibrium constants obtained from potentiometric and spectrophotometric measurements. The concentration of nickel(II) ions at equilibrium may be assumed to be equal to Ni_0 in the whole pH-range. Figure 6.3 shows that besides the reactant in excess (Ni^{2+}), the species LH_2 , LH^- , $NiLH^+$ and NiL have to be considered in the reaction scheme. Analogously the reaction of Ni^{2+} with LH_2 has been taken into account. The equilibrium concentration of the species $NiOH^+$ is always much smaller than Ni^{2+} ($K_M = 10^{9.996} \text{ M}^{-1}$, see 5.22) and therefore nickel(II) ions reacts with Asp only as Ni^{2+} . Since Ni^{2+} ions occur in excess, no 1:2 complexes form. This leads to scheme 6.1.



Scheme 6.1

A) Fitting of the data assuming a water-release rate-determining step

In this section it is assumed that the stopped-flow experiments are accurately described by fitting the change of absorption by a single relaxation effect. Furthermore a water-release rate-determining step is assumed (see section 3.1.1).

The derivation of the reciprocal of the relaxation time of the reaction of Ni(II) ions with Asp as a function of proton concentration was done as follows:

The rate law for the formation of free nickel(II) ions is given by

$$\frac{d[\text{Ni}^{2+}]}{dt} = -k_{0H}[\text{Ni}^{2+}][\text{LH}_2] + k_{-0H}[\text{NiLH}_2^{2+}] - k_{1H}[\text{Ni}^{2+}][\text{LH}^-] + k_{-1H}[\text{NiLH}^+] - k_1[\text{Ni}^{2+}][\text{L}^{2-}] + k_{-1}[\text{NiL}] \quad (6.1)$$

$$\text{Let } [\text{LH}_2] = \gamma_{\text{LH}_2} [\text{L}] \quad (6.2)$$

$$[\text{LH}^-] = \gamma_{\text{LH}} [\text{L}] \quad (6.3)$$

$$\text{and } [\text{L}^{2-}] = \gamma_{\text{L}} [\text{L}] \quad (6.4)$$

$$\text{where } [\text{L}] = [\text{LH}_2] + [\text{LH}^-] + [\text{L}^{2-}]$$

$$\text{and hence } \gamma_{\text{LH}_2} = \frac{[\text{LH}_2]}{[\text{LH}_2] + [\text{LH}^-] + [\text{L}^{2-}]},$$

$$\gamma_{\text{LH}} = \frac{[\text{LH}^-]}{[\text{LH}_2] + [\text{LH}^-] + [\text{L}^{2-}]},$$

$$\text{and } \gamma_L = \frac{[L^{2-}]}{[LH_2] + [LH^-] + [L^{2-}]},$$

Analogously,

$$[NiLH_2^{2+}] = \gamma_{NiLH_2} [ML] \quad (6.5)$$

$$[NiLH^+] = \gamma_{NiLH} [ML] \quad (6.6)$$

$$\text{and } [NiL] = \gamma_{NiL} [ML] \quad (6.7)$$

where $[ML] = [NiLH_2^{2+}] + [NiLH^+] + [NiL]$,

$$\text{and hence } \gamma_{NiL} = \frac{[NiL]}{[NiL] + [NiLH^+] + [NiLH_2^{2+}]},$$

$$\gamma_{NiLH} = \frac{[NiLH^+]}{[NiL] + [NiLH^+] + [NiLH_2^{2+}]}$$

$$\text{and } \gamma_{NiLH_2} = \frac{[NiLH_2^{2+}]}{[NiL] + [NiLH^+] + [NiLH_2^{2+}]}$$

Substituting (6.2 – 6.7) into (6.1) results in

$$\begin{aligned} \frac{d[Ni^{2+}]}{dt} = & -k_{0H} \left\{ \gamma_{LH_2} ([Ni^{2+}][L]) - \frac{k_{-0H}}{k_{0H}} [ML] \gamma_{NiLH_2} \right\} + k_{1H} \left\{ \gamma_{LH} ([Ni^{2+}][L]) - \frac{k_{-1H}}{k_{1H}} [ML] \gamma_{NiLH} \right\} \dots \\ & \dots - k_1 \left\{ \gamma_L ([Ni^{2+}][L]) - \frac{k_{-1}}{k_1} [ML] \gamma_{NiL} \right\} \end{aligned} \quad (6.8)$$

The values of γ_{NiLH_2} , γ_{NiLH} , γ_{NiL} , γ_{LH_2} , γ_{LH} and γ_L are constant since all the solutions were buffered. Substituting $[Y] = [Y]_e + x_Y$ (where $[Y]_e$ is the concentration of species Y at equilibrium and the term x represents the deviation of the respective concentrations from the equilibrium state) into (6.8) gives

$$\begin{aligned} \frac{dx_{Ni^{2+}}}{dt} = & -k_{0H} \left\{ \gamma_{LH_2} ([Ni^{2+}]_e x_{[L]} + [L]_e x_{Ni^{2+}}) - \frac{k_{-0H}}{k_{0H}} x_{ML} \gamma_{NiLH_2} \right\} \dots \\ & + k_{1H} \left\{ \gamma_{LH} ([Ni^{2+}]_e x_{[L]} + [L]_e x_{Ni^{2+}}) - \frac{k_{-1H}}{k_{1H}} x_{ML} \gamma_{NiLH} \right\} - k_1 \left\{ \gamma_L ([Ni^{2+}]_e x_{[L]} + [L]_e x_{Ni^{2+}}) - \frac{k_{-1}}{k_1} x_{ML} \gamma_{NiL} \right\} \end{aligned} \quad (6.9)$$

In equation (6.9) $x_{[L]} x_{Ni^{2+}}$ has been neglected since this product is small compared to

$$x_{[L]} [Ni^{2+}]_e, Ni_0 \gg L_0 \text{ and } |x_{Ni^{2+}}| \leq L_0.$$

The following balances are used:

$$X_{LH_2} + X_{LH^-} + X_{L^{2-}} + X_{NiLH_2^{2+}} + X_{NiLH^+} + X_{NiL} = 0$$

$$X_{Ni^{2+}} + X_{NiLH_2^{2+}} + X_{NiLH^+} + X_{NiL} = 0$$

such that $X_{LH_2} + X_{LH^-} + X_{L^{2-}} = X_{[L]} = X_{Ni^{2+}}$

and $X_{Ni^{2+}} = -X_{NiLH_2^{2+}} - X_{NiLH^+} - X_{NiL}$

Hence $\frac{X_{[L]}}{X_{Ni^{2+}}} = 1$ and $\frac{X_{[ML]}}{X_{Ni^{2+}}} = -1$ giving

$$\begin{aligned} \frac{1}{\tau} = & k_{0H} \left\{ \gamma_{LH_2} ([Ni^{2+}]_e + [L]_e) + \frac{k_{-0H}}{k_{0H}} \gamma_{NiLH_2} \right\} \dots \\ & + k_{1H} \left\{ \gamma_{LH} ([Ni^{2+}]_e + [L]_e) - \frac{k_{-1H}}{k_{1H}} \gamma_{NiLH} \right\} + k_1 \left\{ \gamma_L ([Ni^{2+}]_e + [L]_e) + \frac{k_{-1}}{k_1} \gamma_{NiL} \right\} \end{aligned} \quad (6.10)$$

$([Ni^{2+}]_e + [L]_e) \approx [Ni^{2+}]_e \approx Ni_0$ since $Ni_0 \gg L_0$.

Applying this approximation and substituting the following equations

$$\begin{aligned} K_{a2} &= \frac{[LH^-][H^+]}{[LH_2]} & K_{a3} &= \frac{[L^{2-}][H^+]}{[LH^-]} \\ K_{cLH_2} &= \frac{[NiLH_2^{2+}]}{[NiLH^+][H^+]} & K_{cH} &= \frac{[NiLH^+]}{[NiL][H^+]} \end{aligned}$$

in (6.10) and rearranging, results in

$$\frac{1}{\tau} = \left(k_{0H} \frac{[H^+]}{K_{a2}} + k_{1H} + k_1 \frac{K_{a3}}{[H^+]} \right) \left(\frac{K_{a2} Ni_0}{K_{a2} + [H^+]} + \frac{[H^+]}{K_{c1} K_{a3} (K_{cLH_2} K_{cH} [H^+]^2 + K_{cH} [H^+] + 1)} \right) \quad (6.11)$$

At the end of this section it will be shown that the terms $k_{0H} \frac{[H^+]}{K_{a2}}$ and

$K_{c1} K_{a3} K_{cLH_2} K_{cH} [H^+]^2$ may be neglected. This reduces equation (6.11) to (6.12).

$$\frac{1}{\tau} = \left(k_{1H} + k_1 \frac{K_{a3}}{[H^+]} \right) \left(\frac{K_{a2} Ni_0}{K_{a2} + [H^+]} + \frac{[H^+]}{K_{c1} K_{a3} (K_{cH} [H^+] + 1)} \right) \quad (6.12)$$

The experimental data were fitted using this equation. For the derivation of this equation it was taken into account that:

- the solutions were buffered
- $Ni_0 \gg L_0$

c) The term proportional to k_{0H} may be neglected.

Considering the values of $K_{a2} = 10^{-3.74}$ M, $K_{a3} = 10^{-9.89}$ and $K_{c1} = 10^{7.47}$ M⁻¹, fitted from thermodynamic experiments (see section 5.3), it becomes evident that equation (6.12) can be divided into 4 pcH-dependent terms as follows:

i) at high pcH (pcH > 6):

$$k_{1H} < k_1 \frac{K_{a3}}{[H^+]},$$

$$\frac{[H^+]}{K_{c1}K_{a3}(K_{cH}[H^+] + 1)} < \frac{K_{a2}Ni_o}{K_{a2} + [H^+]}$$
 and

$$[H^+] \ll K_{a2} \text{ such that equation (6.12) reduces to } \frac{1}{\tau} = \left(k_1 \frac{K_{a3}}{[H^+]} Ni_o \right) \quad (6.12a) \text{ (curve (a) in}$$

figure 6.4). Fitting of this function yields the value for the reaction rate constant k_1 .

The best fit yields the value of $k_1 = 91000 (\pm 2000)$ M⁻¹s⁻¹; $\chi^2 = 0.006$.

ii) at low pcH (pcH < 6):

$$k_{1H} \text{ becomes significant, such that } \frac{1}{\tau} = \left(k_{1H} + k_1 \frac{K_{a3}}{[H^+]} \right) \left(\frac{K_{a2}Ni_o}{K_{a2} + [H^+]} \right) \quad (6.12b) \text{ (curve (b) in}$$

figure 6.4). Fitting of this function describes only approximately the deviation of the function from the straight line obtained previously. Therefore the rate constant k_{1H} cannot be obtained from this fit.

The best fit yields the value of $k_{1H} = 0.89 (\pm 0.14)$ M⁻¹s⁻¹; $\chi^2 = 0.004$.

iii) at even lower pcH (pcH < 5):

the following equation below should be used:

$$\frac{1}{\tau} = \left(k_{1H} + k_1 \frac{K_{a3}}{[H^+]} \right) \left(\frac{K_{a2}Ni_o}{K_{a2} + [H^+]} + \frac{[H^+]}{K_{c1}K_{a3}} \right) \quad (6.12c) \text{ (curve (c) in figure 6.4). Fitting of this}$$

function should yield a value for the reaction rate constant K_{c1} . However there are systematic deviations between the experimental data and the fitted curve and hence no reliable values for K_{c1} can be obtained.

The best fit yields the value of $\log (K_{c1} \cdot M) = 8.41 (\pm 0.08)$; $\chi^2 = 0.003$.

iv) Finally, the complete equation (6.12) is fitted to the experimental data (curve (d) in figure 6.4). Fitting of this function results in a good fit and yields values for the constants k_{1H} , K_{c1} and K_{cH} . These influence collectively the pCH-dependence of the relaxation time at $5.50 > \text{pCH} > 3.50$ and hence cannot be fitted separately (as k_1 in case i).

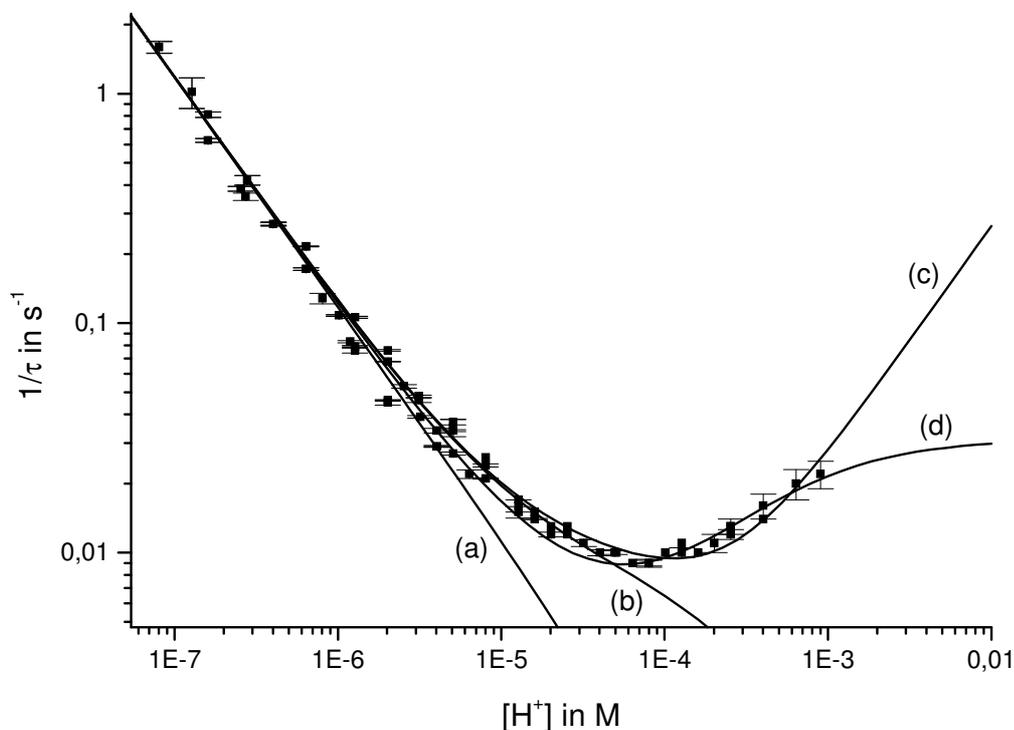


Figure 6.4

Stepwise fitting of the reciprocal of the longer relaxation time of the reaction of Ni(II) ions with Asp as a function of proton concentration: (a) according to equation (6.12a); (b) according to equation (6.12b); (c) according to equation (6.12c); (d) according to equation (6.12);

$\text{Ni}_0 = 10^{-2} \text{ M}$, $\text{Asp}_0 = 2.5 \times 10^{-4} \text{ M}$, $I = 0.1 \text{ M}$ (NaCl), $\text{buffer}_0 = 5.10^{-3} \text{ M}$, $\text{indicator}_0 = 2.10^{-5} \text{ M}$; $T = 25^\circ\text{C}$

Using the values of $K_{a2} = 10^{-3.74} \text{ M}$, $K_{a3} = 10^{-9.89} \text{ M}$ (see table 5.6), the values for the reaction rate constants k_{1H} and k_1 and for K_{cH} and K_{c1} shown in table 6.2 were obtained.

Table 6.2

Constants fitted from the reciprocal of the longer relaxation time of the reaction of nickel(II) ions with Asp as a function of proton concentration for the case where nickel(II) ions were present in excess.

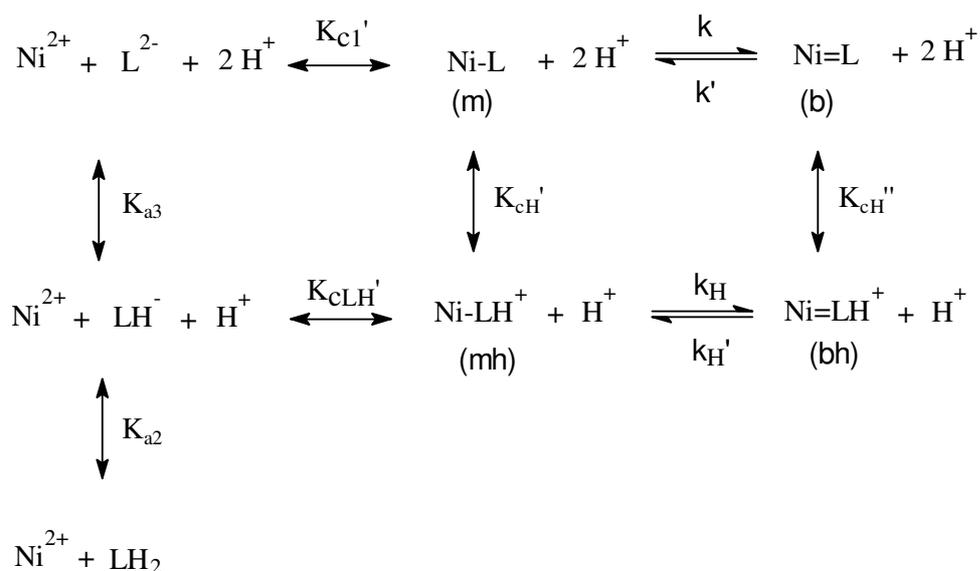
	Results
k_{1H} in $\text{M}^{-1}\text{s}^{-1}$	0.20 ± 0.07
k_1 in $\text{M}^{-1}\text{s}^{-1}$	$90\,000 \pm 4\,000$
$\log(K_{cH} \cdot \text{M})$	3.7 ± 0.3
$\log(K_{c1} \cdot \text{M})$	7.35 ± 0.09

$\chi^2 = 0.0028$

Considering scheme 6.1, the rate constant k_{OH} has to be taken into account. Using $K_{a2} = 10^{-3.74}$ M, $K_{a3} = 10^{-9.89}$ M, $K_{cH} = 10^{3.70}$ M⁻¹, $K_{c1} = 10^{7.20}$ M⁻¹ and $K_{cLH_2} = 10$ M⁻¹ (see table 5.6), the value of $k_{OH} = 0.027 \pm 0.008$ M⁻¹s⁻¹ was obtained. The fitted curve is indistinguishable from the curve (d) in figure 6.4 indicating that in scheme 6.1, the lower reaction path does not contribute to the reaction rate.

B) Fitting of the data assuming a metal chelate ring-closure rate-determining step

As in part A), in this section it is assumed that the stopped-flow experiments are accurately described by fitting the change of absorption by a single relaxation effect. However, in contrast to part A), the rate-determining step is here assumed to be the metal chelate ring-closure (see section 3.1.3).



where \longleftrightarrow : fast step

\rightleftharpoons : slow step

Scheme 6.2

$$\frac{1}{\tau} = (k + k_H K_{cH}' [H^+]) \left(\frac{K_{c1}' \frac{1 + K_{cH}' [H^+]}{1 + \frac{[H^+]}{K_{a3}} + \frac{[H^+]^2}{K_{a2} K_{a3}}} Ni_o}{\left\{ 1 + K_{c1}' \frac{1 + K_{cH}' [H^+]}{1 + \frac{[H^+]}{K_{a3}} + \frac{[H^+]^2}{K_{a2} K_{a3}}} Ni_o \right\} (1 + K_{cH}' [H^+])} + \frac{K}{(1 + K_{cH}' [H^+])} \right) \quad (6.13)$$

Fitting of the data assuming scheme 6.2 was not possible.

6.1.1.2 Asp in excess

Using the equilibrium constants obtained from potentiometric and spectrophotometric measurements shown in figure 5.3 and 5.4, the following species distribution diagram results for the case in which Asp was in excess:

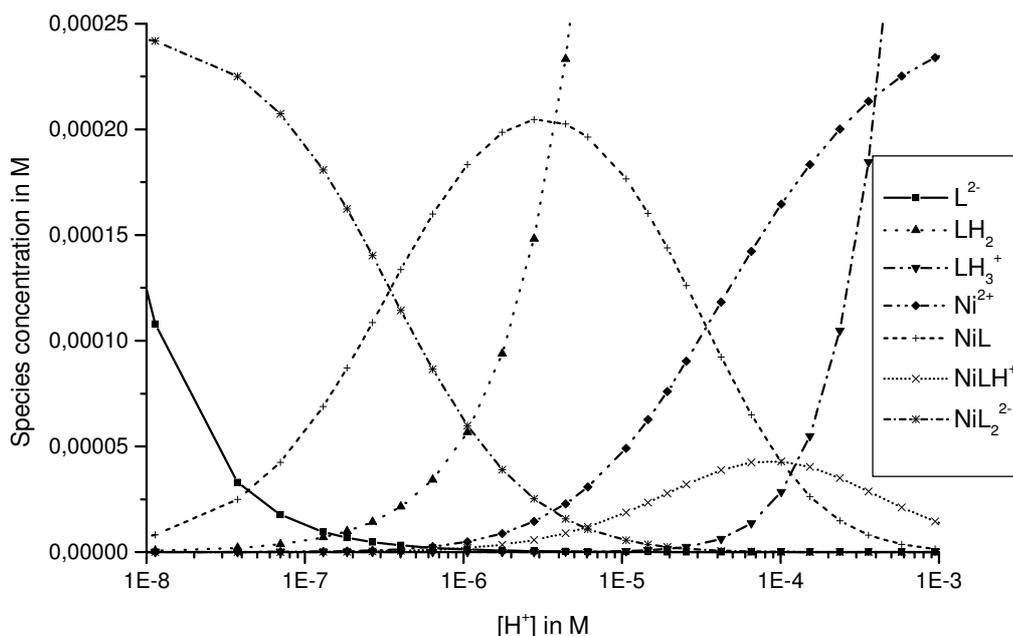


Figure 6.5

Species distribution diagram for the case where Asp was in excess;

$Asp_o = 10^{-2}$ M, $Ni_o = 2.5 \times 10^{-4}$ M, $I = 0.1$ M (NaCl), $buffer_o = 5.10^{-3}$ M, $indicator_o = 2.10^{-5}$ M; $T=25^\circ\text{C}$

The concentrations of $NiOH^+$ and $Ni(OH)_2$, are negligibly small in the whole pCh-range.

When aspartic acid was present in excess, two different types of relaxation behaviour were observed:

- i) from pCh 3.0 to pCh 5.0: only one relaxation process
- ii) from pCh 6.0 to pCh 8.0: two relaxation processes.

From pCh 5.0 to pCh 6.0 is an 'overlap region' where it cannot be unambiguously decided whether a single or a double relaxation processes best describes the data.

The relaxation times obtained by these fits are shown in figure 6.6. The fact that at $3 < \text{pCh} < 5$ the measurements can be very accurately fitted by single relaxation times aroused doubts regarding the value of K_{MLLH} obtained from thermodynamic measurements (table 5.4).

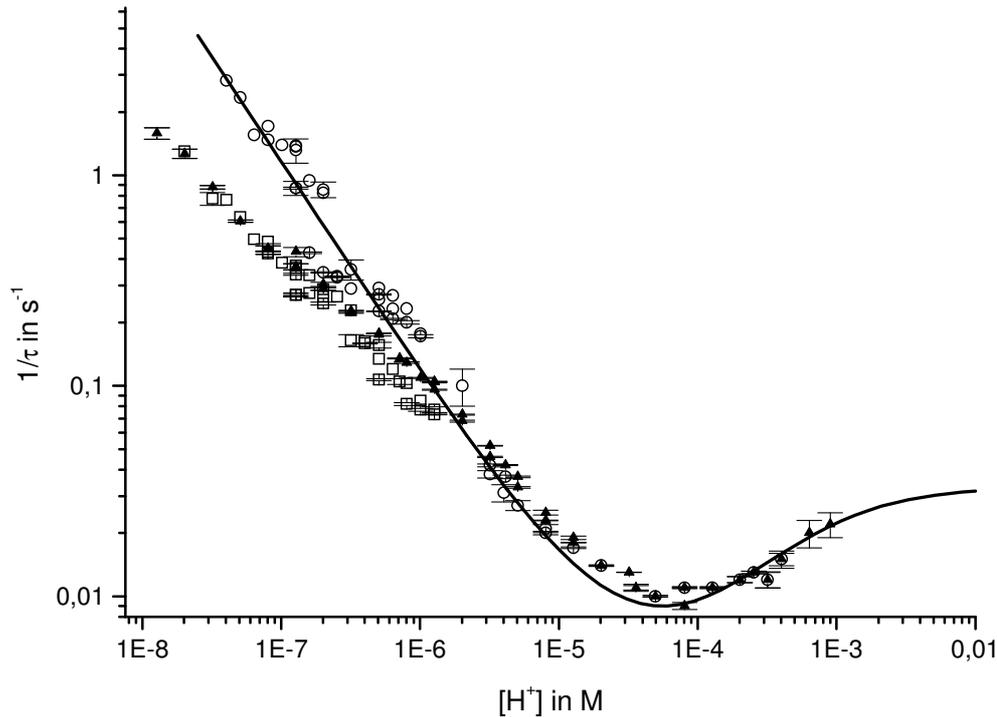


Figure 6.6

Reciprocals of the relaxation times of the reaction of Ni(II) ions with Asp as a function of proton concentration for the case where Asp was present in excess;

$Asp_0 = 10^{-2}$ M, $Ni_0 = 2.5 \times 10^{-5}$ M, $I = 0.1$ M (NaCl), $buffer_0 = 5.10^{-3}$ M, $indicator_0 = 2.10^{-5}$ M; $T = 25^\circ\text{C}$

▲ : Data fitted to a single relaxation effect; □ and ○ : Data fitted to two relaxation effects; (The fit for nickel(II) ions in excess is also shown (solid line) as a comparison).

The ratios of the relaxation amplitudes (A_{II} / A_I) and of the relaxation times τ_{II} / τ_I are shown in figure 6.7.

Figures 6.6 and 6.7 show that:

- i) the longer relaxation time τ_{II} is similar to the value for τ obtained from the fitting by a single relaxation effect
- ii) the ratio of the relaxation amplitudes (A_{II} / A_I) is greater than unity at $[H^+] < 2 \times 10^{-7}$ M.
- iii) the ratio of the relaxation times at $pH > 5.70$ is constant at $\tau_{II} / \tau_I \approx 3.5$ at $[H^+] < 2 \times 10^{-7}$ M

However, in contrast to figures 6.1 and 6.2

- iv) both ratios show a systematic dependence to the proton concentration such that it is concluded that the shorter time is a real effect, in spite of observation (i).

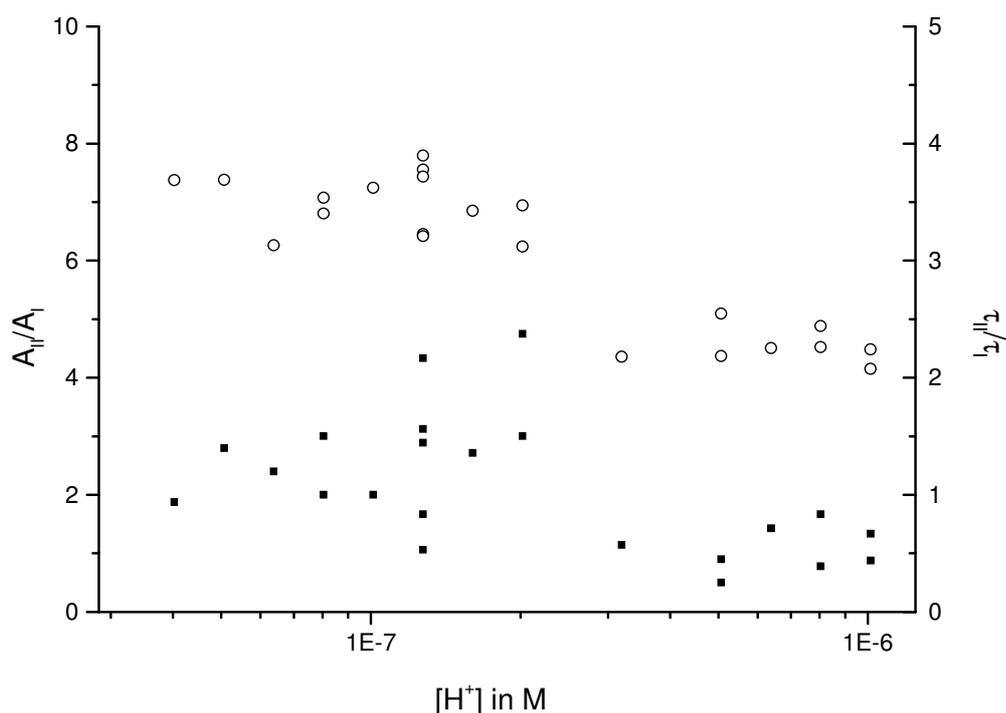


Figure 6.7

The ratio of the relaxation amplitudes (A_{II} / A_I ; ■) and of the relaxation times (τ_{II} / τ_I ; ○) for the case where Asp is in excess; I refers to the faster relaxation effect and II refers to the slower relaxation effect;

$Ni_o = 2.5 \times 10^{-4}$ M, $Asp_o = 10^{-2}$ M, $I = 0.1$ M (NaCl), $buffer_o = 5.10^{-3}$ M, $indicator_o = 2.10^{-5}$ M; $T = 25^\circ\text{C}$

Moreover the pCH-dependence of the relaxation times obtained for solutions in which nickel(II) ions were present in excess agrees with the results presented here when only one relaxation effect is observed (pCH < 6) and with the faster effect (pCH > 6) when two relaxation effects are present. The second relaxation times were longer, see figure 6.6.

These observations can be explained by a scheme in which the formation of the 1:2 complexes is slow, and coupled to the 1:1 complexes' formation such that evaluation of the 1:2 complexes' kinetics requires the decoupling of the two values of τ using secular equations.

A) Fitting of the two-relaxation-time curves

In this section it is assumed that the stopped-flow experiments are accurately described by fitting the change of absorption to two relaxation effects. Furthermore a water-release rate-determining step is assumed (see section 3.1.1). Since $\tau_{II} < 10 \tau_I$, the two consecutive reactions have similar speeds and cannot be treated separately. For the evaluation of the rate laws, scheme 5.2 is simplified to the following scheme:



Scheme 6.3

where

$$[M] = [Ni^{2+}]$$

$$[L] = [LH_3^+] + [LH_2] + [LH^-] + [L^{2-}]$$

$$[ML] = [NiLH_2^{2+}] + [NiLH^+] + [NiL]$$

$$[ML_2] = [Ni(LH)_2] + [NiLLH^-] + [NiL_2^{2-}]$$

The values of κ_i are functions of rate constants, equilibrium constants and proton concentration.

For scheme 5.2 they are given in equations (6.14) to (6.19):

$$\kappa_1 = \left(k_{1H} + \frac{k_1 K_{a3}}{[H]} + \frac{k_{0H}[H]}{K_{a2}} \right) \gamma_{LH} \quad (6.14)$$

$$\kappa_{-1} = \left(\frac{k_{1H}}{K_{c1} K_{cH} K_{a3}} + \frac{k_1}{K_{c1} K_{cH} [H]} + \frac{k_{0H} K_{a2}}{K_{c1} K_{cH} K_{a3} [H]} \right) \gamma_{NiLH} \quad (6.15)$$

$$\kappa_2 = \left(k_{2H} + \frac{k_2 K_{a3}}{K_{cH} [H]^2} \right) \gamma_{NiLH} \gamma_{LH} \quad (6.16)$$

$$\kappa_{-2} = \left(\frac{\frac{k_{2H} K_{cH} [H]^2}{K_{a3}} + k_2}{K_{c2} + \frac{K_{M(LH)_2} K_{cH} [H]^2}{K_{a3}} + K_{ML2} [H] K_{c2}} \right) \quad (6.17)$$

and

$$\gamma_{LH} = \left(\frac{K_{a1} K_{a2} [H]}{K_{a1} (K_{a2} K_{a3} + K_{a2} [H] + [H]^2) + [H]^3} \right) \quad (6.18)$$

$$\gamma_{NiLH} = \left(\frac{K_{cH} [H]}{K_{cH2} K_{cH} [H]^2 + K_{cH} [H] + 1} \right) \quad (6.19)$$

The rate equations for the general reaction shown in scheme 6.3 are given by

$$\frac{d[M]}{dt} = -\kappa_1 [M][L] + \kappa_{-1} [ML] \quad (6.20)$$

$$\frac{d[ML_2]}{dt} = \kappa_2 [ML][L] - \kappa_{-2} [ML_2] \quad (6.21)$$

The reactions occur under pseudo first order conditions, since

- i) the solutions were buffered and
- ii) $Ni_0 \ll L_0$

Therefore, substituting $[Y] = [Y]_e + x_Y$ (where the term x represents the deviation of the respective concentrations from the equilibrium state) into (6.20) and (6.21) we obtain

$$\frac{dx_M}{dt} = -\kappa_1[M]x_L - \kappa_1[L]x_M + \kappa_{-1}x_{ML} \quad (6.22)$$

$$\frac{dx_{ML_2}}{dt} = \kappa_2[ML]x_L + \kappa_2[L]x_{ML} - \kappa_{-2}x_{ML_2} \quad (6.23)$$

x_L and x_{ML} can be eliminated by the balance equations

$$x_M + x_{ML} + x_{ML_2} = 0 \quad (6.24)$$

$$x_L + x_{ML} + 2x_{ML_2} = 0 \quad (6.25)$$

giving

$$\frac{dx_M}{dt} = -\kappa_1[M](x_M - x_{ML_2}) - \kappa_1[L]x_M + \kappa_{-1}(-x_M - x_{ML_2}) \quad (6.26)$$

$$\frac{dx_{ML_2}}{dt} = \kappa_2[ML](x_M - x_{ML_2}) + \kappa_2[L](-x_M - x_{ML_2}) - \kappa_{-2}x_{ML_2} \quad (6.27)$$

with the result

$$\frac{dx_M}{dt} = a_{++}x_M + a_{+2}x_{ML_2} \quad (6.28)$$

$$\frac{dx_{ML_2}}{dt} = a_{2+}x_M + a_{22}x_{ML_2} \quad (6.29)$$

where

$$a_{++} = -\{\kappa_1([M] + [L]) + \kappa_{-1}\} \quad (6.30)$$

$$a_{+2} = \kappa_1[M] - \kappa_{-1} \quad (6.31)$$

$$a_{2+} = \kappa_2([ML] - [L]) \quad (6.32)$$

$$a_{22} = -\{\kappa_2([ML] + [L]) + \kappa_{-2}\} \quad (6.33)$$

As opposed to the κ_i values, the above a_{xy} values are always valid for the above generalized scheme and its assigned quantity balances and are independent of the proposed mechanism. Such a treatment is convenient at the stage where different reaction schemes were tried out.

The two simultaneous differential equations (6.28) and (6.29) are solved by transforming them into two equations of the form

$$\frac{dy_i}{dt} = -\frac{1}{\tau} y_i \quad (6.34)$$

where the y_i are linear combinations of the x_i , i.e.

$$y_i = \beta_{iM} x_M + \beta_{iML_2} x_{ML_2} \quad (6.35)$$

Since equation (6.34) is invariant to a constant factor of y_i , the following can be set $\beta_{iML_2} = 1$ and

$\beta_{iM} = \beta_i$, giving

$$y_i = \beta_i x_M + x_{ML_2} \quad (6.36)$$

Substituting equations (6.28), (6.29) and (6.36) in (6.34) we get

$$\left(\frac{1}{\tau_i} \beta_i + \beta_i a_{++} + a_{2+} \right) x_M + \left(\frac{1}{\tau_i} + \beta_i a_{+2} + a_{22} \right) x_{ML_2} = 0 \quad (6.37)$$

Since the coefficients of the independent variables x_M and x_{ML_2} must vanish separately, two

equations for $\frac{1}{\tau_i}$ and β_i are obtained. Eliminating β_i a quadratic in $\frac{1}{\tau_i}$ is obtained, whose roots

are

$$\frac{1}{\tau_{I,II}} = \frac{1}{2} \left(-a_{++} - a_{22} \pm \sqrt{(-a_{++} - a_{22})^2 - 4a_{++}a_{22} - 4a_{+2}a_{2+}} \right) \quad (6.38)$$

This may be abbreviated as

$$\frac{1}{\tau_{I,II}} = \frac{1}{2} \left(\Sigma \pm \sqrt{\Sigma^2 - 4\Pi} \right) \quad (6.39)$$

with

$$\Sigma = -a_{++} - a_{22} \quad (6.40)$$

and

$$\Pi = a_{++}a_{22} - a_{+2}a_{2+} \quad (6.41)$$

Substituting equations (6.30) - (6.33) into (6.40) and (6.41) yields respectively

$$\Sigma = \{ \kappa_1([M] + [L]) + \kappa_{-1} \} + \{ \kappa_2([ML] + [L]) + \kappa_{-2} \} \quad (6.42)$$

$$\Pi = \{ \kappa_1([M] + [L]) + \kappa_{-1} \} \{ \kappa_2([ML] + [L]) + \kappa_{-2} \} - (\kappa_1[M] - \kappa_{-1})(\kappa_2([ML] - [L])) \quad (6.43)$$

i.e. Σ is a sum over terms of which each refers to one of the four rate constants. On the other hand, Π is a sum over terms of which each contains the product of a rate constant of the first step and a rate constant of the second step.

For the case where Asp occurs in excess, the following approximations can be done:

i) $[ML] \ll [L]$ or $\kappa_1[M] \ll \kappa_{-1}$

ii) $[ML_2] \ll [L]$ or $\kappa_2[ML] \ll \kappa_{-2}$

iii) $[M_o] \ll [L_o]$ giving $[L] \approx L_o$, resulting in

$$a_{++} \approx -(\kappa_1 L_o + \kappa_{-1}) \quad (6.44)$$

$$a_{+2} \approx -\kappa_{-1} \quad (6.45)$$

$$a_{2+} \approx -\kappa_2 L_o \quad (6.46)$$

$$a_{22} \approx -(\kappa_2 L_o + \kappa_{-2}) \quad (6.47)$$

Equation (6.38) then reads

$$\frac{1}{\tau_I} = \frac{1}{2} \left([\kappa_1 L_o + \kappa_{-1} + \kappa_2 L_o + \kappa_{-2}] + \sqrt{\{(\kappa_1 L_o + \kappa_{-1}) - (\kappa_2 L_o + \kappa_{-2})\}^2 + 4\kappa_{-1}\kappa_2 L_o} \right) \quad (6.48)$$

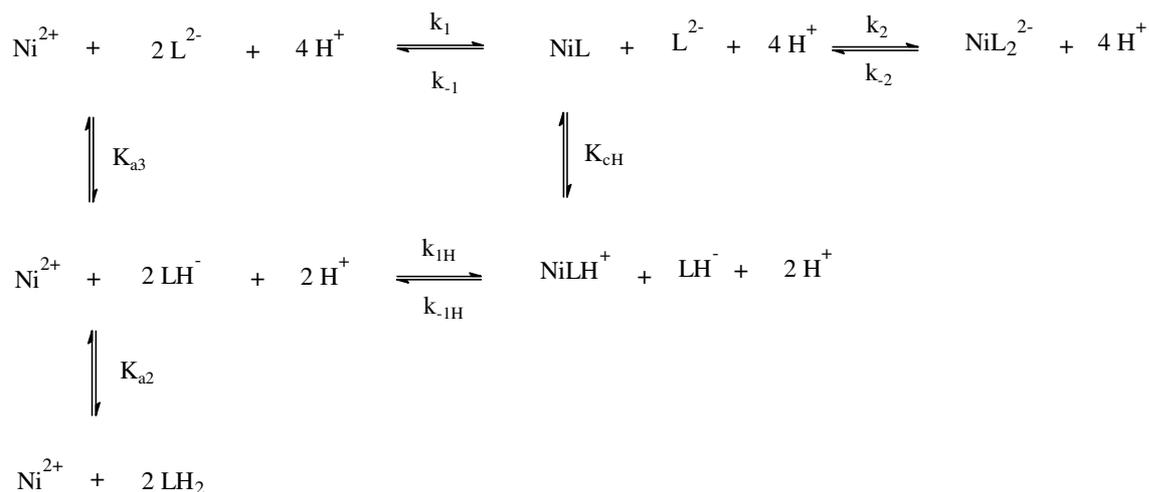
and

$$\frac{1}{\tau_{II}} = \frac{1}{2} \left([\kappa_1 L_o + \kappa_{-1} + \kappa_2 L_o + \kappa_{-2}] - \sqrt{\{(\kappa_1 L_o + \kappa_{-1}) - (\kappa_2 L_o + \kappa_{-2})\}^2 + 4\kappa_{-1}\kappa_2 L_o} \right) \quad (6.49)$$

Equation (6.48): describes the faster relaxation effect; equation (6.49): describes the slower relaxation effect;

i) Assuming a reaction scheme without the species NiLLH⁻ and Ni(LH)₂

Due to the highly erroneous value for the stability constant K_{MLLH} , (see table 5.4) it is concluded that the species Ni(LH)₂ may occur in insignificant amounts. Consequently, evaluations of the above equations was carried out, assuming the reaction scheme 6.4, i.e. the terms in equations (6.14) to (6.19) containing k_{OH} , k_{2H} , K_{ML2} and $K_{M(LH)2}$ are neglected.



Scheme 6.4

At $\text{pCH} < 5.5$, the approximation that $[\text{ML}_2] \ll [\text{ML}]$, or $\kappa_2 L_o \ll \kappa_{-2}$ can be done (see figure 6.5).

This leads to $a_{22} \approx -\kappa_{-2}$ and to the following solutions:

$$\frac{1}{\tau_I} = \kappa_1 L_o + \kappa_{-1} \quad (6.50)$$

and

$$\frac{1}{\tau_{II}} = \kappa_{-2} \quad (6.51)$$

The second relaxation time depends on κ_{-2} and therefore corresponds to the formation of NiL₂²⁻. Since this species is neglected at $\text{pCH} > 5.5$, the amplitude of the second relaxation effect is undetectably small. This is why at this pCH range, only one relaxation effect is observed and hence no new constants can be fitted. For scheme 6.4, equation (6.50) is identical to equation (6.12), indicating that the same relaxation time is expected for the case when Asp is in excess at $\text{pCH} < 5$ as that obtained for the case when Ni(II) ions are present in excess.

On the other hand at $\text{pH} > 5.5$ the approximation $[M] \ll [ML]$, or $\kappa_1 L_o \gg \kappa_{-1}$ can be done, (see figure 6.5) leading to $a_{++} \approx \kappa_1 L_o$. Furthermore, since the approximation $[ML_2] \ll [ML]$ no longer holds, $a_{22} \approx -(\kappa_2 L_o + \kappa_{-2})$ yielding the following solutions:

$$\frac{1}{\tau_I} = \kappa_1 L_o \quad (6.52)$$

and

$$\frac{1}{\tau_{II}} = \kappa_2 L_o + \kappa_{-2} \quad (6.53)$$

Hence for the whole pH range equations (6.48) and (6.49) will be simplified to

$$\frac{1}{\tau_I} = \kappa_1 L_o + \kappa_{-1} \quad (6.54)$$

and

$$\frac{1}{\tau_{II}} = \kappa_2 L_o + \kappa_{-2} \quad (6.55)$$

Fitting of equations (6.54) and (6.55) for $\text{pH} > 6$.

These solutions are much simpler than equations (6.48) and (6.49) and hence are used to estimate the values of k_2 and K_{c2} .

Equation 6.55 for scheme 6.4 reads

$$\frac{1}{\tau_{II}} = \left(\frac{k_2 K_{a3}}{K_{cH} [H]^2} \right) \left(\frac{K_{cH} [H]}{K_{cH} [H] + 1} \right) \left(\frac{K_{a2}}{K_{a2} + [H^+]} \right) L_o + \left(\frac{k_2}{K_{c2}} \right).$$

Using $K_{a2} = 10^{-3.74}$ M, $K_{a3} = 10^{-9.89}$ M, $K_{cH} = 10^{3.70}$ M⁻¹, the values shown in table 6.3 were obtained for k_2 and K_{c2} (dotted line).

Table 6.3 Thermodynamic and kinetic constants fitted from the reciprocal of the longer relaxation time of the reaction of Ni(II) ions with Asp as a function of proton concentration for the case where Asp was present in excess for the reaction scheme 6.4

	Results
k_2 in M ⁻¹ s ⁻¹	24000 ± 2200
log (K_{c2} .M)	5.42 ± 0.04

Equation (6.52) can be rewritten as $\frac{1}{\tau_l} \approx \left(k_1 \frac{K_{a3}}{[H^+]} L_o \right)$. Fitting of this equation gives curve (a) shown in figure 6.4. Using the values of $k_{1H} = 0.2 \text{ M}^{-1}\text{s}^{-1}$, $K_{a2} = 10^{-3.74} \text{ M}$ and $K_{a3} = 10^{-9.89} \text{ M}$, (see table 5.6 and table 6.2), the value of $90000 \pm 5000 \text{ M}^{-1}\text{s}^{-1}$ is obtained for k_1 (solid line in figure 6.8).

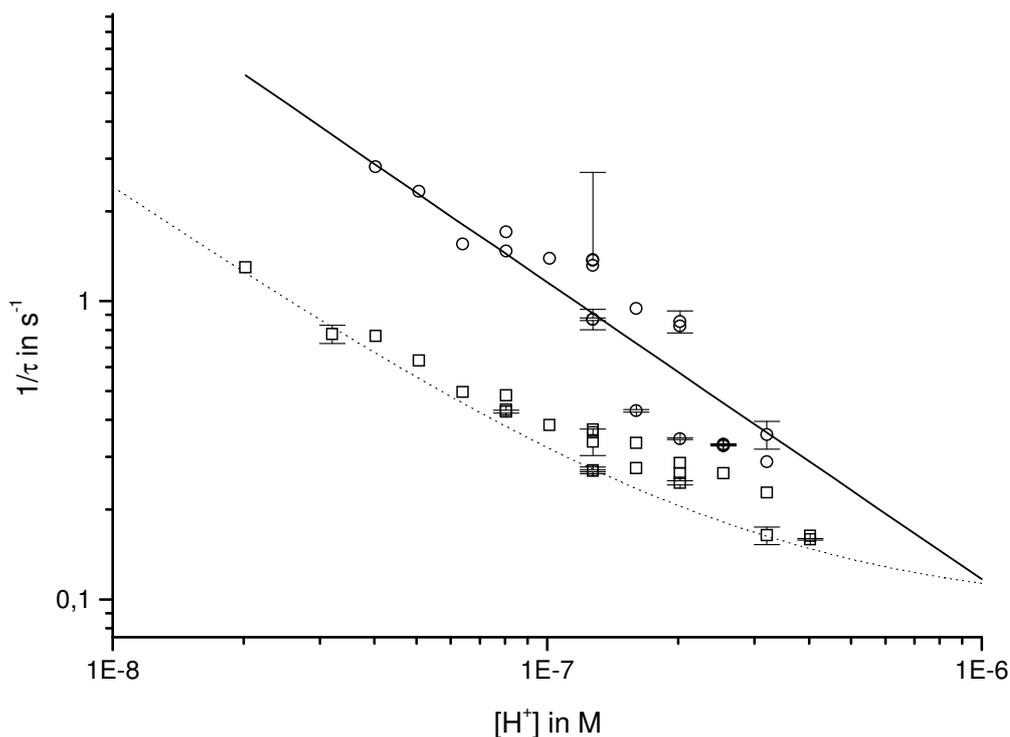


Figure 6.8

Fitted dependencies of the reciprocals of the short (o and solid line) and long (□ and dotted line) relaxation times for the reaction of Ni(II) ions with Asp as a function of proton concentration for the case where Asp was present in excess for the range $6 \leq \text{pH} \leq 8$;

$\text{Asp}_o = 10^{-2} \text{ M}$, $\text{Ni}_o = 2.5 \times 10^{-4} \text{ M}$, $I = 0.1 \text{ M}$ (NaCl), $\text{buffer}_o = 5.10^{-3} \text{ M}$, $\text{indicator}_o = 2.10^{-5} \text{ M}$; $T = 25^\circ\text{C}$

Fitting of equations (6.54) and (6.55) for $3 < \text{pH} < 8$.

Equations 6.54 and 6.55 gave the fits (for the whole pH range) shown in fig 6.9.

Equation 6.54 is identical to equation 6.12 and hence yields the same constants as shown in table 6.2.

For equation 6.55, the values for K_{a2} , K_{a3} and K_{cH} shown in tables 5.7 and 5.8 are used, yielding the values shown in table 6.4 for k_2 and K_{c2} .

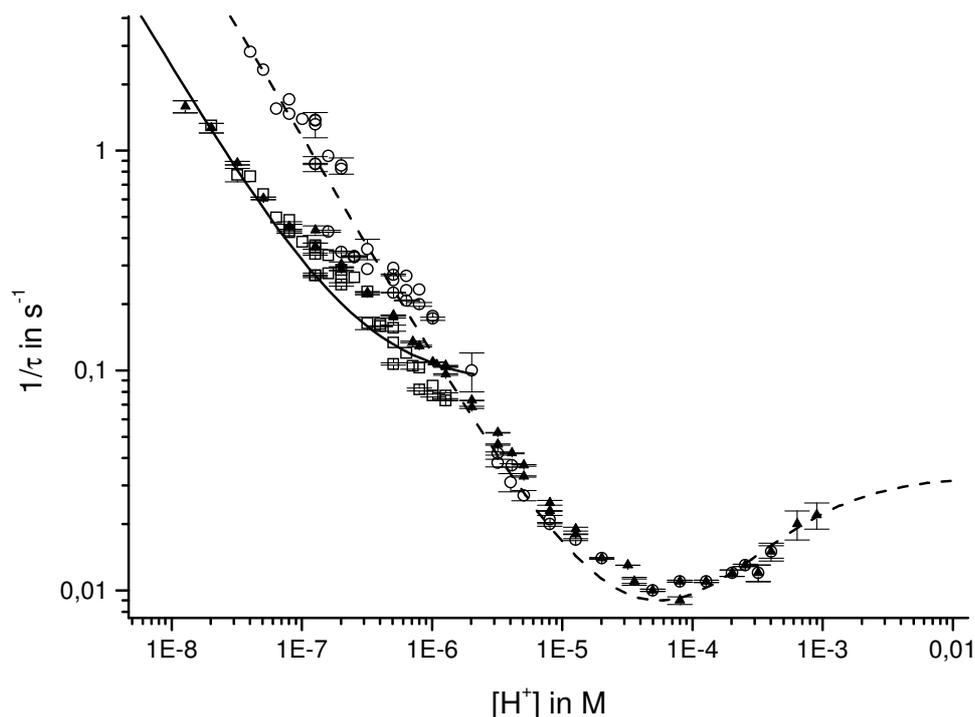


Figure 6.9

Fitted dependencies of the reciprocals of the relaxation times for the reaction of Ni(II) ions with Asp as a function of proton concentration for the case where Asp was present in excess, using equation 6.36 (segmented line) and 6.37 (solid line).

$Asp_0 = 10^{-2}$ M, $Ni_0 = 2.5 \times 10^{-4}$ M, $I = 0.1$ M (NaCl), $buffer_0 = 5.10^{-3}$ M, $indicator_0 = 2.10^{-5}$ M; $T = 25^\circ\text{C}$

Table 6.4 Thermodynamic and kinetic constants fitted from the reciprocal of the longer relaxation time of the reaction of Ni(II) ions with Asp as a function of proton concentration for the case where Asp was present in excess for the reaction scheme 6.4, using equation 6.55

	Results
k_2 in $\text{M}^{-1}\text{s}^{-1}$	22000 ± 2000
$\log(K_{c2} \cdot M)$	5.41 ± 0.03

ii) Assuming a reaction scheme with the species $NiLLH^+$ and $Ni(LH)_2$

Using the equilibrium constants (obtained from potentiometric and spectrophotometric measurements) shown in table 5.4, the species distribution diagram in figure 6.10 results for the case in which Asp was in excess.

The existence of the species $Ni(LH)_2$ at significant concentrations at the pCH range 3.5 to 5.5 is in contradiction to the observed single relaxation effect in this pCH range. Simulations of equation 6.48 can however be used to indicate the maximal value of K_{MLLH} , figure 6.11.

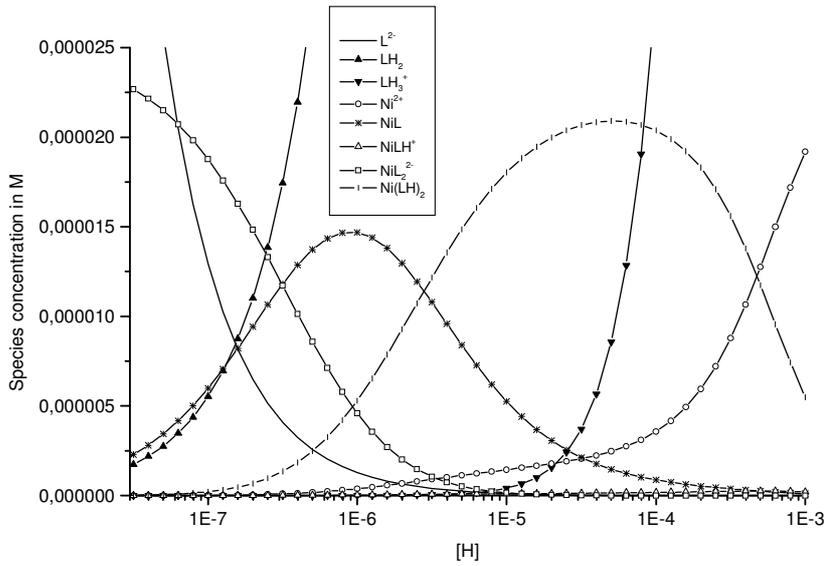


Figure 6.10
Species distribution diagram for the case where Asp was in excess using a scheme involving the species NiLLH and Ni(LH)₂ in addition to NiLH⁺, NiL and NiL₂²⁻.

Asp₀ = 10⁻² M, Ni₀ = 2.5x10⁻⁴ M, I = 0.1 M (NaCl), buffer₀ = 5.10⁻³ M, indicator₀ = 2.10⁻⁵ M; T=25°C

Equation 6.48 fitted the pCH region 3 to 5 only when K_{MLLH} was reduced to 10⁶ M⁻¹. However, the constant for the formation of Ni(LH)₂ in scheme 5.2 could not be reasonably fitted.

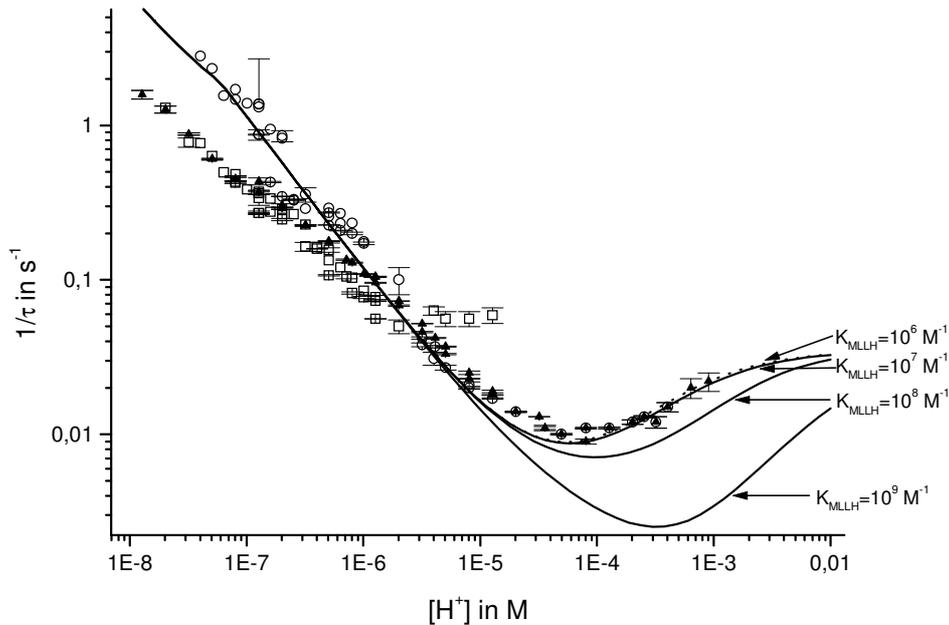


Figure 6.11
Simulations for the reciprocals of the relaxation times for the reaction of Ni(II) ions with Asp as a function of proton concentration showing the sensitivity of the function to K_{MLLH}; The dotted line shows the fit for τ_1 .

Asp₀ = 10⁻² M, Ni₀ = 2.5x10⁻⁴ M, I = 0.1 M (NaCl), buffer₀ = 5.10⁻³ M, indicator₀ = 2.10⁻⁵ M; T=25°C

Additional experiments indicated that the value of $\log (K_{MLLH} \cdot M)$ should be less than 9. These are:

i) Solubility

In an attempt to crystallise $Ni(LH)_2$, NiL and NiL_2 , three separate solutions were prepared containing Asp (0.125M) and nickel (II) ions (0.05M) set at pH 3.50, pH 6.00 and pH 10.50 and freeze-dried. A light green, blue and darker blue samples were formed. On re-dissolving the resulting powders, the first sample gave a white powder (presumably aspartic acid) and a green solution (presumably hexaaquanickel(II)). On the other hand, the samples at pH 6.00 and pH 10.50 formed blue solutions.

ii) UV-Vis Spectroscopy

The much smaller blue shift for $NiLH^+$ (and eventually $Ni(LH)_2$) in comparison to NiL and NiL_2 indicates the absence of amino group bonding to nickel ions (see figure 5.7 and figure 5.10).

iii) IR and Raman Spectroscopy

IR (figures 10.3 – 10.7 in section 10.1.2.2) and Raman measurements (figures 10.8 - 10.12 in section 10.1.2.2) also indicate the presence of a free amino group in $NiLH^+$ (and eventually $Ni(LH)_2$).

iv) Stability constant

The stability constant for monosuccinatonickel(II) is 40 M^{-1} (compared to $K_{M(LH)_2} = 18000 \text{ M}^{-1}$ for $K_{MLLH} = 10^9 \text{ M}^{-1}$ and to $K_{M(LH)_2} = 18 - 180 \text{ M}^{-1}$ for $K_{MLLH} = 10^6 - 10^7 \text{ M}^{-1}$).

These observations suggested that in the species $Ni(LH)_2$ there is no Ni-amino group bonding and hence its structure is more likely to be that in figure 6.12 (a) rather than (b).

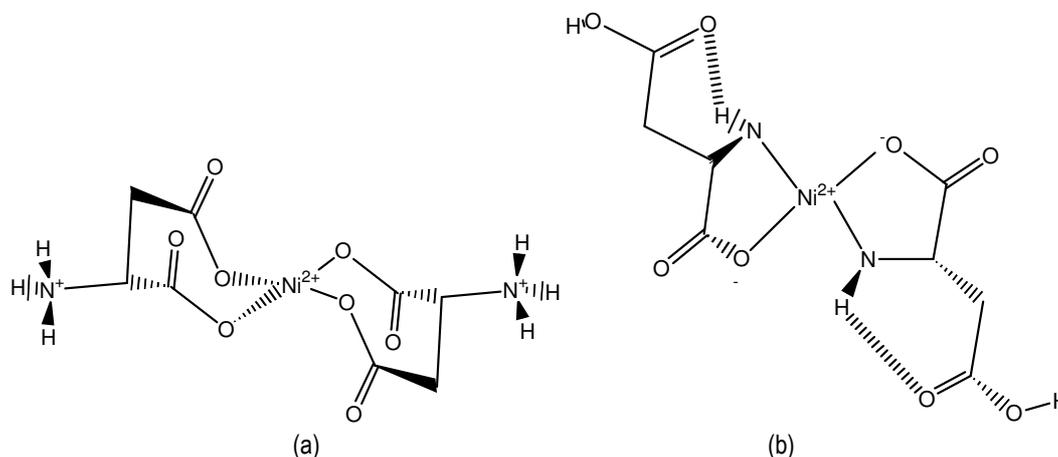


Figure 6.12
Probable structure of $Ni(LH)_2$

Moreover, using $K_{MLLH} = 10^7 \text{ M}^{-1}$, the concentration of $\text{Ni}(\text{LH})_2$ becomes negligible (see figure 6.13 in contrast to figure 6.5) and hence the nickel complexes occurring in significant amounts at $\text{pH} < 5.5$ are NiLH^+ and NiL , i.e. identical to the case where $\text{Ni}(\text{II})$ ion occur in excess.

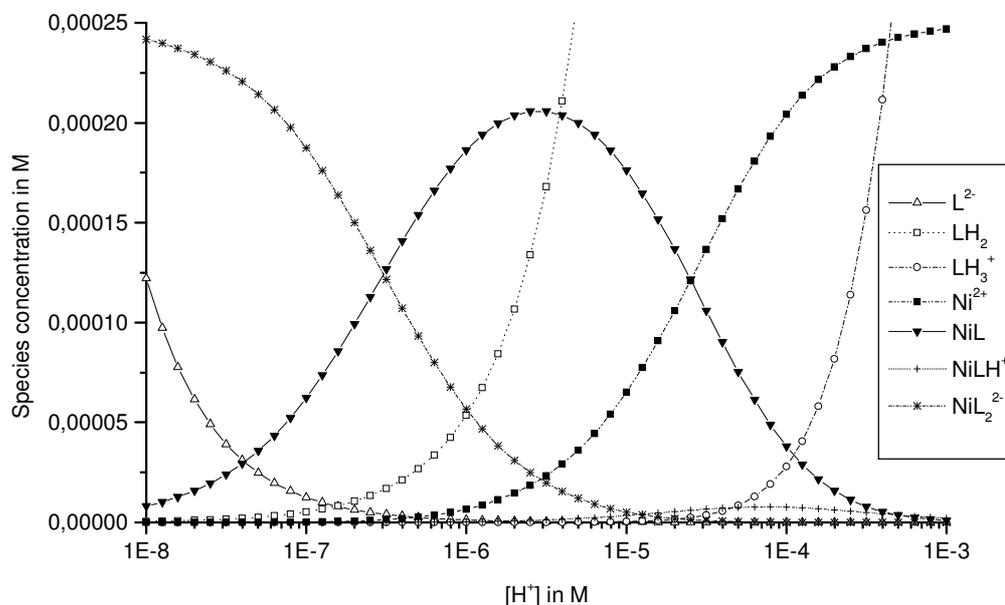


Figure 6.13

Species distribution diagram for the case where Asp was in excess, using $K_{MLLH} = 10^7 \text{ M}^{-1}$; The concentrations of NiOH^+ and $\text{Ni}(\text{OH})_2$ are negligibly small.

$\text{Asp}_o = 10^{-2} \text{ M}$, $\text{Ni}_o = 2.5 \times 10^{-4} \text{ M}$, $I = 0.1 \text{ M}$ (NaCl), $\text{buffer}_o = 5 \cdot 10^{-3} \text{ M}$, $\text{indicator}_o = 2 \cdot 10^{-5} \text{ M}$; $T = 25^\circ \text{C}$

Since $\text{Ni}(\text{LH})_2$ occurs in insignificantly small concentration, if at all, the value of the rate constant for its formation cannot be fitted. Additionally, fitting equation 6.48 using scheme 6.4 gave an identical curve to the one shown in figure 6.11 for $K_{MLLH} = 10^6 \text{ M}^{-1}$. Hence it can be concluded that scheme 6.4 is the simplest mechanism with which all the thermodynamic and kinetic results can be explained.

6.1.2 Concentration-Dependence of the Reaction Rate

As discussed in section 6.1.1.1Ai, for $\text{pH} 7.0$, equation 6.12 can be approximated by the equation

$$\frac{1}{\tau} = k_1 \frac{K_{a3}}{[\text{H}^+]} (\text{Ni}_o + L_o). \quad (6.56)$$

6.1.2.1 Dependence of the Reaction Rate on the Concentration of Nickel(II) ions; Nickel(II) ions in excess

Substituting the value of $k_1 = 90000 \text{ M}^{-1}\text{s}^{-1}$ in equation (6.54), the gradient of the fitted line shown in figure 6.14 yields the value of $\text{p}K_{a3} = 9.80 (\pm 0.1)$. This agrees well with the value obtained from thermodynamic measurements ($\text{p}K_{a3} = 9.89$, see table 5.7).

The value of the intercept c is too small for reliable calculations regarding K_{c1} . In fact, as discussed in section 6.1.1.1Aiii, equation 6.12 becomes sensitive to K_{c1} at $\text{p}H < 5$.

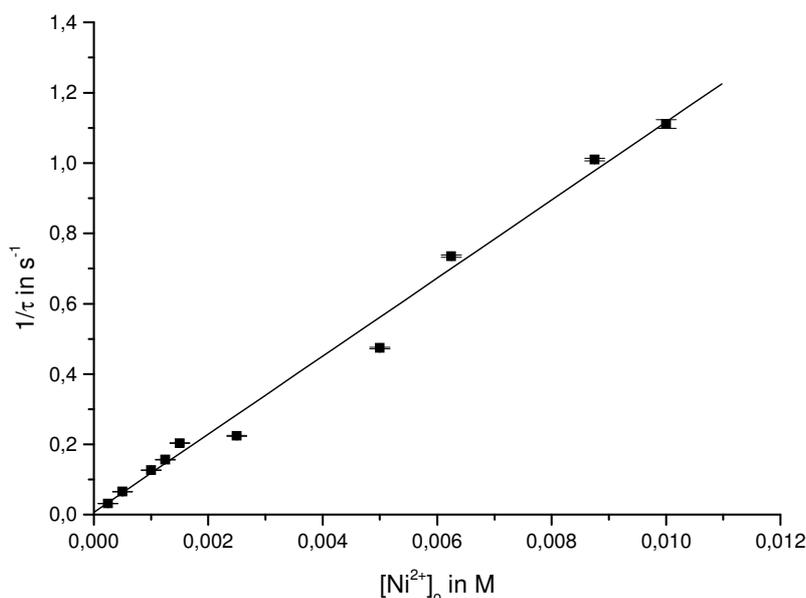


Figure 6.14

Fitted dependencies of the reciprocals of the relaxation times for the reaction of Ni(II) ions with Asp as a function of the concentration of Ni(II) ions for the case where Ni(II) ions were present in excess;

[Asp]₀ = 2.5×10^{-5} M, $I = 0.1$ M (NaCl), $\text{Lut}_0 = 5 \cdot 10^{-3}$ M, $\text{BTB}_0 = 2 \cdot 10^{-5}$ M, $\text{p}H = 7.00$; $T = 25^\circ\text{C}$

In order to fit the value of K_{cH} , experiments were carried out at $\text{p}H 4.30$, figure 6.15. At this $\text{p}H$, the function becomes sensitive to the value of K_{cH} such that equation 6.12 has to be used. From this equation, the ratio of the gradient m to the intercept c of the plot in figure 6.15, yields the equation 6.57.

$$\frac{m}{c} = \left(\frac{K_{a2}}{K_{a2} + [H^+]} \right) \left(\frac{K_{c1} K_{a3} (K_{cH} [H^+] + 1)}{[H^+]} \right) \quad (6.57)$$

Using the value of $K_{a2} = 10^{-3.74}$ M, $K_{a3} = 10^{-9.89}$ M and $\log(K_{c1} \cdot M) = 7.20$ (see tables 5.7 and 5.8), the value of $\log(K_{cH} \cdot M) = 4.3 \pm 0.1$ is obtained. A high error is always associated with the value of K_{cH} , since the term $(K_{cH} [H^+] + 1)$ is actually fitted in a range where $K_{cH} [H^+] \approx 1$.

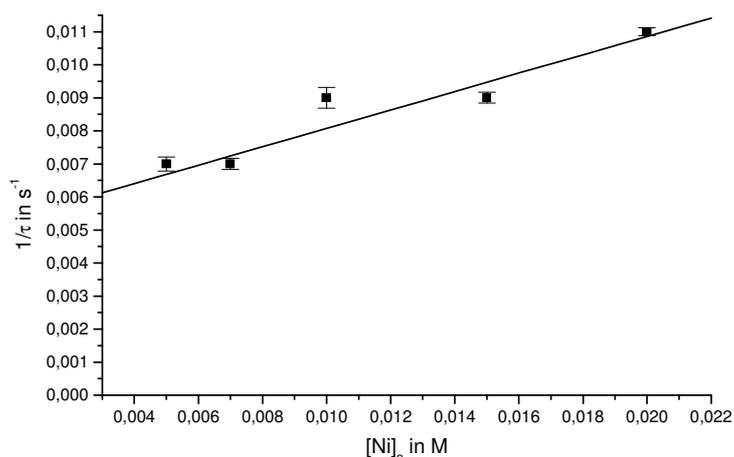


Figure 6.15

Fitted dependencies of the reciprocals of the relaxation times for the reaction of Ni(II) ions with Asp as a function of Ni(II) ions' concentration for the case where Ni(II) ions were present in excess; Asp₀ = 5.10⁻⁴ M, I = 0.1 M (NaCl), Ac₀ = 5.10⁻³ M, BCG₀ = 2.10⁻⁵ M, pH = 4.30; T=25°C

6.1.2.2 Dependence of the Reaction Rate on the Aspartic Acid Concentration; Aspartic Acid in excess

When aspartic acid is in excess, at pH 4.20, the relationship between the reciprocals of the relaxation times as a function of Asp concentration is identical, within experimental errors to that as a function of the concentration of Ni(II) ions, figure 6.16. Using the value of $K_{a2} = 10^{-3.74}$ M, $K_{a3} = 10^{-9.89}$ M and $\log(K_{c1} \cdot M) = 7.20$ (see table 5.7 and 5.8), the value of $\log(K_{cH} \cdot M) = 4.5 \pm 0.1$ is obtained.

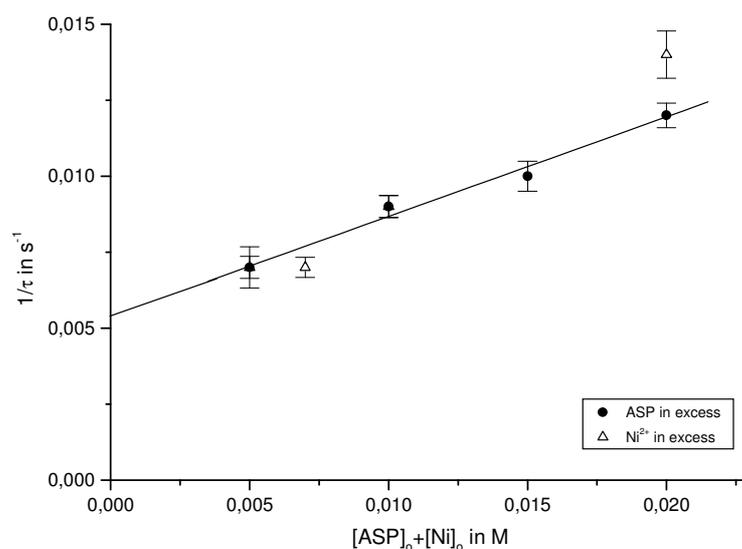


Figure 6.16

Fitted dependencies of the reciprocals of the relaxation times for the reaction of Ni(II) ions with Asp; [limiting reactant]₀ = 5.10⁻⁴ M, I = 0.1 M (NaCl), Ac₀ = 5.10⁻³ M, BCG₀ = 2.10⁻⁵ M, pH = 4.20; T=25°C

Furthermore the amplitudes for the experiments in which nickel(II) ions were present in excess followed opposite trends to those in which Asp was present in excess, indicating that while a deprotonated species (probably NiL) increased with increasing Nickel ion concentration, the same species decreased with increasing Asp concentration, figure 6.17.

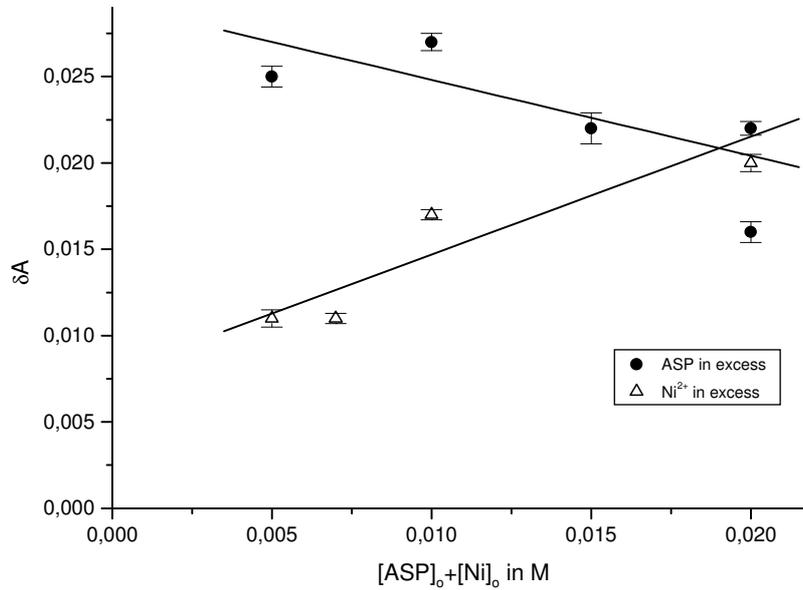


Figure 6.17

Dependencies of the amplitudes for the reaction of Ni(II) ions with Asp; [limiting reactant]₀ = 5.10⁻⁴ M, I = 0.1 M (NaCl), Ac₀ = 5.10⁻³ M, BCG₀ = 2.10⁻⁵ M, pH = 4.20; T=25°C The lines are the best fits assuming a linear dependency.

These results indicate that essentially the same (rate-limiting) reaction is being observed and that the constants k_{2H} , $K_{cM(LH)2}$ and K_{MLLH} cannot be fitted.

Analogous to the experiments in section 6.1.1.2, at pH 7, two relaxation effect were observed, with the faster one being very similar to that obtained for the case where nickel (II) ions were present in excess, see figure 6.18. As previously discussed, at pH 7, the dependence of the relaxation times to Asp concentration (for the case where Asp is present in excess) can be described by equations 6.52 and 6.53. Considering scheme 6.4, equation 6.52 yields the value of k_1 and equation 6.53 yields the value of K_{c2} as follows:

$$\frac{1}{\tau_I} = \left(\frac{k_1 K_{a3}}{[H^+]} \right) \left(\frac{K_{a2}}{K_{a2} + [H^+]} \right) L_o \quad (6.58)$$

and

$$\frac{1}{\tau_{II}} = \left(\frac{k_2 K_{a3}}{K_{cH} [H^+]^2} \right) \left(\frac{K_{cH} [H]}{K_{cH} [H^+] + 1} \right) \left(\frac{K_{a2}}{K_{a2} + [H^+]} \right) L_o + \left(\frac{k_2}{K_{c2}} \right). \quad (6.59)$$

Moreover, at pH 7.00, $[H^+] \ll K_{cH}, K_{a2}$, $(K_{cH}[H^+] + 1) \approx 1$ and $K_{a2} + [H^+] \approx K_{a2}$ giving

$$\frac{1}{\tau_I} = \left(\frac{k_1 K_{a3}}{[H^+]} \right) L_o \quad (6.60)$$

and

$$\frac{1}{\tau_{II}} = \left(\frac{k_2 K_{a3}}{[H^+]} \right) L_o + \left(\frac{k_2}{K_{c2}} \right). \quad (6.61)$$

The ratio of the gradient m to the intercept c of the segmented plot in figure 6.18, yields the equation

$$\frac{m}{c} = \left(\frac{K_{c2} K_{a3}}{[H^+]} \right). \quad (6.62)$$

Using the value of $K_{a3} = 10^{-9.89}$ M, the value of $\log(K_{c2} \cdot M) = 5.34$ is obtained, which agrees well with the value (5.41), obtained in section 6.1.1.2 A, table 6.4, with the value obtained from thermodynamic measurements and with the value reported in the literature (5.25, see table 5.8).

Using the value of $K_{c2} = 10^{5.34} \text{ M}^{-1}$ the intercept yields the value of $k_2 = 33000 \text{ M}^{-1}\text{s}^{-1}$.

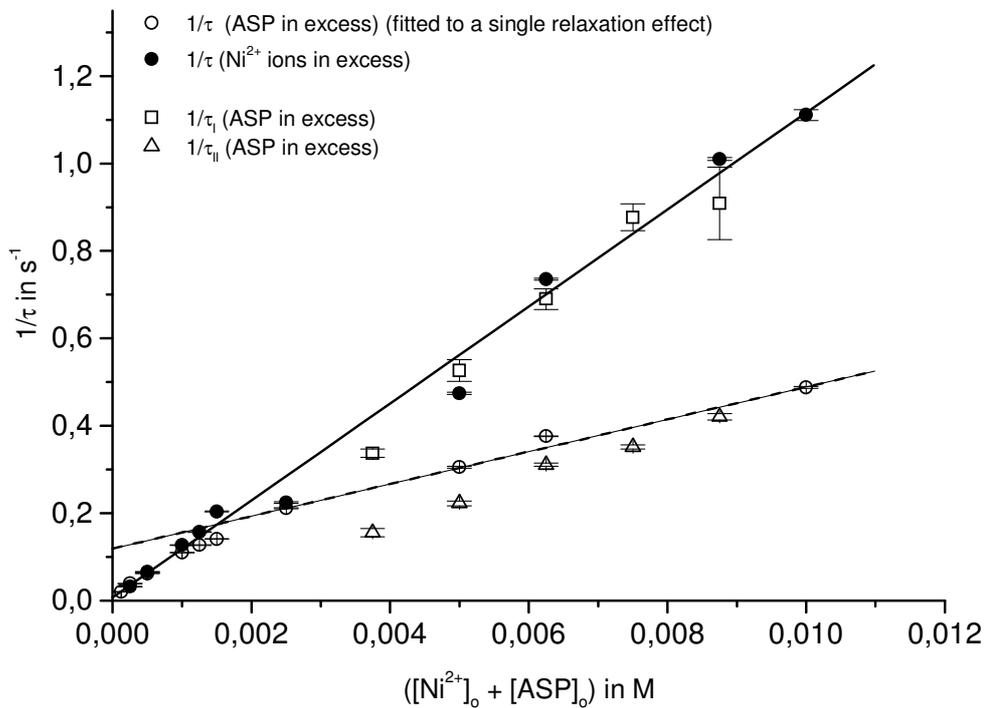


Figure 6.18

Fitted dependencies of the reciprocals of the relaxation times for the reaction of Ni(II) ions with Asp; $[Ni]_o$ or $[Asp]_o = 2.5 \times 10^{-5} \text{ M}$, $I = 0.1 \text{ M}$ (NaCl), $A_{c0} = 5.10^{-3} \text{ M}$, $BTB_0 = 2.10^{-5} \text{ M}$, $\text{pH} = 7.00$; $T = 25^\circ\text{C}$

6.1.2.3 Dependence of the Reaction Rate on the Buffer Concentration

In order to investigate whether the buffer influenced the reaction of nickel(II) ions with Asp, stopped-flow experiments were performed with varying concentrations sodium formate, sodium acetate and 2,6-lutidine respectively. For sodium formate at pH 4.0, assuming a linear interdependence, a slight increase of 5% in the reaction rate was observed at 5×10^{-3} M buffer, figure 6.19. For sodium acetate at pH 5.0 and for 2,6-lutidine at pH 7.0 no influence on the reaction rate was observed from 2.5×10^{-3} M till 0.009 M, figures 6.20 and 6.21 respectively. All stopped-flow experiments described above were carried out using 5×10^{-3} M buffer such that the influence of the buffer on the reaction rate can be assumed to be negligible.

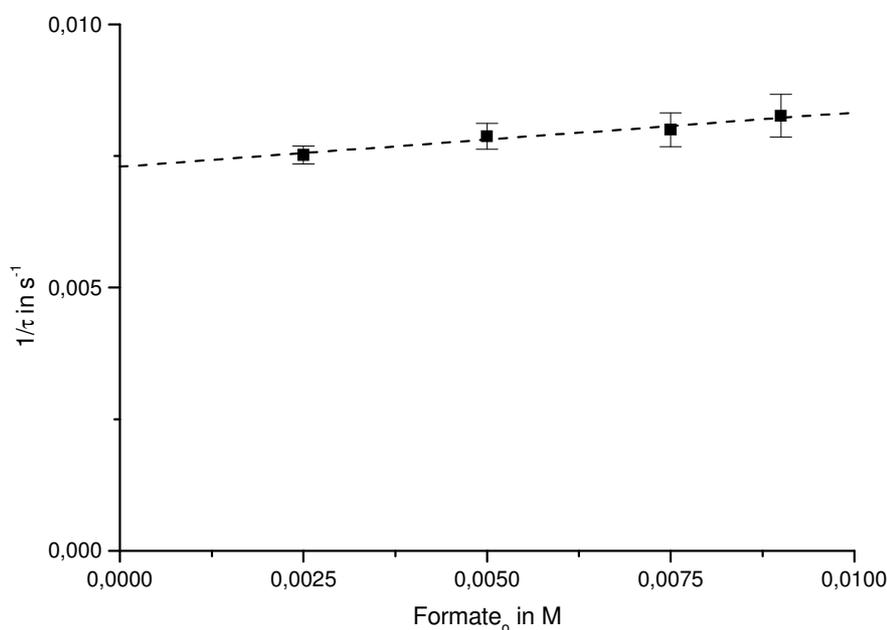


Figure 6.19

Fitted dependencies of the reciprocals of the relaxation times for the reaction of Ni(II) ions with Asp;

[Ni]₀ = 0.01 M, [Asp]₀ = 2.5×10^{-4} M, I = 0.1 M (NaCl), BPB₀ = $2 \cdot 10^{-5}$ M, pH = 4.0; T = 25°C

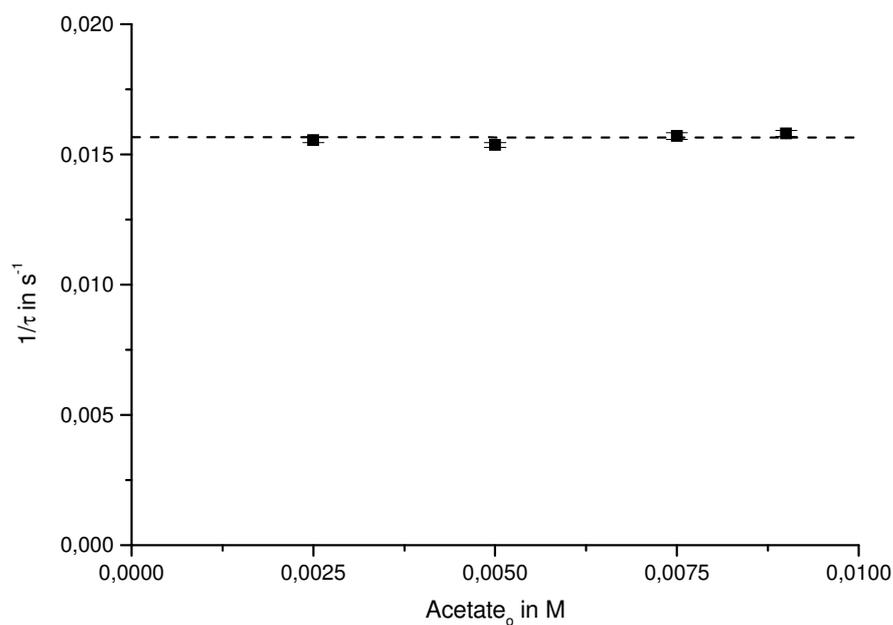


Figure 6.20

Fitted dependencies of the reciprocals of the relaxation times for the reaction of Ni(II) ions with Asp; $[\text{Ni}]_0 = 0.01 \text{ M}$, $[\text{Asp}]_0 = 2.5 \times 10^{-4} \text{ M}$, $I = 0.1 \text{ M}$ (NaCl), $\text{BCG}_0 = 2 \cdot 10^{-5} \text{ M}$, $\text{pH} = 5.0$; $T = 25^\circ\text{C}$

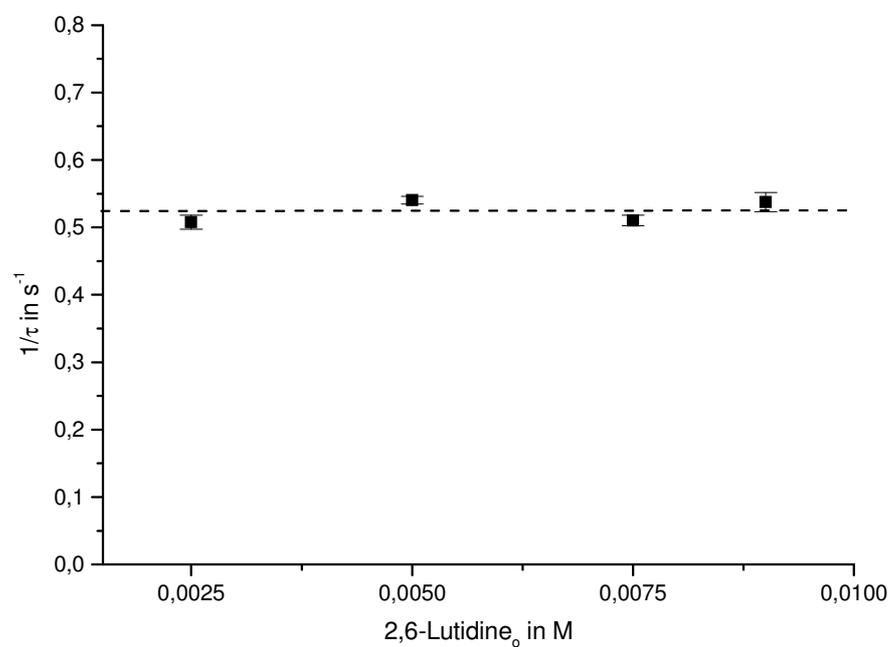


Figure 6.21

Fitted dependencies of the reciprocals of the relaxation times for the reaction of Ni(II) ions with Asp; $[\text{Ni}]_0 = 0.01 \text{ M}$, $[\text{Asp}]_0 = 2.5 \times 10^{-4} \text{ M}$, $I = 0.1 \text{ M}$ (NaCl), $\text{BTB}_0 = 2 \cdot 10^{-5} \text{ M}$, $\text{pH} = 7.0$; $T = 25^\circ\text{C}$

The following two tables summarize the results obtained so far.

Table 6.5

Fitted values for the complexation constants of Asp and Ni(II) ions in solution obtained from Potentiometric and Spectrophotometric experiments.

	Results	Literature
$K_{c1} = \frac{[NiL]}{[Ni^{2+}][L^{2-}]}$	$\log(K_{c1}.M) = 7.20 \pm 0.04$	$7.15 \pm 0.02^*$ 7.25^{**} $7.17 \blacktriangle$
$K_{cH} = \frac{[NiLH^+]}{[NiL][H^+]}$	$\log(K_{cH}.M) = 4.29 \pm 0.22$	4.05^*
$K_{c2} = \frac{[NiL_2^{2+}]}{[NiL][L^{2-}]}$	$\log(K_{c2}.M) = 5.27 \pm 0.03$	$5.25 \pm 0.10^*$ $5.32 \blacktriangle$

Table 6.6 Kinetic constants and equilibrium conditional constants fitted for the 1:1 and the 1:2 complexes' formation as obtained from kinetic experiments.

	Stopped-Flow Results from pH-Dependence of the relaxation times	Stopped-Flow Results from Concentration-Dependence of the relaxation times	Literature
k_{1H} in $M^{-1}s^{-1}$	0.20 ± 0.07		Not reported
k_1 in $M^{-1}s^{-1}$	$90\,000 \pm 4000$		Not reported
$\log(K_{cH}.M)$	3.7 ± 0.3	4.4 ± 0.1	4.05^*
$\log(K_{c1}.M)$	7.35 ± 0.09		$7.15 \pm 0.02^*$ 7.25^{**} $7.17\blacktriangle$
k_2 in $M^{-1}s^{-1}$	$22\,000 \pm 2\,000$	$33\,000 \pm 12\,000$	Not reported
$\log(K_{c2}.M)$	5.41 ± 0.03	5.34 ± 0.15	$5.25 \pm 0.10^*$ $5.32\blacktriangle$
$\log(K_{MLLH}.M)$	< 7		Not reported

* A. E. Martell and R. M. Smith, *Critical Stability Constants*, Plenum Press, New York, (1974 -1989)

** R. N. Patel et. al., *Indian J. Chem. Section A*, 38 (8), 850-853, (1999)

▲ M. R. Patel et al., *J. Indian Chem. Soc.*, 70 (6), 569 – 572, (1993)

6.1.3 Evaluation of Amplitudes

6.1.3.1 Single relaxation effect

Asp, free nickel(II) ions and complexed nickel(II) ions absorb only insignificantly at the chosen wavelengths compared to the coupled proton indicator, such that the observed absorbance is attributed only to the protonated and deprotonated forms of the indicator, InH^- and In^{2-} respectively. Hence, the relation between the signal (absorbance due to the coupled proton

indicator) and the concentration of the coupled proton indicator is given by Beer-Lambert's law as follows:

$$\frac{A}{d} = \varepsilon_{\text{In}^{2-}} \cdot [\text{In}^{2-}] + \varepsilon_{\text{InH}^-} \cdot [\text{InH}^-] \quad (6.63)$$

The following protonation and complexation constants are considered:

$$K_{a1} = \frac{[\text{LH}_2][\text{H}^+]}{[\text{LH}_3^+]} \quad (6.64) \quad K_{a2} = \frac{[\text{LH}^-][\text{H}^+]}{[\text{LH}_2]} \quad (6.65)$$

$$K_{a3} = \frac{[\text{L}^{2-}][\text{H}^+]}{[\text{LH}^-]} \quad (6.66) \quad K_{\text{In}} = \frac{[\text{In}^{2-}][\text{H}^+]}{[\text{InH}^-]} \quad (6.67)$$

$$K_{\text{B}} = \frac{[\text{B}^-][\text{H}^+]}{[\text{BH}]} \quad (6.68) \quad K_{c1} = \frac{[\text{NiL}]}{[\text{Ni}^{2+}][\text{L}^{2-}]} \quad (6.69)$$

$$K_{\text{cH}} = \frac{[\text{NiLH}^+]}{[\text{NiL}][\text{H}^+]} \quad (6.70) \quad K_{c2} = \frac{[\text{NiL}_2^{2+}]}{[\text{NiL}][\text{L}^{2-}]} \quad (6.71)$$

Additionally, the following balances are taken into account:

$$L_o = [\text{LH}_3^+] + [\text{LH}_2] + [\text{LH}^-] + [\text{L}^{2-}] + [\text{NiLH}^+] + [\text{NiL}] + 2 [\text{NiL}_2^{2-}] \quad (6.72)$$

$$\text{Ni}_o = [\text{Ni}^{2+}] + [\text{NiLH}^+] + [\text{NiL}] + [\text{NiL}_2^{2-}] \quad (6.73)$$

$$\text{B}_o = [\text{BH}] + [\text{B}^-] \quad (6.74)$$

$$\text{In}_o = [\text{InH}^-] + [\text{In}^{2-}] \quad (6.75)$$

$$\text{H}_o = [\text{BH}] + [\text{InH}^-] + [\text{H}^+] - [\text{OH}^-] + [\text{LH}^-] + 2 [\text{LH}_2] + 3 [\text{LH}_3^+] + [\text{NiLH}^+] \quad (6.76)$$

From (6.63), the change in absorption corresponding to the progress of the complexation reaction is then given by

$$\frac{\delta A}{d} = \varepsilon_{\text{In}^{2-}} \cdot \delta [\text{In}^{2-}] + \varepsilon_{\text{InH}^-} \cdot \delta [\text{InH}^-] \quad (6.77)$$

where

$\delta A = A(\text{after the complexation reaction have reached equilibrium, i.e. at } t \gg \tau) - A(\text{at the time immediately after mixing of the reactants, i.e. at } t = 0)$

and

$$\delta[X] \equiv [X]_e - [X]_s;$$

$[X]_s$ ("s" for start) being the concentration of species X immediately after mixing of the reactants in the stopped-flow, when the protonation equilibria of aspartic acid, buffer and indicator are already

established and $[X]_e$ ("e" for end) being the concentration of species X after mixing of the reactants and products in the stopped-flow, (at $t \gg \tau$) i.e. at equilibrium.

Substituting (6.75) in (6.77) results in

$$\delta A = \delta[\text{In}^{2-}] \cdot d \cdot (\varepsilon_{\text{in}} - \varepsilon_{\text{InH}}) \quad (6.78)$$

The $\delta[\text{OH}^-]$ is neglected in the following derivations since its contribution is insignificant in the pH range 3.0 to 8.0.

At the point of mixing of the reactants, (at $t = 0$) the species that need to be considered are Ni^{2+} , L^{2-} , LH^- , LH_2 , LH_3^+ , BH^+ , B , H^+ , InH^- and In^{2-} . At equilibrium ($t \gg \tau$) additional to these species, the nickel(II) aspartate complexes (NiLH^+ , NiL and NiL_2^{2-}) have to be taken into account.

From (6.76) we get

$$0 = \delta[\text{BH}^+] + \delta[\text{InH}^-] + \delta[\text{H}^+] + \delta[\text{LH}^-] + 2\delta[\text{LH}_2] + 3\delta[\text{LH}_3^+] + \delta[\text{NiLH}^+] \quad (6.79)$$

The change in the concentration of the protonated buffer is derived by considering the fast equilibrium:



$$\frac{([\text{In}^{2-}]_e - \delta[\text{In}^{2-}])([\text{BH}^+]_e - \delta[\text{BH}^+])}{([\text{InH}^-]_e - \delta[\text{InH}^-])([\text{B}]_e - \delta[\text{B}])} = \frac{[\text{In}^{2-}]_e[\text{BH}^+]_e}{[\text{InH}^-]_e[\text{B}]_e}$$

Considering equations (6.74) and (6.75) and neglecting the quadratic terms⁴, we get

$$\delta[\text{BH}^+] = \delta[\text{InH}^-] \frac{\left(\frac{1}{[\text{InH}^-]_e} + \frac{1}{[\text{In}^{2-}]_e} \right)}{\left(\frac{1}{[\text{BH}^+]_e} + \frac{1}{[\text{B}]_e} \right)} \quad (6.80)$$

Similarly, the change in the concentration of protons is derived by considering the fast protonation of the species B giving

$$\frac{([\text{B}]_e - \delta[\text{B}])([\text{H}^+]_e - \delta[\text{H}^+])}{([\text{BH}^+]_e - \delta[\text{BH}^+])} = \frac{[\text{B}]_e[\text{H}^+]_e}{[\text{BH}^+]_e}$$

⁴ See section 10.3

$$\delta[H^+] = [H^+]_e \left(\frac{1}{[BH^+]_e} + \frac{1}{[B]_e} \right) \delta[BH^+] \quad (6.81)$$

The change in the concentration of the species LH_3^+ is derived by considering the fast deprotonation of this species to the buffer B giving

$$\frac{([LH_3^+]_e - \delta[LH_3^+])([B]_e - \delta[B])}{([LH_2]_e - \delta[LH_2])([BH^-]_e - \delta[BH^-])} = \frac{[LH_3^+]_e[B]_e}{[LH_2]_e[BH^-]_e}$$

$$\delta[LH_3^+] = \frac{[LH_3^+]_e}{[LH_2]_e} \delta[LH_2] + [LH_3^+]_e \left(\frac{1}{[BH^+]_e} + \frac{1}{[B]_e} \right) \delta[BH^+] \quad (6.82)$$

$$\text{Analogously, } \delta[LH_2] = \frac{[LH_2]_e}{[LH]_e} \delta[LH] + [LH]_e \left(\frac{1}{[BH^+]_e} + \frac{1}{[B]_e} \right) \delta[BH^+] \quad (6.83)$$

The change in the concentration of the species LH^- is derived from equation (6.72), giving

$$\delta[LH^-] = -\delta[NiL] - \delta[NiLH^+] - 2\delta[NiL_2^{2-}] - \delta[L^{2-}] - \delta[LH_2] - \delta[LH_3^+] \quad (6.84)$$

Analogously, the change in the concentration of the species L^{2-} is derived by considering the fast protonation of this species to the buffer B resulting in:

$$\frac{([L^{2-}]_e - \delta[L^{2-}])([BH^+]_e - \delta[BH^+])}{([LH^-]_e - \delta[LH^-])} = \frac{[L^{2-}]_e[BH^+]_e}{[LH^-]_e}$$

$$\text{giving } \delta[L^{2-}] = \frac{[L^{2-}]_e}{[LH^-]_e} \delta[LH^-] - [L^{2-}]_e \left(\frac{1}{[BH^+]_e} + \frac{1}{[B]_e} \right) \delta[BH^+] \quad (6.85)$$

Substituting equations 6.82 and 6.83, 6.85 in 6.84 and rearranging, we get

$$\delta[LH^-] \left\{ 1 + \frac{[L^{2-}]_e}{[LH^-]_e} + \frac{[LH_2]_e}{[LH^-]_e} + \frac{[LH_3^+]_e}{[LH^-]_e} \right\} = -\delta[NiLH^+] - \delta[NiL] - 2\delta[NiL_2^{2-}] \dots$$

$$\dots - \left\{ \left(\frac{1}{[BH^+]_e} + \frac{1}{[B]_e} \right) \delta[BH^+] (-[L^{2-}]_e + [LH_2]_e + 2[LH_3^+]_e) \right\} \quad (6.86)$$

$$\delta[LH^-] = \frac{-\delta[NiLH^+] - \delta[NiL] - 2\delta[NiL_2^{2-}] - \left(\frac{1}{[InH^-]_e} + \frac{1}{[In^{2-}]_e} \right) \delta[InH^-] (2[LH_3^+]_e + [LH_2]_e - [L^{2-}]_e)}{\left\{ 1 + \frac{[L^{2-}]_e}{[LH^-]_e} + \frac{[LH_2]_e}{[LH^-]_e} + \frac{[LH_3^+]_e}{[LH^-]_e} \right\} - \left\{ 1 + \frac{[L^{2-}]_e}{[LH^-]_e} + \frac{[LH_2]_e}{[LH^-]_e} + \frac{[LH_3^+]_e}{[LH^-]_e} \right\}} \quad (6.87)$$

Since, immediately after mixing of the reactants in the stopped-flow,

$$[\text{NiLH}^+]_s = [\text{NiL}]_s = [\text{NiL}_2^{2-}]_s = 0, \text{ then}$$

$$\delta[\text{NiLH}^+] = [\text{NiLH}^+]_e \quad (6.88)$$

$$\delta[\text{NiL}] = [\text{NiL}]_e \quad (6.89)$$

$$\delta[\text{NiL}_2^{2-}] = [\text{NiL}_2^{2-}]_e \quad (6.90)$$

The equation relating $\delta[\text{In}^{2-}]$ to $[\text{H}^+]$ is obtained by substituting the values of $\delta[\text{H}^+]$, $\delta[\text{NiLH}^+]$, $\delta[\text{NiL}]$, $\delta[\text{NiL}_2^{2-}]$, $\delta[\text{L}^{2-}]$, $\delta[\text{LH}^-]$, $\delta[\text{LH}_2]$, $\delta[\text{LH}_3^+]$ and $\delta[\text{BH}]$ (equations (6.81), (6.88), (6.89), (6.90), (6.85), (6.87), (6.83), (6.82) and (6.80) respectively) into (6.79). This gives

$$\delta[\text{In}^{2-}] = \frac{\left[-[\text{H}^+]_e \left(\frac{1}{[\text{BH}^+]_e} + \frac{1}{[\text{B}]_e} \right) + \frac{[\text{NiLH}^+]_e + [\text{NiL}]_e + 2 \cdot [\text{NiL}_2^{2-}]_e}{\left(1 + \frac{[\text{L}^{2-}]_e}{[\text{LH}^-]_e} + \frac{[\text{LH}_2]_e}{[\text{LH}^-]_e} + \frac{[\text{LH}_3^+]_e}{[\text{LH}^-]_e} \right)} \left\{ 1 + 2 \frac{[\text{LH}_2]_e}{[\text{LH}^-]_e} + 3 \frac{[\text{LH}_3^+]_e}{[\text{LH}^-]_e} - [\text{NiLH}^+]_e \right\} \right]}{\left(\frac{1}{[\text{InH}^+]_e} + \frac{1}{[\text{In}^{2-}]_e} \right) + 1 - \left(\frac{1}{[\text{InH}^+]_e} + \frac{1}{[\text{In}^{2-}]_e} \right) \left(2[\text{LH}_3^+]_e + [\text{LH}_2]_e - [\text{L}^{2-}]_e \right) \left\{ 1 + 2 \frac{[\text{LH}_2]_e}{[\text{LH}^-]_e} + 3 \frac{[\text{LH}_3^+]_e}{[\text{LH}^-]_e} \right\} + \left(\frac{1}{[\text{InH}^+]_e} + \frac{1}{[\text{In}^{2-}]_e} \right) (2[\text{LH}_2]_e + 3[\text{LH}_3^+]_e) \right.} \\ \left. \left(\frac{1}{[\text{BH}^+]_e} + \frac{1}{[\text{B}]_e} \right) \left\{ 1 + \frac{[\text{L}^{2-}]_e}{[\text{LH}^-]_e} + \frac{[\text{LH}_2]_e}{[\text{LH}^-]_e} + \frac{[\text{LH}_3^+]_e}{[\text{LH}^-]_e} \right\} \right)} \quad (6.91)$$

Substituting equations (6.64), (6.65), (6.66), (6.67), (6.68), (6.70), (6.71) and (6.91) in (6.78) we get

$$\delta A = \frac{\left[\delta[\text{In}^{2-}] \cdot d \cdot (\varepsilon_{\text{In}} - \varepsilon_{\text{InH}}) \cdot [\text{NiL}]_e \cdot \left(\frac{1 + K_{cH}[\text{H}^+] + 2 \cdot K_{c2}[\text{L}^{2-}]}{1 + \frac{[\text{H}^+]}{K_{a2}} + \frac{K_{a3}}{[\text{H}^+]} + \frac{[\text{H}^+]^2}{K_{a1}K_{a2}}} \right) \left\{ 1 + 2 \frac{[\text{H}^+]}{K_{a2}} + 3 \frac{[\text{H}^+]^2}{K_{a1}K_{a2}} \right\} - K_{cH}[\text{H}^+] \right] \cdot [\text{H}^+] \left(\frac{K_B + [\text{H}^+]}{[\text{H}^+]K_B B_o} \right)}{\left[1 + \left(\frac{K_{In} + [\text{H}^+]}{[\text{H}^+]K_m I_{n_o}} \right) \left(\frac{[\text{H}^+]K_B B_o}{(K_B + [\text{H}^+])^2} - \frac{2[\text{LH}_3^+]_e + [\text{LH}_2]_e - [\text{L}^{2-}]_e}{1 + \frac{[\text{H}^+]}{K_{a2}} + \frac{K_{a3}}{[\text{H}^+]} + \frac{[\text{H}^+]^2}{K_{a1}K_{a2}}} \right) \left\{ 1 + 2 \frac{[\text{H}^+]}{K_{a2}} + 3 \frac{[\text{H}^+]^2}{K_{a1}K_{a2}} \right\} + 2[\text{LH}_2]_e + 3[\text{LH}_3^+]_e \right]} \quad (6.92)$$

Equation 6.92 is a general equation which can be used for the experiments in which nickel(II) ions occur in excess as well as for those in which aspartic acid is present in excess. For the case in which nickel(II) ions occur in excess, $[\text{NiL}_2^{2-}]_e$ is small relative to $([\text{NiLH}^+]_e + [\text{NiL}]_e)$ and $[\text{LH}_3^+]_e$ is small relative to $([\text{LH}_2]_e + [\text{LH}^-]_e + [\text{L}^{2-}]_e)$ since $[\text{L}_o] \ll [\text{Ni}_o]$.

Moreover, for the case when Asp is used as an internal buffer (see figure 6.23), the buffering species are LH^- and LH_2 . Equation (6.79) now becomes

$$0 = \delta[\text{InH}^+] + \delta[\text{H}^+] + \delta[\text{LH}^-] + 2\delta[\text{LH}_2] + 3\delta[\text{LH}_3^+] + \delta[\text{NiLH}^+] \quad (6.93)$$

such that equation (6.79) now becomes

$$\delta A = \frac{\left(\delta[\text{In}^{2-}] \cdot d \cdot (\epsilon_{\text{In}} - \epsilon_{\text{InH}}) \cdot [\text{NiL}]_e \cdot \left(\frac{1 + K_{cH}[\text{H}^+] + 2 \cdot K_{c2}[\text{L}^{2-}]}{1 + \frac{[\text{H}^+]}{K_{a2}} + \frac{K_{a3}}{[\text{H}^+]} + \frac{[\text{H}^+]^2}{K_{a1}K_{a2}}} \right) \left\{ 1 + 2 \frac{[\text{H}^+]}{K_{a2}} + 3 \frac{[\text{H}^+]^2}{K_{a1}K_{a2}} \right\} - K_{cH}[\text{H}^+] \right)}{1 + \left(\frac{K_{In} + [\text{H}^+]}{[\text{H}^+]K_{In}n_o} \right) \left(\frac{2[\text{LH}_3^+]_e + [\text{LH}_2]_e - [\text{L}^{2-}]_e}{1 + \frac{[\text{H}^+]}{K_{a2}} + \frac{K_{a3}}{[\text{H}^+]} + \frac{[\text{H}^+]^2}{K_{a1}K_{a2}}} \right) \left\{ 1 + 2 \frac{[\text{H}^+]}{K_{a2}} + 3 \frac{[\text{H}^+]^2}{K_{a1}K_{a2}} \right\} + 2[\text{LH}_2]_e + 3[\text{LH}_3^+]_e } \right) \quad (6.94)$$

δA calculated according to equation 6.92 was compared to the experimentally obtained values for δA as a function of $[\text{H}^+]$. These dependencies are shown in figures 6.22 and 6.23 for the case where Ni(II) and Asp were present in excess respectively.

For the calculations of δA shown in figures 6.22 to 6.25 the following values of ϵ_{In} , ϵ_{InH} (Table 6.7), K_{In} and K_{B} (Table 6.8) were used:

Table 6.7 Extinction coefficients ϵ_{In} , ϵ_{InH} and equilibrium conditional constant K_{In} for the proton indicators used for the kinetic experiments.

Indicator	λ/nm	$\epsilon_{\text{In}} / \text{M}^{-1} \text{cm}^{-1 \diamond}$	$\epsilon_{\text{InH}} / \text{M}^{-1} \text{cm}^{-1 \diamond}$	$K_{\text{In}} / \text{M}^{\diamond}$
BPB	592	67100	0	4.23
BCG	616	45700	0	4.66
CPR	575	17500	260	6.00
BTB	616	39 500	80	7.10

Table 6.8 Equilibrium conditional constant K_{B} for the buffers used for the kinetic experiments.

Buffer	$-\text{Log}(K_{\text{B}} \cdot \text{M}^{-1})$
Sodium formate	3.57 [*]
Sodium acetate	4.56 [*]
2,6-lutidine	6.72 [*]

* A. E. Martell and R. M. Smith, Critical Stability Constants, Plenum Press, New York, (1974 -1989)

\diamond E. Bishop, 1972

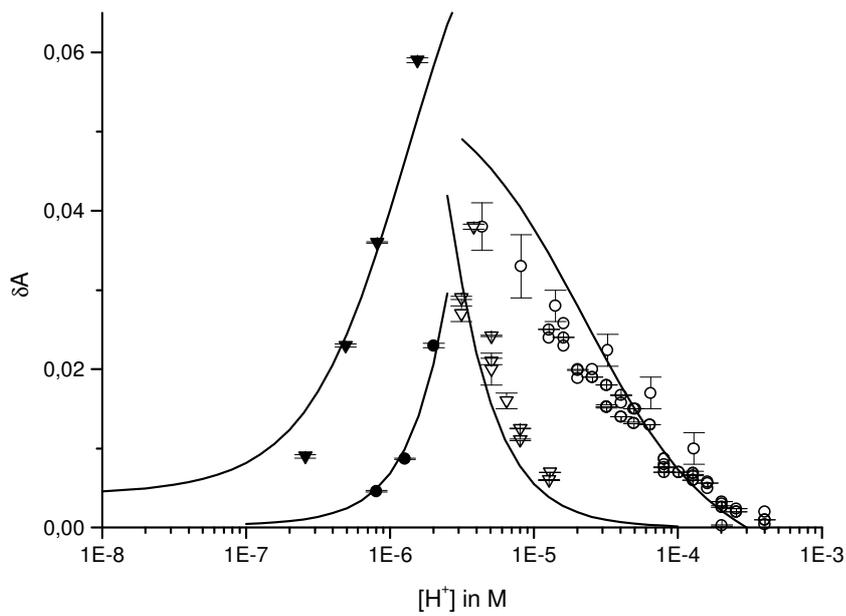


Figure 6.22a

Amplitudes of the complexation reaction of nickel(II) ions to aspartic acid;

$[\text{Ni}]_0 = 0.01 \text{ M}$, $[\text{Asp}]_0 = 2.5 \times 10^{-4} \text{ M}$, $I = 0.1 \text{ M}$ (NaCl), $\text{Buffer}_0 = 5 \times 10^{-3} \text{ M}$; $I_{n_0} = 2 \times 10^{-5} \text{ M}$; $T = 25^\circ\text{C}$;

○ Acetate/BCG ($\lambda = 616 \text{ nm}$); ▽ Acetate/CPR ($\lambda = 575 \text{ nm}$); ● $1 \times 10^{-2} \text{ M}$ Lutidine/BCG ($\lambda = 616 \text{ nm}$); ▼ Lutidine/CPR ($\lambda = 575 \text{ nm}$);

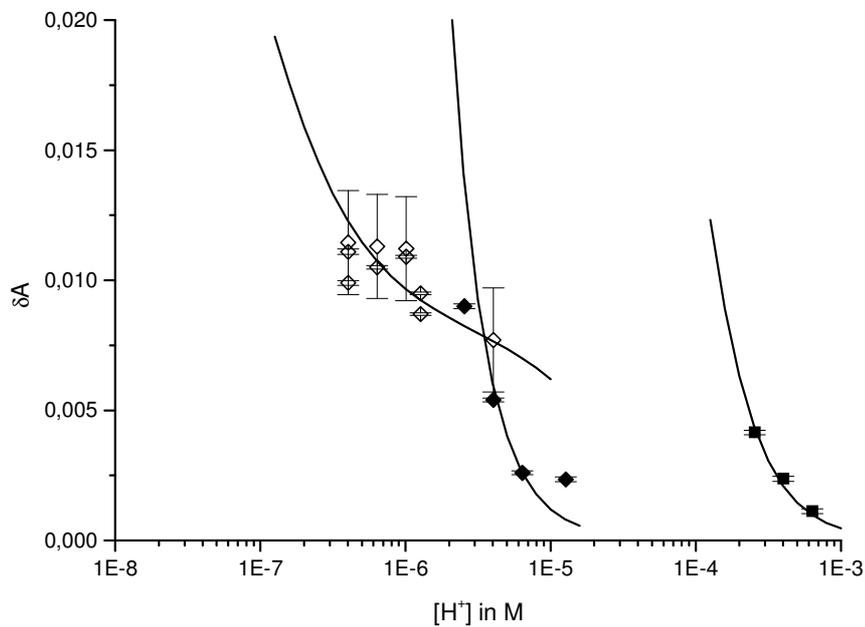


Figure 6.22b

Amplitudes of the complexation reaction of nickel(II) ions to aspartic acid;

$[\text{Ni}]_0 = 0.01 \text{ M}$, $[\text{Asp}]_0 = 2.5 \times 10^{-4} \text{ M}$, $I = 0.1 \text{ M}$ (NaCl), $\text{Buffer}_0 = 5 \times 10^{-3} \text{ M}$; $I_{n_0} = 2 \times 10^{-5} \text{ M}$; $T = 25^\circ\text{C}$;

■ Formate/BPB ($\lambda = 592 \text{ nm}$); ◆ Acetate/BTB ($\lambda = 616 \text{ nm}$); ◇ $1 \times 10^{-2} \text{ M}$ Lutidine/BTB ($\lambda = 616 \text{ nm}$);

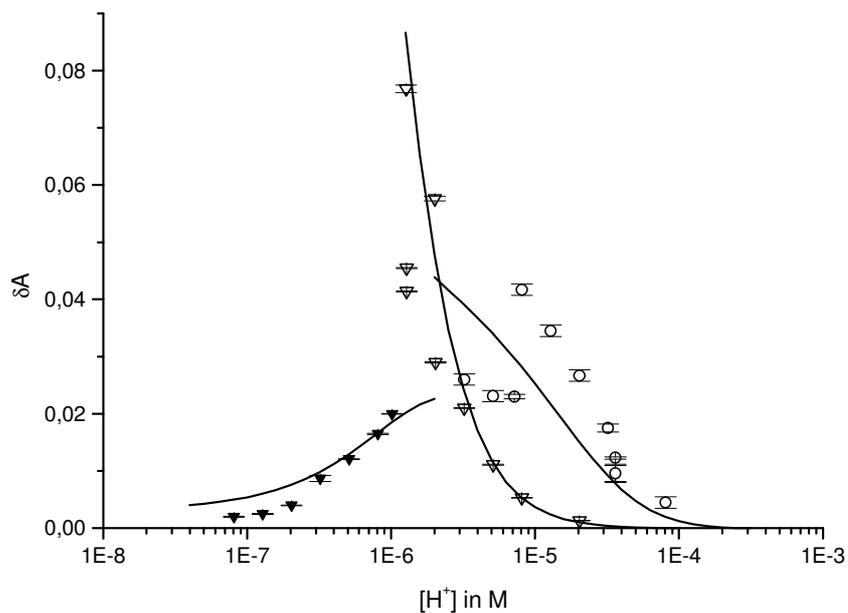


Figure 6.23a

Amplitudes of the complexation reaction of nickel(II) ions to aspartic acid;

$[\text{Asp}]_0 = 0.01 \text{ M}$, $[\text{Ni}]_0 = 2.5 \times 10^{-4} \text{ M}$, $I = 0.1 \text{ M}$ (NaCl), $\text{Buffer}_0 = 5 \times 10^{-3} \text{ M}$; $I_{n_0} = 2 \times 10^{-5} \text{ M}$; $T = 25^\circ\text{C}$;

○ Acetate/BCG ($\lambda = 616 \text{ nm}$); ▽ Acetate/CPR ($\lambda = 575 \text{ nm}$); ▼ $1 \times 10^{-2} \text{ M}$ Lutidine/CPR ($\lambda = 575 \text{ nm}$);

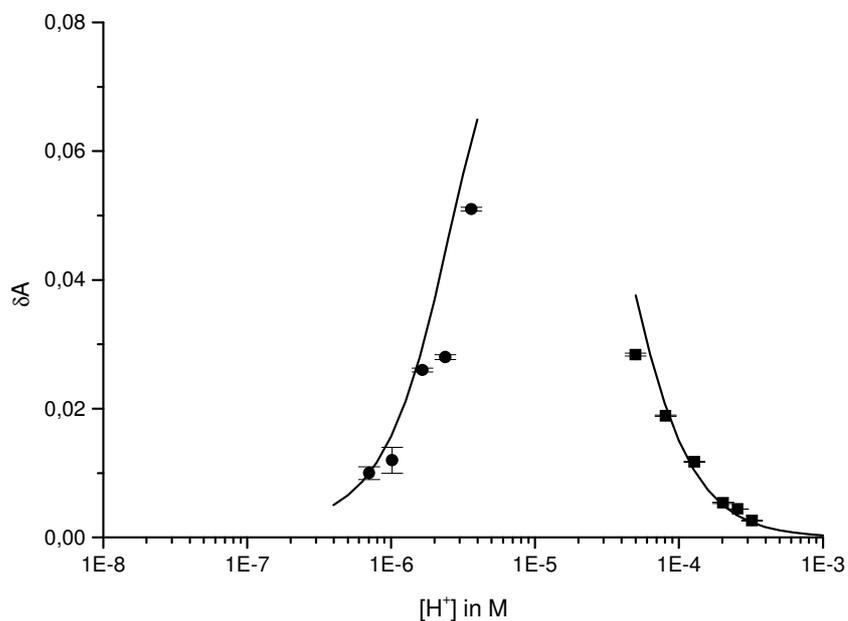


Figure 6.23b

Amplitudes of the complexation reaction of nickel(II) ions to aspartic acid;

$[\text{Asp}]_0 = 0.01 \text{ M}$, $[\text{Ni}]_0 = 2.5 \times 10^{-4} \text{ M}$, $I = 0.1 \text{ M}$ (NaCl), $\text{Buffer}_0 = 5 \times 10^{-3} \text{ M}$; $I_{n_0} = 2 \times 10^{-5} \text{ M}$; $T = 25^\circ\text{C}$;

■ BPB ($\lambda = 592 \text{ nm}$); ● Lutidine/BCG ($\lambda = 616 \text{ nm}$);

The calculated curves fit the experimental data very well.

6.1.3.2 Two relaxation effects

Since at $\text{pH} > 6$, (the range where two relaxation effects are observed) nearly no nickel(II) ions are present at equilibrium (see figure 6.13), the first step is assumed to proceed irreversibly as follows



Scheme 6.5

where

$$[\text{M}] = [\text{Ni}^{2+}]$$

$$[\text{L}] = [\text{LH}_3^+] + [\text{LH}_2] + [\text{LH}^-] + [\text{L}^{2-}]$$

$$[\text{ML}] = [\text{NiLH}^+] + [\text{NiL}]$$

$$[\text{ML}_2] = [\text{NiL}_2^{2-}]$$

and for scheme 6.4,

$$\kappa_1 = \left(k_{1H} + \frac{k_1 K_{a3}}{[\text{H}^+]} \right) \gamma_{LH} \quad (6.95)$$

$$\kappa_2 = \left(\frac{k_2 K_{a3}}{K_{cH} [\text{H}^+]^2} \right) \gamma_{NiLH} \gamma_{LH} \quad (6.96)$$

$$\kappa_{-2} = \left(\frac{k_2}{K_{c2}} \right) \quad (6.97)$$

and

$$\gamma_{LH} = \left(\frac{K_{a1} K_{a2} [\text{H}^+]}{K_{a1} (K_{a2} K_{a3} + K_{a2} [\text{H}^+] + [\text{H}^+]^2) + [\text{H}^+]^3} \right) \quad (6.98)$$

$$\gamma_{NiLH} = \left(\frac{K_{cH} [\text{H}^+]}{K_{cH} [\text{H}^+] + 1} \right) \quad (6.99)$$

The rate equations for the general scheme 6.5 are given by

$$\frac{d[\text{M}]}{dt} = -\kappa_1 [\text{M}] [\text{L}] \quad (6.100)$$

$$\frac{d[\text{ML}_2]}{dt} = \kappa_2 [\text{ML}] [\text{L}] - \kappa_{-2} [\text{ML}_2] \quad (6.101)$$

The reactions occur under pseudo first order conditions, since

- iii) the solutions were buffered and
- iv) $Ni_0 \ll L_0$

Therefore, substituting $[Y] = [Y]_e + x_Y$ (where the term x represents the deviation of the respective concentrations from the equilibrium state) into (6.100) and (6.101) we obtain

$$\frac{dx_M}{dt} = -\kappa_1[M]x_L - \kappa_1[L]x_M \quad (6.102)$$

$$\frac{dx_{ML_2}}{dt} = \kappa_2[ML]x_L + \kappa_2[L]x_{ML} - \kappa_{-2}x_{ML_2} \quad (6.103)$$

since $x_L x_M \ll [L]x_M$ and $x_L x_{ML} \ll [L]x_{ML}$ respectively.

For the case where Asp occurs in excess, $M_0 \ll L_0$ giving $[L] \approx L_0$, resulting in

$$\frac{dx_M}{dt} = -\kappa_1 L_0 x_M, \text{ which when integrated yields}$$

$$[M] = M_0 e^{-\frac{t}{\tau_I}} \quad (6.104)$$

$$\text{with } \frac{1}{\tau_I} = \kappa_1 L_0 \quad (6.105)$$

On the other hand, using the approximation $[L] \approx L_0$ for equation (6.103) yields

$$-\frac{dx_{ML_2}}{dt} = -\kappa_2 L_0 x_{ML} + \kappa_{-2} x_{ML_2} \quad (6.106)$$

Substituting equation 6.104 and $x_{ML} = -x_M - x_{ML_2}$ (from equation 6.24) in (6.106) yields

$$-\frac{dx_{ML_2}}{dt} = \kappa_2 L_0 M_0 e^{-\frac{t}{\tau_I}} + (\kappa_2 L_0 + \kappa_{-2}) x_{ML_2} \quad (6.107)$$

The solution of (6.106) has the following form⁵

$$x_{ML_2} = \alpha_I e^{-\frac{t}{\tau_I}} + \alpha_{II} e^{-\frac{t}{\tau_{II}}} \quad (6.108)$$

$$\text{with } \frac{1}{\tau_{II}} = \kappa_2 L_0 + \kappa_{-2} \quad (6.109)$$

The values of α_I and α_{II} are found by differentiating equation (6.108) as follows:

⁵ The proof is presented in section 10.4

$$\frac{dx_{ML_2}}{dt} = \frac{\alpha_I}{\tau_I} e^{-\frac{t}{\tau_I}} + \frac{\alpha_{II}}{\tau_{II}} e^{-\frac{t}{\tau_{II}}} \quad (6.110)$$

Substituting equation 6.108 and 6.109 in 6.107 yields

$$-\frac{dx_{ML_2}}{dt} = \kappa_2 L_o M_o e^{-\frac{t}{\tau_I}} + \frac{1}{\tau_{II}} \left(\alpha_I e^{-\frac{t}{\tau_I}} + \alpha_{II} e^{-\frac{t}{\tau_{II}}} \right) \quad (6.111)$$

Equating 6.107 to 6.111 results in

$$\kappa_2 L_o M_o e^{-\frac{t}{\tau_I}} = \alpha_I e^{-\frac{t}{\tau_I}} \left(\frac{1}{\tau_I} - \frac{1}{\tau_{II}} \right) \quad (6.112)$$

$$\text{Then } \alpha_I = \frac{\kappa_2 L_o M_o}{\kappa_1 L_o - \kappa_2 L_o - \kappa_{-2}} = -\frac{M_o}{1 + \frac{\kappa_1}{\kappa_2} + \frac{\kappa_{-2}}{\kappa_2 L_o}} \quad (6.113)$$

On the other hand, at $t = 0$, equation 6.108 reads

$$\delta_{ML_2} = -[ML_2]_e = \alpha_I + \alpha_{II} \quad (6.114)$$

$$\text{such that } \alpha_{II} = -[ML_2]_e + \frac{M_o}{1 + \frac{\kappa_1}{\kappa_2} + \frac{\kappa_{-2}}{\kappa_2 L_o}} \quad (6.115)$$

The amplitudes A_I and A_{II} corresponding to the two relaxation effects observed are found by multiplying the coefficients α_I and α_{II} by a factor converting $\delta[\text{NiL}_2^{2-}]$ to δA , as follows.

Converting $[\text{NiL}]_e$ in (6.92) to $[\text{NiL}_2^{2-}]_e$ results in

$$\delta A = -[\text{NiL}_2^{2-}]_e \left\{ \frac{\delta[\text{In}^{2-}] \cdot d \cdot (\varepsilon_{\text{In}} - \varepsilon_{\text{InH}}) \cdot \frac{1}{K_{c2}[\text{L}^{2-}]} \cdot \left(\frac{1 + K_{cH}[\text{H}^+] + 2 \cdot K_{c2}[\text{L}^{2-}]}{1 + \frac{[\text{H}^+]}{K_{a2}} + \frac{K_{a3}}{[\text{H}^+]} + \frac{[\text{H}^+]^2}{K_{a1}K_{a2}}} \right) \left\{ 1 + 2 \frac{[\text{H}^+]}{K_{a2}} + 3 \frac{[\text{H}^+]^2}{K_{a1}K_{a2}} \right\} - K_{cH}[\text{H}^+]}{1 + \left(\frac{K_{\text{In}} + [\text{H}^+]}{[\text{H}^+]K_{\text{In}}\text{In}_o} \right) \left(\frac{[\text{H}^+]K_B B_o}{(K_B + [\text{H}^+])^2} - \frac{2[\text{LH}_3^+]_e + [\text{LH}_2]_e - [\text{L}^2]_e}{1 + \frac{[\text{H}^+]}{K_{a2}} + \frac{K_{a3}}{[\text{H}^+]} + \frac{[\text{H}^+]^2}{K_{a1}K_{a2}}} \right) \left\{ 1 + 2 \frac{[\text{H}^+]}{K_{a2}} + 3 \frac{[\text{H}^+]^2}{K_{a1}K_{a2}} \right\} + 2[\text{LH}_2]_e + 3[\text{LH}_3^+]_e} \right\} \dots \right. \\ \left. \frac{[\text{H}^+]}{[\text{H}^+]K_B B_o} \left(\frac{K_B + [\text{H}^+]}{[\text{H}^+]K_B B_o} \right)}{1 + \left(\frac{K_{\text{In}} + [\text{H}^+]}{[\text{H}^+]K_{\text{In}}\text{In}_o} \right) \left(\frac{[\text{H}^+]K_B B_o}{(K_B + [\text{H}^+])^2} - \frac{2[\text{LH}_3^+]_e + [\text{LH}_2]_e - [\text{L}^2]_e}{1 + \frac{[\text{H}^+]}{K_{a2}} + \frac{K_{a3}}{[\text{H}^+]} + \frac{[\text{H}^+]^2}{K_{a1}K_{a2}}} \right) \left\{ 1 + 2 \frac{[\text{H}^+]}{K_{a2}} + 3 \frac{[\text{H}^+]^2}{K_{a1}K_{a2}} \right\} + 2[\text{LH}_2]_e + 3[\text{LH}_3^+]_e} \right\} \dots \right. \quad (6.116)$$

Then,

$$\delta A_I = -\alpha_I \left\{ \frac{\delta[\text{In}^{2-}] \cdot d \cdot (\varepsilon_{\text{In}} - \varepsilon_{\text{InH}}) \cdot \frac{1}{K_{c2}[\text{L}^{2-}]} \cdot \left(\frac{1 + K_{cH}[\text{H}^+] + 2 \cdot K_{c2}[\text{L}^{2-}]}{1 + \frac{[\text{H}^+]}{K_{a2}} + \frac{K_{a3}}{[\text{H}^+]} + \frac{[\text{H}^+]^2}{K_{a1}K_{a2}}} \right) \left\{ 1 + 2 \frac{[\text{H}^+]}{K_{a2}} + 3 \frac{[\text{H}^+]^2}{K_{a1}K_{a2}} \right\} - K_{cH}[\text{H}^+]}{1 + \left(\frac{K_{\text{In}} + [\text{H}^+]}{[\text{H}^+]K_{\text{In}}I_{\text{No}}} \right) \left(\frac{[\text{H}^+]K_B B_o}{(K_B + [\text{H}^+])^2} - \frac{2[\text{LH}_3^+]_e + [\text{LH}_2]_e - [\text{L}^{2-}]_e}{1 + \frac{[\text{H}^+]}{K_{a2}} + \frac{K_{a3}}{[\text{H}^+]} + \frac{[\text{H}^+]^2}{K_{a1}K_{a2}}} \right) \left\{ 1 + 2 \frac{[\text{H}^+]}{K_{a2}} + 3 \frac{[\text{H}^+]^2}{K_{a1}K_{a2}} \right\} + 2[\text{LH}_2]_e + 3[\text{LH}_3^+]_e} \right\} \dots$$

$$\frac{[\text{H}^+] \left(\frac{K_B + [\text{H}^+]}{[\text{H}^+]K_B B_o} \right)}{1 + \left(\frac{K_{\text{In}} + [\text{H}^+]}{[\text{H}^+]K_{\text{In}}I_{\text{No}}} \right) \left(\frac{[\text{H}^+]K_B B_o}{(K_B + [\text{H}^+])^2} - \frac{2[\text{LH}_3^+]_e + [\text{LH}_2]_e - [\text{L}^{2-}]_e}{1 + \frac{[\text{H}^+]}{K_{a2}} + \frac{K_{a3}}{[\text{H}^+]} + \frac{[\text{H}^+]^2}{K_{a1}K_{a2}}} \right) \left\{ 1 + 2 \frac{[\text{H}^+]}{K_{a2}} + 3 \frac{[\text{H}^+]^2}{K_{a1}K_{a2}} \right\} + 2[\text{LH}_2]_e + 3[\text{LH}_3^+]_e} \right\} \dots$$

(6.117)

$$\delta A_{II} = -\alpha_{II} \left\{ \frac{\delta[\text{In}^{2-}] \cdot d \cdot (\varepsilon_{\text{In}} - \varepsilon_{\text{InH}}) \cdot \frac{1}{K_{c2}[\text{L}^{2-}]} \cdot \left(\frac{1 + K_{cH}[\text{H}^+] + 2 \cdot K_{c2}[\text{L}^{2-}]}{1 + \frac{[\text{H}^+]}{K_{a2}} + \frac{K_{a3}}{[\text{H}^+]} + \frac{[\text{H}^+]^2}{K_{a1}K_{a2}}} \right) \left\{ 1 + 2 \frac{[\text{H}^+]}{K_{a2}} + 3 \frac{[\text{H}^+]^2}{K_{a1}K_{a2}} \right\} - K_{cH}[\text{H}^+]}{1 + \left(\frac{K_{\text{In}} + [\text{H}^+]}{[\text{H}^+]K_{\text{In}}I_{\text{No}}} \right) \left(\frac{[\text{H}^+]K_B B_o}{(K_B + [\text{H}^+])^2} - \frac{2[\text{LH}_3^+]_e + [\text{LH}_2]_e - [\text{L}^{2-}]_e}{1 + \frac{[\text{H}^+]}{K_{a2}} + \frac{K_{a3}}{[\text{H}^+]} + \frac{[\text{H}^+]^2}{K_{a1}K_{a2}}} \right) \left\{ 1 + 2 \frac{[\text{H}^+]}{K_{a2}} + 3 \frac{[\text{H}^+]^2}{K_{a1}K_{a2}} \right\} + 2[\text{LH}_2]_e + 3[\text{LH}_3^+]_e} \right\} \dots$$

$$\frac{[\text{H}^+] \left(\frac{K_B + [\text{H}^+]}{[\text{H}^+]K_B B_o} \right)}{1 + \left(\frac{K_{\text{In}} + [\text{H}^+]}{[\text{H}^+]K_{\text{In}}I_{\text{No}}} \right) \left(\frac{[\text{H}^+]K_B B_o}{(K_B + [\text{H}^+])^2} - \frac{2[\text{LH}_3^+]_e + [\text{LH}_2]_e - [\text{L}^{2-}]_e}{1 + \frac{[\text{H}^+]}{K_{a2}} + \frac{K_{a3}}{[\text{H}^+]} + \frac{[\text{H}^+]^2}{K_{a1}K_{a2}}} \right) \left\{ 1 + 2 \frac{[\text{H}^+]}{K_{a2}} + 3 \frac{[\text{H}^+]^2}{K_{a1}K_{a2}} \right\} + 2[\text{LH}_2]_e + 3[\text{LH}_3^+]_e} \right\} \dots$$

(6.118)

δA_I and δA_{II} calculated according to equations 6.117 and 6.118 were compared to the experimentally obtained values for δA_I and δA_{II} as a function of $[\text{H}^+]$. These dependencies are shown in figures 6.24 and 6.25.

Figure 6.24 shows the experimental data obtained when nickel(II) nitrate was reacted with excess aspartic acid in the presence of 5×10^{-3} M 2,6-lutidine buffer.

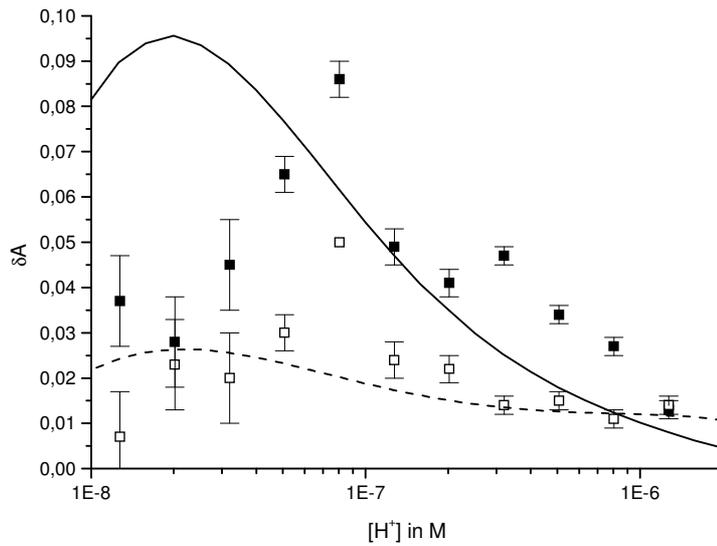


Figure 6.24

Amplitudes of the complexation reaction of nickel(II) ions to aspartic acid in the presence of Aspartic acid in excess and $5 \times 10^{-3} \text{ M}$ 2,6-lutidine buffer;

$[\text{Asp}]_0 = 0.01 \text{ M}$, $[\text{Ni}]_0 = 2.5 \times 10^{-4} \text{ M}$, $I = 0.1 \text{ M}$ (NaCl), $\text{BTB}_0 = 2 \times 10^{-5} \text{ M}$ ($\lambda = 616 \text{ nm}$); $T = 25^\circ \text{C}$; $\text{lut}_0 = 5 \times 10^{-3} \text{ M}$;

□ A_I , ■ A_{II} ;

Figure 6.25 shows the experimental data obtained when nickel(II) nitrate was reacted with excess aspartic acid in the presence of $1 \times 10^{-2} \text{ M}$ 2,6-lutidine buffer.

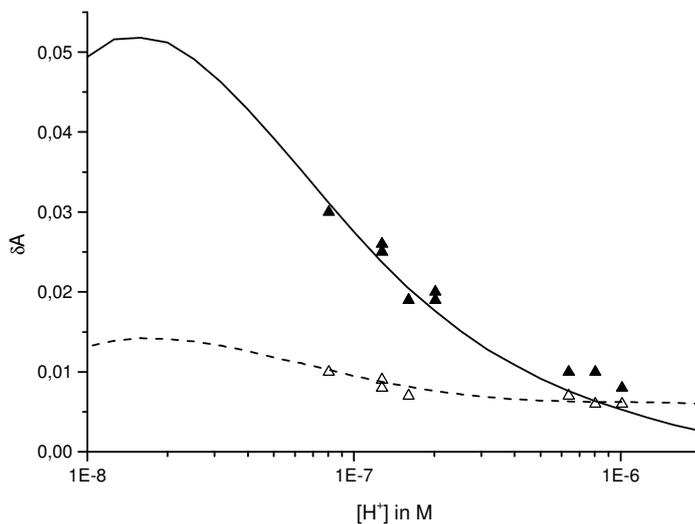


Figure 6.25

Amplitudes of the complexation reaction of nickel(II) ions to aspartic acid in the presence of Aspartic acid in excess and $1 \times 10^{-2} \text{ M}$ 2,6-lutidine buffer;

$[\text{Asp}]_0 = 0.01 \text{ M}$, $[\text{Ni}]_0 = 2.5 \times 10^{-4} \text{ M}$, $I = 0.1 \text{ M}$ (NaCl), $\text{BTB}_0 = 2 \times 10^{-5} \text{ M}$ ($\lambda = 616 \text{ nm}$); $T = 25^\circ \text{C}$; $\text{lut}_0 = 1 \times 10^{-2} \text{ M}$;

Δ A_I , ▲ A_{II}

The calculated curves for δA_I and δA_{II} agree well with the recorded experimental data in both figures. The measurements at $[H^+] \leq 5 \cdot 10^{-8}$ M are highly erroneous due to the resolution of the spectrometer such that the two relaxation times cannot be clearly distinguished from one another.

7. Discussion

7.1 Thermodynamic Experiments

7.1.1 Potentiometrical Results

Fitting of the potentiometric results shows that at equilibrium four different forms of aspartic acid occur, see Scheme 5.1.

The protonation conditional constants obtained are shown in table 7.1.

Table 7.1: Fitted values for the protonation constants of Asp

	Results	Literature
$K_{a1} = \frac{[LH_2][H^+]}{[LH_3^+]}$	$-\log(K_{a1}.M^{-1}) = 1.90 \pm 0.05$	$1.93 \pm 0.01^*$ 1.99^\diamond 1.87^{**}
$K_{a2} = \frac{[LH^-][H^+]}{[LH_2]}$	$-\log(K_{a2}.M^{-1}) = 3.74 \pm 0.03$	$3.70 \pm 0.01^*$ 3.69^\diamond 4.00^{**} 3.60^\blacktriangle
$K_{a3} = \frac{[L^{2-}][H^+]}{[LH^-]}$	$-\log(K_{a3}.M^{-1}) = 9.89 \pm 0.03$	$9.63 \pm 0.01^*$ 9.47^\diamond 9.75^{**} 9.60^\blacktriangle

* A. E. Martell and R. M. Smith, *Critical Stability Constants*, Plenum Press, New York, (1974 -1989)

** R. N. Patel et al., *Indian J. Chem. Section A*, 38 (8), 850-853, (1999)

▲ M. R. Patel et al., *J. Indian Chem. Soc.*, 70 (6), 569 – 572, (1993)

◇ A. Pohlmeier and W. Knoche, *International Journal of Chemical Kinetics*, Vol. 28. , 125-136 (1996)

Since the species $NiLH_2^{2+}$, $NiLLH^-$ and $Ni(LH)_2$, occur in very low concentrations, see figure 5.13, the values of K_{cLH_2} , K_{ML_2} and K_{MLLH} cannot be accurately evaluated. Global fitting of the potentiometric and spectrophotometric results, assuming scheme 5.2 gave the complexation constants shown in table 7.2.

Table 7.2: Fitted values for the complexation constants of Asp and Ni(II) ions in solution

	Results	Literature
$K_{c1} = \frac{[NiL]}{[Ni^{2+}][L^{2-}]}$	$\log(K_{c1}.M) = 7.20 \pm 0.04$	$7.15 \pm 0.02^*$ 7.25^{**} 7.17^\blacktriangle
$K_{cH} = \frac{[NiLH^+]}{[NiL][H^+]}$	$\log(K_{cH}.M) = 4.29 \pm 0.22$	4.05^*
$K_{c2} = \frac{[NiL_2^{2+}]}{[NiL][L^{2-}]}$	$\log(K_{c2}.M) = 5.27 \pm 0.03$	$5.25 \pm 0.10^*$ 5.32^\blacktriangle

* A. E. Martell and R. M. Smith, *Critical Stability Constants*, Plenum Press, New York, (1974 -1989)

** R. N. Patel et al., *Indian J. Chem. Section A*, 38 (8), 850-853, (1999)

▲ M. R. Patel et al., *J. Indian Chem. Soc.*, 70 (6), 569 – 572, (1993)

All the thermodynamic and kinetic results can be fitted using scheme 6.4, i.e. neglecting the species $\text{Ni}(\text{LH})_2$, NiLH_2^{2+} and NiLLH^- . All those species are present in insignificant concentrations in the pH range investigated.

7.1.2 Spectrophotometrical results - analysing the spectral changes due to the formation of the various nickel(II)aspartate complexes

7.1.2.1 Asp-Ni Binding Mode

The peak maxima at 395 nm and 659 nm of the hexaaquaonickel(II) ions shift to 380 nm and 632 nm for the nickel (II) mono-aspartate complex (NiL) and finally to 363 nm and 600 nm for the nickel (II) di-aspartate complex (NiL_2^{2-}). This shift at the higher wavelength (ca. 30 nm) is exactly double that at the lower wavelength (ca. 15 nm). This indicates the binding of the amino group to the nickel(II)ion.

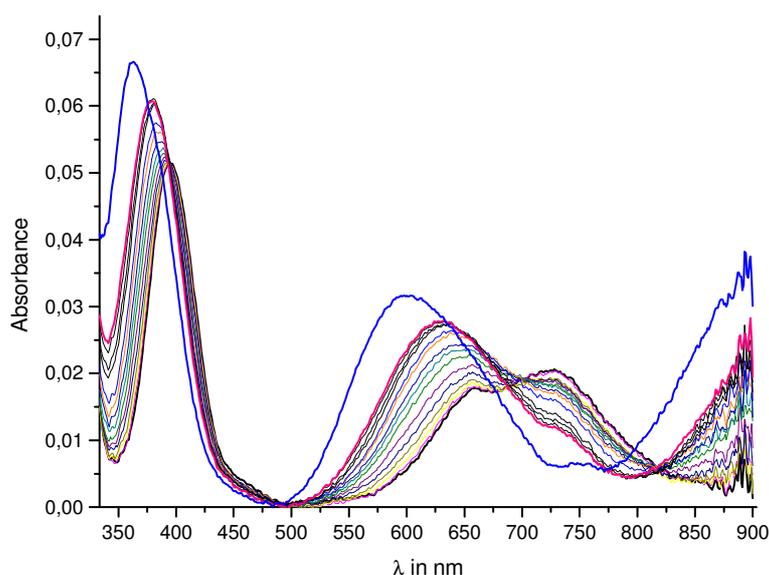


Figure 7.1: pH-dependence of the equilibrium absorption of $2 \cdot 10^{-3}$ M nickel(II) nitrate in the presence of $5 \cdot 10^{-3}$ M Asp and 0.1M NaCl at 25°C at pH 2.90, 3.92, 4.10, 4.29, 4.48, 4.70, 4.94, 5.08, 5.32, 5.46, 5.66, 6.09, 6.30, 6.50, 6.68 and 9.24 (in the order of increasing absorption at 600nm);

7.1.2.2 Ni(II) Binding Mode to protonated Asp and to PAsp

The absence of blue shifts for the calculated extinction coefficient for the species NiLH^+ (as compared to $\epsilon(\text{NiL})$ and $\epsilon(\text{NiL}_2^{2-})$, figure 5.10) is similar to the spectra of solutions of PAsp and nickel(II) nitrate (figure 5.12). This indicates the absence of binding of the amino group to the

nickel(II) ions in NiLH^+ (figure 7.2) and in Ni(PAsp) (figure 7.3). Additionally, the spectra of solutions of PAsp and nickel nitrate show an increase in the absorption intensity with increasing pH due to the fact that complexes formed have no longer a centre of symmetry, making the d-d transitions 'less forbidden', F. A. Cotton and G. Wilkinson, 1995. This spectral variation is similar to the spectral change observed for the species $[\text{Ni}(\text{H}_2\text{O})]^{2+}$ and NiLH^+ (see figure 5.10), indicating that the interaction of Ni(II) ions to LH_2 and to PAsp is weak electrostatic bonding of the hydrated nickel(II) ions to the carboxyl groups as seen below. This accounts for the lower value of K_{cH} compared to K_{c1} and for the insignificant amounts of NiLLH^- and $\text{Ni}(\text{LH})_2$.

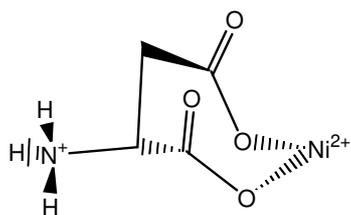


Figure 7.2 The binding in NiLH^+

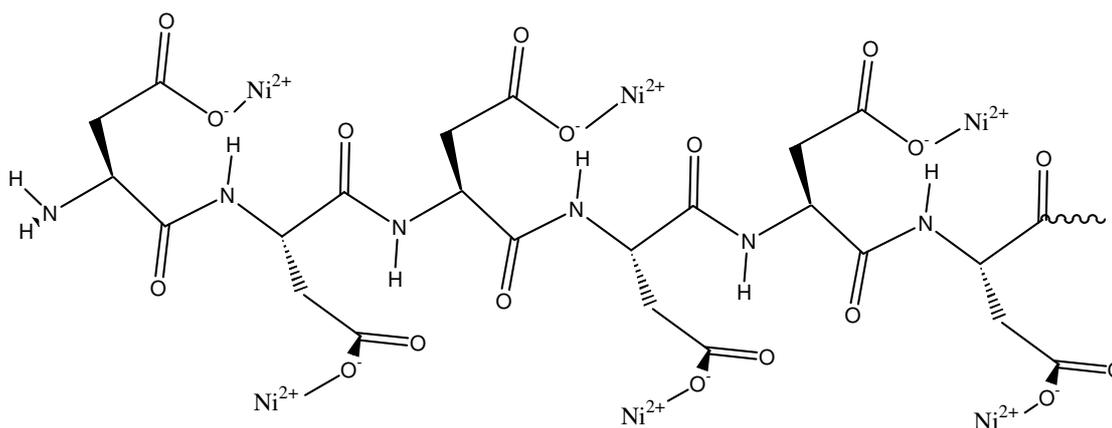


Figure 7.3 Schematic diagram showing the binding mode of nickel(II) ions to PAsp

Figure 7.4 shows the species distribution diagram for the different types of 1:1 and 1:2 aspartatonickel(II) complexes formed as well as free nickel(II) ions (as hexaaquaonickel(II) ions) as percent of the total nickel(II) species at equilibrium, using the equilibrium constants obtained from potentiometric and spectrophotometric measurements (tables 7.1 and 7.2), as a function of proton concentration.

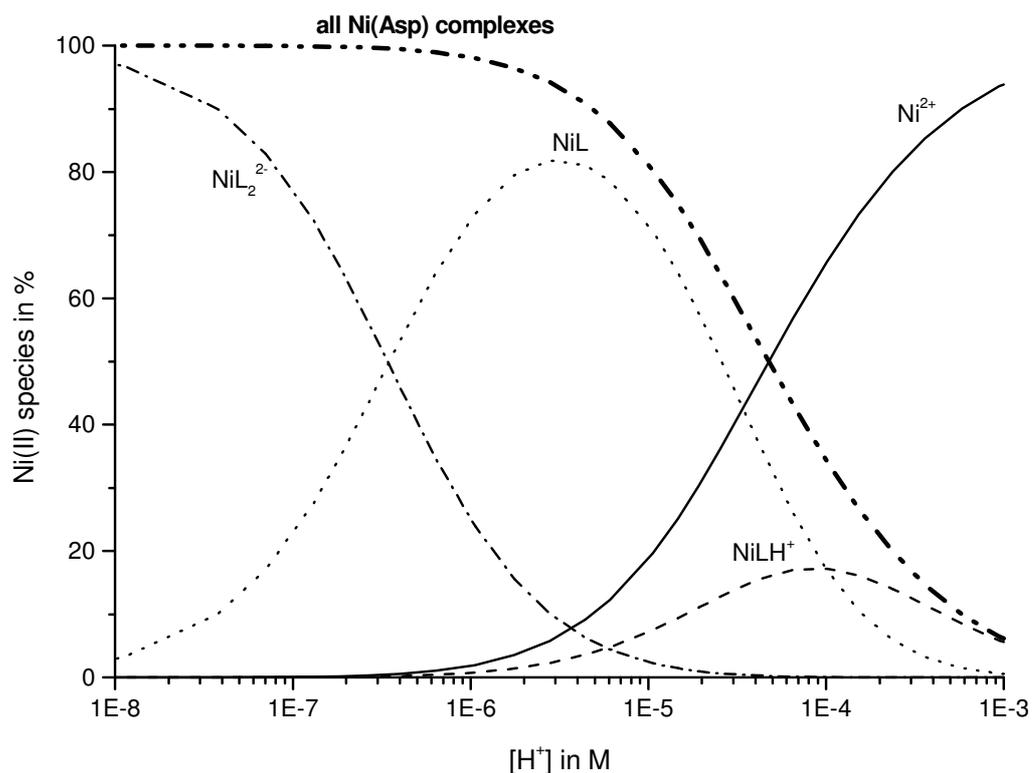


Figure 7.4

Species distribution diagram showing the nickel(II) species present at equilibrium for the case where Asp was in excess, as a function of proton concentration;

$Asp_0 = 10^{-2}$ M, $Ni_0 = 2.5 \times 10^{-4}$ M, $I = 0.1$ M (NaCl), $buffer_0 = 5 \cdot 10^{-3}$ M, $indicator_0 = 2 \cdot 10^{-5}$ M; $T = 25^\circ\text{C}$

This figure shows that:

- i) the fact that NiLH⁺ is present at equilibrium with a maximum concentration of 17 % of the total Ni(II) species present indicates that a relatively larger error would be associated to the value of the stability constant K_{cH} as opposed to K_{c1} and K_{c2} .
- ii) for typical concentrations of ligand and heavy metal ions as found in environmentally polluted areas, as presented here, Asp binds the nickel(II) ions almost completely at $p\text{cH} \geq 6$, while 50% of the nickel(II) ions are already free at $p\text{cH} 4.5$. This observation has several interdisciplinary implications as referred to in the Introduction.

7.2 Kinetics

7.2.1 Stopped-flow experiments

The kinetics of the complexation reaction between nickel(II) ions and Asp in solution were investigated using the Stopped-Flow technique. In this study, kinetic experiments were done in the p_H range 3 to 8, such that as seen in figures 5.10, 6.3 and 6.13, Asp is present mainly as LH₂ and LH⁻.

However, since

- i) no fit of the experimental data was possible when L²⁻ is omitted in the reaction scheme,
- ii) Asp in its full-deprotonated state occurs in very small concentrations (less than 1% of the ligand species in the pH range 3 – 8),
- iii) a very large rate constant (k_1) was obtained for the monoaspartatonicel(II) complex (NiL) forming through L²⁻ as compared to that for the protonated complex formed by the reaction of the much more abundant species LH⁻ (k_{1H}),

the complexation reaction of nickel(II) ions with Asp may be described as base-catalysed at p_H 4.3 - 8.0.

Analogously, since,

- i) NiLH⁺ is present at low concentrations compared to NiL,
- ii) the reaction rate increases as p_H decreases from 4.3 to 3.0 (see fig 6.9),
- iii) the curve (c) in figure 6.4 does not fit the experimental data accurately, showing the kinetic significance of the species NiLH⁺,

this complexation reaction may be also described as acid catalysed in this p_H range 3.0 to 4.3.

The reactions were assumed to proceed in a pseudo-first order mode due to a large excess of nickel(II) ions or Asp and well buffered solutions. The buffers used for the above mentioned p_H range (formate, acetate and 2,6-lutidine) did not have any influence on the reaction rate and hence no buffer catalysis was detected.

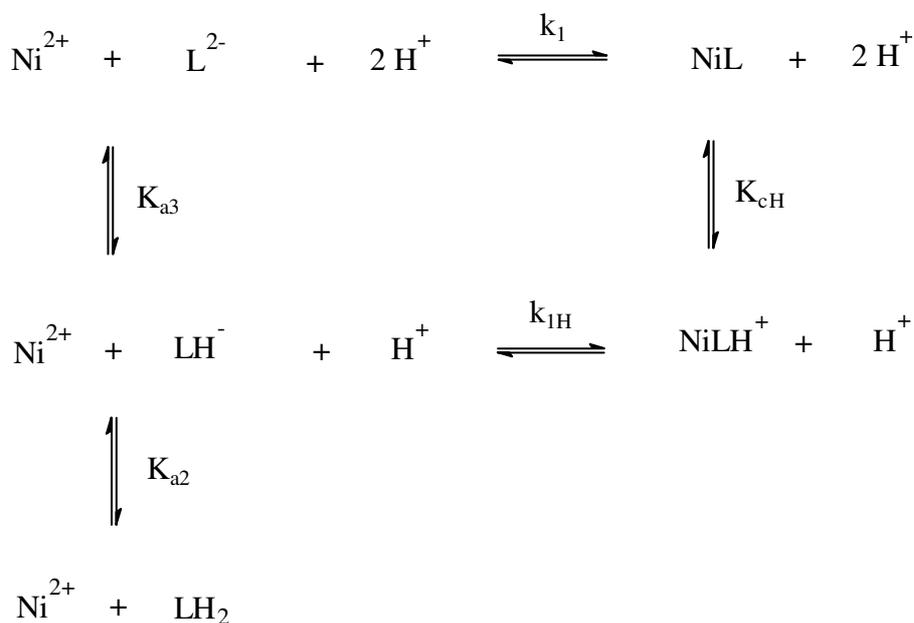
7.2.1.1 pH-Dependence

The complexation reaction of nickel (II) ions with Asp was investigated at varying pCH keeping the concentrations of nickel(II) nitrate and Asp constant. Furthermore, the results were evaluated using reaction schemes assuming the rate-determining step to be the exchange rate of one water molecule of the nickel(II) ion's inner hydration shell, (see section 3.1.1). Attempts to fit the experimental data using a scheme in which the chelation of the tridentate aspartatonickel(II) complex as the rate-limiting step were unsuccessful (see section 6.1.1.1B).

7.2.1.1.1 Ni in excess

Equation (7.1) describes the dependence of the reciprocal of the relaxation time to the proton concentration for reaction scheme 7.1, i.e. when nickel(II) ions were present in excess.

$$\frac{1}{\tau} = \left(k_{1H} + k_1 \frac{K_{a3}}{[H^+]} \right) \left(\frac{K_{a2} Ni_o}{K_{a2} + [H^+]} + \frac{[H^+]}{K_{c1} K_{a3} (K_{cH} [H^+] + 1)} \right) \quad (7.1)$$



Scheme 7.1

The reaction scheme for the formation of the 1:1 complexes of nickel(II) ions with Asp

All the experimental data recorded can be very well fitted by equation (7.1), yielding the rate constants k_1 and k_{1H} , as well as the stability constants K_{c1} and K_{cH} . The latter are in good agreement with the values obtained from the evaluation of the thermodynamic measurements, confirming the validity of the reaction scheme.

Figure 7.5 shows the splitting of equation (7.1) into its constituting four terms as a function of proton concentration.

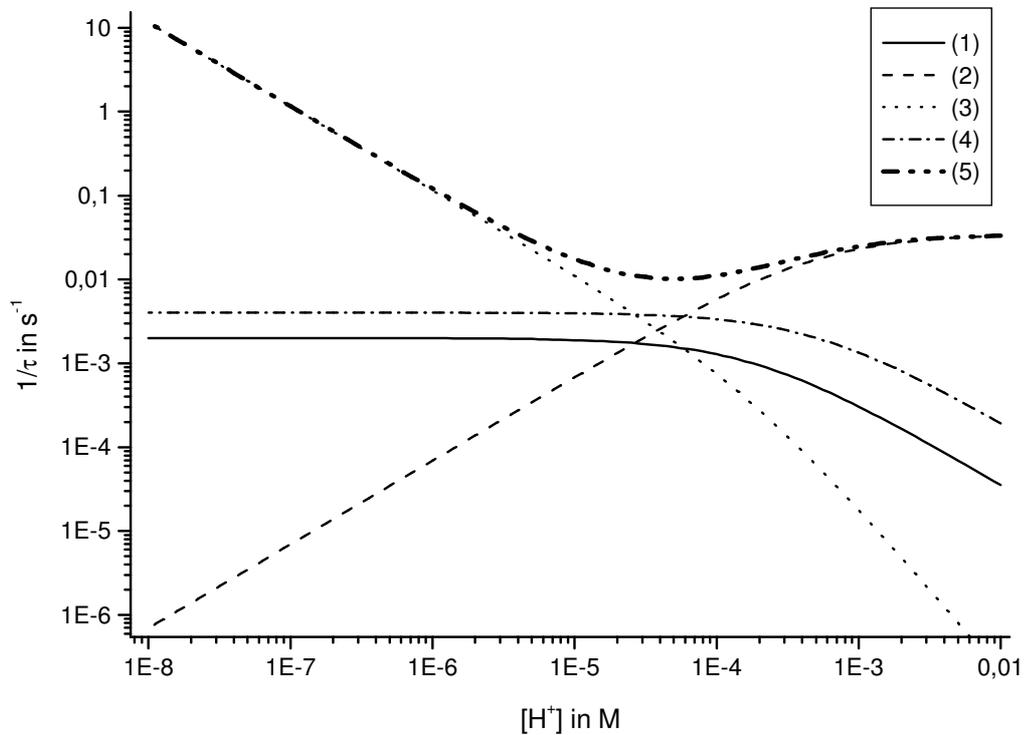


Figure 7.5

Analysis of the relationship obtained for the reciprocal of the relaxation time of the reaction of Ni(II) ions with Asp as a function of proton concentration for the case when nickel(II) ion are present in excess.

$$\text{Curve (1): } \frac{1}{\tau} = (k_{1H}) \left(\frac{K_{a2} Ni_o}{K_{a2} + [H^+]} \right)$$

$$\text{Curve (2): } \frac{1}{\tau} = (k_{1H}) \left(\frac{[H^+]}{K_{c1} K_{a3} (K_{cH} [H^+] + 1)} \right)$$

$$\text{Curve (3): } \frac{1}{\tau} = \left(k_1 \frac{K_{a3}}{[H^+]} \right) \left(\frac{K_{a2} Ni_o}{K_{a2} + [H^+]} \right)$$

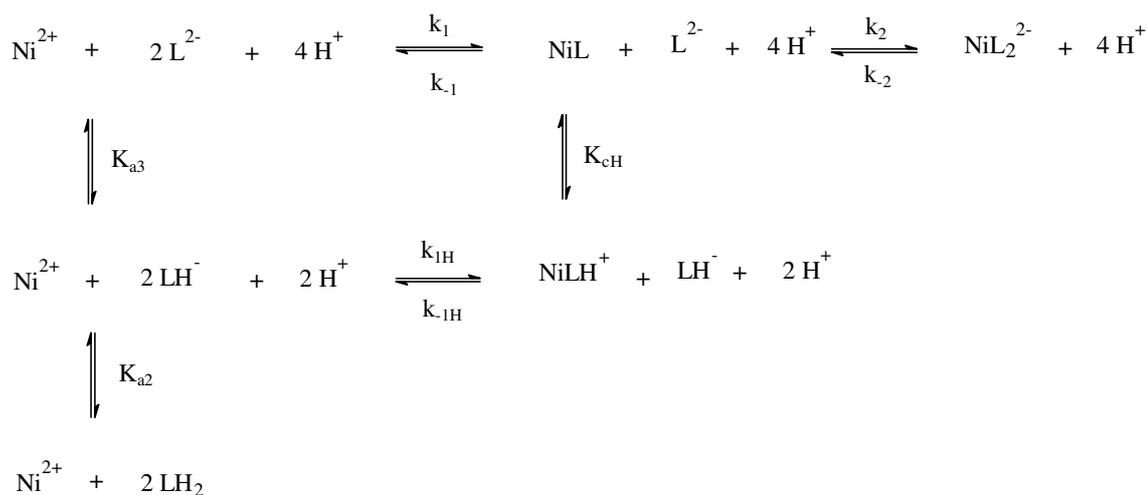
$$\text{Curve (4): } \frac{1}{\tau} = \left(k_1 \frac{K_{a3}}{[H^+]} \right) \left(\frac{[H^+]}{K_{c1} K_{a3} (K_{cH} [H^+] + 1)} \right)$$

$$\text{Curve (5): } \frac{1}{\tau} = \left(k_{1H} + k_1 \frac{K_{a3}}{[H^+]} \right) \left(\frac{K_{a2} Ni_o}{K_{a2} + [H^+]} + \frac{[H^+]}{K_{c1} K_{a3} (K_{cH} [H^+] + 1)} \right)$$

Curves (1) to (5) are calculated using the values shown in table 6.2.

This analysis gives the chemical significance to the mathematical analysis carried out in section 6.1.1.1A. It indicates that:

These observations can be explained by a scheme in which the formation of the 1:2 complexes is slow, and coupled to the 1:1 complexes' formation. Since the coupling is a strong one ($\tau_I / \tau_{II} < 10$), evaluation of the 1:2 complexes' kinetics cannot be treated separately from the 1:1 complexes' formation. On the other hand, the longer relaxation time τ_{II} is similar to the value for τ obtained from the fitting (of the absorption vs time results) to a single relaxation effect. The 1:1 complex is very stable and in fact its formation goes to completion. This leads to the complete reaction (consumption) of the free nickel(II) ions, as is shown in figure 7.4, such that NiL_2^{2-} forms only from NiL and not from Ni^{2+} . This is an example of consecutive reactions with comparable speed. Additionally the much higher stability of the tris-complex NiL , in comparison to NiLH^+ explains why the latter occurs in smaller amounts at equilibrium. This leads to even smaller amounts of protonated 1:2 complexes ($\text{Ni}(\text{LH})_2$ and NiLLH^+) such that scheme 7.3 is sufficient to explain quantitatively all the experimental thermodynamic and kinetic data observed.



Scheme 7.3

The calculated rate constants for the forward and backward reactions are presented in table 7.3

Table 7.3

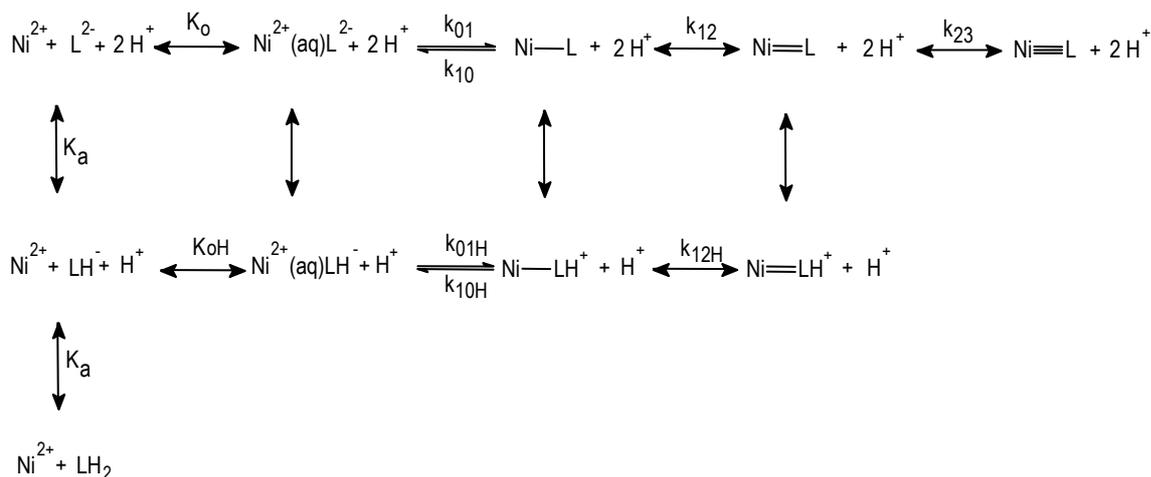
Fitted values for the rate constants obtained from pH-dependent and concentration-dependent Stopped-Flow results at $I = 0.1 \text{ M}$ (NaCl), $T = 25^\circ\text{C}$

Association	Dissociation
$k_{1H} = 0.20 \pm 0.07 \text{ (M}^{-1}\text{s}^{-1}\text{)}$	$k_{-1H} = 0.00010 \pm 0.00009 \text{ (M}^{-1}\text{s}^{-1}\text{)}$
$k_1 = 90000 \pm 4000 \text{ (M}^{-1}\text{s}^{-1}\text{)}$	$k_{-1} = 0.0040 \pm 0.0002 \text{ (M}^{-1}\text{s}^{-1}\text{)}$
$k_2 = 22000 \pm 2000 \text{ (M}^{-1}\text{s}^{-1}\text{)}$	$k_{-2} = 0.0958 \pm 0.0008 \text{ (M}^{-1}\text{s}^{-1}\text{)}$

The generally accepted Eigen-Tamm mechanism (M. Eigen and K. Tamm, 1962) for the complexation of metal ions is applied to our system such that the formation of nickel complexes proceeds via a multi-step mechanism:

- i) in a first diffusion controlled step, an outer-sphere complex is formed ($M(aq)L$), where the Ni^{2+} ion and the ligand are separated by the complete inner hydration shell of the metal ion and bound electrostatically,
- ii) the second step is the formation of the monodentate inner-sphere complex, where metal ion and ligand are in direct contact. In this step, a single water molecule is exchanged for a carboxylate group of the aspartic acid molecule,
- iii) the sequential formation of the bi- and tridentate complexes occurs fast in comparison to the inner-sphere complex formation

Scheme 7.1 then reads



Scheme 7.4

Eigen-Tamm mechanism for the reaction yielding the 1:1 nickel(II) aspartate complexes.

The second step is the rate limiting step and is controlled by the exchange rate of one water molecule of the inner hydration shell, such that the rate constant k_{01} (and k_{01H}) is a measure of the rate with which this water molecule is exchanged (H. Diebler et. al., 1969). For nickel(II) ions this value is almost independent of the type of complexing ligand and its typical value is around 10^4 s^{-1} (M. Eigen, 1963, Table 5.2).

At $pH = 7$ the reaction path via $NiLH^+$ may be neglected such that the rate law for the formation of the monoaspartatonickel(II) complex NiL is given by

$$\frac{d[NiL]}{dt} = k_{01}[Ni(aq)L] - k_{10}[Ni-L] \quad (7.2)$$

$$\text{where } K_o = \frac{[Ni(aq)L]}{[Ni^{2+}][L^{2-}]} \quad (7.3)$$

$$K_2 = \frac{[Ni = L]}{[Ni - L]} \quad (7.4)$$

$$K_3 = \frac{[Ni \equiv L]}{[Ni = L]} \quad (7.5)$$

$$[NiL] = [Ni - L] + [Ni = L] + [Ni \equiv L] \quad (7.6)$$

$$L_o = [L] + [Ni(aq)L] + [Ni - L] + [Ni = L] + [Ni \equiv L] \quad (7.7)$$

where $[L] = [LH_2] + [LH^-] + [L^{2-}]$ and hence

$$\gamma_{LH_2} = \frac{[LH_2]}{[LH_2] + [LH^-] + [L^{2-}]},$$

$$\gamma_{LH} = \frac{[LH^-]}{[LH_2] + [LH^-] + [L^{2-}]},$$

$$\text{and } \gamma_L = \frac{[L^{2-}]}{[LH_2] + [LH^-] + [L^{2-}]},$$

$$Ni_o = [Ni^{2+}] + [Ni(aq)L] + [Ni - L] + [Ni = L] + [Ni \equiv L] \quad (7.8)$$

Substituting $[Y] = [Y]_e + x_Y$ (where the term x represents the deviation of the respective concentrations from the equilibrium state) into (7.2) gives

$$-\frac{dx_{[Ni-L]+[Ni=L]+[Ni\equiv L]}}{dt} \cdot \frac{1}{x_{[Ni-L]+[Ni=L]+[Ni\equiv L]}} = k_{01} \frac{x_{[Ni(aq)L]}}{x_{[Ni-L]+[Ni=L]+[Ni\equiv L]}} - k_{10} \frac{x_{[Ni-L]}}{x_{[Ni-L]+[Ni=L]+[Ni\equiv L]}} \quad (7.9)$$

Since we work under pseudo-first order conditions, equation (7.3) yields

$$\frac{x_{[Ni(aq)L]}}{[Ni(aq)L]_e} = \frac{x_{Ni^{2+}}}{[Ni^{2+}]_e} + \frac{x_{L^{2-}}}{[L^{2-}]_e} \quad (7.10)$$

$$x_{[Ni(aq)L]} = K_o \gamma_L ([Ni^{2+}]_e + [L]_e) x_{Ni^{2+}} \quad (7.11)$$

from (7.8) we get

$$x_{Ni^{2+}} = -x_{[Ni(aq)L]} - (x_{[Ni-L]} + x_{[Ni=L]} + x_{[Ni\equiv L]}) \quad (7.12)$$

Substituting (7.12) into (7.11) and rearranging we get

$$\frac{x_{[Ni(aq)L]}}{x_{[Ni-L]} + x_{[Ni=L]} + x_{[Ni\equiv L]}} = -\frac{K_o \gamma_L ([Ni^{2+}]_e + [L]_e)}{1 + K_o \gamma_L ([Ni^{2+}]_e + [L]_e)} \quad (7.13)$$

Analogously to equation (7.10), the fast equilibria for the formation of the bi- and tridentate complexes yield

$$x_{[Ni=L]} = \frac{[Ni=L]_e}{[Ni-L]_e} x_{[Ni-L]} \quad (7.14)$$

$$\text{and } x_{[Ni\equiv L]} = \frac{[Ni\equiv L]_e}{[Ni-L]_e} x_{[Ni-L]} \quad (7.15)$$

respectively. Then

$$\frac{x_{[Ni-L]}}{x_{[Ni-L]+[Ni=L]+[Ni\equiv L]}} = \frac{1}{1 + K_2 + K_2 K_3} \quad (7.16)$$

Substituting the (7.13) and (7.16) into (7.9) we get

$$\frac{1}{\tau} = k_{01} \frac{K_o \gamma_L ([Ni^{2+}]_e + [L]_e)}{1 + K_o \gamma_L ([Ni^{2+}]_e + [L]_e)} + k_{10} \frac{1}{1 + K_2 + K_2 K_3} \quad (7.17)$$

Since $K_o \gamma_L ([Ni^{2+}]_e + [L]_e) \ll 1$ equation (7.17) reduces to

$$\frac{1}{\tau} = k_{01} K_o \gamma_L ([Ni^{2+}]_e + [L]_e) + k_{10} \frac{1}{1 + K_2 + K_2 K_3} \quad (7.18)$$

From this function the value of $k_1 = k_{01} K_o$ can be obtained. For the reaction of Ni^{2+} with ligand Y, the experimentally obtained rate constant relates to equation 7.18 by $k_1 = k_{01} K_o f_{Ni^{2+}} f_{Y^{n-}} f_{NiY^{2-n}}^{-1}$ independently of the charge of Y. The value of K_o for the formation of the outer sphere complex can be estimated using the Fuoss equation (equation 3.1) which relates K_o to the ionic radii, ionic charges and the electrostatic attractions (Fuoss, 1958). For a doubly charged anion and doubly charged cation, Fuoss equation yields $K_{o,2:2}^6 \approx 20$. The thermodynamic, dimensionless $K_{o,2:2}$ estimated from figure 7.6 is defined as

$$K_o (\text{thermodynamic}) = \frac{[Ni(aq)L] \cdot M^{-1}}{[Ni^{2+}][L^{2-}] \cdot M^{-2}} \cdot \frac{f_{Ni(aq)L}}{f_{Ni^{2+}} f_{L^{2-}}}$$

such that the conditional constant $K_{o,2:2}$ is obtained from

$$K_o (\text{conditional}) = \frac{20}{M} \cdot \frac{f_{Ni^{2+}} f_{L^{2-}}}{f_{Ni(aq)L}} = 2.89 M^{-1}$$

$$\text{Hence for } I = 0.1M, k_{01} = \frac{k_1}{K_o} \approx 3 \cdot 10^4 s^{-1}.$$

The reason for this value being around three times that obtained for acetate (see table 7.4) is due to the fact that in the species L^{2-} there are three groups where nickel(II) ions can bind.

⁶ Estimated from figure 7.6

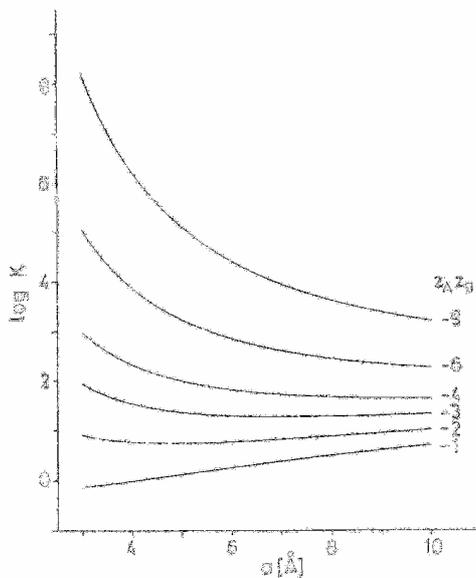


Figure 7.6

The association constant as calculated using the Fuoss formula, against the distance of closest approach for different values of $Z_A Z_B$ in water at 25°C. (Reproduced from Strehlow, H., Knoche, W., 1977, p 105);

K refers to K_0 in this work.

Table 7.4

Values of the observed rate constants k and the rate constants k_{01} for the formation of the inner-sphere complexes of a range of ligands with nickel(II) ions

Ligand	$k_1 / M^{-1}s^{-1}$	k_{01} / s^{-1}	I / M	T / K	Literature
LH (aspartate)	0.2	$\approx 5 \cdot 10^{-2}$	0.10	298.15	this Study
L ²⁻ (aspartate)	$9 \cdot 10^4$	$\approx 3 \cdot 10^4$	0.10	298.15	this Study
Citrate ³⁻	$3.7 \cdot 10^5$	$\approx 1 \cdot 10^4$	0.10	298.15	B. Engel, 2003
Citrate ²⁻	$8.0 \cdot 10^4$	$\approx 4 \cdot 10^3$	0.10	298.15	B. Engel, 2003
Citrate ⁻	$1.1 \cdot 10^4$	$\approx 1 \cdot 10^3$	0.10	298.15	B. Engel, 2003
Acetate ⁻		$\approx 3 \cdot 10^3$		283.15	Bonsen et al., 1975
Acetate ⁻	$5 \cdot 10^5$			298.15	Hoffmann et al., 1969
Acetate ⁻		$\approx 1 \cdot 10^4$			Strehlow et al., 1977
Oxalate ²⁻	$7.5 \cdot 10^4$	$\approx 6 \cdot 10^3$	0.10	298.15	Nancollas et al., 1964
Bioxalate ⁻	$5 \cdot 10^3$	$\approx 3 \cdot 10^3$	0.10	298.15	Nancollas et al., 1964
Glutarate ²⁻		$\approx 1 \cdot 10^3$	0	278.15	Hoffmann et al., 1971
2-Hydroxyglutarate		$\approx 1 \cdot 10^3$ $\approx 3 \cdot 10^3$	0	278.15	Hoffmann et al., 1971
3-Hydroxyglutarate		$\approx 1 \cdot 10^3$	0	278.15	Hoffmann et al., 1971
Malonate ²⁻	$7.0 \cdot 10^4$	$\approx 5 \cdot 10^3$	0.10	298.15	Cavasino, 1965
Malate ²⁻	$3.1 \cdot 10^4$		0.04	297.15	Hoffmann et al., 1968
Bimalonate ⁻	$3.1 \cdot 10^3$	$\approx 2 \cdot 10^3$	0.10	298.15	Cavasino, 1965
Succinate ²⁻	$4.3 \cdot 10^5$	$\approx 2 \cdot 10^4$	0	293.15	Bear et al., 1968
Tartarate ²⁻		$\approx 3 \cdot 10^4$		298.15	Hoffmann et al., 1968
Water		$\approx 3 \cdot 10^4$	0.10		Swift et al., 1962 & 1966

For the reaction of LH^- with Ni^{2+} , $k_{1H} = k_{01H}K_{oH}$ and using $K_{oH,1,2}^7 \approx 10$, $k_{01H} \approx 5 \cdot 10^{-2} \text{ s}^{-1}$. The reason for such a lower value compared to that obtained for the acetate anion is due to stronger intramolecular hydrogen bonds (between the α - and β - carboxylate groups and the amino group) in LH^- than in L^{2-} (see figure 7.7). These slow the complexation reaction significantly since these intramolecular hydrogen bonds must be broken prior to the reaction with nickel(II) ions. A more important reason is the protonation of the amino group which slows the reaction significantly.

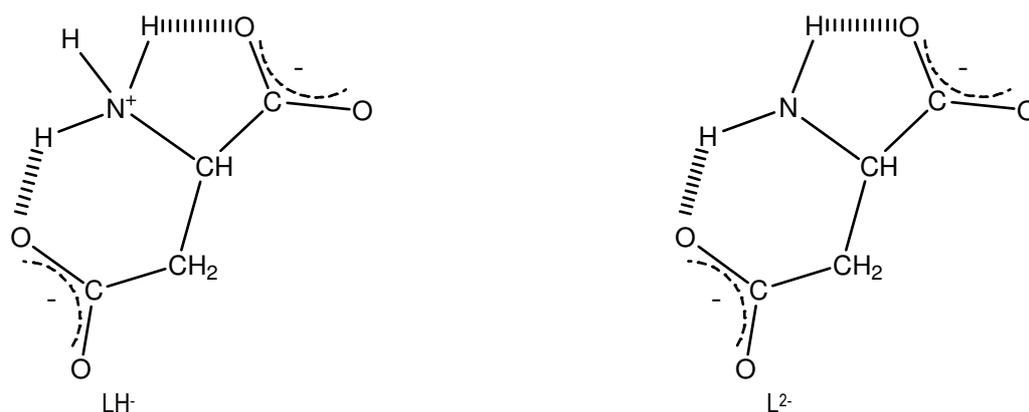


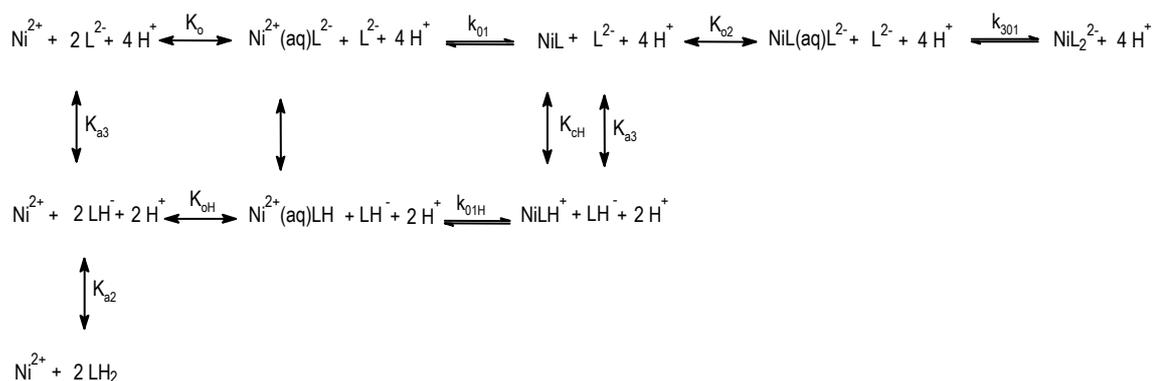
Figure 7.7

Schematic representation of the possible H-Bonds in the reacting aspartic acid species LH^- and L^{2-} .

In spite of the fact that such intramolecular hydrogen bonds are also possible for the species L^{2-} , the reaction of this species to nickel(II) ions is observed to be much faster than that involving LH^- . This may be due to the fact that in this species, the nitrogen lone pairs of the amino group are free, such that on the approach of the nickel(II) ion, these coordinate the metal ion, together with the carboxylate anions in a stable tridentate geometry.

Applying the Eigen-Tamm mechanism to the case in which Asp was present in excess, scheme 7.3 then reads

⁷ Estimated from figure 7.6



Scheme 7.5

Eigen-Tamm mechanism for the reaction yielding the 1:1 and 1:2 Ni(II) aspartate complexes.

The species $\text{NiL}(\text{aq})\text{L}^{2-}$ includes the species $\text{Ni-L}(\text{aq})\text{L}^{2-}$, $\text{Ni}=\text{L}(\text{aq})\text{L}^{2-}$ and $\text{Ni}\equiv\text{L}(\text{aq})\text{L}^{2-}$, such that the species NiL_2^{2-} includes the species $[\text{L-Ni-L}]^{2-}$, $[\text{L-Ni}=\text{L}]^{2-}$, $[\text{L-Ni}\equiv\text{L}]^{2-}$, $[\text{L}=\text{Ni-L}]^{2-}$, $[\text{L}=\text{Ni}=\text{L}]^{2-}$, $[\text{L}=\text{Ni}\equiv\text{L}]^{2-}$, $[\text{L}\equiv\text{Ni-L}]^{2-}$, $[\text{L}\equiv\text{Ni}=\text{L}]^{2-}$ and $[\text{L}\equiv\text{Ni}\equiv\text{L}]^{2-}$ which are all in (fast) equilibrium to one another and hence do not influence the rate of the forward reaction.

Again, in this case the rate constant k_2 is composed of

- i) a term describing the fast formation of an outer-sphere complex generally denoted as $\text{ML}(\text{aq})\text{L}$ and
- ii) a term describing the slow rate-limiting formation of the inner-sphere complex, where the complex ML and second ligand are in direct contact. In this step, a fourth water molecule is exchanged for a binding group of the aspartic acid molecule.

7.2.1.2 Why is the formation of the 1:2 complex slower than the formation of the 1:1 complex?

The observed slower formation of the 1:2 complexes is attributed to four possible reasons:

A) Weak intermediate monodentate and bidentate complexes

The 1:2 complex formation reaction proceeds via the monodentate complex Ni-L (and $[\text{L-Ni-L}]^{2-}$), and the bidentate complex $\text{Ni}=\text{L}$ (and $[\text{L}=\text{Ni}=\text{L}]^{2-}$) which would occur in very small amounts, due to their much weaker stability compared to the tridentate complexes. Apart from the chelate effect, (see section 2.1.1) the monodentate complexes and the bidentate complexes in Asp are weak complexes since they do not involve coordination by the amino group. In contrast to Asp, in histidine, the bidentate complexes are coordinated by the imidazole group and hence are much more stable.

B) Slow metal-chelate ring closure step

The rate-determining step yielding the 1:2 complex is the closing of the chelate ring rather than the release of the water molecule from the inner coordination sphere of the metal ion.

Two types of rate-limiting steps are encountered in the literature for metal complexation reactions depending on various factors as discussed in chapter 3. These are:

- water release step
- metal-chelate ring closure step.

In Asp, it is thought that both these steps play a part in the mechanism of the reaction, depending on the degree of protonation of Asp as follows:

a) Asp as L^{2-} :

i) fast water abstraction step

Bonding the nickel(II) ion with two negatively charged groups decreases its effective positive charge. This loosens the water molecules in the primary hydration sheath as suggested by G. G. Hammes and J. I. Steinfeld, (1962) making the water abstraction step faster. Thus, it is thought that the chelation step is relatively slower and is the rate-determining step when Asp is fully deprotonated.

ii) slow (second) chelation step

the formation of the hexadentate nickel(II) di-aspartate complex (NiL_2^{2-}) involves the formation of a 5- and 6-ring in addition to the 7-ring nickel(II) mono-aspartate complex (NiL) initially formed. This results in negative entropic contributions due to the steric strain involved.

b) Asp as LH^- :

due to its negative charge Asp can be compared to glycine. Similarly to glycine, (G. G. Hammes and J. I. Steinfeld, 1962) the complexation of the second Asp molecule is made easier through reduction of the charge of the metal complex. In this pH range the water abstraction is slower than for the above case such that its rate may become comparable to the chelation step.

c) Asp as LH₂:

When only one carboxyl group is deprotonated, weak electrostatic bonding is possible through the deprotonated carboxyl group and no chelation is possible. The water abstraction step is here very slow due to the absence of reduction of the charge of the metal complex by negatively charged ligand's functional groups. Hence, the rate-limiting step depends on the degree of protonation of the carboxyl groups.

C) The availability of the nitrogen lone pairs for coordination

Functional groups containing nitrogen lone pairs tend to slow the complexation reaction with nickel(II) ions. This can be seen when one compares the relaxation times in the seconds' range measured for reactions of nickel(II) ions to ligands containing nitrogen lone pairs groups (as in histidine {B. Goette, 2000}, alanine {C. Kreczinski, 2001} and aspartic acid {this study}) to the relaxation times in the millisecond range measured for reactions of nickel(II) ions to anionic ligands having no nitrogen lone pairs groups (e.g. carboxylate groups in citric acid {B. Engel, 2003}, PMA {S. Meyer, 1999, pg 74-76}, pectin {A. Schauer, 2001} and humic acid {Barwinski, 2002}). This is due to the fact that the pK values of these groups are higher than those of carboxyl groups such that in the pH range 3 – 8 these nitrogen-containing functionalities are still protonated in solution.

Additionally this factor explains why the formation of the 1:2 nickel(II) histidin complex is fast; four nitrogen lone pairs are in this complex available for coordination in comparison to two in the 1:1 nickel(II) histidin complex (assuming a tris-complex in both cases).

However, this factor alone is not enough to explain our results. Using this factor alone would also result in a faster 1:2 nickel(II) aspartate complex in comparison to the 1:1 complex, since the former involves two coordinated nitrogen lone pairs to the central nickel(II) ion in comparison to the one in the latter.

D) The charge product of the metal ion and ligand ($Z_M \cdot Z_L$ see section 3.1.4) rather than solely ligand charge

An interesting observation was that contrary to our results, in histidine (B. Goette, 2000) and alanine (C. Kreczinski, 2001), the formation of the 1:2 complex is faster than the formation of the 1:1 complex. This is attributed to the fact that as in glycine (G. G. Hammes and J. I. Steinfeld, 1962), in histidine and alanine the rate of formation of metal complexes can be correlated with the rate of water substitution of the aquo-metal ion, becoming faster with additional substitution of ligand. Glycine, histidine and alanine follow this reacting mode since they are all singly (negatively) charged when fully deprotonated, see section 3.1.2.

Following this trend, Asp, being doubly-negatively charged when fully deprotonated should react faster since the nickel-coordinated water molecules are further weakened by the increasing negative charge around the nickel ion centre. Since the opposite is observed, some other factor should be operating. Steric strain (entropic contribution) is not likely to be the cause since it is probably of the same extent as in His; in both cases

- i. additional 5, 6 and 7- rings are formed and
- ii. the stability constant for the 1:2 complex is ca. a factor 100 less stable than the stability constant for the 1:1 complex ($K_{c1} = 10^{7.20}$ M in Asp (this study, see table 7.2) and $10^{8.63}$ M in His (B. Goette, 2000); $K_{c2} = 10^{5.27}$ M in Asp (this study, see table 7.2) and $10^{6.84}$ M in His (B. Goette, 2000)).

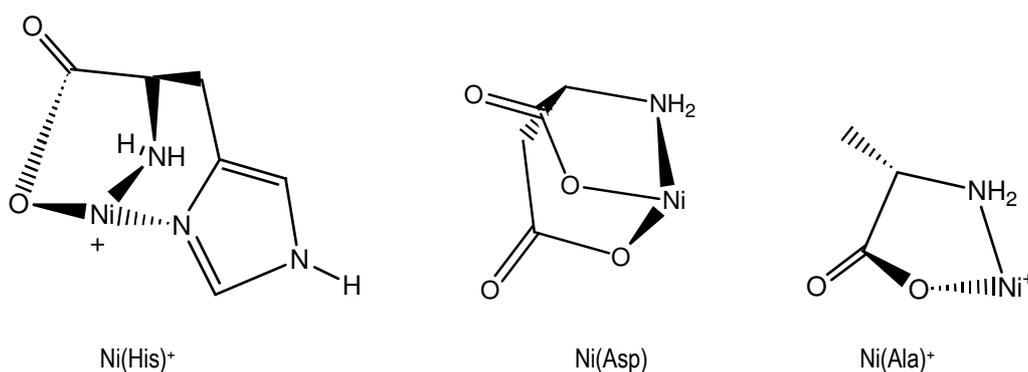


Figure 7.8

Schematic representation of the 1:1 complexes of nickel(II) ions with histidine, aspartic acid and alanine.

A more important contribution to the rate of the complexation reaction of the second Asp ligand to nickel(II) ions is thought to be the **electrostatic factor** involved in bringing the reactant species together. The charge product of the metal ion and ligand $Z_M \cdot Z_L$ in equation (3.3) is zero for the formation of the 1:2 nickel(II) aspartate complex from L^{2-} and

NiL in comparison to the value of minus four for the formation of the 1:1 nickel(II) aspartate complex from the approach of L^{2-} to Ni^{2+} .

The dependence of the rate of the complexation reaction on the electrostatic factor is also evidenced by the fact that ligands in their neutral form react much slower than in their cationic form⁸ and why a very small value obtained for $k_{1\text{H}}$ (and $k_{01\text{H}}$) is obtained in comparison to k_1 (and k_{01}) (table 7.4)

7.3 Poly-L-Aspartic acid

From the information obtained through the well studied Asp ligand, the binding groups in PAsp, RCOO^- and RCOOH would be represented by Asp in its forms LH^- or LH_2 respectively. In this case however the amino group is not available (being an imido group whose pK is around 20), and hence does not bind to the nickel(II) ion, as confirmed from UV-Vis measurements reported earlier. Hence, no chelate formation is possible, reducing the binding of nickel(II) ions to a weak monodentate interaction as shown below.

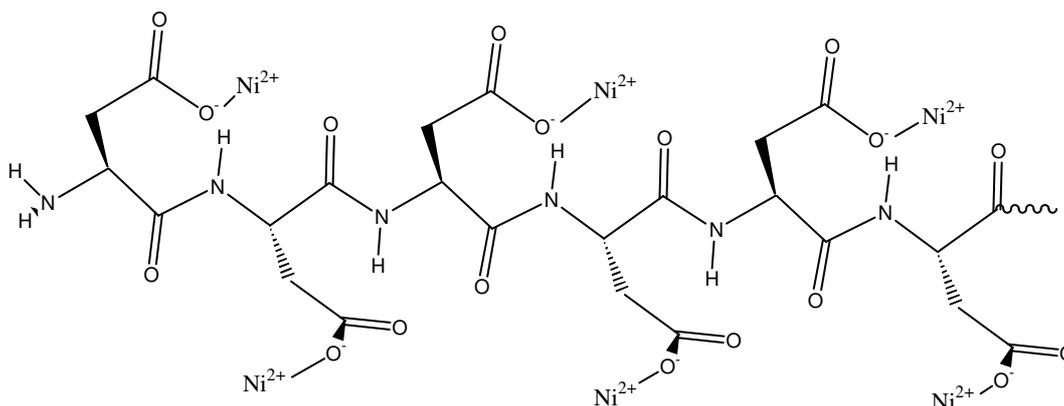


Figure 7.9

A schematic segment of the poly-L-Asp showing the complexation mode to nickel(II) ions.

The complexation equilibria of the separate carboxyl groups cannot be described quantitatively by discrete constants, since this is influenced by the electrostatic interactions with neighbouring free or complexed groups. Additionally, secondary effects such as polyelectrolyte properties and conformational changes need to be considered for the P(Asp)_{300} . Hence, quantitative description of the binding mode of Ni^{2+} ions to Pasp can only be done using distribution functions of $\text{pK}'\text{s}$.

Regarding the kinetics of this complexation reaction, it is expected that:

- since the kinetic analysis depends on the change in absorbance of a coupled proton indicator to the system, no signal would be expected at $\text{pH} > 6$ when all the carboxylate groups would be deprotonated;

⁸ i) For histidine: Ni^{2+} and NiL^+ react ten times slower to LH compared to L^- ; see B.Goette, p 66-67;

ii) LH in aminobutyric acid (A. Kowalak et. al., 1966) and LH_2 (Asp, section 6.1.1.1A) are relatively inert to Ni^{2+}

- the relaxation time for the binding of Nickel (II) ions to the carboxylate groups of P(Asp) to be in the ms region as observed for acetic acid (Strehlow et al., 1977), citric acid (Engel, 2003), PMA (S. Meyer, 1999), Pectin (Schauer, 2001) and Humic acid (Barwinski, 2002). Such a fast effect cannot be studied by the stopped-flow technique. Pressure Jump or even Temperature jump would be needed making the evaluation of the results much more complex.
- a longer relaxation effect (typical of polyelectrolytes) due to change in the conformation induced by the addition of the cation (nickel(II)).

8. Summary

This study focuses on the thermodynamics and kinetics of the complexation of nickel (II) ions to aspartic acid (Asp), the building block of poly-aspartic acid (PAsp), a biodegradable polyelectrolyte that is extensively used for water and protein purification. Similar to other toxic heavy metal ions, the toxicity of Ni²⁺ is determined mainly by pH and its speciation. The studies have been performed in aqueous solution, at constant temperature (25°C) and ionic strength (0.1 mol l⁻¹ NaCl), between pH 3 and 8 applying potentiometry, UV-Vis-spectrophotometry and stopped-flow technique. These conditions represent the ionic strength and the pH in natural environments (surface waters, soils, plants).

Evaluation of potentiometric titrations of aspartic acid with HCl and NaOH in the absence of nickel (II) ions yielded the protonation conditional constants shown in table 8.1.

Table 8.1

Fitted values for the protonation constants of Asp

	Results	Literature
$K_{a1} = \frac{[LH_2][H^+]}{[LH_3^+]}$	$-\log(K_{a1} \cdot M^{-1}) = 1.90 \pm 0.05$	1.93 + 0.01* 1.99 [◇] 1.87**
$K_{a2} = \frac{[LH^-][H^+]}{[LH_2]}$	$-\log(K_{a2} \cdot M^{-1}) = 3.74 \pm 0.03$	3.70 + 0.01* 3.69 [◇] 4.00** 3.60▲
$K_{a3} = \frac{[L^{2-}][H^+]}{[LH^-]}$	$-\log(K_{a3} \cdot M^{-1}) = 9.89 \pm 0.03$	9.63 + 0.01* 9.47 [◇] 9.75** 9.60▲

* A. E. Martell and R. M. Smith, Critical Stability Constants, Plenum Press, New York, (1974 -1989)

** R. N. Patel et. al., Indian J. Chem. Section A, 38 (8), 850-853, (1999)

▲ M. R. Patel et al., J. Indian Chem. Soc., 70 (6), 569 – 572, (1993)

◇ A. Pohlmeier and W. Knoche, International Journal of Chemical Kinetics, Vol. 28. , 125-136 (1996)

Global least-squares fitting of the potentiometric and spectrophotometric experiments of solutions of aspartic acid (LH₂) and nickel(II) nitrate indicated two mono-L-aspartatonicel(II) complexes (NiL and NiLH⁺) and one bis(L-aspartato)nickel(II) complex (NiL₂²⁻) as the major complexes formed. The fitted complexation conditional constants are shown in table 8.2. The species NiLH₂²⁺, Ni(LH)₂ and NiLLH⁻ occurred at insignificant concentrations such that no reliable stability constants for them could be fitted.

Table 8.2

Fitted values for the complexation constants of Asp and Ni(II) ions in solution

	Results	Literature
$K_{c1} = \frac{[\text{NiL}]}{[\text{Ni}^{2+}][\text{L}^{2-}]}$	$\log(K_{c1}M) = 7.20 \pm 0.04$	$7.15 \pm 0.02^*$ 7.25^{**} 7.17^\blacktriangle
$K_{cH} = \frac{[\text{NiLH}^+]}{[\text{NiL}][\text{H}^+]}$	$\log(K_{cH}M) = 4.29 \pm 0.22$	4.05^*
$K_{c2} = \frac{[\text{NiL}_2^{2+}]}{[\text{NiL}][\text{L}^{2-}]}$	$\log(K_{c2}M) = 5.27 \pm 0.03$	$5.25 \pm 0.10^*$ 5.32^\blacktriangle

* A. E. Martell and R. M. Smith, Critical Stability Constants, Plenum Press, New York, (1974 -1989)

** R. N. Patel et al., Indian J. Chem. Section A, 38 (8), 850-853, (1999)

▲ M. R. Patel et al., J. Indian Chem. Soc., 70 (6), 569 – 572, (1993)

Comparing the spectra obtained for solutions of nickel(II) ions and PAsp to spectra obtained for solutions of nickel(II) ions and Asp and to calculated absorption coefficients for Ni^{2+} , NiL , NiL_2^{2-} and NiLH^+ , it was found out that PAsp binds nickel using only its carboxyl groups even at pH 12.

The dynamics of the complexation reaction of nickel(II) ions and Asp were followed using the stopped-flow technique. Since protons are set free on the binding of nickel(II) ions to Asp, the reaction was investigated by coupling it to a proton indicator and the change in its optical absorbance was monitored. Solutions were buffered and one of the two reactants was always present in excess such that pseudo first order kinetics could be used.

In the stopped-flow experiments, a single relaxation effect is observed in the whole pCH range ($3 \leq \text{pCH} \leq 8$) when nickel(II) ions are present in excess. On the other hand, in the presence of aspartic acid in excess, two different types of relaxation behaviour were observed:

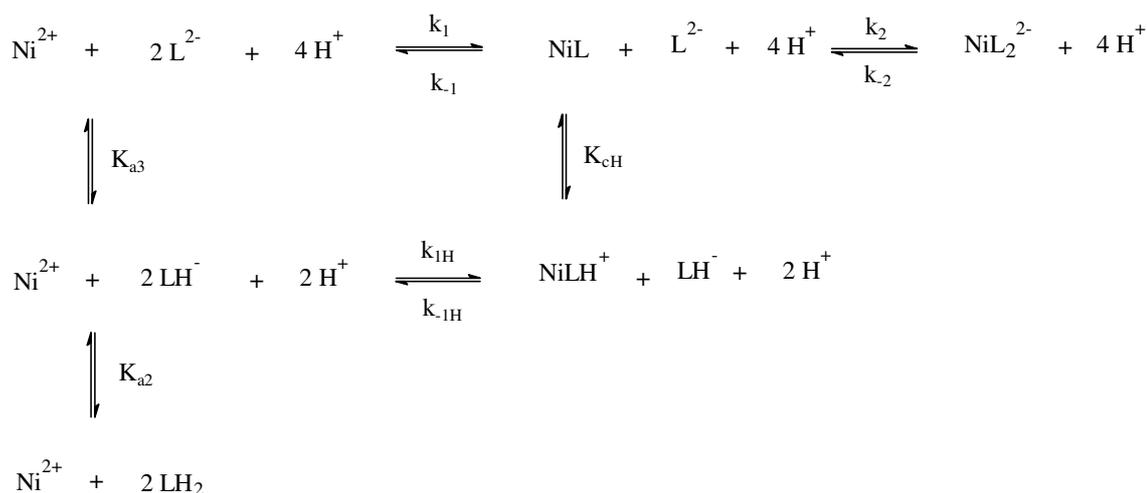
(a) one relaxation process from pCH 3 to pCH 5 with identical rate to the case in which nickel(II) ions are in excess.

This is due to the fact that the total concentration of the weighed-in metal and ligand ($\text{Ni}_o + \text{L}_o$) is the same in both cases. The relationship of the relaxation time to the proton concentration is given by the equation 8.1 below.

$$\frac{1}{\tau_l} = \left(k_{1H} + k_1 \frac{K_{a3}}{[\text{H}^+]} \right) \left(\frac{K_{a2}(\text{Ni}_o + \text{L}_o)}{K_{a2} + [\text{H}^+]} + \frac{[\text{H}^+]}{K_{c1}K_{a3}(K_{cH}[\text{H}^+] + 1)} \right) \quad (8.1)$$

(b) two relaxation processes from pCH 6 to pCH 8.

These observations were explained by scheme 8.1 in which the formation of the 1:2-complex is coupled to and slower than that of the 1:1-complexes.



Scheme 8.1

Solution of the simultaneous differential rate equations using secular equations resulted in the rate constants and conditional constants shown in table 8.3.

Table 8.3 Kinetic constants and equilibrium conditional constants fitted for the 1:1 and the 1:2 complexes' formation as obtained from kinetic experiments.

	Stopped-Flow Results from pH-Dependence of the relaxation times	Stopped-Flow Results from Concentration-Dependence of the relaxation times	Literature
k_{1H} in $M^{-1}s^{-1}$	0.20 ± 0.07		Not reported
k_1 in $M^{-1}s^{-1}$	$90\,000 \pm 4\,000$		Not reported
$\log(K_{cH}M)$	3.7 ± 0.3	4.4 ± 0.1	4.05^*
$\log(K_{c1}M)$	7.35 ± 0.09		$7.15 \pm 0.02^*$ 7.25^{**} 7.17^\blacktriangle
k_2 in $M^{-1}s^{-1}$	$22\,000 \pm 2\,000$	$33\,000 \pm 12\,000$	Not reported
$\log(K_{c2}M)$	5.41 ± 0.03	5.34 ± 0.15	$5.25 \pm 0.10^*$ 5.32^\blacktriangle
$\log(K_{MLLH}M)$	< 7		Not reported

* A. E. Martell and R. M. Smith, *Critical Stability Constants*, Plenum Press, New York, (1974 -1989)

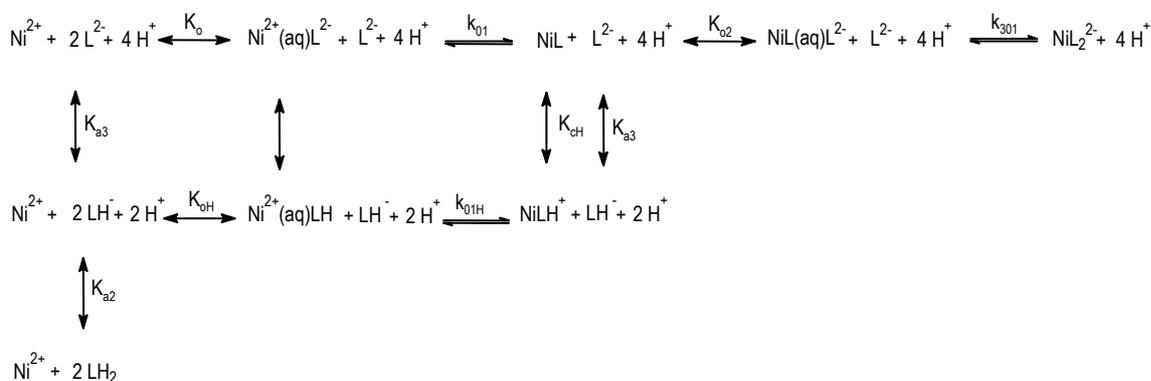
** R. N. Patel et. al., *Indian J. Chem. Section A*, 38 (8), 850-853, (1999)

▲ M. R. Patel et al., *J. Indian Chem. Soc.*, 70 (6), 569 – 572, (1993)

Analysis of the amplitudes of relaxations observed using these constants resulted in very good fits shown in figures 6.22 to 6.25. This confirms the accuracy of these constants.

The pH- and concentration-dependence of the relaxation times measured could be only explained by a mechanism involving (a) the diffusion-controlled outer-sphere complex formation followed by (b) the formation of an inner-sphere complex, where the metal ion and ligand are in direct contact

after the loss of an inner coordinated water molecule. The sequential formation of the bi- and tridentate (for both 1:1 and 1:2) complexes occurs fast in comparison to the inner-sphere complex formation as represented in scheme 8.2 below.



Scheme 8.2

Eigen-Tamm mechanism for the reaction yielding the 1:1 and 1:2 nickel(II) aspartate complexes.

The reaction proceeds mainly through the deprotonated species, L^{2-} , such that the reaction rate increases from pCH 4.3 to 8.0.

The main reasons for the slower formation of the 1:2 nickel(II) aspartate complex compared to the 1:1 nickel(II) aspartate complex are thought to be an interplay between the weak intermediate monodentate and bidentate complexes involved and the electrostatic factor involved in bringing the reactant species together.

In this study the thermodynamics and kinetics of the complexation of nickel (II) ions to aspartic acid are fully explained in the wide pCH range (pCH 3 to pCH 8) providing useful information regarding the binding mode of the commonly occurring amino- and carboxyl- functionalities in a wide range of natural and synthetic more complex molecules.

When sufficient ligand is present, complexation of nickel(II) to Asp occurs in the pH range 3-9, with the predominant species being NiL at pCH < 6.5 and NiL_2^{2-} at pCH > 6.5. The complexes formed are so strong that the nickel hydroxides' formation occurs only at pCH > 11.

Absorption studies of solutions of nickel(II) nitrate and P(Asp) indicated that P(Asp) binds the nickel(II) ions only weakly through the carboxyl groups. Hence it can be concluded that the nickel(II) ions will not be efficiently complexed by a P(Asp) stationary phase, making P(Asp) an inefficient nickel(II) ions "scavenger". An effective stationary phase for nickel(II) ions requires the use of chelating amino groups.

9. References and Notes

1. Adamo F. et. al., *Europ. J. Pharm. Sc.*, 13, 213 – 217, (2001).
2. Adamson A. W., *J. Am. Chem. Soc.* 76, 1578 (1954).
3. Altheide, A., *Diploma Thesis*, Bielefeld (1999).
4. Anderson N. E. and Solne T. O, *J. Am. Pharm. Assoc., Sci. Ed.*, 39, 460 (1950).
5. Artola A, Balaguer MD, Rigola M, *Water Research*, 31, 5, 997-1004 (1997).
6. Baes F. and Mesmer R. E., *The Hydrolysis of Cations*, Wiley Interscience, (1976).
7. Barwinski A., *Ph.D Thesis*, Bielefeld, (2002).
8. Bates R.G., *J. Res. Nat. Bur. Stand.*, 66a, 179 (1962).
9. Bates, R. G., *J. Res. Nat. Bur. Stand.*, 66a, 179 (1962).
10. Battaglia L. P. et al., *J. Am. Chem. Soc.*, 104, 2407-2411 (1982).
11. Bethe H., *Ann. Physik*, 5, 3, 135, (1929).
12. Bishop E., *Indicators*, Pergamon Press, Oxford, New York, Braunschweig, (1972).
13. Bonson A., Eggers F., Knoche W., *Inorg. Chem.*, 15, 1212, (1976).
14. Byadelek T. J. and Blomster M. L., *Inorg. Chem.*, 3, 667 (1964).
15. Byadelek T. J. and Constant A. H., *Inorg. Chem.*, 4, 833, (1965).
16. Cassatt J. C. and Wilkins R. G., *J. Am Chem Soc.*, 90: 22 (1968).
17. Cavasino F. P., *J. Phys. Chem.*, 69, 4380 (1965), reported the values of 7×10^4 and $3.1 \times 10^3 \text{ M}^{-1} \text{ sec}^{-1}$ at 25°C , $I = 0.1$ for the reaction of $\text{CH}_2(\text{CO}_2)_2^{2-}$ and $\text{CH}_2(\text{CO}_2)_2\text{H}^-$ with nickel(II)
18. Chapman D., Lloyd D. R., and Prince R. H., *J. Chem. Soc.*, 3645 (1963).
19. Chapman, D. et. al., *J. Chem. Soc.*, 3645 (1963).
20. Cobbett C. S., *Plant Physiol.*, 123, 825 – 832, (2000).
21. Cotton F. A., *J. Chem. Ed.*, 41, 466 (1964).
22. Cotton F. A., Wilkinson G., *Basic Inorganic Chemistry*, Wiley, New York, 1995, p. 518.
23. Davies W., *Ion Association*, Butterworth, London, (1962).
24. Diebler H. et. al. *Pure Appl. Chem.*, 20, 93 - 115 (1969).
25. E. Martell and R. D. Hancock, *Metal Complexes in Aqueous Solutions*, Plenum Press, New York, (1996).
26. Ehsan M. Q. et al., *Indian J. Chem. Section A*, 38 (8), 826-828, (1999).
27. Eigen M. and Tamm K., *Z. Elektrochem.*, 66, 107 (1962).
28. Eigen M. and Wilkins R, G., *Advances in Chemistry Series*, No. 49, American Chemical Society, Washington, D. C., 1965, p 55;
29. Sutin N., *Ann. Rev. Phys. Chem.*, 17, 119 (1966).

-
30. Eigen M. and Wilkins R., *Mechanisms of Inorganic Reactions*, R.F. Gould, Ed., Advances in Chemistry Series, No.49, 18, American Chemical Society, Washington D.C., (1965), 55-81;
 31. Eigen M., *Z. Elektrochem., Ber. Buns. Ges. Phy.Chem.*, 67, 753 - 762 (1963).
 32. Eigen, M., *Pure Appl. Chem.* 6, 97 (1963)
 33. Emsley J., *Die Elemente*, Walter de Gruyter & Co., Berlin (1994).
 34. Engel, B., *Ph.D Thesis*, Bielefeld, 2003.
 35. Evans H. B. and Goldstein B. H., *Spectro Chim. Acta*, 24A, 73 (1968).
 36. Fuoss R. M., *J. Am. Chem. Soc.* 80, 5059 - 5063 (1958).
 37. Gaberc-Porekar V. et. al., *J. Biochem. Biophys. Methods*, 49, 336 – 360, (2001).
 38. Goette B., *Ph.D Thesis*, Bielefeld, 2000.
 39. Gooding J. J. et. al., *Sensors*, 1, 75-90, (2001).
 40. H. Sigel, *Metal Ions in Biological Systems*, New York, 1979.
 41. Halloran B. A. et. al., *J. E. Comp. Biochem. Physiol.*, 111B, 221-231 (1995).
 42. Hammes G. G. and Steinfeld J. I., *J. Am. Chem. Soc.*, 84, 4639, (1962).
 43. Hancock R. D., *Acc. Chem. Res.*, 23, 253, (1990).
 44. Hoffmann H., Nickel U., , *Ber. Buns. Ges. Phy. Chem.*, 72, 1096 – 1101 (1968).
 45. Hoffmann H., Nickel U., , *Ber. Buns. Ges. Phy. Chem.*, 73, 432 – 437 (1969).
 46. Hoffmann H., Nickel U., *Zeitschrift f. Naturforsch.*, 26b, 299 – 306 (1971).
 47. Holyer R. H., Hubbard C. D., Kettle S. F. A., and Wilkins R. *Inorg. Chem*, 4,929 (1965); 5, 622 (1966).
 48. Katzin L. I. and Gulyas E., *J. Am. Chem. Soc.*, 86, 1655 (1964).
 49. Kauffman G.B. *Inorganic Coordination Compounds*, Heyden & Son Ltd, (1981).
 50. Kowalak, K. Kustin, R. F. Pasternack, and S. Petrucci, *Ibid.*, 89, 3126 (1967).
 51. Kreczinski C., *Teachers' Diploma Thesis*, Bielefeld, 2001.
 52. Kustin K., Pasternack R. F., and Weinstock E. M., *J. Am. Chem. Soc.*, 88 (20), 4610, (1966).
 53. Mandal R., et.al., *Environ. Sci. Technol.*, 36, 1477-1484 (2002).
 54. Margerum D. W. and Rosen H. M., *J. Am. Chem. Soc.*, 89, 1088 (1967).
 55. Martell A. E. et. al., R. J. Motekaitis and R. M. Smith, *Environmental Inorganic Chemistry* VCH Publishers, Deerfield Beach, FL, p.89 (1985).
 56. Martell E. and Smith R. M., *Critical Stability Constants*, Plenum Press, New York, Vols 1-6, (1974 -1989).
 57. Meyer S., *Diploma Thesis*, Bielefeld, 1999.

58. Nancollas G. H. and Sutin N., *Inorg. Chem.*, 3, 360 (1964), have found that the rate constants for reaction of $C_2O_4^{2-}$ and $HC_2O_4^{2-}$ with nickel(II) are 7.5×10^4 and $5 \times 10^3 \text{ M}^{-1} \text{ sec}^{-1}$ at 25°C respectively.
59. Nancollas G. H., *Interactions in Electrolyte Solutions*, Elsevier Publishing, Co., Amsterdam, 1966, p 17.
60. Patel M. R. et al., *J. Indian Chem. Soc.*, 70 (6), 569 – 572, (1993).
61. Patel R. N. et. al., *Indian J. Chem. Section A*, 38 (8), 850-853, (1999).
62. Pearlmutter F. and Stuehr J., *J. Am. Chem. Soc.*, 90, 858 (1968).
63. Pearson R. G., *Chem. Br.*, 3, 103, (1967).
64. Perrin D. D. and Dempsey B., *Buffers for pH and Metal Ion Control*, Chapman and Hall, London, (1974).
65. Pohlmeier A. and Knoche W., *International Journal of Chemical Kinetics*, Vol. 28. ,125-136 (1996).
66. Schauer A., *Ph.D Thesis*, Bielefeld, 2001.
67. Schwarzenbach and H. Ackermann, *Helv. Chim. Acta*, 30, 1798 (1947).
68. Schwarzenbach G., *Helv. Chim. Acta*, 35, 2344, (1952).
69. Steinhaus K. and Margerum D. W., *J. Am. Chem. Soc.*, 88, 441 (1966).
70. Stokes P. *Metal Ions in Biological Systems*, Siegel, H., Ed. Marcel Dekker, New York, Vol. 23, 31-46, (1988).
71. Strehlow, H., Knoche, W., *Fundamentals of Chemical Relaxations*, aus der Serie: *Mono-graphs in Modern Chemistry*, Verlag Chemie, Weinheim, Vol. 10, (1977).
72. Swift T. J., Connick R. E., *J. Chem. Phys.*, 37, 307 – 320 (1962).
73. Swift T. J., Stephenson T. A., *Inorg. Chem.*, 5, 1100 – 1105 (1966).
74. Van Vleck J. H., *Phys. Rev.*, 1932, 41, 208; *J. Chem. Phys.*, 3, 803, 807 (1945).
75. Watanabe K. et. al., *Analytical Sciences*, 17, 671-674 (2001).
76. Weiner S. et. al., *Science*, 212, 987-989, (1975).

10. Appendix

10.1 Experimental data

In this section the experimental data of the most important experiments are summarised in table form.

10.1.1 Potentiometrical data

Table 11.1 pcH-values und volumes of added 0.1M HCl to 50 ml of $5 \cdot 10^{-3}$ M Asp; $I = 0.1$ M (NaCl); $T = 25^\circ\text{C}$.

V/ml	pcH	V/ml	pcH	V/ml	pcH	V/ml	pcH	V/ml	pcH	V/ml	pcH	V/ml	pcH
0.00	3.11	4.24	2.21	8.48	1.92	12.72	1.76	16.96	1.65	21.20	1.58	25.44	1.52
0.04	3.09	4.28	2.21	8.52	1.92	12.76	1.76	17.00	1.65	21.24	1.58	25.48	1.52
0.08	3.07	4.32	2.20	8.56	1.91	12.80	1.76	17.04	1.65	21.28	1.57	25.52	1.52
0.12	3.05	4.36	2.20	8.60	1.91	12.84	1.76	17.08	1.65	21.32	1.57	25.56	1.52
0.16	3.04	4.40	2.19	8.64	1.91	12.88	1.75	17.12	1.65	21.36	1.57	25.60	1.52
0.20	3.02	4.44	2.19	8.68	1.91	12.92	1.75	17.16	1.65	21.40	1.57	25.64	1.52
0.24	3.00	4.48	2.19	8.72	1.91	12.96	1.75	17.20	1.65	21.44	1.57	25.68	1.52
0.28	2.99	4.52	2.18	8.76	1.90	13.00	1.75	17.24	1.65	21.48	1.57	25.72	1.51
0.32	2.97	4.56	2.18	8.80	1.90	13.04	1.75	17.28	1.65	21.52	1.57	25.76	1.51
0.36	2.96	4.60	2.18	8.84	1.90	13.08	1.75	17.32	1.64	21.56	1.57	25.80	1.51
0.40	2.94	4.64	2.17	8.88	1.90	13.12	1.75	17.36	1.64	21.60	1.57	25.84	1.51
0.44	2.93	4.68	2.17	8.92	1.90	13.16	1.75	17.40	1.64	21.64	1.57	25.88	1.51
0.48	2.91	4.72	2.16	8.96	1.90	13.20	1.75	17.44	1.64	21.68	1.57	25.92	1.51
0.52	2.90	4.76	2.16	9.00	1.89	13.24	1.74	17.48	1.64	21.72	1.57	25.96	1.51
0.56	2.88	4.80	2.16	9.04	1.89	13.28	1.74	17.52	1.64	21.76	1.57	26.00	1.51
0.60	2.87	4.84	2.15	9.08	1.89	13.32	1.74	17.56	1.64	21.80	1.57	26.04	1.51
0.64	2.86	4.88	2.15	9.12	1.89	13.36	1.74	17.60	1.64	21.84	1.57	26.08	1.51
0.68	2.84	4.92	2.15	9.16	1.89	13.40	1.74	17.64	1.64	21.88	1.57	26.12	1.51
0.72	2.83	4.96	2.14	9.20	1.88	13.44	1.74	17.68	1.64	21.92	1.56	26.16	1.51
0.76	2.82	5.00	2.14	9.24	1.88	13.48	1.74	17.72	1.64	21.96	1.56	26.20	1.51
0.80	2.81	5.04	2.14	9.28	1.88	13.52	1.74	17.76	1.64	22.00	1.56	26.24	1.51
0.84	2.79	5.08	2.13	9.32	1.88	13.56	1.73	17.80	1.63	22.04	1.56	26.28	1.51
0.88	2.78	5.12	2.13	9.36	1.88	13.60	1.73	17.84	1.63	22.08	1.56	26.32	1.51
0.92	2.77	5.16	2.13	9.40	1.88	13.64	1.73	17.88	1.63	22.12	1.56	26.36	1.51
0.96	2.76	5.20	2.12	9.44	1.87	13.68	1.73	17.92	1.63	22.16	1.56	26.40	1.51
1.00	2.75	5.24	2.12	9.48	1.87	13.72	1.73	17.96	1.63	22.20	1.56	26.44	1.51
1.04	2.74	5.28	2.12	9.52	1.87	13.76	1.73	18.00	1.63	22.24	1.56	26.48	1.51
1.08	2.72	5.32	2.11	9.56	1.87	13.80	1.73	18.04	1.63	22.28	1.56	26.52	1.51
1.12	2.71	5.36	2.11	9.60	1.87	13.84	1.73	18.08	1.63	22.32	1.56	26.56	1.51
1.16	2.70	5.40	2.11	9.64	1.87	13.88	1.73	18.12	1.63	22.36	1.56	26.60	1.50
1.20	2.69	5.44	2.10	9.68	1.86	13.92	1.72	18.16	1.63	22.40	1.56	26.64	1.50
1.24	2.68	5.48	2.10	9.72	1.86	13.96	1.72	18.20	1.63	22.44	1.56	26.68	1.50
1.28	2.67	5.52	2.10	9.76	1.86	14.00	1.72	18.24	1.63	22.48	1.56	26.72	1.50
1.32	2.66	5.56	2.09	9.80	1.86	14.04	1.72	18.28	1.63	22.52	1.56	26.76	1.50
1.36	2.65	5.60	2.09	9.84	1.86	14.08	1.72	18.32	1.63	22.56	1.56	26.80	1.50
1.40	2.64	5.64	2.09	9.88	1.86	14.12	1.72	18.36	1.62	22.60	1.55	26.84	1.50
1.44	2.63	5.68	2.09	9.92	1.85	14.16	1.72	18.40	1.62	22.64	1.55	26.88	1.50
1.48	2.62	5.72	2.08	9.96	1.85	14.20	1.72	18.44	1.62	22.68	1.55	26.92	1.50
1.52	2.62	5.76	2.08	10.00	1.85	14.24	1.72	18.48	1.62	22.72	1.55	26.96	1.50
1.56	2.61	5.80	2.08	10.04	1.85	14.28	1.72	18.52	1.62	22.76	1.55	27.00	1.50
1.60	2.60	5.84	2.07	10.08	1.85	14.32	1.71	18.56	1.62	22.80	1.55	27.04	1.50
1.64	2.59	5.88	2.07	10.12	1.85	14.36	1.71	18.60	1.62	22.84	1.55	27.08	1.50

V/ml	pCH	V/ml	pCH	V/ml	pCH	V/ml	pCH	V/ml	pCH	V/ml	pCH	V/ml	pCH
1.68	2.58	5.92	2.07	10.16	1.85	14.40	1.71	18.64	1.62	22.88	1.55	27.12	1.50
1.72	2.57	5.96	2.07	10.20	1.85	14.44	1.71	18.68	1.62	22.92	1.55	27.16	1.50
1.76	2.56	6.00	2.06	10.24	1.84	14.48	1.71	18.72	1.62	22.96	1.55	27.20	1.50
1.80	2.55	6.04	2.06	10.28	1.84	14.52	1.71	18.76	1.62	23.00	1.55	27.24	1.50
1.84	2.55	6.08	2.06	10.32	1.84	14.56	1.71	18.80	1.62	23.04	1.55	27.28	1.50
1.88	2.54	6.12	2.05	10.36	1.84	14.60	1.71	18.84	1.62	23.08	1.55	27.32	1.50
1.92	2.53	6.16	2.05	10.40	1.84	14.64	1.71	18.88	1.61	23.12	1.55	27.36	1.50
1.96	2.52	6.20	2.05	10.44	1.84	14.68	1.71	18.92	1.61	23.16	1.55	27.40	1.50
2.00	2.52	6.24	2.05	10.48	1.83	14.72	1.70	18.96	1.61	23.20	1.55	27.44	1.50
2.04	2.51	6.28	2.04	10.52	1.83	14.76	1.70	19.00	1.61	23.24	1.55	27.48	1.49
2.08	2.50	6.32	2.04	10.56	1.83	14.80	1.70	19.04	1.61	23.28	1.55	27.52	1.49
2.12	2.49	6.36	2.04	10.60	1.83	14.84	1.70	19.08	1.61	23.32	1.55	27.56	1.49
2.16	2.49	6.40	2.04	10.64	1.83	14.88	1.70	19.12	1.61	23.36	1.55	27.60	1.49
2.20	2.48	6.44	2.03	10.68	1.83	14.92	1.70	19.16	1.61	23.40	1.54	27.64	1.49
2.24	2.47	6.48	2.03	10.72	1.83	14.96	1.70	19.20	1.61	23.44	1.54	27.68	1.49
2.28	2.46	6.52	2.03	10.76	1.82	15.00	1.70	19.24	1.61	23.48	1.54	27.72	1.49
2.32	2.46	6.56	2.03	10.80	1.82	15.04	1.70	19.28	1.61	23.52	1.54	27.76	1.49
2.36	2.45	6.60	2.02	10.84	1.82	15.08	1.70	19.32	1.61	23.56	1.54	27.80	1.49
2.40	2.44	6.64	2.02	10.88	1.82	15.12	1.69	19.36	1.61	23.60	1.54	27.84	1.49
2.44	2.44	6.68	2.02	10.92	1.82	15.16	1.69	19.40	1.61	23.64	1.54	27.88	1.49
2.48	2.43	6.72	2.02	10.96	1.82	15.20	1.69	19.44	1.60	23.68	1.54	27.92	1.49
2.52	2.43	6.76	2.01	11.00	1.82	15.24	1.69	19.48	1.60	23.72	1.54	27.96	1.49
2.56	2.42	6.80	2.01	11.04	1.81	15.28	1.69	19.52	1.60	23.76	1.54	28.00	1.49
2.60	2.41	6.84	2.01	11.08	1.81	15.32	1.69	19.56	1.60	23.80	1.54	28.04	1.49
2.64	2.41	6.88	2.00	11.12	1.81	15.36	1.69	19.60	1.60	23.84	1.54	28.08	1.49
2.68	2.40	6.92	2.00	11.16	1.81	15.40	1.69	19.64	1.60	23.88	1.54	28.12	1.49
2.72	2.40	6.96	2.00	11.20	1.81	15.44	1.69	19.68	1.60	23.92	1.54	28.16	1.49
2.76	2.39	7.00	2.00	11.24	1.81	15.48	1.69	19.72	1.60	23.96	1.54	28.20	1.49
2.80	2.38	7.04	2.00	11.28	1.81	15.52	1.68	19.76	1.60	24.00	1.54	28.24	1.49
2.84	2.38	7.08	1.99	11.32	1.80	15.56	1.68	19.80	1.60	24.04	1.54	28.28	1.49
2.88	2.37	7.12	1.99	11.36	1.80	15.60	1.68	19.84	1.60	24.08	1.54	28.32	1.49
2.92	2.37	7.16	1.99	11.40	1.80	15.64	1.68	19.88	1.60	24.12	1.53	28.36	1.49
2.96	2.36	7.20	1.99	11.44	1.80	15.68	1.68	19.92	1.60	24.16	1.53	28.40	1.49
3.00	2.35	7.24	1.98	11.48	1.80	15.72	1.68	19.96	1.60	24.20	1.53	28.44	1.48
3.04	2.35	7.28	1.98	11.52	1.80	15.76	1.68	20.00	1.60	24.24	1.53	28.48	1.48
3.08	2.34	7.32	1.98	11.56	1.80	15.80	1.68	20.04	1.59	24.28	1.53	28.52	1.48
3.12	2.34	7.36	1.98	11.60	1.79	15.84	1.68	20.08	1.59	24.32	1.53	28.56	1.48
3.16	2.33	7.40	1.97	11.64	1.79	15.88	1.68	20.12	1.59	24.36	1.53	28.60	1.48
3.20	2.33	7.44	1.97	11.68	1.79	15.92	1.67	20.16	1.59	24.40	1.53	28.64	1.48
3.24	2.32	7.48	1.97	11.72	1.79	15.96	1.67	20.20	1.59	24.44	1.53	28.68	1.48
3.28	2.32	7.52	1.97	11.76	1.79	16.00	1.67	20.24	1.59	24.48	1.53	28.72	1.48
3.32	2.31	7.56	1.97	11.80	1.79	16.04	1.67	20.28	1.59	24.52	1.53	28.76	1.48
3.36	2.31	7.60	1.96	11.84	1.79	16.08	1.67	20.32	1.59	24.56	1.53	28.80	1.48
3.40	2.30	7.64	1.96	11.88	1.79	16.12	1.67	20.36	1.59	24.60	1.53	28.84	1.48
3.44	2.30	7.68	1.96	11.92	1.78	16.16	1.67	20.40	1.59	24.64	1.53	28.88	1.48
3.48	2.29	7.72	1.96	11.96	1.78	16.20	1.67	20.44	1.59	24.68	1.53	28.92	1.48
3.52	2.29	7.76	1.95	12.00	1.78	16.24	1.67	20.48	1.59	24.72	1.53	28.96	1.48
3.56	2.28	7.80	1.95	12.04	1.78	16.28	1.67	20.52	1.59	24.76	1.53	29.00	1.48
3.60	2.28	7.84	1.95	12.08	1.78	16.32	1.67	20.56	1.59	24.80	1.53	29.04	1.48
3.64	2.27	7.88	1.95	12.12	1.78	16.36	1.67	20.60	1.59	24.84	1.53	29.08	1.48
3.68	2.27	7.92	1.95	12.16	1.78	16.40	1.66	20.64	1.59	24.88	1.52	29.12	1.48
3.72	2.26	7.96	1.94	12.20	1.78	16.44	1.66	20.68	1.58	24.92	1.52	29.16	1.48
3.76	2.26	8.00	1.94	12.24	1.77	16.48	1.66	20.72	1.58	24.96	1.52	29.20	1.48
3.80	2.26	8.04	1.94	12.28	1.77	16.52	1.66	20.76	1.58	25.00	1.52	29.24	1.48

V/ml	pH	V/ml	pH	V/ml	pH	V/ml	pH	V/ml	pH	V/ml	pH	V/ml	pH
3.84	2.25	8.08	1.94	12.32	1.77	16.56	1.66	20.80	1.58	25.04	1.52	29.28	1.48
3.88	2.25	8.12	1.94	12.36	1.77	16.60	1.66	20.84	1.58	25.08	1.52	29.32	1.48
3.92	2.24	8.16	1.93	12.40	1.77	16.64	1.66	20.88	1.58	25.12	1.52	29.36	1.48
3.96	2.24	8.20	1.93	12.44	1.77	16.68	1.66	20.92	1.58	25.16	1.52	29.40	1.48
4.00	2.23	8.24	1.93	12.48	1.77	16.72	1.66	20.96	1.58	25.20	1.52	29.44	1.47
4.04	2.23	8.28	1.93	12.52	1.77	16.76	1.66	21.00	1.58	25.24	1.52	29.48	1.47
4.08	2.23	8.32	1.93	12.56	1.76	16.80	1.66	21.04	1.58	25.28	1.52	29.52	1.47
4.12	2.22	8.36	1.92	12.60	1.76	16.84	1.65	21.08	1.58	25.32	1.52	29.56	1.47
4.16	2.22	8.40	1.92	12.64	1.76	16.88	1.65	21.12	1.58	25.36	1.52	29.60	1.47
4.20	2.21	8.44	1.92	12.68	1.76	16.92	1.65	21.16	1.58	25.40	1.52	29.64	1.47

Table 10.2 pH-values und volumes of added 0.1M NaOH to 50 ml of $5 \cdot 10^{-3}$ M Asp; $I = 0.1$ M (NaCl); $T = 25^\circ\text{C}$.

V/ml	pH	V/ml	pH	V/ml	pH	V/ml	pH	V/ml	pH	V/ml	pH
0.00	3.13	2.12	4.47	4.24	10.17	6.36	11.24	8.48	11.58	10.60	11.77
0.04	3.15	2.16	4.53	4.28	10.20	6.40	11.25	8.52	11.59	10.64	11.77
0.08	3.17	2.20	4.59	4.32	10.22	6.44	11.26	8.56	11.59	10.68	11.77
0.12	3.19	2.24	4.67	4.36	10.25	6.48	11.27	8.60	11.60	10.72	11.77
0.16	3.21	2.28	4.75	4.40	10.28	6.52	11.28	8.64	11.60	10.76	11.78
0.20	3.22	2.32	4.86	4.44	10.30	6.56	11.29	8.68	11.61	10.80	11.78
0.24	3.24	2.36	4.99	4.48	10.33	6.60	11.30	8.72	11.61	10.84	11.78
0.28	3.26	2.40	5.17	4.52	10.35	6.64	11.31	8.76	11.61	10.88	11.78
0.32	3.28	2.44	5.44	4.56	10.38	6.68	11.32	8.80	11.62	10.92	11.79
0.36	3.30	2.48	5.85	4.60	10.40	6.72	11.32	8.84	11.62	10.96	11.79
0.40	3.32	2.52	6.41	4.64	10.43	6.76	11.33	8.88	11.62	11.00	11.79
0.44	3.34	2.56	7.13	4.68	10.46	6.80	11.34	8.92	11.63	11.04	11.79
0.48	3.36	2.60	7.85	4.72	10.48	6.84	11.35	8.96	11.63	11.08	11.80
0.52	3.38	2.64	8.33	4.76	10.51	6.88	11.35	9.00	11.64	11.12	11.80
0.56	3.40	2.68	8.58	4.80	10.53	6.92	11.36	9.04	11.64	11.16	11.80
0.60	3.42	2.72	8.72	4.84	10.56	6.96	11.37	9.08	11.64	11.20	11.80
0.64	3.44	2.76	8.82	4.88	10.58	7.00	11.38	9.12	11.65	11.24	11.81
0.68	3.46	2.80	8.90	4.92	10.61	7.04	11.38	9.16	11.65	11.28	11.81
0.72	3.48	2.84	8.97	4.96	10.63	7.08	11.39	9.20	11.66	11.32	11.81
0.76	3.50	2.88	9.04	5.00	10.66	7.12	11.40	9.24	11.66	11.36	11.81
0.80	3.52	2.92	9.09	5.04	10.68	7.16	11.40	9.28	11.66	11.40	11.82
0.84	3.54	2.96	9.15	5.08	10.71	7.20	11.41	9.32	11.66	11.44	11.82
0.88	3.57	3.00	9.20	5.12	10.73	7.24	11.42	9.36	11.67	11.48	11.82
0.92	3.59	3.04	9.25	5.16	10.76	7.28	11.42	9.40	11.67	11.52	11.82
0.96	3.61	3.08	9.29	5.20	10.78	7.32	11.43	9.44	11.68	11.56	11.83
1.00	3.63	3.12	9.33	5.24	10.80	7.36	11.43	9.48	11.68	11.60	11.83
1.04	3.65	3.16	9.38	5.28	10.83	7.40	11.44	9.52	11.68	11.64	11.83
1.08	3.67	3.20	9.41	5.32	10.85	7.44	11.44	9.56	11.69	11.68	11.83
1.12	3.70	3.24	9.45	5.36	10.87	7.48	11.45	9.60	11.69	11.72	11.84
1.16	3.72	3.28	9.49	5.40	10.89	7.52	11.46	9.64	11.69	11.76	11.84
1.20	3.74	3.32	9.52	5.44	10.91	7.56	11.46	9.68	11.70	11.80	11.84
1.24	3.76	3.36	9.56	5.48	10.93	7.60	11.47	9.72	11.70	11.84	11.84
1.28	3.78	3.40	9.59	5.52	10.95	7.64	11.48	9.76	11.70	11.88	11.85
1.32	3.81	3.44	9.62	5.56	10.97	7.68	11.48	9.80	11.71	11.92	11.85
1.36	3.83	3.48	9.65	5.60	10.98	7.72	11.49	9.84	11.71	11.96	11.85
1.40	3.86	3.52	9.69	5.64	11.00	7.76	11.49	9.88	11.71	12.00	11.85
1.44	3.88	3.56	9.72	5.68	11.02	7.80	11.50	9.92	11.72		
1.48	3.91	3.60	9.75	5.72	11.04	7.84	11.50	9.96	11.72		
1.52	3.93	3.64	9.77	5.76	11.05	7.88	11.51	10.00	11.72		
1.56	3.96	3.68	9.80	5.80	11.07	7.92	11.51	10.04	11.72		
1.60	3.99	3.72	9.83	5.84	11.08	7.96	11.52	10.08	11.73		
1.64	4.02	3.76	9.86	5.88	11.10	8.00	11.53	10.12	11.73		

V/ml	pcH	V/ml	pcH	V/ml	pcH	V/ml	pcH	V/ml	pcH	V/ml	pcH
1.68	4.05	3.80	9.89	5.92	11.11	8.04	11.53	10.16	11.73		
1.72	4.08	3.84	9.91	5.96	11.12	8.08	11.53	10.20	11.74		
1.76	4.11	3.88	9.94	6.00	11.14	8.12	11.54	10.24	11.74		
1.80	4.14	3.92	9.97	6.04	11.15	8.16	11.55	10.28	11.74		
1.84	4.17	3.96	9.99	6.08	11.16	8.20	11.55	10.32	11.74		
1.88	4.21	4.00	10.02	6.12	11.17	8.24	11.55	10.36	11.75		
1.92	4.25	4.04	10.05	6.16	11.19	8.28	11.56	10.40	11.75		
1.96	4.28	4.08	10.07	6.20	11.20	8.32	11.56	10.44	11.75		
2.00	4.33	4.12	10.10	6.24	11.21	8.36	11.57	10.48	11.76		
2.04	4.37	4.16	10.12	6.28	11.22	8.40	11.57	10.52	11.76		
2.08	4.42	4.20	10.15	6.32	11.23	8.44	11.58	10.56	11.76		

Table 10.3 pcH-values und volumes of added 0.1M NaOH to 40 ml of $5 \cdot 10^{-3}$ M Asp. 0.02 M HCl. 0.1 M NaCl and $1 \cdot 10^{-3}$ M Ni(NO₃)₂; T = 25°C.

V/ml	pcH	V/ml	pcH	V/ml	pcH	V/ml	pcH	V/ml	pcH	V/ml	pcH
0.00	1.77	8.52	3.29	10.53	5.56	11.09	7.96	11.66	9.71	13.87	11.23
0.03	1.77	8.67	3.37	10.56	5.65	11.11	8.10	11.71	9.78	14.08	11.28
0.05	1.77	8.82	3.46	10.59	5.74	11.13	8.24	11.77	9.85	14.33	11.34
0.08	1.77	8.96	3.54	10.61	5.83	11.14	8.35	11.83	9.92	14.60	11.39
0.10	1.77	9.10	3.62	10.64	5.92	11.15	8.45	11.90	9.99	14.92	11.44
0.60	1.81	9.23	3.71	10.66	6.00	11.16	8.54	11.96	10.06	15.28	11.50
1.10	1.84	9.36	3.80	10.69	6.09	11.18	8.61	12.03	10.14	15.70	11.55
1.60	1.88	9.48	3.89	10.71	6.18	11.19	8.68	12.11	10.22	16.20	11.60
2.10	1.92	9.60	3.98	10.73	6.27	11.20	8.74	12.18	10.29	16.70	11.65
2.60	1.97	9.71	4.08	10.76	6.36	11.21	8.80	12.25	10.36	17.20	11.70
3.10	2.02	9.82	4.18	10.78	6.44	11.23	8.86	12.33	10.43	17.70	11.74
3.60	2.07	9.91	4.28	10.80	6.52	11.24	8.91	12.40	10.50	18.20	11.77
4.10	2.12	10.00	4.39	10.82	6.61	11.25	8.96	12.47	10.57	18.70	11.80
4.60	2.19	10.08	4.50	10.84	6.69	11.27	9.02	12.55	10.63	19.20	11.83
5.10	2.26	10.14	4.61	10.86	6.77	11.29	9.07	12.62	10.68	19.70	11.86
5.60	2.34	10.20	4.71	10.89	6.86	11.31	9.13	12.70	10.74	20.20	11.88
6.10	2.43	10.24	4.81	10.91	6.95	11.33	9.18	12.77	10.79	20.70	11.91
6.57	2.53	10.28	4.90	10.93	7.04	11.36	9.23	12.86	10.84	21.20	11.93
6.94	2.63	10.32	4.99	10.96	7.14	11.38	9.29	12.94	10.89	21.70	11.95
7.27	2.73	10.35	5.07	10.98	7.24	11.41	9.34	13.04	10.94	22.20	11.97
7.54	2.83	10.38	5.15	11.00	7.34	11.44	9.40	13.14	10.98	22.70	11.99
7.77	2.92	10.41	5.23	11.02	7.45	11.48	9.46	13.25	11.03	23.20	12.00
7.99	3.02	10.44	5.31	11.04	7.57	11.52	9.52	13.38	11.08	23.70	12.02
8.18	3.11	10.47	5.39	11.06	7.68	11.56	9.58	13.52	11.13		
8.36	3.20	10.50	5.47	11.08	7.82	11.61	9.65	13.69	11.18		

Table 10.4 pcH-values und volumes of added 0.1M NaOH to 40 ml of $5 \cdot 10^{-3}$ M Asp. 0.02 M HCl. 0.1 M NaCl and $2 \cdot 10^{-3}$ M Ni(NO₃)₂; T = 25°C.

V/ml	pcH	V/ml	pcH	V/ml	pcH	V/ml	pcH	V/ml	pcH	V/ml	pcH
0.08	1.77	8.86	3.33	10.84	5.40	11.70	7.55	12.27	9.83	15.35	11.48
0.10	1.77	9.01	3.40	10.88	5.48	11.72	7.62	12.30	9.91	15.81	11.54
0.18	1.78	9.15	3.48	10.92	5.56	11.74	7.69	12.34	9.99	16.31	11.60
0.31	1.79	9.29	3.55	10.96	5.64	11.76	7.75	12.37	10.06	16.81	11.65
0.60	1.81	9.42	3.63	11.00	5.71	11.78	7.80	12.41	10.14	17.31	11.69
1.10	1.84	9.55	3.72	11.04	5.79	11.80	7.86	12.45	10.21	17.81	11.73
1.60	1.88	9.68	3.80	11.07	5.86	11.82	7.93	12.49	10.28	18.31	11.76
2.10	1.92	9.79	3.90	11.11	5.94	11.83	7.99	12.54	10.35	18.81	11.80
2.60	1.97	9.90	3.99	11.14	6.01	11.85	8.05	12.58	10.42	19.31	11.82
3.10	2.01	9.96	4.04	11.17	6.09	11.87	8.11	12.64	10.49	19.81	11.85

V/ml	pcH	V/ml	pcH	V/ml	pcH	V/ml	pcH	V/ml	pcH	V/ml	pcH
3.60	2.06	10.00	4.09	11.20	6.17	11.88	8.18	12.69	10.55	20.31	11.88
4.10	2.12	10.05	4.14	11.23	6.26	11.90	8.25	12.75	10.62	20.81	11.90
4.60	2.18	10.13	4.24	11.26	6.34	11.92	8.33	12.82	10.68	21.31	11.92
5.10	2.25	10.21	4.34	11.29	6.44	11.94	8.41	12.90	10.74	21.81	11.94
5.60	2.33	10.28	4.44	11.32	6.53	11.95	8.50	12.99	10.81	22.31	11.96
6.10	2.42	10.34	4.53	11.36	6.63	11.97	8.60	13.09	10.87	22.81	11.98
6.57	2.51	10.39	4.61	11.39	6.73	11.99	8.71	13.20	10.93	23.31	12.00
6.95	2.61	10.44	4.70	11.42	6.82	12.01	8.85	13.33	10.99	23.81	12.01
7.28	2.70	10.48	4.77	11.45	6.91	12.04	8.99	13.48	11.06	24.31	12.03
7.55	2.79	10.52	4.84	11.49	6.99	12.06	9.12	13.65	11.12	24.81	12.04
7.79	2.87	10.56	4.92	11.52	7.08	12.09	9.24	13.84	11.18	25.31	12.06
8.01	2.95	10.61	5.00	11.55	7.17	12.12	9.35	14.06	11.24		
8.21	3.03	10.65	5.08	11.58	7.24	12.14	9.46	14.31	11.30		
8.39	3.11	10.70	5.16	11.61	7.32	12.17	9.56	14.60	11.36		
8.56	3.18	10.74	5.24	11.64	7.40	12.20	9.65	14.95	11.42		
8.71	3.26	10.79	5.32	11.67	7.47	12.24	9.74	15.35	11.48		

10.1.2 Spectrophotometrical data

10.1.2.1 Uv-Vis Spectrophotometrical data

a) pH-titrations

Table 10.5a pcH-dependence of the equilibrium absorption of $2 \cdot 10^{-3}$ M nickel(II) nitrate in the presence of $5 \cdot 10^{-3}$ M Asp, $d = 5$ cm and 0.1M NaCl at 25°C at different wavelengths.

pcH	A (360 nm)	A (389 nm)	A (405 nm)	A (593 nm)	A (641 nm)	A (724 nm)
2.80	0.009	0.050	0.044	0.003	0.013	0.018
3.03	0.009	0.049	0.045	0.004	0.014	0.019
3.24	0.010	0.049	0.044	0.003	0.014	0.019
3.45	0.010	0.049	0.045	0.004	0.014	0.019
3.63	0.009	0.049	0.044	0.004	0.014	0.018
3.82	0.010	0.050	0.044	0.004	0.015	0.019
4.00	0.012	0.050	0.044	0.005	0.015	0.018
4.19	0.013	0.051	0.044	0.006	0.016	0.018
4.38	0.015	0.052	0.043	0.007	0.017	0.018
4.60	0.018	0.052	0.043	0.010	0.020	0.019
4.72	0.020	0.052	0.042	0.011	0.021	0.019
4.84	0.021	0.053	0.041	0.012	0.022	0.018
4.98	0.023	0.054	0.041	0.014	0.023	0.018
5.22	0.027	0.055	0.042	0.016	0.025	0.019
5.36	0.031	0.056	0.041	0.018	0.027	0.018
5.56	0.034	0.056	0.041	0.019	0.028	0.018
5.76	0.038	0.057	0.042	0.022	0.030	0.018
5.98	0.041	0.057	0.042	0.023	0.031	0.018
6.20	0.045	0.057	0.042	0.025	0.032	0.018
6.40	0.048	0.057	0.043	0.027	0.033	0.018
6.58	0.051	0.056	0.043	0.029	0.034	0.019
6.74	0.056	0.055	0.042	0.030	0.034	0.019
6.89	0.057	0.054	0.042	0.031	0.034	0.018
7.16	0.064	0.053	0.042	0.034	0.036	0.018
7.43	0.067	0.053	0.041	0.036	0.036	0.018
7.95	0.066	0.048	0.038	0.039	0.036	0.017

120 pH-Sensitive Binding of Nickel(II) Ions to Aspartic Acid

pcH	A (360 nm)	A (389 nm)	A (405 nm)	A (593 nm)	A (641 nm)	A (724 nm)
8.13	0.071	0.050	0.037	0.039	0.035	0.016
8.52	0.075	0.049	0.039	0.041	0.037	0.017
8.87	0.077	0.049	0.038	0.042	0.037	0.017
9.14	0.076	0.049	0.038	0.041	0.036	0.016
9.34	0.081	0.051	0.041	0.043	0.038	0.018
9.50	0.079	0.049	0.039	0.042	0.037	0.017
9.64	0.078	0.049	0.038	0.042	0.037	0.017
9.76	0.082	0.050	0.041	0.043	0.038	0.017
9.86	0.078	0.049	0.039	0.042	0.036	0.016
9.98	0.071	0.048	0.036	0.041	0.036	0.016

Table 10.5b pcH-dependence of the equilibrium absorption of $2 \cdot 10^{-3}$ M nickel(II) nitrate in the presence of $5 \cdot 10^{-3}$ M Asp, $d = 5$ cm and 0.1M NaCl at 25°C at different wavelengths.

pcH	A (363 nm)	A (380 nm)	A (395 nm)	A (600 nm)	A (632 nm)
2.80	0.013	0.038	0.051	0.005	0.013
3.03	0.013	0.037	0.051	0.005	0.013
3.24	0.013	0.038	0.051	0.005	0.013
3.45	0.013	0.038	0.051	0.005	0.013
3.63	0.014	0.038	0.051	0.006	0.013
3.82	0.015	0.039	0.051	0.006	0.014
4.00	0.016	0.04	0.052	0.007	0.015
4.19	0.017	0.041	0.051	0.008	0.016
4.38	0.02	0.043	0.052	0.009	0.017
4.60	0.022	0.046	0.051	0.012	0.019
4.72	0.024	0.047	0.051	0.013	0.02
4.84	0.025	0.048	0.051	0.014	0.021
4.98	0.028	0.05	0.051	0.015	0.023
5.22	0.031	0.053	0.051	0.017	0.024
5.36	0.034	0.055	0.051	0.018	0.025
5.56	0.037	0.057	0.051	0.019	0.026
5.76	0.04	0.059	0.051	0.02	0.027
5.98	0.043	0.06	0.051	0.021	0.027
6.20	0.045	0.06	0.05	0.022	0.027
6.40	0.048	0.061	0.05	0.023	0.028
6.58	0.049	0.061	0.049	0.023	0.028
6.74	0.051	0.06	0.049	0.024	0.027
6.89	0.052	0.06	0.047	0.025	0.027
7.16	0.056	0.06	0.046	0.025	0.027
7.43	0.059	0.059	0.045	0.027	0.027
7.95	0.062	0.056	0.04	0.029	0.027
8.13	0.063	0.057	0.042	0.03	0.028
8.52	0.065	0.057	0.041	0.03	0.027
8.87	0.066	0.057	0.041	0.031	0.029
9.14	0.067	0.057	0.041	0.032	0.028
9.34	0.069	0.059	0.042	0.031	0.028
9.50	0.067	0.057	0.041	0.03	0.027
9.64	0.067	0.058	0.041	0.031	0.028
9.76	0.07	0.059	0.042	0.03	0.027
9.86	0.068	0.058	0.041	0.031	0.027
9.98	0.068	0.057	0.04	0.032	0.028

b) Nickel(II) nitrate - titrations - Separate solution experiments

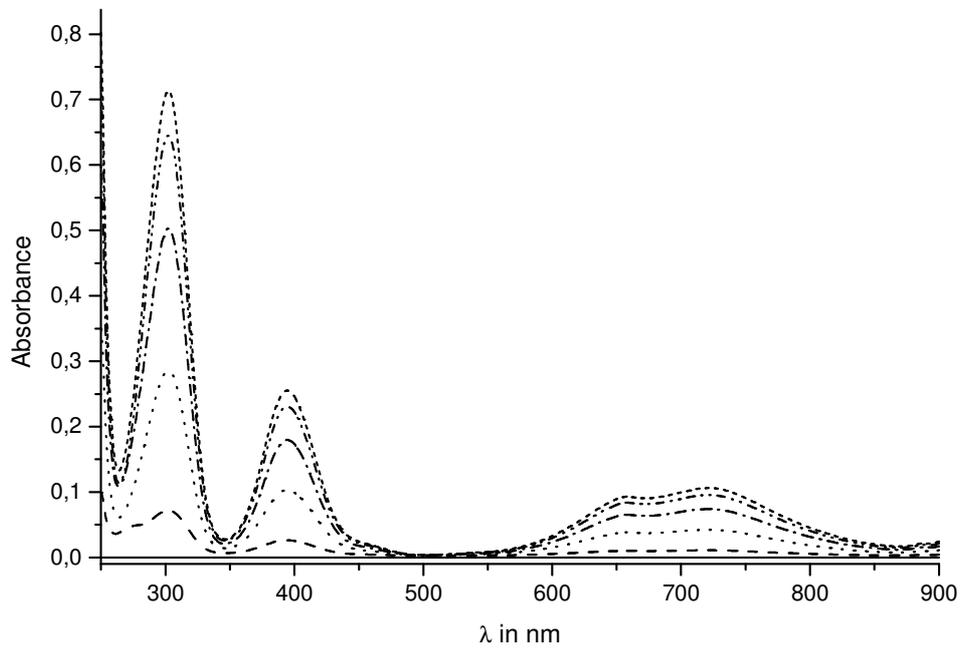
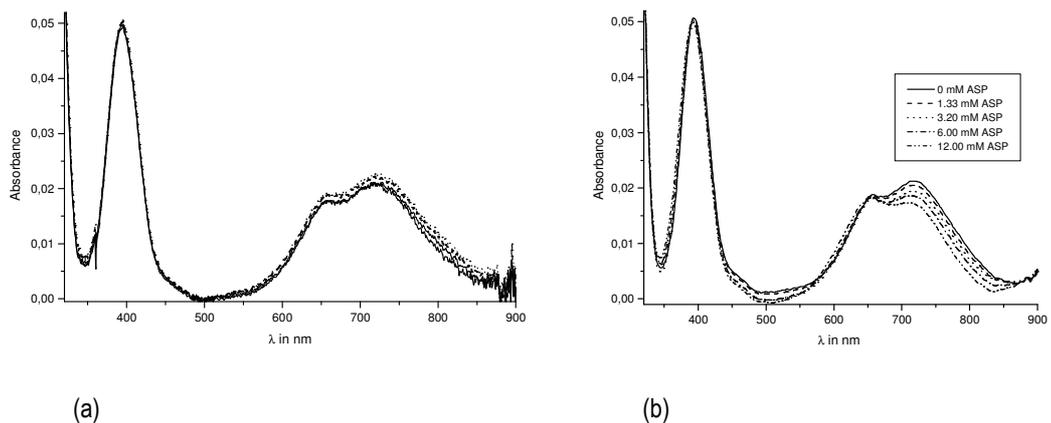


Figure 10.1 Nickel(II) nitrate concentration-dependence of the equilibrium absorption of solutions of $2 \cdot 10^{-4}$ M Asp at varying nickel(II) nitrate concentration, $d = 5$ cm and 0.1 M NaCl at 25°C (a) at $\text{pH } 5.22$; $[\text{buffer}]_{\text{NaAc}} = 5 \cdot 10^{-3}$ M; $[\text{Nickel(II) nitrate}] = 0$ M, $1 \cdot 10^{-3}$ M, $4 \cdot 10^{-3}$ M, $7 \cdot 10^{-3}$ M, $9 \cdot 10^{-3}$ M and $1 \cdot 10^{-2}$ M (in the order of increasing absorption at 700nm); Spectra for $\text{pH } 6.80$ are similar to the ones shown here and hence are not shown.

c) Asp-titrations - Separate solution experiments



(a)

(b)

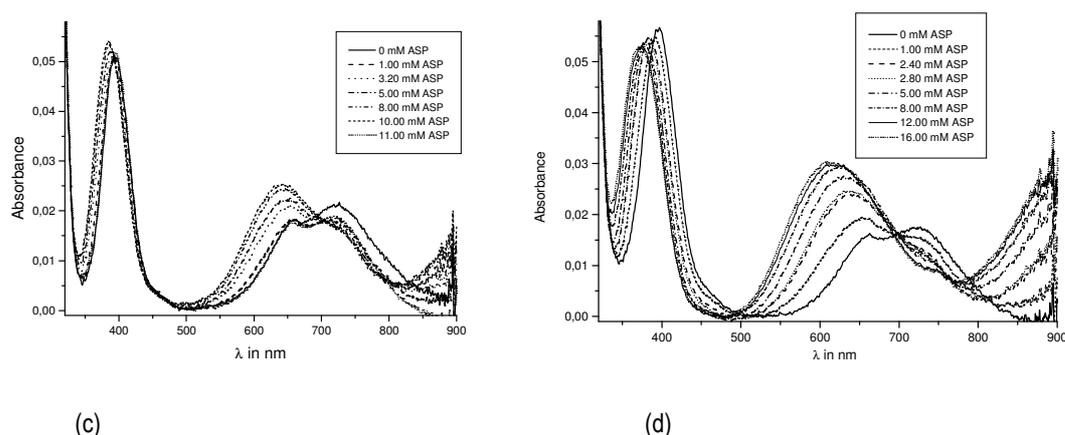


Figure 10.2 Asp concentration-dependence of the equilibrium absorption of $2 \cdot 10^{-3}$ M nickel(II) nitrate solution, $d = 5$ cm and 0.1M NaCl at 25°C (a) at pCh 3.45; $[\text{Asp}]_0 = 0$ M, $0.33 \cdot 10^{-3}$ M, $3.2 \cdot 10^{-3}$ M and $8 \cdot 10^{-3}$ M (in the order of increasing absorption at 800nm); (b) at pCh 4.00; $[\text{Asp}]_0$ - see legend; (c) at pCh 5.22; $[\text{Asp}]_0$ - see legend; $[\text{buffer}]_{\text{NaAc}} = 5 \cdot 10^{-3}$ M (d) at pCh 6.80; $[\text{buffer}]_{\text{lutidine}} = 5 \cdot 10^{-3}$ M. $[\text{Asp}]_0$ - see legend;

10.1.2.2 IR and Raman data

IR and Raman experiments were especially performed in order to get evidence about the chemical structure of the nickel complexes formed at low pH (NiLH^+ and possibly $\text{Ni}(\text{LH})_2$).

a) IR Spectroscopy

The band at 3423 cm^{-1} (seen also in Asp) indicates a free NH_2 group in sample P. This peak is shifted to 3443 cm^{-1} in NiL and NiL_2^{2-} due to chelation (see L.J. Bellamy, 1975). Additionally, the band at around 1600 (1599 cm^{-1} in NiL and 1589 cm^{-1} in NiL_2^{2-}) indicates an ionised carbonyl absorption and is typically shifted by 35 cm^{-1} to higher frequencies indicating the presence of NH_3^+ group in sample P as reported by L.J. Bellamy, 1975, M. Q. Ehsan et al., 1999 and L. P. Battaglia et al., 1982.

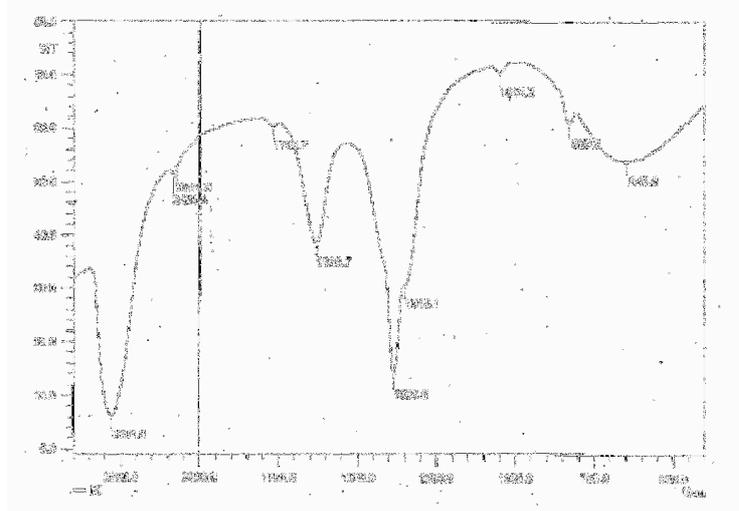


Figure 10.3: IR spectrum of nickel(II) nitrate

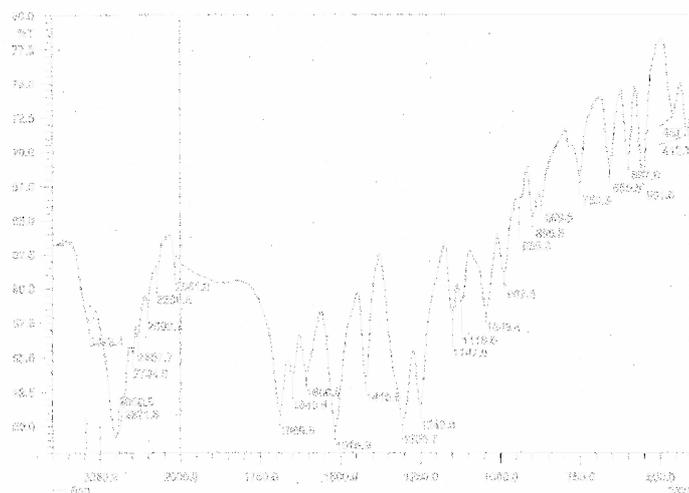
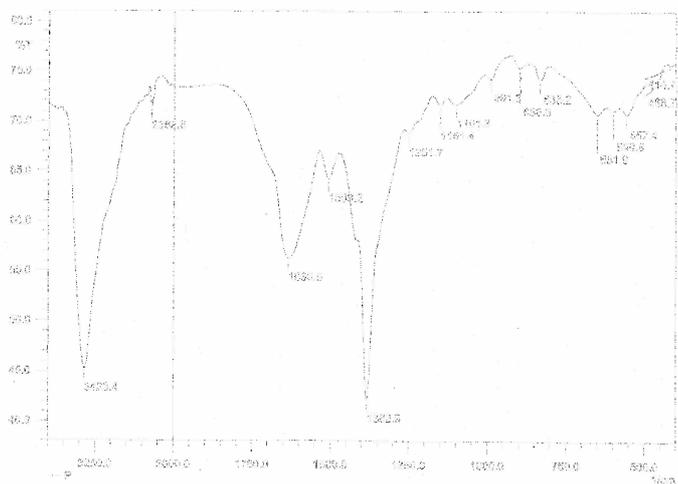
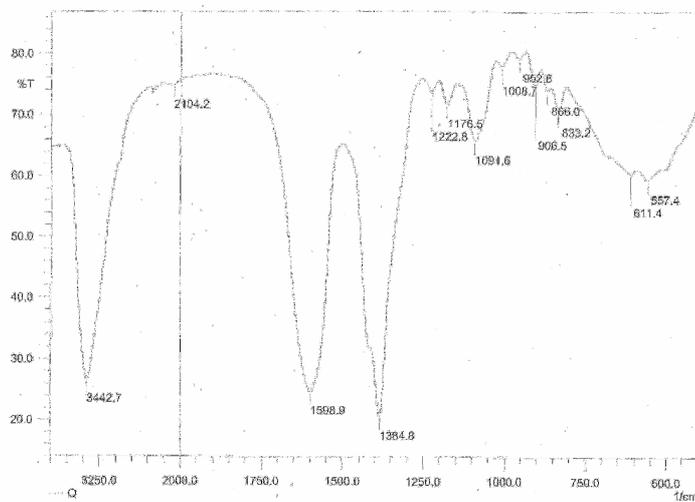


Figure 10.4: IR spectrum of aspartic acid

Figure 10.5: IR spectrum of a freeze-dried solution of 0.05M Ni(NO₃)₂ and 0.125M Asp at pH 3.5 (sample P)Figure 10.6: IR spectrum of a freeze-dried solution of 0.05M Ni(NO₃)₂ and 0.125M Asp at pH 6.0 (sample Q)

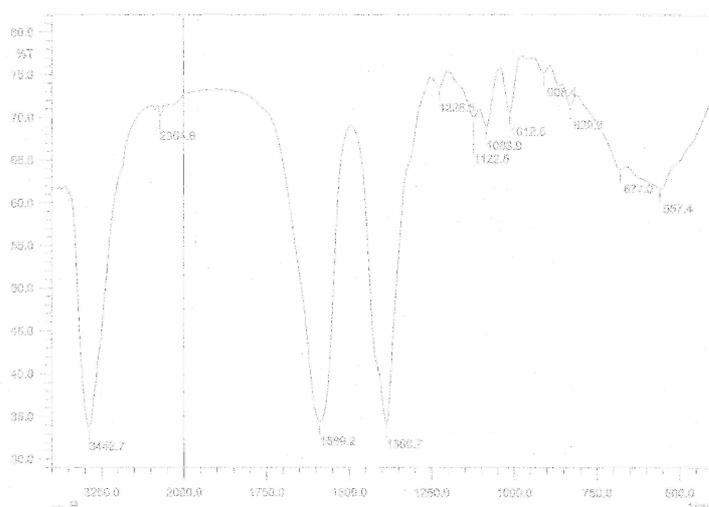


Figure 10.7: IR spectrum of a freeze-dried solution of 0.05M Ni(NO₃)₂ and 0.125M Asp at pH 10.5 (sample R)

b) Raman Spectroscopy

The typical NH stretching vibration seen at 2953 cm⁻¹ in Asp occurs also in NiLH⁺ (eventually in Ni(LH)₂) at 2950 cm⁻¹ and is shifted to 2937 cm⁻¹ in NiL and to 2924 cm⁻¹ in NiL₂²⁻ indicating a free NH₂ in sample P.

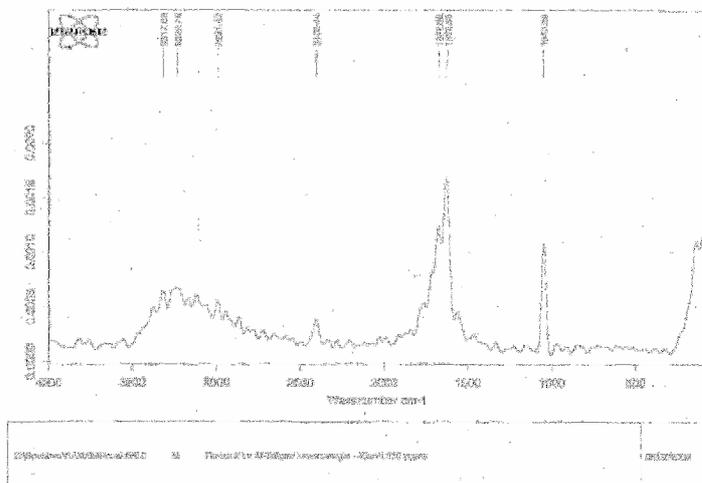


Figure 10.8: Raman spectrum of nickel(II) nitrate

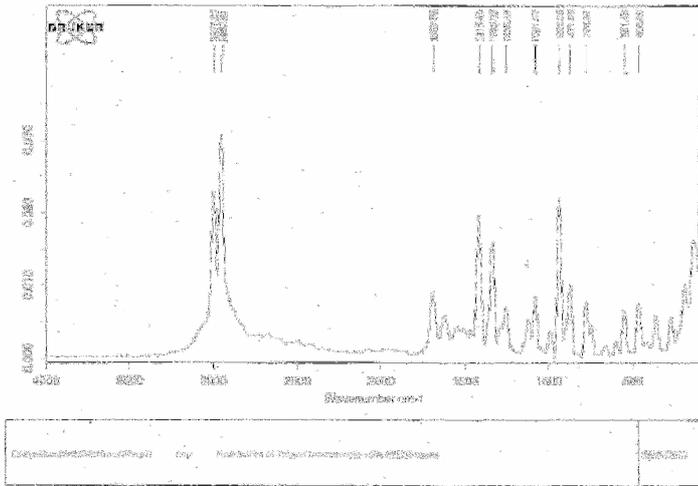


Figure 10.9: Raman spectrum of aspartic acid

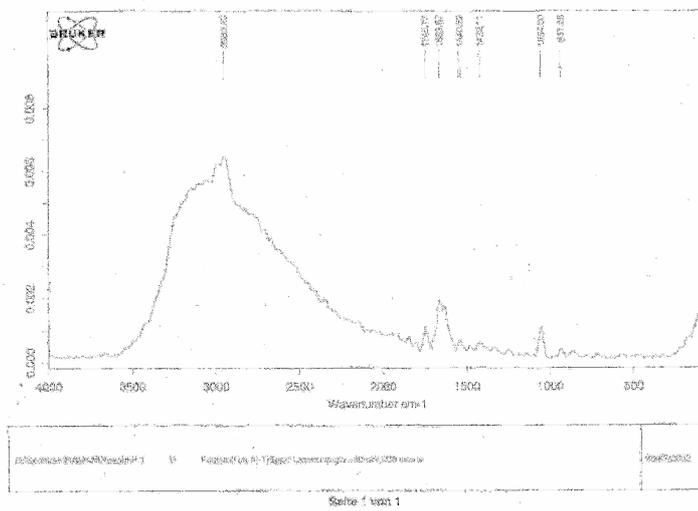


Figure 10.10: Raman spectrum of a freeze-dried solution of 0.05M Ni(NO₃)₂ and 0.125M Asp at pH 3.5 (sample P)

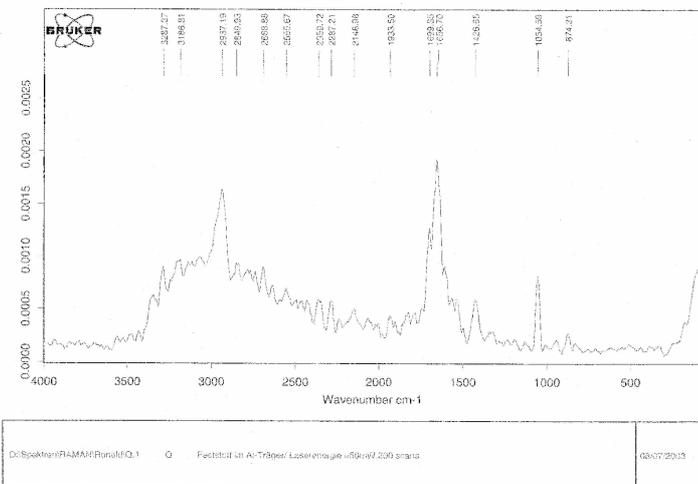
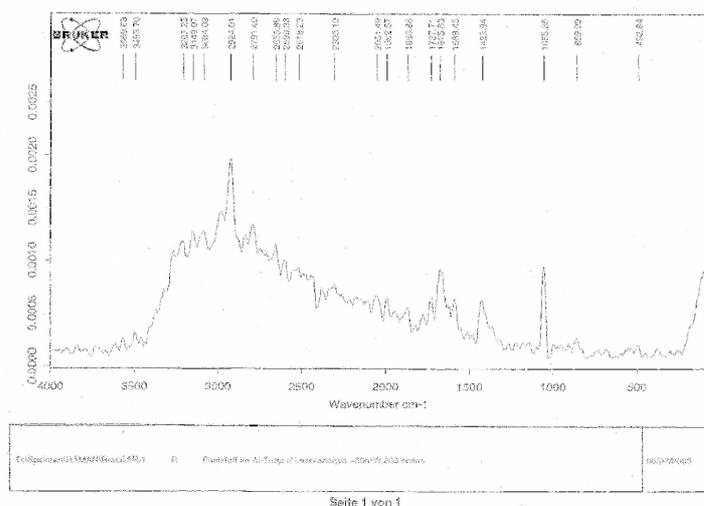


Figure 10.11: Raman spectrum of a freeze-dried solution of 0.05M Ni(NO₃)₂ and 0.125M Asp at pH 6.0 (sample Q)

Figure 10.12: Raman spectrum of a freeze-dried solution of 0.05M Ni(NO₃)₂ and 0.125M Asp at pH 10.5 (sample R)

10.1.3 Kinetic data - Stopped-flow Experiments

Table 10.6 Reciprocal of the relaxation times and amplitudes of the reaction of Ni(II) ions with Asp as a function of pCh; Ni₀ = 10⁻² M, Asp₀ = 2.5 × 10⁻⁴ M, I = 0.1 M (NaCl), buffer₀ = 5 · 10⁻³ M, indicator₀ = 2 · 10⁻⁵ M; T = 25°C;

Fo:Formate; Ac: Acetate; Lu: Lutidine

[H ⁺] /M	pCh	τ /s	$1/\tau$ /s ⁻¹	$\delta A/mOD$ BPB/Fo	$\delta A/mOD$ BCG/Ac	$\delta A/mOD$ BCG/Lu	$\delta A/mOD$ CPR/Ac	$\delta A/mOD$ CPR/Lu	$\delta A/mOD$ BTB/Ac	$\delta A/mOD$ BTB/Lu
6.38E-04	3.19			1.12						
4.03E-04	3.39				2.00					
4.03E-04	3.39	69.0	0.0145		1.00					
4.03E-04	3.39	89.0	0.0112		0.44					
4.03E-04	3.39				1.00					
4.03E-04	3.39			2.37						
2.54E-04	3.59	80.6	0.0124							
2.54E-04	3.59	78.8	0.0127		2.00					
2.54E-04	3.59				2.00					
2.54E-04	3.59				2.40					
2.54E-04	3.59			4.15						
2.02E-04	3.69	90.5	0.0111		2.61					
2.02E-04	3.69	90.3	0.0111		3.00					
2.02E-04	3.69	90.5	0.0111		2.65					
2.02E-04	3.69	87.2	0.0115		0.26					
2.02E-04	3.69				3.30					
1.60E-04	3.79				5.80					
1.60E-04	3.79	103.1	0.0097		5.00					
1.60E-04	3.79				5.60					
1.27E-04	3.89	105.0	0.0095		10.00					
1.27E-04	3.89	100.0	0.0100		6.90					
1.27E-04	3.89	95.0	0.0105		6.00					
1.27E-04	3.89	83.0	0.0121		6.58					
1.27E-04	3.89	100.0	0.0100		6.90					
1.01E-04	3.99	105.0	0.0095		7.00					
8.04E-05	4.09	106.0	0.0094		8.70					
8.04E-05	4.09	106.5	0.0094		8.00					
8.04E-05	4.09	105.0	0.0095		7.62					

[H ⁺] /M	pCh	τ /s	$1/\tau$ /s ⁻¹	$\delta A/mOD$ BPB/Fo	$\delta A/mOD$ BCG/Ac	$\delta A/mOD$ BCG/Lu	$\delta A/mOD$ CPR/Ac	$\delta A/mOD$ CPR/Lu	$\delta A/mOD$ BTB/Ac	$\delta A/mOD$ BTB/Lu
8.04E-05	4.09	106.0	0.0094		8.70					
6.38E-05	4.19	131.0	0.0076		17.00					
6.38E-05	4.19	108.0	0.0093		13.00					
5.07E-05	4.29	102.8	0.0097		15.00					
4.96E-05	4.30	102.0	0.0098		13.20					
4.96E-05	4.30	102.0	0.0098		13.20					
4.03E-05	4.39	100.0	0.0100		15.80					
4.03E-05	4.39	97.5	0.0103		14.00					
4.03E-05	4.39	103.0	0.0097		16.75					
3.20E-05	4.49	88.0	0.0114		22.40					
3.20E-05	4.49	90.0	0.0111		15.30					
3.20E-05	4.49	93.9	0.0107		18.00					
3.20E-05	4.49	99.2	0.0101		15.24					
3.20E-05	4.49	90.0	0.0111		15.30					
2.54E-05	4.59	82.0	0.0122		19.00					
2.54E-05	4.59	80.0	0.0125		20.00					
2.02E-05	4.69	83.8	0.0119		18.90					
2.02E-05	4.69	77.6	0.0129		20.00					
2.02E-05	4.69	89.2	0.0112		19.90					
1.60E-05	4.79	70.8	0.0141		25.80					
1.60E-05	4.79	66.5	0.0150		23.00					
1.60E-05	4.79				24.00					
1.40E-05	4.85	59.0	0.0170		28.00					
1.27E-05	4.89	62.0	0.0161				7.00			
1.27E-05	4.89	57.9	0.0173		24.00					
1.27E-05	4.89				25.00					
1.27E-05	4.89	63.7	0.0157				6.03			
1.27E-05	4.89	61.8	0.0162						2.35	
8.04E-06	5.09	41.7	0.0240		33.00					
8.04E-06	5.09	41.3	0.0242				11.10			
8.04E-06	5.09	38.3	0.0261				12.50			
6.38E-06	5.19	38.0	0.0263				16.00			
6.38E-06	5.19	46.3	0.0216						2.60	
5.07E-06	5.29	27.0	0.0370				21.00			
5.07E-06	5.29	28.2	0.0355				20.00			
5.07E-06	5.29	28.6	0.0350				24.20			
4.32E-06	5.36	30.0	0.0333		38.00					
4.03E-06	5.39	34.3	0.0292							7.70
4.03E-06	5.39	29.3	0.0341						5.40	
3.76E-06	5.42	22.3	0.0448				38.00			
3.13E-06	5.50	20.7	0.0483				29.00			
3.13E-06	5.50	21.8	0.0459				27.00			
2.54E-06	5.59	18.7	0.0535						9.00	
2.02E-06	5.69	22.1	0.0453			23.00				
1.53E-06	5.81	13.9	0.0719					59.00		
1.27E-06	5.89	13.2	0.0756			8.70				
1.27E-06	5.89	9.4	0.1060							8.70
1.27E-06	5.89	12.6	0.0793							9.50
1.01E-06	5.99	3.2	0.3155							11.21
1.01E-06	5.99	9.3	0.1075							10.90
8.04E-07	6.09	6.5	0.1541					36.00		
8.04E-07	6.09	7.8	0.1277			4.60				

128 pH-Sensitive Binding of Nickel(II) Ions to Aspartic Acid

[H ⁺] /M	pCh	τ /s	$1/\tau$ /s ⁻¹	$\delta A/mOD$ BPB/Fo	$\delta A/mOD$ BCG/Ac	$\delta A/mOD$ BCG/Lu	$\delta A/mOD$ CPR/Ac	$\delta A/mOD$ CPR/Lu	$\delta A/mOD$ BTB/Ac	$\delta A/mOD$ BTB/Lu
6.38E-07	6.19	5.7	0.1745							11.30
6.38E-07	6.19	5.8	0.1721							10.50
4.84E-07	6.31	5.0	0.2008					23.00		
4.03E-07	6.39	3.7	0.2740							11.45
4.03E-07	6.39	3.7	0.2695							11.10
4.03E-07	6.39	3.7	0.2703							9.90
2.54E-07	6.59	3.0	0.3333					9.00		

Table 10.7 Reciprocal of the relaxation times and amplitudes of the reaction of Ni(II) ions with Asp as a function of pCh; Asp₀ = 10⁻² M, Ni₀ = 2.5x10⁻⁴ M, I = 0.1 M (NaCl), buffer₀ = 5.10⁻³ M, indicator₀ = 2.10⁻⁵ M; T=25°C; Fo:Formate; Ac: Acetate; Lu: Lutidine

[H ⁺] /M	pCh	τ /s	$1/\tau$ /s ⁻¹	δA /mOD BPB/Fo	δA /mOD BCG/Ac	δA /mOD BCG/Lu	δA /mOD CPR/Ac	δA /mOD CPR/Lu			$\delta A1$ /mOD BTB/ 5mM Lu	$\delta A1$ /mOD BTB/ 10mM Lu	$\delta A2$ /mOD BTB/ 5mM Lu	$\delta A2$ /mOD BTB/ 10mM Lu
3,22E-04	3,49	80,7	0,0124	2,61										
2,56E-04	3,59	78,8	0,0127	4,42										
2,03E-04	3,69	86,2	0,0116	5,40										
1,28E-04	3,89	92,1	0,0109	11,74										
8,09E-05	4,09	106,5	0,0094		4,50									
8,09E-05	4,09	94,9	0,0105	18,90										
4,99E-05	4,30	98,0	0,0102	28,40										
3,61E-05	4,44	82,0	0,0122		12,30									
3,61E-05	4,44	94,1	0,0106		9,60									
3,61E-05	4,44	87,1	0,0115		9,60									
3,22E-05	4,49	78,4	0,0128		17,51									
2,03E-05	4,69	69,2	0,0145		26,70									
2,03E-05	4,69									1,30				
1,28E-05	4,89	55,9	0,0179		34,51									
8,09E-06	5,09	43,1	0,0232		41,70									
8,09E-06	5,09	40,0	0,0250							5,30				
7,21E-06	5,14	35,0	0,0286		23,00									
5,10E-06	5,29	30,4	0,0330		23,10									
5,10E-06	5,29	26,9	0,0372							11,10				
3,61E-06	5,44	30,0								51,00				
3,22E-06	5,49	21,8	0,0459		26,00									
3,22E-06	5,49	19,3	0,0518							21,00				
[H ⁺] /M	pCh	τ_{II} /s	τ_{II}^{-1} /s ⁻¹	δA /mOD BPB/Fo	δA /mOD BCG/Ac	δA /mOD BCG/Lu	δA /mOD CPR/Ac	δA /mOD CPR/Lu	τ_I /s	τ_I^{-1} /s ⁻¹	$\delta A1$ /mOD BTB/ 5mM Lu	$\delta A1$ /mOD BTB/ 10mM Lu	$\delta A2$ /mOD BTB/ 5mM Lu	$\delta A2$ /mOD BTB/ 10mM Lu
2,50E-06	5,60	3,8	0,2632						33,0	0,0303				
2,39E-06	5,62	16,9				28,00								
2,03E-06	5,69	13,8	0,0725				29,00							
2,02E-06	5,69	13,5	0,0741				57,60							
1,65E-06	5,78	15,6				26,00								
1,28E-06	5,89	9,6	0,1046				45,50							
1,28E-06	5,89	9,6	0,1041				41,40		18,0	0,0556				
1,27E-06	5,89	10,0	0,1000				76,80							
1,27E-06	5,89	4,9	0,2041						13,4		14,00		13,00	
1,02E-06	5,99	9,0				12,00			13,4					
1,01E-06	5,99	4,4							5,6	0,1770				
1,02E-06	5,99	9,1	0,1094					20,00						

[H ⁺] /M	pCh	τ_{II} /s	τ_{II}^{-1} /s ⁻¹	δA /mOD BPB/Fo	δA /mOD BCG/Ac	δA /mOD BCG/Lu	δA /mOD CPR/Ac	δA /mOD CPR/Lu	τ_I /s	τ_I^{-1} /s ⁻¹	$\delta A1$ /mOD BTB/ 5mM Lu	$\delta A1$ /mOD BTB/ 10mM Lu	$\delta A2$ /mOD BTB/ 5mM Lu	$\delta A2$ /mOD BTB/ 10mM Lu
1,01E-06	5,99	11,7	0,0850						4,3	0,2330		8,00		6,00
8,09E-07	6,09	7,8	0,1290					16,50	6,3					
8,04E-07	6,09	5,7	0,1754						3,7	0,2690	11,00		27,00	
8,04E-07	6,09	9,7	0,1030									10,00		6,00
7,21E-07	6,14	7,4	0,1348						7,2	0,1389				
7,05E-07	6,15	6,5				10,00			4,0					
6,38E-07	6,19	8,4	0,1200						5,1	0,1965		10,00		7,00
5,10E-07	6,29	5,6	0,1776					12,10	3,8					
5,07E-07	6,29	2,3	0,4348								15,00		34,00	
3,22E-07	6,49	4,4	0,2257					8,70	1,2	0,8260				
3,20E-07	6,49	1,5	0,6667								14,00		47,00	
3,01E-07	6,52	0,8							3,1					
2,03E-07	6,69	3,3	0,3040					4,00	1,1	0,9450				
2,02E-07	6,69	1,4	0,7143								22,00		41,00	
2,02E-07	6,69	3,8	0,2650						3,6	0,2762		19,00		
2,02E-07	6,69	3,5	0,2870						0,7	1,3700		20,00		
1,69E-07	6,77	0,9							0,7	1,3790				
1,60E-07	6,79	3,6	0,2760						1,8			19,00		7,00
1,28E-07	6,89	2,3	0,4329					2,50						
1,27E-07	6,89	1,1	0,9091						7,0	0,1429	24,00		49,00	
1,27E-07	6,89	2,8	0,3630						0,6	1,7090		25,00		8,00
1,27E-07	6,89	2,7	0,3710						2,0			26,00		9,00
9,73E-08	7,01								7,4	0,1351				
8,09E-08	7,09	2,2	0,4484					2,00	0,4	2,8170				
8,04E-08	7,09	2,0	0,5000						2,0		50,00		86,00	
8,04E-08	7,09	2,1	0,4830						6,7	0,1493		30,00		10,00
6,43E-08	7,19	0,5												
5,07E-08	7,29	2,1	0,4762						5,1	0,1961	30,00		65,00	
3,20E-08	7,49	2,3	0,4348						0,9		20,00		45,00	
2,02E-08	7,69	2,1	0,4762								23,00		28,00	
1,27E-08	7,89	1,2	0,8333								7,00		37,00	

Table 11.8 Reciprocal of the relaxation times of the reaction of Ni(II) ions with Asp as a function of nickel(II) nitrate concentration for the case where Ni(II) ions were present in excess;

pH = 7; Asp₀ = 2.5 × 10⁻⁵ M, I = 0.1 M (NaCl), lutidine₀ = 5.10⁻³ M, BTB₀ = 2.10⁻⁵ M; T = 25°C;

Ni ₀ / 10 ⁻³ M	τ / s	τ^{-1} / s ⁻¹
0.25	31.2	0.0321
0.50	15.2	0.0658
1.00	7.9	0.1267
1.25	6.4	0.1567
1.50	4.9	0.2037
2.50	4.5	0.2240
5.00	2.1	0.4740
6.25	1.4	0.7353
8.75	1.0	1.0101
10.00	0.9	1.1111

Table 10.9 Reciprocals of the relaxation times for the reaction of Ni(II) ions with Asp as a function of nickel(II) nitrate concentration for the case where Ni(II) ions were present in excess;

pH = 4.30; Asp₀ = 5.10⁻⁴ M, I = 0.1 M (NaCl), Acetate₀ = 5.10⁻³ M, BCG₀ = 2.10⁻⁵ M, T=25°C;

Ni ₀ /10 ⁻³ M	τ /s	τ ⁻¹ /s ⁻¹
5.0	137	0.0073
7.5	135	0.0074
10.0	113	0.0088
15.0	110	0.0091
20.0	90	0.0111

Table 10.10 Reciprocal of the relaxation times of the reaction of Ni(II) ions with Asp as a function of nickel(II) nitrate concentration for the case where Asp was present in excess;

pH = 7; Ni₀ = 2.5x10⁻⁵ M, I = 0.1 M (NaCl), lutidine₀ = 5.10⁻³ M, BTB₀ = 2.10⁻⁵ M; T=25°C;

L ₀ /10 ⁻³ M	τ _I /s	τ _I ⁻¹ /s ⁻¹	τ _{II} /s	τ _{II} ⁻¹ /s ⁻¹
3.75	2.97	0.3370	6.46	0.1548
5.00	1.90	0.5260	4.50	0.2222
6.25	1.45	0.6900	3.22	0.3106
7.50	1.14	0.8770	2.85	0.3509
8.75	1.10	0.9090	2.38	0.4202

Table 10.11 Reciprocal of the relaxation times of the reaction of Ni(II) ions with Asp as a function of nickel(II) nitrate concentration for the case where Asp was present in excess;

pH = 4.20; Asp₀ = 5x10⁻⁴ M, I = 0.1 M (NaCl), Acetate₀ = 5.10⁻³ M, BCG₀ = 2.10⁻⁵ M, T=25°C;

Ni ₀ /10 ⁻³ M	τ /s	τ ⁻¹ /s ⁻¹	δA /mOD BCG/Ac
5,0	139	0,0072	0,011
7,5	135	0,0074	0,011
10,0	106	0,0094	0,017
20,0	72	0,0139	0,020

Table 10.12 Reciprocal of the relaxation times of the reaction of Ni(II) ions with Asp as a function of nickel(II) nitrate concentration for the case where Asp was present in excess;

pH = 4.20; Ni₀ = 5x10⁻⁴ M, I = 0.1 M (NaCl), Acetate₀ = 5.10⁻³ M, BCG₀ = 2.10⁻⁵ M, T=25°C;

L ₀ /10 ⁻³ M	τ /s	τ ⁻¹ /s ⁻¹	δA /mOD BCG/Ac
5	148	0.0068	0.025
10	117	0.0085	0.027
15	101	0.0099	0.022
20	62	0.0161	0.016
20	86	0.0116	0.022

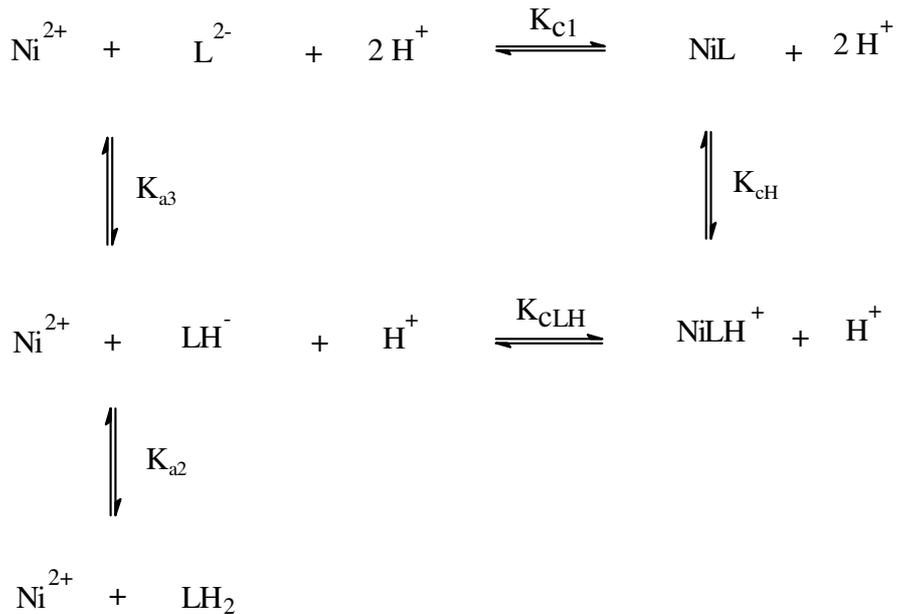
10.2 The fitting programmes used

10.2.1 Fitting of Potentiometric and spectrophotometric data

The computer programs used in this study for the collection and evaluation of experimental data were developed in our research group.

Potentiometric and spectrophotometric data are evaluated by expressing the particular reaction scheme in a system of n non-linear equations (whose number is equal to the number of species reacting) inhomogeneous equations containing the quantity balances of nickel, aspartic acid protons and each equilibrium.

For instance for the simple scheme 10.1, the equation system shown in equations 10.2.1 – 10.2.6 results.



Scheme 10.1

$$\bar{M}_1 = L_o = [\text{LH}_2] + [\text{LH}^-] + [\text{L}^{2-}] + [\text{NiLH}^+] + [\text{NiL}] \quad (10.2.1)$$

$$\bar{M}_2 = \text{Ni}_o = [\text{Ni}^{2+}] + [\text{NiLH}^+] + [\text{NiL}] \quad (10.2.2)$$

$$\bar{M}_3 = \log K_{a2} = \log[\text{LH}_2] - \log[\text{LH}^-] - \log[\text{H}^+] \quad (10.2.3)^9$$

$$\bar{M}_4 = \log K_{a3} = \log[\text{LH}^-] - \log[\text{L}^{2-}] - \log[\text{H}^+] \quad (10.2.4)$$

$$\bar{M}_5 = \log K_{cH} = \log[\text{NiLH}^+] - \log[\text{NiL}] - \log[\text{H}^+] \quad (10.2.5)$$

$$\bar{M}_6 = \log K_{c1} = \log[\text{NiL}] - \log[\text{Ni}^{2+}] - \log[\text{L}^{2-}] \quad (10.2.6)$$

$$\bar{M}_7 = A_o - B_o + 2 \cdot L_o = 2 \cdot [\text{LH}_2] + [\text{LH}^-] + [\text{NiLH}^+] + [\text{H}^+] - \frac{K_w}{[\text{H}^+]} \quad (10.2.7)$$

The quantities Ni_o , L_o , A_o and B_o represent the originally weighted-in concentrations of nickel(II) nitrate and aspartic acid (in the form LH_2) and/or acid (hydrochloric acid) and base (NaOH solution). K_w is the ionic product of the water and has the value $\text{p}K_w = 13.78$ (CSC. 1991) at $T =$

⁹ „log“ und „l“ are abbreviations for the Briggs logarithm of the size divided by the unit.

298.15 K and $I_{\text{NaCl}} = 0.10$ M. After the Newton-Raphson's iterative method the vector \vec{M} is developed in a Taylor series around the estimate \vec{M}_0 .

$$\vec{M} = \vec{M}_0 + \vec{M}' + \frac{1}{2!} \vec{M}'' + \frac{1}{3!} \vec{M}''' + \dots \quad (10.2.8)$$

For the zero order solution is $\vec{M} - \vec{M}_0 = 0$. Thus one obtains the following zeros (set of equations II) using the originally weighted-in quantity concentrations and equilibrium constants:

$$\vec{M}_1 - \vec{M}_{1,0} = [\text{LH}_2] + [\text{LH}^-] + [\text{L}^{2-}] + [\text{NiLH}^+] + [\text{NiL}] - L_o \quad (10.2.9)$$

$$\vec{M}_2 - \vec{M}_{2,0} = [\text{Ni}^{2+}] + [\text{NiLH}^+] + [\text{NiL}] - \text{Ni}_o \quad (10.2.10)$$

$$\vec{M}_3 - \vec{M}_{3,0} = \log[\text{LH}_2] - \log[\text{LH}^-] - \log[\text{H}^+] - \log K_{a2} \quad (10.2.10)$$

$$\vec{M}_4 - \vec{M}_{4,0} = \log[\text{LH}^-] - \log[\text{L}^{2-}] - \log[\text{H}^+] - \log K_{a3} \quad (10.2.12)$$

$$\vec{M}_5 - \vec{M}_{5,0} = \log[\text{NiLH}^+] - \log[\text{NiL}] - \log[\text{H}^+] - \log K_{cH} \quad (10.2.13)$$

$$\vec{M}_6 - \vec{M}_{6,0} = \log[\text{NiL}] - \log[\text{Ni}^{2+}] - \log[\text{L}^{2-}] - \log K_{c1} \quad (10.2.14)$$

$$\vec{M}_7 - \vec{M}_{7,0} = 2 \cdot [\text{LH}_2] + [\text{LH}^-] + [\text{NiLH}^+] + [\text{H}^+] - \frac{K_w}{[\text{H}^+]} - A_o + B_o - 2 \cdot L_o \quad (10.2.15)$$

If the estimated values are in the proximity of the mathematical solution, then the Taylor series can be broken off after the first order term, \vec{M}' yielding the value for the equilibrium concentration of a particular reacting species.

$$\vec{M} - \vec{M}_{1,0} = \vec{M}' \quad \text{where} \quad \vec{M}' = \sum_{i=1}^n \frac{\partial \vec{M}}{\partial c_i} \quad (10.2.16)$$

In the iterative process, the infinitesimal changes dc_i become finite differences δc_i . The looked for equilibrium concentration $c_{i,0}$ is approached through:

$$c_{i,0} = c_{i,0} + \delta c_i \quad (10.2.17)$$

The iterations are accomplished until the difference vector fulfills a certain abort criterion. It can be computed using equation (10.2.18)

$$\delta \vec{c}_i = \vec{M} \cdot \mathbf{J}^{-1} \quad (10.2.18)$$

where J is the Jakobi matrix. It contains the partial derivative of the set of equations II over the concentrations c_i .

$$\mathbf{J} = \begin{pmatrix} \frac{\partial M_1(c)}{\partial c_1} & \frac{\partial M_1(c)}{\partial c_2} & \dots & \frac{\partial M_1(c)}{\partial c_9} \\ \frac{\partial M_2(c)}{\partial c_1} & \frac{\partial M_2(c)}{\partial c_2} & \dots & \frac{\partial M_2(c)}{\partial c_9} \\ \vdots & \vdots & \vdots & \vdots \\ \frac{\partial M_9(c)}{\partial c_1} & \frac{\partial M_9(c)}{\partial c_2} & \dots & \frac{\partial M_9(c)}{\partial c_9} \end{pmatrix} \quad (10.2.19)$$

For scheme 10.1, the Jacobi matrix has the following form:

$$\mathbf{J} = \begin{pmatrix} -l[\text{LH}_2] & -l[\text{LH}^-] & -l[\text{L}^{2-}] & -l[\text{NiLH}^+] & -l[\text{NiL}] & 0 & 0 \\ 0 & 0 & 0 & -l[\text{NiLH}^+] & -l[\text{NiL}] & -l[\text{Ni}^{2+}] & 0 \\ -1 & 1 & 0 & 0 & 0 & 0 & 1 \\ 0 & -1 & 1 & 0 & 0 & 0 & 1 \\ 0 & 0 & 0 & -1 & 1 & 0 & 1 \\ 0 & 0 & 1 & 0 & -1 & 1 & 0 \\ -2 \cdot l[\text{LH}_2] & -l[\text{LH}^-] & -l[\text{L}^{2-}] & -l[\text{NiLH}^+] & 0 & 0 & \frac{[\text{H}^+] + K_w}{[\text{H}^+]} \end{pmatrix} \quad (10.2.20)$$

Due to lack of space the symbol “l” is used as an abbreviation for the Briggs logarithm of the size divided by the unit. Equation (10.2.18) can be solved using this matrix yielding estimated values for the equilibrium concentration of each species. After each iteration step the equilibrium concentrations will be obtained, from which new differences can be formed etc.. Iterations are accomplished until the abort criterion is fulfilled in equation (10.2.21). The system possesses only one solution in the range $0 \leq c_i \leq c_{i,0}$.

$$\left| \frac{\delta c_i}{c_i} \right| \leq 0.002 \quad \text{for } i = 1, n \quad (10.2.21)$$

Thus the the equilibrium concentration of each reacting species and hence the equilibrium constants can be fitted from the originally weighted-in quantity concentrations, the proton concentration and the estimated equilibrium constants.

The Newton-Raphson refined equilibrium concentrations are used to calculate the theoretical pH, theoretical absorbance (for a maximum of five wavelengths, using Beer-Lambert's law) and the partial chi squares (χ^2) for multiple potentiometric and spectrophotometric titrations. The partial

chi squares are summed up to the global χ^2 such that the globally optimised pK's and absorption coefficients (for a maximum of five wavelengths) are fitted using the method of least-squares or through a grid search. Additionally the programme enables the titre value to be fitted. A theoretical titration curve is calculated from the fitted equilibrium concentrations and constants. For each wavelength (in intervals of 1nm) the absorbance is optimised (through the minimisation of χ^2) knowing the equilibrium concentrations of each absorbing species as a function of pCh.

In a separate programme, the absorbance values (in intervals of 1nm) for each pH and the equilibrium concentrations of the nickel(II) aspartate complexes calculated by the programme described above are given as input. Using Beer-Lambert's law the theoretical absorbance for each wavelength is calculated, (using the Newton-Raphson's method) from which optimised absorption coefficients for the given nickel(II) aspartate complexes are fitted using the method of least-squares. Through comparison of the theoretical and experimental absorbance values, the chi squares (χ^2) values are calculated from which a standard deviation value for each absorption coefficient at each wavelength is calculated.

10.2.2 Fitting of Kinetic data

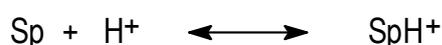
Kinetic measurements are evaluated with the help of the program Fit (Kardel, 1991). in which iterations are carried out using the Marquardt Algorithm and the parameters $A_{0,i}$, A_e , τ_i and D are fitted by the method of least squares fit. This program permits adjustments of up to three exponential functions at measuring data, whereby additionally a linear drift D of the measured signal can be also fitted such that the general equation has the following form:

$$A(t) = \sum_i A_{0,i} e^{-\frac{t}{\tau_i}} + Dt + A_e \quad (10.2.22)$$

The parameters with the smallest deviation from the experimental values are computed.

10.3 Justification of the neglect of the quadratic terms in the derivation of the equation relating δA and $[H^+]$ (See section 6.1.3)

For the protonation of a species Sp, the following fast equilibrium is always established



giving

$$\frac{([\text{Sp}]_e - \delta[\text{Sp}])([\text{H}^+]_e - \delta[\text{H}^+])}{([\text{SpH}^+]_e - \delta[\text{SpH}^+])} = \frac{[\text{Sp}]_e [\text{H}^+]_e}{[\text{SpH}^+]_e} \quad (10.3.1)$$

$$\left\{1 - \frac{\delta[\text{Sp}]}{[\text{Sp}]_e}\right\} \left\{1 - \frac{\delta[\text{H}^+]}{[\text{H}^+]_e}\right\} = \left\{1 - \frac{\delta[\text{SpH}^+]}{[\text{SpH}^+]_e}\right\} \quad (10.3.2)$$

In the above equation it is not trivial that $\frac{\delta[\text{H}^+]}{[\text{H}^+]_e} \ll 1$. Therefore, the quadratic terms

$$\left\{\frac{\delta[\text{Sp}]}{[\text{Sp}]_e} \frac{\delta[\text{H}^+]}{[\text{H}^+]_e}\right\} \text{ cannot be neglected.}$$

On the other hand, when Sp reacts with the buffer BH^+ , the protons are exchanged according to



and if equilibrium is established

$$\frac{([\text{Sp}]_e - \delta[\text{Sp}])([\text{BH}^+]_e - \delta[\text{BH}^+])}{([\text{SpH}^+]_e - \delta[\text{SpH}^+])([\text{B}]_e - \delta[\text{B}])} = \frac{[\text{Sp}]_e[\text{BH}^+]_e}{[\text{SpH}^+]_e[\text{B}]_e} \quad (10.3.3)$$

$$\left\{1 - \frac{\delta[\text{Sp}]}{[\text{Sp}]_e}\right\} \left\{1 - \frac{\delta[\text{BH}^+]}{[\text{BH}^+]_e}\right\} = \left\{1 - \frac{\delta[\text{SpH}^+]}{[\text{SpH}^+]_e}\right\} \left\{1 - \frac{\delta[\text{B}]}{[\text{B}]_e}\right\} \quad (10.3.4)$$

$$\left\{\frac{\delta[\text{Sp}]}{[\text{Sp}]_e}\right\} \left\{1 - \frac{\delta[\text{BH}^+]}{[\text{BH}^+]_e}\right\} + \frac{\delta[\text{BH}^+]}{[\text{BH}^+]_e} = \left\{\frac{\delta[\text{SpH}^+]}{[\text{SpH}^+]_e}\right\} \left\{1 - \frac{\delta[\text{B}]}{[\text{B}]_e}\right\} + \frac{\delta[\text{B}]}{[\text{B}]_e} \quad (10.3.5)$$

In this case, however, since the solution is buffered, i.e. $\delta[\text{B}], \delta[\text{BH}^+] \ll B_0$, the

terms $\frac{\delta[\text{BH}^+]}{[\text{BH}^+]_e}, \frac{\delta[\text{B}]}{[\text{B}]_e} \ll 1$, such that the quadratic terms $\left\{\frac{\delta[\text{Sp}]}{[\text{Sp}]_e} \frac{\delta[\text{BH}^+]}{[\text{BH}^+]_e}\right\}$ and

$\left\{\frac{\delta[\text{SpH}^+]}{[\text{SpH}^+]_e} \frac{\delta[\text{B}]}{[\text{B}]_e}\right\}$ can be neglected, giving

$$\left\{\frac{\delta[\text{Sp}]}{[\text{Sp}]_e}\right\} + \frac{\delta[\text{BH}^+]}{[\text{BH}^+]_e} = \left\{\frac{\delta[\text{SpH}^+]}{[\text{SpH}^+]_e}\right\} + \frac{\delta[\text{B}]}{[\text{B}]_e} \quad (10.3.6)$$

Analogously, the quadratic term can be neglected for any species reacting with the buffer (BH^+ or B ; but not with H^+ or producing H^+). This is the reason why the values of $\delta[\text{H}^+]$, $\delta[\text{L}^{2-}]$, $\delta[\text{LH}^-]$, $\delta[\text{LH}_2]$ and $\delta[\text{LH}_3^+]$ (equations (6.81), (6.85), (6.87), (6.83), and (6.82) respectively) were derived assuming reaction with the buffer (BH^+ or B) in section 6.1.3.1.

10.4 Proof of the Integration for the evaluation of the amplitudes for two relaxation effects (See section 6.1.3.2)

In section 6.1.3.2 it was claimed that the solution of (6.106) is

$$x_{ML_2} = \alpha_I e^{-\frac{t}{\tau_I}} + \alpha_{II} e^{-\frac{t}{\tau_{II}}} \quad (10.4.1)$$

This is proved by differentiating (6.108) and comparing the result to (6.106), as follows:

$$\frac{dx_{ML_2}}{dt} = -\frac{\alpha_I}{\tau_I} e^{-\frac{t}{\tau_I}} - \frac{\alpha_{II}}{\tau_{II}} e^{-\frac{t}{\tau_{II}}} \quad (10.4.2)$$

Substituting (6.108) and (6.115) into (10.4.2) gives

$$\frac{dx_{ML_2}}{dt} = \left(\frac{M_o}{1 + \frac{\kappa_1}{\kappa_2} + \frac{\kappa_{-2}}{\kappa_2 L_o}} \right) \frac{1}{\tau_I} e^{-\frac{t}{\tau_I}} - \left(-[ML_2]_e + \frac{M_o}{1 + \frac{\kappa_1}{\kappa_2} + \frac{\kappa_{-2}}{\kappa_2 L_o}} \right) \frac{1}{\tau_{II}} e^{-\frac{t}{\tau_{II}}} \quad (10.4.3)$$

Substituting (6.113) and (6.115) into (10.4.1) and rearranging gives

$$\left(-[ML_2]_e + \frac{M_o}{1 + \frac{\kappa_1}{\kappa_2} + \frac{\kappa_{-2}}{\kappa_2 L_o}} \right) e^{-\frac{t}{\tau_{II}}} = x_{ML_2} + \frac{M_o}{1 + \frac{\kappa_1}{\kappa_2} + \frac{\kappa_{-2}}{\kappa_2 L_o}} e^{-\frac{t}{\tau_I}} \quad (10.4.4)$$

Substituting (10.4.4) into (10.4.3) we obtain

$$\frac{dx_{ML_2}}{dt} = \left(\frac{M_o}{1 + \frac{\kappa_1}{\kappa_2} + \frac{\kappa_{-2}}{\kappa_2 L_o}} \right) \frac{1}{\tau_I} e^{-\frac{t}{\tau_I}} - \frac{1}{\tau_{II}} \left(x_{ML_2} + \frac{M_o}{1 + \frac{\kappa_1}{\kappa_2} + \frac{\kappa_{-2}}{\kappa_2 L_o}} e^{-\frac{t}{\tau_I}} \right) \quad (10.4.5)$$

$$\frac{dx_{ML_2}}{dt} = \left(\frac{M_o}{1 + \frac{\kappa_1}{\kappa_2} + \frac{\kappa_{-2}}{\kappa_2 L_o}} \right) e^{-\frac{t}{\tau_I}} \left\{ \frac{1}{\tau_I} - \frac{1}{\tau_{II}} \right\} - \frac{1}{\tau_{II}} x_{ML_2} \quad (10.4.6)$$

Substituting the values of τ_I and τ_{II} , equations (6.105) and (6.109) respectively into (10.4.6) gives

$$\frac{dx_{ML_2}}{dt} = \left(\frac{M_o}{1 + \frac{\kappa_1}{\kappa_2} + \frac{\kappa_{-2}}{\kappa_2 L_o}} \right) e^{-\frac{t}{\tau_I}} \{ \kappa_1 L_o - \kappa_2 L_o - \kappa_{-2} \} - (\kappa_2 L_o + \kappa_{-2}) x_{ML_2} \quad (10.4.7)$$

$$\frac{dx_{ML_2}}{dt} = \left(\frac{-\frac{\kappa_1 L_o}{\kappa_2 L_o} - 1 - \frac{\kappa_{-2}}{\kappa_2 L_o}}{1 + \frac{\kappa_1}{\kappa_2} + \frac{\kappa_{-2}}{\kappa_2 L_o}} \right) M_o e^{-\frac{t}{\tau_1}} \{\kappa_2 L_o\} - (\kappa_2 L_o + \kappa_{-2}) x_{ML_2} \quad (10.4.8)$$

$$-\frac{dx_{ML_2}}{dt} = \kappa_2 L_o M_o e^{-\frac{t}{\tau_1}} + (\kappa_2 L_o + \kappa_{-2}) x_{ML_2} \quad (10.4.9)$$

Equation (10.4.9) is identical to (6.107) confirming that $x_{ML_2} = \alpha_I e^{-\frac{t}{\tau_I}} + \alpha_{II} e^{-\frac{t}{\tau_{II}}}$ is its solution as claimed.

Curriculum Vitae

Personal information		
Name	Ronald Agius	
Address	57, Melanchthonstraße, 33615, Bielefeld, Germany	
Nationality	Maltese	
Marital Status	Single	
Date of birth	13 th October, 1972	

Education	1976 - 1983	<u>Primary Education:</u> Siggiewi Primary School, Siggiewi, Malta
	1983 - 1988	<u>Secondary Education:</u> Tal-Handaq Junior Lyceum, Qormi, Malta
	1988 - 1990	<u>Tertiary Education:</u> The New Lyceum, Msida, Malta
	Oct.1990 - Sept. 1997	<u>Tertiary Education:</u> The University of Malta
	Nov. 1993	Obtained Bachelor of Science degree in Chemistry and Biology <u>B.Sc. Thesis:</u> <i>The Photosubstitution reaction between 1,4-dicyanobenzene and 2,3-dimethyl-2-butene: Studies of the effects of solvent, sensitizer and additives</i>
	Oct. 1996	Obtained Post Graduate Course in Education; (P.G.C.E.) <u>Thesis:</u> <i>Teaching Science: An Effective Approach</i>
	Nov. 1997	Obtained Master of Science degree in Chemistry <u>M.Sc. Thesis:</u> <i>The effect of alcohols and solvents on the synthesis of CdS nanoparticles in reverse micellar media</i>
	Oct.1999 - Dec. 2000	Studies of Physical Chemistry and of the German language at the University of Bielefeld
Jan. 2001 - March 2004	PhD student at the University of Bielefeld <u>Ph.D. Thesis:</u> <i>pH-Sensitive Binding of Nickel(II) Ions to Aspartic acid</i>	
Work Experience	Oct. 1993 - Sept. 1994	Lecturer at the <i>Institute of Agriculture</i> , University of Malta
	Sept. 1993 - Sept.1999	Teacher at <i>St. Albert the Great College</i> , Valletta, Malta
	Oct. 1994 - June 1995	Laboratory Demonstrator at the Faculty of Chemistry, University of Malta
	Oct. 1997 - June 1999	Tutor for Chemistry Advanced Level Practicals and Tutorials at the <i>Department of Chemistry, Junior College</i> , University of Malta
	Oct. 2000 - Sept. 2003	Research Assistant for Physical Chemistry Practicals and Tutorials at the Faculty of Chemistry, University of Bielefeld
Language Skills		Maltese and English - Mother tongues Italian and German - fluent in writing and verbally, French and Arabic - school knowledge